Molecular pharmacology of AMPA receptor trafficking proteins - TARPs - evidence for an association with 5HT(_2c) receptors

Peter Donoghue

Molecular Pharmacology of AMPA Receptor Trafficking Proteins – TARPs – Evidence for an Association with $5HT_{2C}$ Receptors.

Peter Donoghue

A thesis submitted to the University of Durham in accordance with the requirements for the degree of Doctor of Philosophy

School of Biological and Biomedical Sciences

2009

Supervisors: Dr Christopher L Thompson and Dr Paul L Chazot

Abstract

There has been an increasing awareness of the involvement of neurotransmitters other than serotonin in depression, with new antidepressants possessing effects on other receptor types, such as Agomelatine®, an antagonist of $5HT_{2C}$ receptors that functions as an agonist at melatonin receptors.

AMPA receptors are one of the families of ionotropic glutamate receptors and another neurotransmitter receptor type that have been demonstrated to be important in the function of new antidepressants. AMPA receptors possess effects upon brain-derived neurotrophic factor (BDNF) expression, a protein involved in neurogenesis in the hippocampus, which is believed to be pivotal to antidepressant efficacy, with BDNF expression diminishing in critical brain areas in response to chronic stress, but increasing in the hippocampus in response to treatment with both antidepressants and/or AMPA receptor modulators.

AMPA receptors interact with a family of accessory proteins, the transmembrane AMPA receptor regulatory proteins (TARPs), which not only possess important roles in the trafficking and targeting of AMPA receptors, but also function as auxillary subunits to AMPA receptors. Present in several isoforms, each individual TARP also directly modifies AMPA receptor kinetics. As such TARPs and their effects must be taken into account for any pathophysiological or drug-induced change involving AMPA receptors. Despite the vast literature on AMPA receptors, there is comparatively little information regarding how TARPs modify AMPA receptor function, largely due to the absence of the necessary tools.

We developed polyclonal antibodies specific to each of the known TARP isoforms ($\gamma 2$, $\gamma 4$, $\gamma 8$) mapping the distribution of the TARPs in the mouse CNS, displaying a different distribution profile for each of the TARP isoforms. TARP $\gamma 8$ is of particular interest, being shown to have a wide expression in the CNS from the frontal cortex to the spinal cord, but also a regional distribution in the forebrain that shares similarities to a positive allosteric modulator of AMPA receptors. There is also some evidence of a strain

dependent distribution of TARP γ8, possibly contributing to some of the behavioural differences between strains.

With the extensive distribution of TARP γ8 in the forebrain, particularly in those structures shown to experience severe neuronal atrophy in depression, such as the hippocampus, we focused on the antibodies generated to this isoform to generate immunoaffinity columns and immunopurify TARP γ8 and its interacting proteins from Triton X-100™ solubilised, so effectively non-synaptic, cerebral cortex.

Examination of the purified TARP γ8 and its interacting partners by both immunological and proteomic techniques revealed a range of proteins previously not implicated as TARP interacting proteins important in several pathophysiological situations, including several isoforms of actin. Furthermore, the immunopurified TARP γ8 material also contained a protein identified with multiple $5HT_{2C}$ receptor antibodies at ~60 kDa, the molecular weight correlating to fully glycosylated $5HT_{2C}$ receptor.

Further study of TARP and AMPA receptor levels in the forebrain of mice with either forebrain-specific over-expression, or forebrain-specific knockdown of $5HT_{2C}$ receptors, identified several differences in total protein levels of the TARPs and AMPA receptor subunits. TARP γ8 was shown to possess higher levels of expression in both of the mice strains with altered $5HT_{2C}$ receptor expression, suggesting a complex functional interaction between TARPs/AMPA receptors and $5HT_{2C}$ receptors.

These results, in addition to providing evidence of strain variations with regard to TARP distributions, have also identified several previously unknown TARP γ8 interacting proteins, including, but not limited to cytoskeletal proteins. The results also show evidence of both a physical and functional interaction of TARP γ8 and AMPA receptors with $5HT_{2C}$ receptors in the forebrain, particularly the cerebral cortex – findings of potential importance regarding the role of AMPA receptors in mood disorders.

Acknowledgements

Firstly I would like to acknowledge the support of my family and friends throughout my PhD – people who have been there throughout a time of constant challenge and change for me. In particular, I'd like to thank my partner Samantha, who has put up with the second-hand stress this PhD has caused.

Secondly I would like to acknowledge the support of the people I've worked with. This project has by no means been easy, and I feel fortunate to have been in the company of some excellent colleagues. In particular I'd like to thank Dr Helen Payne, Dr Victoria Hann, Joanne Robson and Dr Paul Chazot for the assistance they have provided throughout the more challenging points of this project – Dr Chazot in particular, who, late in the day assumed the role of supervisor at short notice during a difficult personal time for himself.

Thirdly I'd like to acknowledge Professor Michael Spedding, who has always been on hand with advice, support and who is someone I am indebted to for everything he's done ensuring this projects completion.

I'd also like to acknowledge the organisations that have funded this project and provided financial support – the BBSRC and SERVIER I'd also like to thank everyone at the University of Durham who has helped over the years, not the least of which are the people in the LSSU.

Finally I'd like to acknowledge someone who I wish was around to receive the first acknowledgment, my initial supervisor, the late Dr Christopher L Thompson – someone I am honoured and humbled to have worked for, and who will influence my career constantly. A true inspiration and role model.

Declaration

I confirm that no part of the material presented has previously been submitted for a degree in this or any other university. If material has been generated through joint work, my independent contribution has been clearly indicated. In all other cases, material from the work of others has been clearly indicated, acknowledged and quotations and paragraphs indicated.

Contents

List of Abbreviations Used in this Thesis

5HT = 5-hydroxytryptamine, eg. $5HT_{2C}$ receptor = 5-hydroxytryptamine 2C receptor

γ8C = Antibody generated using the TARP γ8 C terminal domain

γ8N = Antibody generated using the TARP γ8 C terminal domain

AMPA = α-amino-3-hydroxyl-5-methyl-4-isoxazole-propionate

BDNF = Brain derived neurotrophic factor

CA1-3 = Cornu Ammonis

CACN = Voltage dependent calcium channel

CAMKII = Calmodulin dependent protein kinase II

cAMP = Cyclic adenosine monophosphate

CBM = Cerebellum

CHO = Chinese Hamster Ovary

CNPase = 2',3'-cyclic-nucleotide 3'-phosphodiesterase

CNS = Central Nervous System

CTX = Cerebral Cortex

CTZ = Cyclothiazide

DAB = 3,3'-Diaminobenzidine

DG = Dentate Gyrus

DH = Dorsal Horn of the spinal cord

dH_2O = De-ionised water

DHPG = 3,5-Dihydroxyphenylglycine

DMSO = Dimethyl sulfoxide

EDTA = Ethylenediaminetetraacetic acid

ELISA = Enzyme-Linked ImmunoSorbent Assay

ER = Endoplasmic Reticulum

F1-5 = Purified fractions eluted from the immunoaffinity columns – an subscript number refers to the day of elution.

FB = Forebrain

FT = Flow through from the immunoaffinity columns

GABA = Gamma-aminobutyric acid

GluR1-4 = Glutamate Receptor subunit

GPCR = G Protein-coupled Receptor

GRIP1 = Glutamate Receptor Interacting Protein

HEK293 = Human Embryonic Kidney 293

HP = Hippocampus

HRP = Horseradish Peroxidase

HSP90 = Heat Shock Protein 90

JNK = c-Jun N-terminal kinase

KA = Kainate (Kainic Acid). KAR = Kainate Receptor

KD = Knockdown, as in $5HT_{2C}$ Receptor knockdown mice

kDa = Kilo Dalton(s)

KSCN = Potassium thiocyanate

LTD = Long-term Depression

LTP = Long-term Potentiation

MAGI-2 = Membrane Associated Guanylate Kinase 2

MALDI-TOF = Matrix-Assisted Laser Desorption/Ionization – Time of Flight mass spectroscopy

MALDI-TOF/TOF = Matrix-Assisted Laser Desorption/Ionization – Time of Flight conducted in tandem

MAP-1A = Microtubule Associated Protein 1A. Also MAP-1A LC2, where LC2= Light Chain 2.

MBP = Myelin Basic Protein

mcKLH = Marine Culture Keyhole Limpet Hemocyanin

MEA = β-mercaptoethylamine

mGluR = Metabotropic Glutamate Receptor

Mol wt = Molecular Weight Markers

mRNA = Messenger Ribonucleic Acid

MS/MS = Tandem Mass Spectroscopy

NAc = Nucleus Accumbans

NaCl = Sodium Chloride

$NaHCO_3$ = Sodium Hydrogen Carbonate

$NaNO_3$ = Sodium Nitrate

NEEP21 = Neuron-Enriched Endosomal Protein of 21 kD

NMDA = N-methyl-D-aspartic acid

nPIST = Neuronal Isoform of Protein-Interacting Specifically with TC10

NSF = N-ethylmaleimide Sensitive Fusion Protein

NuPAGE = Gel Used for Proteomics

OE = Over-expressing, as in $5HT_{2C}$ Receptor over-expressing mice

P38 MAPK = P38 Mitogen-Activated Protein Kinase

PBS = Phosphate Buffered Saline

PDZ = Post synaptic density protein 95, Drosophila disc large tumor suppressor, Zonula occludens-1

PICK 1 = Protein Interacting with Protein Kinase C Alpha

PKC = Protein Kinase C

PMSF = phenylmethanesulphonylfluoride

PP1A = Protein Phosphatase 1A

PP2A = Protein Phosphatase 2A

PSD-93 = Post-synaptic Density Protein 93

PSD-95 = Post-synaptic Density Protein 95

RT = Room Temperature

SAP 97 = Synapse Associated Protein 97

SAP 102 = Synapse Associated Protein 102

SDS = Sodium Dodecyl Sulfate polyacrylamide gel electrophoresis

SDS-PAGE = Sodium Dodecyl Sulfate - Polyacrylamide Gel Electrophoresis

SPC = Spinal Cord

SSRI = Selective Serotonin Reuptake Inhibitor

STG = Stargazin (TARP γ2)

STR = Striatum

TARPs = Transmembrane AMPA Receptor Regulatory Proteins

TBS = Tris-Buffered Saline

TFA = Trifluoroacetic Acid

TH = Thalamus

Tx Sol = Triton X-100^{TM} Solublised material

Tx Insol = Triton X-100^{TM} Insoluble material

VGCC = Voltage-gated Calcium Channel

VH = Ventral Horn of the spinal cord

VTA = Ventral Tegmental Area

Whole Prep. = Homogenised tissue prior to solubilisation

1.1 The glutamatergic nervous system

The central nervous system (CNS) is a collection of cells with a variety of functions, of which the most obvious cell type are the neurones. Signalling in the CNS is mediated by a variety of chemicals termed neurotransmitters, which have specific effects and, as with all chemical signalling in biological systems, specific receptors to mediate these effects.

One critical system of neurotransmitters and receptors is the glutamatergic system, a variety of cells that use the neurotransmitter glutamate to mediate their effects. In the CNS, activation of glutamate receptors is predominantly excitatory to the cell concerned, but some glutamate receptors are inhibitory in their effects on neuronal activity.

Whilst essential for survival, there is a darker side to the glutamatergic nervous system, with the abnormal and excessive release of glutamate being a major contributory factor in the spread of damage during a stroke.

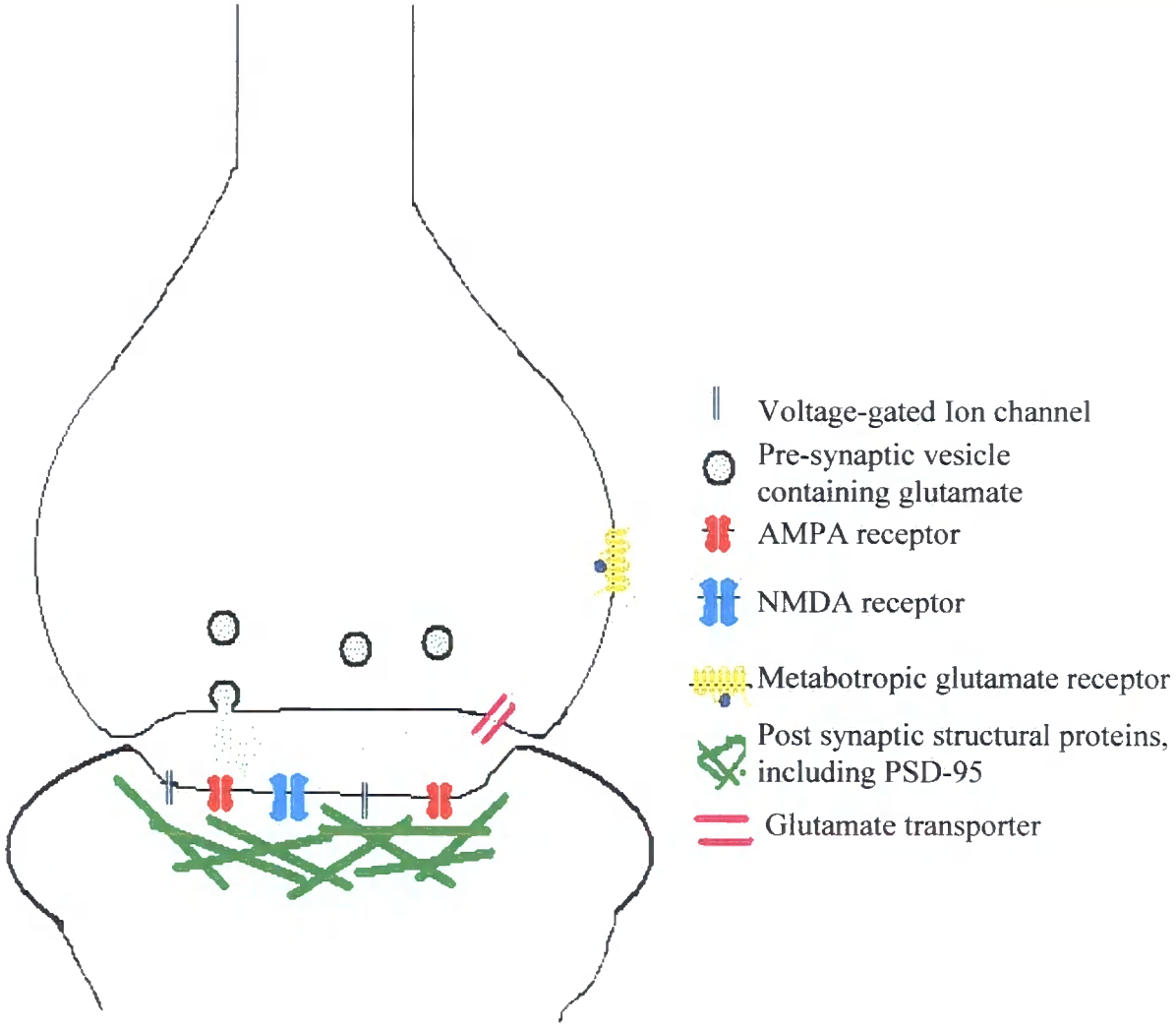

Figure 1.1: A simplified diagram of a glutamatergic synapse showing the typical distribution of the glutamatergic receptors. *Based on information from Boeckers Cell and Tissue Research 2006.*

There are two currently known families of glutamate receptor, the metabotropic and the ionotropic, both of which possess different methods of function and roles in the CNS.

1.2 Metabotropic glutamate receptors (mGluRs)

A family of receptors consisting of eight distinct subtypes (mGluR1-8), mGluRs are wholly distinct from ionotropic glutamate receptors both in compostion and function, the

only similarity being their sensitivity to glutamate (Bockaert et al. 1993, Schoepp 1994 – Reviews).

The first and perhaps most noticeable distinction is the fact that mGluRs are actually a family of G-protein coupled receptors, mediating their effects via intracellular messengers that are secondary to the receptor itself (Nakanishi et al. 1998).

Depending upon the G-protein system to which the mGluR is coupled, in addition to responses to specific compounds, it is possible to sub-divide the mGluR receptor family into 3 groups:

- Group I: This group consists of the mGluRs 1 and 5, which are positively coupled to phosphoinositide hydrolysis. They can be selectively activated by 3, 5 dihydroxy-phenylglycine (3,5 DHPG). They are frequently coupled to phospholipase C and when activated stimulate increased release of intracellular Ca^{2+}, whilst inhibiting voltage-gated Ca^{2+} channels.

- Group II: This group consists of the mGluRs 2 and 3, which are negatively coupled to adenylyl cyclase. They can be selectively activated by the agonist LY379268. This group is coupled to an inhibition of cyclic AMP cascade in addition to regulatory roles in both G-protein coupled, inwardly rectifying K^{+} channels, and intracellular Ca^{2+}.

- Group III: This group consists of the mGluRs 4, 6, 7 and 8, which are again negatively coupled to adenylyl cyclase, but unlike group II mGluRs, are activated by 2-amino-4-phosphobutyrate. The function primarily associated with this group of mGluRs is the inhibition of synaptic transmission via the suppression of presynaptic voltage-gated Ca^{2+} channels. As such, despite being a glutamate receptor, these mGluRs are located in a wide variety of different synapses, including GABAergic synapses.

All mGluRs possess a 7-transmembrane domain topology commonly associated with G-protein coupled receptors, with an extracellular N-terminal domain, and a large intracellular C-terminal domain, which in the cases of mGluRs 1, 3, 5 and 8, can undergo extensive editing resulting in numerous splice variants.

Besides the differences in membrane topology from the ionotropic glutamate receptors, the mGluRs also have a contradictory function in the CNS. Whereas the ionotropic glutamate receptors are associated with excitatory neurotransmission, the principle role of mGluRs is to regulate pre and post-synaptic events, frequently by utilising inhibition. Little is known on the functional roles of each of the mGluR subtypes, but they each have a distinct distribution within the CNS (Ferraguti et al. 2006).

1.3 Ionotropic glutamate receptors

There are three known forms of ionotropic receptors present in the CNS that are responsive to L-glutamate: NMDA receptors, Kainate receptors and AMPA receptors, all of which are so named due to their relative sensitivity to compounds that function as agonist at ionotropic glutamate receptors. All the ionotropic glutamate receptors are similar in general receptor properties and function, but with pronounced differences in their specific roles, localisation, and composition.

All ionotropic glutamate receptors are comprised of several constituent subunits, unique to each receptor type, that possess unique attributes which in turn influence the resultant receptors pharmacology and functional role.

The topology of the individual subunits for these ionotropic glutamate receptors is the same, with an extracellular N-terminal domain, four transmembrane domains (MD1-4) and a cytoplasmic C-terminal domain. Without exception the second transmembrane domain enters the plasma membrane via the cytoplasmic side, and does not fully transect the membrane, instead re-entering the cytoplasm, and as such forms the pore created by co-assembly of these subunits in their constituent receptor.

The ligand binding domain is formed by the extracellular N-terminal region and the first extra-cellular loop, located between MD2 and MD4.

1.3.1 *N*-methyl D-aspartate (NMDA) receptors

NMDA receptors are an extensively studied class of ionotropic glutamate receptors integral for excitatory neurotransmission throughout the CNS. They are potentially either tetrameric or pentameric structures consisting of two NR1 subunits and usually two NR2 subunits although some receptors contain NR3 subunits. The NR2 and NR3 subunits can be further divided into NR2A-D and NR3A-B. The exact composition of the receptor subunits has been shown to confer different functional properties to the receptor, with specific subunit subtypes being associated with specific neurological processes. The NR2 subtypes also possess differential expression throughout the both the CNS, but also within a cell, in addition to possessing a developmentally regulated expression with some NR2B and NR2D containing receptors being replaced with NR2A and NR2C containing receptors during development.

Figure 1.2 Table of NMDAR subunits

Subunit	**Variants**	**Location in CNS**	**Associated Physiological Role** Li et al. (2007)
NR1 Anantharam et al. (1992), Nakanishi et al.. (1992), Sugihara et al. (1992), Kusiak and Norton (1993)	8 Splice Variants (NR1a – NR1h)	Throughout the CNS. Nakanishi (1992), Standaert et al. (1993)	All NMDA receptor-related processes. Durand et al. (1993), Hollmann et al. (1993), Micu et al. (2006)
NR2 Monyer et al. (1992) Nakanishi (1992) Ishii et al. (1993), Buller et al. (1994), Wenzel et al. (1995),	NR 2A	A distribution similar to the NR1 subunit. Uniform distribution between cortex, hippocampus and cerebellum. Low levels in the striatum. Petralia et al. (1994), Vallano et al.	Integral for induction of synaptic Long Term Potentiation (LTP)

Karadottir et al. (2005)		(1995)	
	NR 2B	Primarily the forebrain. Present in the cerebellum during early development. Petralia et al. (1994), Vallano et al. (1995)	Integral for induction of synaptic Long Term Depression (LTD)
	NR 2C	Enriched in the cerebellum. Also present in myelinated cells, thalamus and olfactory structures. Absent in hippocampus. Vallano et al. (1995)	Some neuroprotective effects. Also influences NMDA receptor channel permeability. Pizzi et al. (1999), Micu et al. (2006)
	NR 2D	Distribution follows a developmental pattern. Regions of expression in adults include the striatum, hippocampus and superior colliculus. Concentrated in thalamus and spinal cord in addition to mid-brain and brainstem.	Important in retinal Rod bipolar cells. Also important, but not essential for the developing hippocampal formation. Potential role in excitatory pathways in mature hippocampus. Thompson et al. (2002)
NR 3 Chatterton et al. (2002)	NR 3A Nishi et al. (2001)	Associated with myelinated cells. Karadottir et al. (2005)	Poorly defined, may have roles mediating ischaemic insult in oligodendrocytes. Salter et al. (2005), Micu et al. (2006)
	NR 3B	Highest levels in motor neurones within the pons, medulla and spinal cord. Developmentally dependent expression pattern. Fukaya et al. (2005)	Important in cell surface trafficking of NMDARs and influences Calcium permeability. Forms excitatory glycine receptor with NR1 subunit, although this result is still controversial. (Micu et al. 2006)

The NR1 subunit of NMDA receptors are essential components of a functional receptor, and the majority are believed to combine with the NR2A subunit, with this being the prevalent NR2 subunit in the CNS. The NR1 subunit itself contains a glycine binding domain, a property unique to NMDA receptors when compared with other ionotropic glutamate receptors, and equates to the NMDA receptor requiring co-activation by both glutamate (or a suitable equivalent agonist) and glycine. Once active, the NMDA receptor is permeable to both Na^{+} but primarily Ca^{2+} and is responsible for the much of the Ca^{2+} influx that occurs as a consequence of excitatory neurotransmission.

Another property unique to NMDA receptors compared to other ionotropic glutamate receptors is that at resting membrane potential, the Ca^{2+} ion channel is blocked by Mg^{2+}, with the NMDA receptor requiring a depolarising event to occur in the membrane potential to remove the Mg^{2+} and allow the receptor to function.

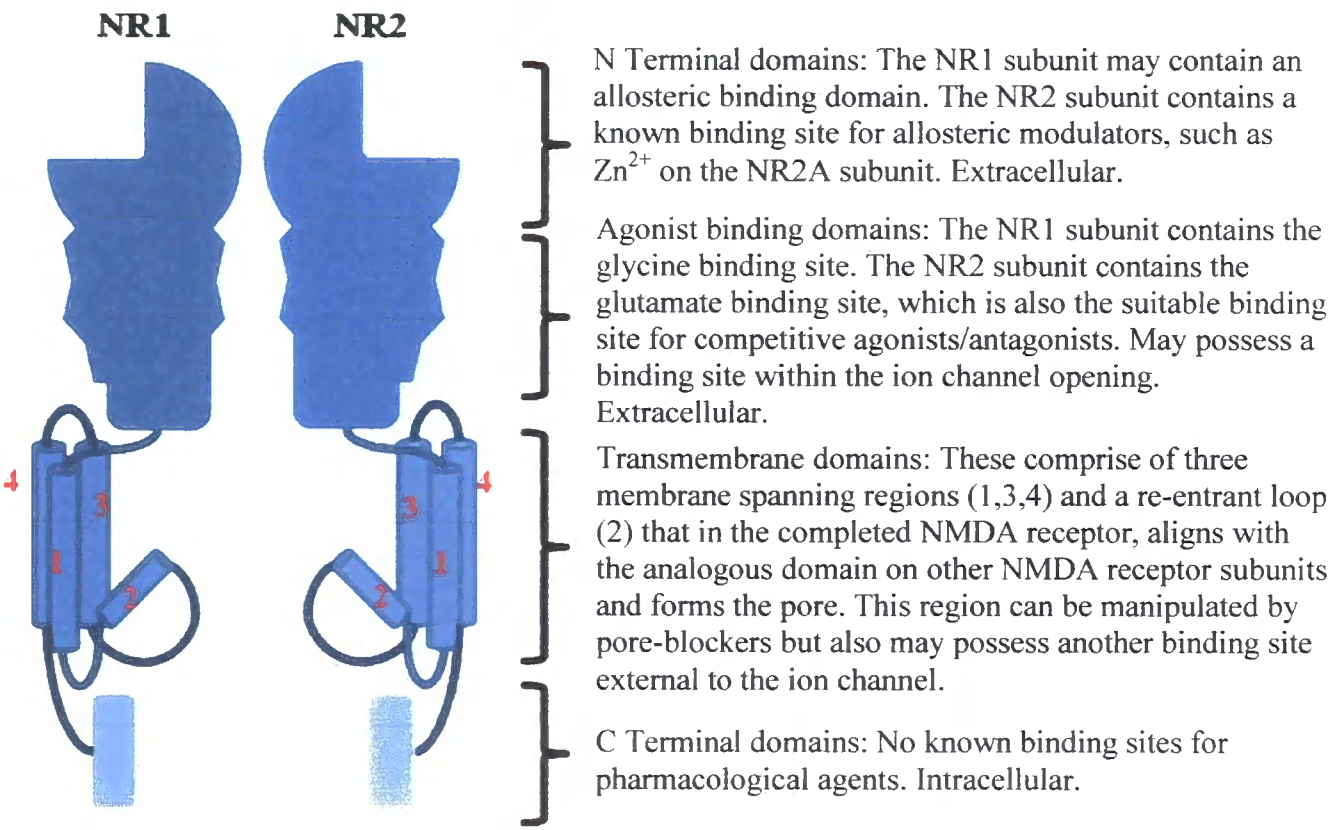

Figure 1.3: Diagram showing the potential binding sites present on the NMDA receptor Extensively adapted from Paoletti and Neyton 2007

The NMDA receptor also has several important interactions with AMPA receptors in several key neurological processes including synaptic LTP and LTD, both of which are discussed in more detail in section 1.4.

1.3.2 Kainate receptors (KA receptors)

Kainate receptors, are one of the two non-NMDA ionotropic glutamate receptors identified in the CNS that are a component of the glutamatergic nervous system. They were originally identified by their preferential response to kainate, namely a rapid desensitization in its presence that distinguished them from the other class of non-NMDA ionotropic glutamate receptor; AMPA receptors (Davies et al. 1979, Bettler and Mulle, 1995).

Kainate receptors are comprised of five receptor subunits GluR5, GluR6, GluR7, Ka1 and Ka2 (Hollmann and Heinemann 1994), which have been shown to co-assemble into both homomeric and heteromeric receptors depending upon the subunits investigated and conditions in which they were expressed.

Compared to other ionotropic glutamate receptors, the kainite receptors are poorly understood, with very few neurological processes where the roles of the kainate receptors are fully understood. As such they are perhaps unique in the sense that they are the only ionotropic glutamate receptors with no known fundamental role in synaptic LTP and LTD.

1.3.3 α-amino-3-hydroxy-5-methyl-4-isoxazolepropionate (AMPA) receptors

AMPA receptors are part of the family of ionotropic glutamate receptors present in the central nervous system and are responsible for rapid excitatory glutamatergic

neurotransmission. Frequently found in the post synaptic density, they also occur pre-synaptically, most frequently mediating the release of neurotransmitters – although the former location is the most extensively studied.

They possess a tetrameric structure existing as either heteromers or homomers of four possible subunits – GluR1, GluR2, GluR3 and GluR4 all of which can undergo some RNA editing, and exist as either *flip* or *flop* splice isoforms (Sommer et al. 1990, Derkach et al. 2007), with these RNA edits affecting their inherent trafficking properties (Coleman et al. 2006).

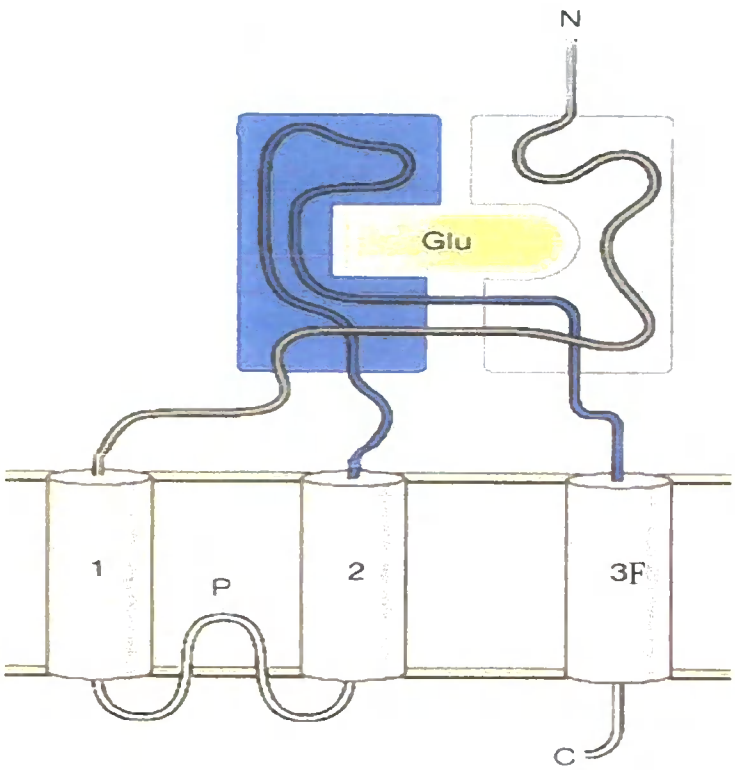

Figure 1.4: Generic structure of an AMPA receptor GluR subunit (Amended from Sun et al. 2002).

Each GluR subunit of an AMPA receptor possesses an extra-cellular N terminus, an intracellular C terminus and four membrane transecting domains, of which the second (P in Figure) only partially transects the plasma membrane before

returning to the cytoplasm. In the fully assembled AMPA receptor, this region (P) forms the ion channel pore. Region F shows the *flip-flop* domain.

The majority of AMPA receptors expressed endogenously *in vivo* are either GluR1/2 or GluR2/3 heteromers. Their cycling both to and from the cell surface and the synapse is widely regarded as of essential importance with regard to their function, and they seem to possess at least several forms of cycling, some of which are activity-dependant (Lüscher et al. 1999). They are also believed to undergo constitutive cycling from extra-synaptic regions in the plasma membrane either translocating into the synapse, or entering intracellular pools of AMPA receptors, of which some are degraded, but others can be recycled back to the cytoplasmic membrane (Liang F et al. 2001).

AMPA receptors are believed to be involved in a couple of neurological phenomena that are regarded as being fundamental to not only learning and memory, but also to synaptic plasticity in excitatory synapses – namely synaptic Long term potentiation (LTP), and synaptic Long term depression (LTD) (Earnshaw et al. 2006). Both of these processes involve the activity-dependant trafficking of AMPA receptors that serves to either strengthen a synapse, as is the case of the former, or weaken it, as is the case of the latter.

During constitutive AMPA receptor synaptic cycling GluR2 containing AMPA receptors are shuttled between extra-synaptic locations and the synapse in an activity-independent manner. The cycling is rapid (Adesnik et al. 2005), and appears to be regulated by synaptic anchoring interactions of the GluR2 PDZ domain with various proteins, although it is uncertain as to what extent these interactions affect the constitutive state cycling compared with an activity-induced cycling process. In the post-synaptic density GluR2 PDZ binding appears to show a preference for Glutamate Receptor Interacting Protein 1 (GRIP1) (Dong et al. 1997 Wyszynski et al. 1999, Osten et al. 2000). However, phosphorylation of ser880 of the GluR2, occurring as a consequence of PKC activation (Matsuda et al. 1999, Chung et al. 2000, Daw et al. 2000), disrupts GRIP1 binding, with the phosphorylated GluR2 diffusing from synaptic locations, seemingly via interactions with Protein Interacting with C Kinase 1 (PICK1) (Perez et al. 2001, Iwakura et al. 2001,

Kim et al. 2001). There is also evidence that the constitutive cycling of GluR2 containing AMPA receptors to the cell surface and their subsequent synaptic trafficking requires interactions with various other cytosolic proteins. These include NSF (Nishimune et al. 1998, Song et al. 1998, Lúscher et al. 1999, Huang et al. 2005), HSP90 (Gerges et al. 2004), NEEP21 (Steiner et al. 2002) and Rab8 (Gerges et al. 2004), in addition to unknown palmitoylating enzymes, such as GODZ, whereby palmitoylation of the GluR2 subunit limits exiting from the Golgi apparatus (Hayashi et al. 2005).

Interestingly GluR3 contains the same PDZ binding motif as GluR2, but does not appear to be the important AMPA receptor subunit regulating constitutive AMPA receptor cycling (Sans et al. 2001, Sheng and Lee 2001), with GluR2-regulated constitutive cycling being important even for those AMPA receptors located at pre-synaptic sites (Pittaluga et al. 2005).

Several forms of LTP, a process that requires the activity-dependant synaptic targeting of AMPA receptors does not appear to be mediated via the GluR2 subunit rather it is the GluR1 subunit that appears to be crucial for the activity of LTP (Oh et al.. 2005).

GluR1 containing AMPA receptors, particularly those which do not contain the GluR2 subunit, are predominantly located in non-synaptic neuronal regions during baseline levels of activity (Chen et al. 1998). Their trafficking to the cell surface and synaptic targeting possesses notable differences in interacting proteins to GluR2, not least in the demonstrated interaction of GluR1 with Synapse Associating Protein 97 (Sap-97) – a protein that is related to PSD-95, but is located predominantly in the cytoplasm (Sans et al. 2001), but also their interaction with the 4.1N protein located in the PSD cytoarchitecture. This interaction is disrupted following palmitoylation of the GluR1 subunit, promoting removal of the GluR1 containing AMPA receptor from the synapse (Hayashi et al. 2005).

However, following the induction of LTP, which stimulates the activation of NMDA receptors and an increase in intracellular Ca^{2+} levels, there is an increase of GluR2-

lacking AMPA receptors frequently homomeric GluR1 receptors being detectable in the PSD, in the first 30 minutes following the induction of LTP, suggesting that it is the increase in Ca^{2+} permeable AMPA receptors that enables the synaptic strengthening involved in LTP (Kauer and Malenka 2006). The precise mechanism for this induction of GluR1 containing AMPA receptors in LTP is unknown, but phosphorylation of the ser845 of GluR1 via multiple candidate kinases, not the least significant of which being CAMKII – activated as a consequence of NMDA receptor activation – has been shown to be important for the synaptic targeting of GluR1 (Sheng and Lee 2001).

The interactions of PSD-95 have also been shown to be important in the recruitment of GluR2-lacking AMPA receptors to the PSD following LTP. This interaction appears to be indirect, but dependant upon the palmitoylation state of PSD-95, with N-terminal palmitoylation being required for cell-surface targeting – indeed expression of dominant negative forms of PSD-95 abolish LTP induction. PSD-95 has no discernable effect on the constitutive induction of GluR2 into the PSD (Ehrlich and Malinow 2004).

It has been shown however, that following LTP and the increase in GluR2 lacking AMPA receptors, there is a long-term increase in the number of GluR2 containing AMPA receptors detectable at the synapse several days after the induction of LTP (Kauer and Malenka 2006, McCormack et al. 2006). – most likely because the LTP and subsequent increase in synaptic strength, not to mention an increase in synaptic size – a consequence of recruitment of additional PSD proteins - has led to an increase in the number of active AMPA receptors likely to be present under 'normal' physiological conditions.

Induction of LTD also promotes an activity-dependant increase in the removal of GluR2 containing AMPA receptors from a synapse, suggesting that it is their removal that is important in the subsequent loss of synaptic strength.

Several possible mechanisms for this have been suggested for both LTD induced and constitutive AMPA receptor endocytosis, with PSD-95 being cited as important in

regulating the rate of AMPA receptor removal from a synapse via ubiquitination of PSD-95 and its subsequent proteolytic degradation (Colledge et al. 2003).

Each of the mechanisms, despite having different inducers, appear to possess a similar mechanism of action, with the AMPA receptor dissociating from the synapse and undergoing dynamin-dependent endocytosis in clathrin-coated vesicles (Man et al. 2000, Lin et al. 2000). One of the mechanisms has been shown to be dependant upon Ca^{2+} influx, ironically via NMDA receptor activation, with evidence suggesting it is the subunit composition of the NMDA receptor that determines whether LTP or LTD is induced following activation, activating PP1, PP2A and calcineurin, which serve to dephosphorylate the AMPA receptor subunit in the C-terminal domain, promoting its removal from the synapse and subsequent endocytosis in a ligand-independent manner (Lin et al. 2000, Beattie et al. 2000).

With particular reference to the subunit composition of NMDA receptors involved in AMPA receptor internalization it has been shown that NR2B containing NMDA receptors promote LTD by activation of Rap1, a small GTPase that promotes activity in the p38-MAPK signalling pathway, which appears to facilitate internalisation of heteromeric AMPA receptors containing the GluR1 and GluR2 subunits. Rap2 on the other hand, promotes depotentiation of AMPA receptors containing the GluR2 and GluR3 subunits via NR2A NMDA receptor activation of the JNK signalling pathway (Zhu et al. 2005).

AMPA receptor subunits also appear to undergo ligand-promoted endocytosis, which is distinguishable from that promoted by NMDA receptor activation, with AMPA-induced endocytosis resulting in AMPA receptors being targeted to late endosomes for proteolytic degradation, and a subsequently slow recovery of AMPA receptor activity compared with those internalised following NMDA receptor activation (Ehlers 2000).

1.4 Transmembrane AMPA receptor interacting proteins (TARPs)

TARPs are a unique family of AMPA receptor interacting proteins consisting of five identified members; TARP γ2 (also known as stargazin), γ3, γ4, γ7 and γ8 (Tomita et al. 2003; Kato et al. 2007) that have some sequence homology, and are believed to be related to the γ subunit of Voltage-gated Calcium channels (Chu et al. 2001).

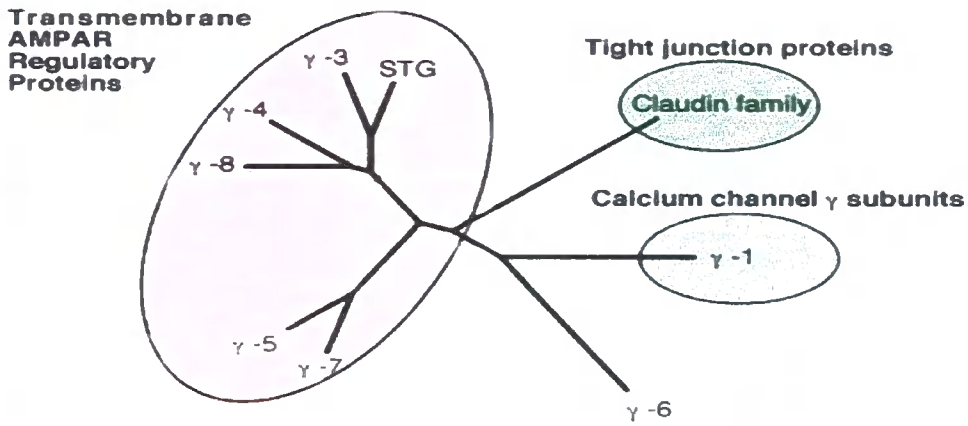

Figure 1.5: Tree diagram showing the relationship between the TARPs and other members of the CACN protein family, including the voltage-gated Ca^{2+} channel subunit γ1. Amended (Now showing that γ5 and γ7 are considered TARP proteins) from Tomita et al., 2003 The *Journal of Cell Biology.*

They consist of four transmembrane spanning regions and intracellular N and C terminals – the C-terminus of the γ2, γ3, γ4 and γ8 isoforms containing a PDZ binding motif.

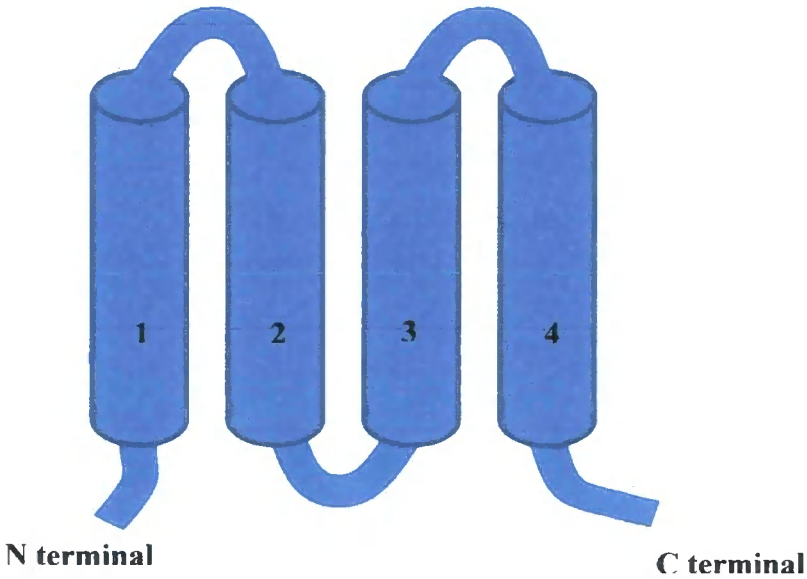

Figure 1.6: Simplified generic structure of a TARP. N and C terminals are located within the cytoplasm, transmembrane domains are highlighted (1-4). Extreme C-terminal contains PDZ binding motif.

Of the five isoforms, TARP γ2 is the most extensively studied and was the initial TARP isoform identified, primarily due to the defining of the *stargazer* mutant mouse – a model of cerebella ataxia that also experiences absence epilepsy – which was shown to possess a truncated version of the CACNγII gene that resulted in a failure to express the TARP γ2 protein. A direct consequence of this failure in TARP γ2 expression was the absence of spontaneous AMPA receptor activity detectable in cultured cerebellar granule neurones (CGNs), leading to the realisation, that rather than, as originally thought, being a neuronal homologue of the γ1 VGCC, TARP γ2 was actually involved in the expression of AMPA receptors at the cell surface. This discovery, in turn led to the identification of the other TARP isoforms of which TARP γ7 is the most recent (identified in 2008).

Whilst still being considered to be related to VGCC's, with TARP γ2, γ3 and γ4 being known to co-immunoprecipitate with both AMPA receptor subunits and the α 1B subunit of VGCCs (Black 2003), TARPs demonstrate little to no effect when expressed with

VGCCs in heterologous cells (Osten and Stern-Bach 2006), with any VGCC role being considered at best, a secondary function.

The primary role of TARPs, as their name suggests, is to be found in the nature of their interactions with AMPA receptors and the numerous functions that these interactions serve. The earliest investigation into TARPs demonstrated their ability to rescue AMPA receptor current when TARP γ2 was transfected into cultured CGNs derived from the stargazer mutant mouse (Chen et al. 2000) – a property also shared, and indeed used to identify the other TARP isoforms (Tomita et al. 2003). These studies implied two major properties of TARPs, namely to both traffick AMPA receptors to the cell membrane, and to be involved in the subsequent synaptic targeting of AMPA receptors.

The N-terminal extracellular loop of stargazin has been identified as being a domain critical for conferring the ability to traffic AMPA receptors to the cytoplasmic membrane. This was demonstrated using the γ5 subunit of the related protein family, that possesses no inherent TARP function developing these properties following domain swapping of the N-terminal extracellular loop with TARP γ2 (Tomita et al. 2004).

Whilst the precise mechanism by how TARPs are responsible for the surface trafficking of AMPA receptors is unknown, facets of their interaction have been glimpsed and important insights gained. It is known that TARP γ2 interacts with AMPA receptor subunits in the endoplasmic reticulum (ER) where the two proteins have been shown to be detectable in close proximity and whilst it is unknown at what stage of AMPA receptor assembly TARP γ2 interacts with AMPA receptors, it appears that TARP γ2 plays a role in the correct folding of AMPA receptor subunits prior to their exiting the ER (Vandenberghe et al. 2005, Ziff 2007). At the current time however, the exact ratio of TARP molecules to AMPA receptor subunits is unknown, indeed speculatively it is possible that it might even be more than one TARP isoform involved in interaction with some AMPA receptor subunit combinations. What is known however is that the interactions are sufficiently durable to warrant TARP γ2 the title of an AMPA receptor auxillary subunit – effectively present together with AMPA receptors from their exiting

the ER, their passage through the Golgi until their subsequent from the cell surface (Vandenburghe et al. 2004, Tomita et al. 2004).

It has also been demonstrated that upon exiting the ER the TARP-AMPA receptor complex interacts both with the cytosolic Golgi-preferring protein nPIST, which may be at least in part responsible for synaptic clustering (Cuadra et al. 2004), but also microtubule associating protein light chain 2 (MAP1A-LC2), which again may be important in transporting the TARP-AMPA receptor complex via the cytoskeleton both to the cytoplasmic membrane and subsequently the synapse (Ives et al. 2004).

The synaptic targeting of AMPA receptors appears to be dependant upon the C-terminal tail of the TARP isoform (Chen et al. 2000), most likely because of the PDZ motif present there, which has been shown to interact with a variety of proteins typically associated with the post synaptic density including PSD-95, PSD-93, SAP-97, SAP-102 and the afore-mentioned MAGI-2 and nPIST (Dakoji et al. 2003).

Certainly with regard to PSD-95 there is increasing evidence supporting this hypothesis. Over-expression of PSD-95 in cultured neurones shows an increased expression of AMPA receptors detectable in the synapse, with a corresponding decrease in AMPA receptor expression non-synaptically. Conversely, over-expression of TARP $\gamma 2$ whilst causing an increase in the overall surface expression of AMPA receptors does not alter the ratio of synaptic AMPA receptors to non-synaptic AMPA receptors, suggesting that in this instance, the amount of PSD-95 – an effective correlate of the size of post-synaptic density, is the limiting factor in determining the number of synaptic AMPA receptors in addition to their ratio to diffuse AMPA receptors (Bats et al. 2007).

MAGI-2 on the other hand is another post synaptic density protein possessing similar PDZ domains to PSD-95, with its interaction with TARP $\gamma 2$ being suggested by yeast two hybrid analysis. Unusually, this protein possesses several PDZ binding motifs, 3 of which (1, 3, and 5) possess the theoretical capacity to bind to TARPs, but one of these regions

(namely 5) also interacts with NMDA receptors – suggesting a direct physical link between AMPA receptors and NMDA receptors within a synapse (Deng et al. 2006).

Studies have also shown that, as is the case with AMPA receptor subunits themselves, the phosphorylation states of TARP isoforms are important in the initiation and maintenance of synaptic localisation of AMPA receptors. Phosphorylation of the TARP γ2 isoform by CAM KII and PKC – which as stated earlier are activated as a consequence of Ca^{2+} influx during NMDA receptor activation, promotes trafficking of TARP-AMPA receptor complexes to a synaptic localisation due to the phosphorylation of serines in the C-terminal tail, enhancing the complexes binding capability with PSD-95. Conversely, NMDA receptor mediated activation of phosphatases PP1 and PP2 promotes dephosphorylation of TARPs, which in turn promotes their dissociation from PSD-95 and subsequent loss from a synapse. These two processes, effectively suggest a mechanism of action for LTP and LTD respectively (Tomita et al. 2005).

The most recent studies have also demonstrated, at least for some TARP isoforms, that they have the capacity to influence AMPA receptor kinetics by at least two distinct mechanisms.

Firstly, via an interaction between the N-terminal extracellular domain and AMPA receptor subunits, TARP isoforms are able to increase the efficacy of kainate, a partial agonist of AMPA receptors expressed in heterologous cells, increasing its functional role to that of a full agonist and vastly enhancing its effects on AMPA receptor activation. These effects are dependent upon the TARP isoform present – the γ2 and γ3 isoforms having greater effects than γ4, γ7 and γ8 (Turetsky et al. 2005, Tomita et al. 2005).

Secondly, via the C-terminal domain, TARPs are capable of decreasing the rate of AMPA receptor desensitization in response to glutamate, in addition to increasing the rate of recovery from a desensitized state (Turetsky et al. 2005), again this being variable dependent upon the TARP isoform involved (Kott et al. 2007). TARPs also enhance the evoked response of AMPA receptors following application of glutamate, via what is

believed to be an allosteric mechanism that may affect the functional properties of the glutamate binding domain of the AMPA receptor (Priel et al. 2005, Tomita et al. 2006).

Perhaps more importantly considering the aim of this research project is the evidence that in addition to their effects on AMPA receptor trafficking, targeting and kinetics, TARPs can also influence the pharmacology of AMPA receptor potentiators, in the case of cyclothiazide (CTZ), an inhibitor of AMPA receptor deactivation. TARP γ2 demonstrated the capacity to not only enhance the effect of CTZ, but also lessened CTZs preference for the *flip* isoform of AMPA receptor subunits by increasing its affinity for *flop* isoforms via a currently unknown mechanism (Tomita et al. 2006).

These data demonstrating the importance of TARP-AMPA receptor interactions, highlights the potential of utilising TARP isoforms as a possible target for future pharmacological treatments, permitting modulatory effects on AMPA receptors minimising the risk usually present with compounds that interact directly upon AMPA receptors or of any non-specific interaction with KA receptors. It also, by demonstrating a known interacting protein of AMPA receptors, opens up possible avenues of investigation for other proteins that may interact with AMPA receptors indirectly.

1.5 AMPA receptors in neurological disorders

As the principle excitatory amino acid in the CNS, the importance of glutamate and its receptors is obvious. However, despite, or perhaps because of this importance the number of neurological conditions where dysfunction in the glutamatergic system was considered to be a contributory factor in disease pathology was limited.

One such condition believed to have a critical glutamatergic component is Schizophrenia, for which a glutamate hypothesis was developed in the early 1990's based upon the observation that non-competitive antagonists to the NMDA receptor were capable of eliciting schizophrenia-like symptoms in healthy individuals and could worsen

schizophrenic symptoms in those who already suffered from the condition (Hertzmann et al., 1990).

This hypothesis was expanded to include non-NMDA ionotropic glutamate receptors, most significantly AMPA receptors, which have become the current focus of study into the glutamatergic basis of schizophrenia.

Studies of human tissue have shown minimal differences between schizophrenics and non-sufferers in AMPA receptor protein and mRNA levels in a variety of brain regions, with the notable exception of the hippocampus; with the current hypothesis regarding AMPA receptor involvement in schizophrenia believed to be an abnormal function of the interacting proteins associated with the receptor (Gao et al. 2000, Woodruff et al. 2001, Beneyto et al. 2006). Obviously there are complications with approaches to treating a neurological disorder by targeting the glutamatergic system, not the least of which being excitotoxicity. As a consequence individual aspects of that system, such as the composition of the AMPA receptors in Schizophrenic patients, including the *flip/flop* variants, identified as being altered in Schizophrenics (Eastwood et al. 1997), are being examined to determine their functional significance. Using the *flip/flop* variants of the AMPA receptor subunits as an example, it is known that the expression of these variants appears to be affected by the chronic administration of anti-psychotics (O'Connor et al. 2007).

Schizophrenia is not the only neurological disorder where a glutamatergic component has been investigated, recent studies have also began to investigate the possibility of a glutamatergic component in disorders traditionally associated with different neurotransmitters and receptors, such as depression – a condition traditionally believed to be predominantly involving the serotonergic system, which was in some form or other, the most common pharmaceutical target for traditional therapeutics.

For example, there is evidence that acute stress and chronic affective disorders, including depression, can elicit several neurological responses that affect the glutamatergic aspect

of neurotransmission, with acute stress and chronic stress having different effects and requiring different treatments. Acute stress can cause the impairment of LTP (Watanabe et al. 1992) and the disruption of signalling pathways in the CNS in favour of others. A prevalent example of this is the disruption of the hippocampal-frontal cortical and hippocampal-amgdala pathways that are disrupted following severe acute stress, whilst the amygdala-frontal cortical pathway is unaffected. This can have effects on memory formation, particularly the emotional context, although it can be prevented by the administration of tianeptine, an antidepressant with effects on AMPA receptors.

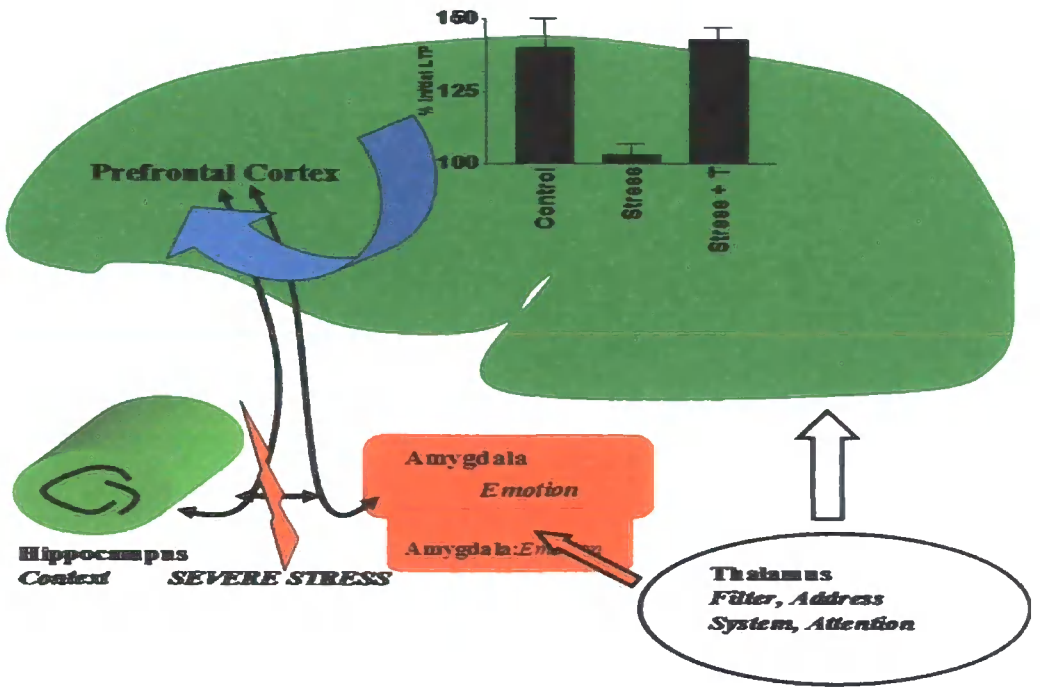

Figure 1.7: Diagram showing the effect of acute stress on neuronal signalling pathways and its reversal by tianeptine. *Kindly provided by Michael Spedding.*

Chronic stress can lead to several morphological changes within the CNS, particularly within the hippocampal formation, with dendritic atrophy and decreased neurogenesis being predominant features, this in turn decreases total hippocampal volume. Antidepressants can also reverse this loss of arborisation following chronic administration of treatment, which also alters the pharmacological properties of the regions of the CNS that had been aberrant as a consequence of the chronic depression,

primarily the hippocampal formation. There is also evidence that the administration of antidepressants alters the expression of AMPA receptor subunits within the regions of effect (Martinez-Turrillas et al. 2002, Martínez-Turrillas et al. 2005).

Tianeptine is not the only antidepressant compound possessing effects on AMPA receptors, in fact there is an increasing number of antidepressant drugs that either possess effects on AMPA or display enhanced potency following administration of AMPA receptor modulators (Lia X et al. 2002). These discoveries have led to an increase in the investigation of chronic and acute application of antidepressants on the proteins downstream of glutamatergic signalling pathways.

An early observation made following the chronic application of antidepressants was the upregulation of Brain derived neurotrophic factor (BDNF) (Coppell et al. 2003), a trophic agent present in the CNS that has since been shown to have important effects both in neuroprotection, but also in neurogenesis. Such is the importance of BDNF, that it has been attributed to being a protein lynchpin in the treatment of depression, with the upregulation of BDNF seemingly being essential to limit neuronal atrophy and loss of dendritic arborisation typically associated with chronic exposure to stress, such as that in seen in depression. This upregulation of BDNF in response to chronic antidepressant administration occurs predominantly in the hippocampus, one of the areas most affected by depression and chronic stress, which when coupled with the restoration of neurogenesis and neuronal architecture, is compelling evidence supporting the importance of BDNF in both the treatment of depression, but also alluding to the importance of BDNF in the healthy brain.

This importance of BDNF in the treatment of depression appears to underlie the importance of AMPA receptors within the condition, with increased phosphorylation of AMPA receptors, as a consequence of restored/enhanced LTP, seemingly being linked to an increase in BDNF expression within the hippocampus in particular. Indeed, some AMPA receptor modulatory compounds, the AMPAkines, possess compounds that

promote the upregulation of BDNF when used as an antidepressant treatment, suggesting that modulation of AMPA receptors influences BDNF expression (Mathew et al. 2005).

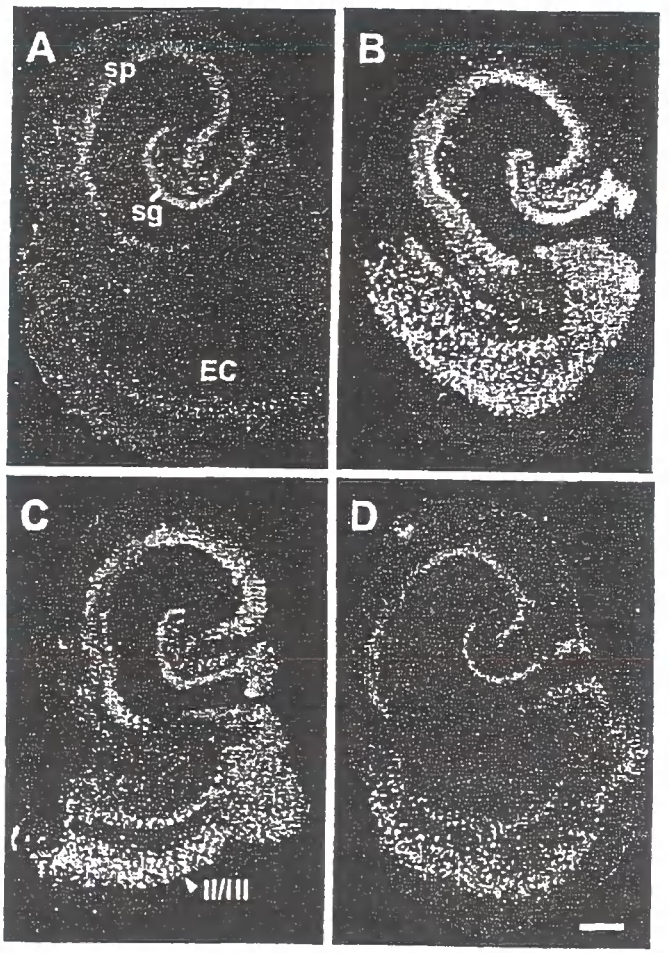

Figure 1.8: Changes in BDNF mRNA expression in the hippocampus following administration of AMPAkines.

Slide A is the control following no administration of AMPAkines. As can be seen the AMPAkines enhance BDNF mRNA levels significantly following application, suggesting AMPA receptors influence BDNF expression.

Provided c/o M. Spedding, personal communication.

It has also been observed that application of antidepressants has several secondary effects, notably on glutamatergic neurotransmission, such as the restoration of LTP and reversal of dendritic atrophy (Shakesby et al. 2002).

This of course has implications in other disorders, such as dementia, with both synaptic LTP and the hippocampus being believed as being integral to cognition, learning and memory, and modulators of AMPA receptors (AMPAkines) have been shown to have effects enhancing cognition, making them a potential pharmaceutical agent to treat the symptoms of dementias (Francis 2008). However, with dementia being predominantly a neurodegenerative condition as opposed to a 'mood disorder', which, as will become apparent in section 1.6 is the primary area of clinical relevance promoting the work undertaken in this PhD, outlining the glutamatergic component of dementia would disrupt the narrative of the thesis, so it must be excluded from any elaborate consideration.

Interestingly, the mechanism of action for AMPAkines reveals that they bind to the S1S2 domain of the GluR2 subunit (Jin et al. 2005), which is the same site of action for tricyclic antidepressants (Stoll et al. 2007).

1.6 AMPA receptors and the Serotonergic nervous system

With the primary focus of historical antidepressant treatments being on the serotonergic nervous system, predominantly in the form of selective serotonin reuptake inhibitors such as Fluoxetine, the increasingly apparent influences of AMPA receptor modulators on antidepressant function and emerging significance of AMPA receptor interacting proteins in the treatment of depression logically opens a vein of investigation regarding potential interactions between serotonergic neurones and glutamatergic neurones.

The serotonergic nervous system utilises the neurotransmitter serotonin (5-hydroxy-tryptamine – 5HT) as its primary neurotransmitter and possesses a diverse variety of receptors sensitive to serotonin.

There are seven subdivisions of 5HT receptors, with at least 13 known subtypes of 5HT receptor divided across the seven subdivisions with $5HT_{1A\text{-}F}$ (minus $5HT_{1C}$ which was renamed $5HT_{2C}$), $5HT_{2A\text{-}C}$, $5HT_{3A\text{-}C}$, $5HT_4$, $5ht_{5A}$, $5ht_{5B}$ $5HT_6$, $5HT_7$. The $5ht_{1E}$ and $5ht_5$

receptors use lower case naming due to an absence of any identified functional role. (Marsden et al. 1989, Hoyer et al. 1994, Hannon and Hoyer 2008).

Figure 1.9: Table of 5HT receptors (Roth et al. 1998, Hoyer et al. 2002, Hannon and Hoyer 2008).

Receptor Name	Receptor Class and Effector	Distribution and Function
$5HT_{1A}$	GPCR - $G_{i/o}$	Located in the CNS, peripheral nervous system and gastrointestinal tract. Concentrated in limbic regions of CNS. Several functions, prominently as inhibitory autoreceptors.
$5HT_{1B}$	GPCR - $G_{i/o}$	Negatively coupled to cAMP. Present in the CNS, particularly the basal ganglia, where it displays inhibitory effects. Also present in vascular tissue throughout the body, with exact functional role unknown but suspected to be functionally 'silent' until vascular dysfunction, such as atherosclerosis.
$5HT_{1D}$	GPCR - $G_{i/o}$	Very similar to $5HT_{1B}$ in function. Expressed at very low levels in the CNS, also detectable in other tissues, including the heart.
$5ht_{1E}$	GPCR - $G_{i/o}$	Detected in human frontal cortex, speculated to be negatively coupled to adenylate cyclase.
$5HT_{1F}$	GPCR - $G_{i/o}$	Detected in the CNS, very similar to $5HT_{1B/1D}$ receptors. Believed to have a

		role in migraine.
$5HT_{2A}$	GPCR - $G_{q/11}$. May couple to $G_{12/13}$	Expressed in the CNS. Highest levels in brain stem nuclei, moderate levels in the striatum and basal ganglia. Also located in smooth muscle and on blood platelets.
$5HT_{2B}$	GPCR - $G_{q/11}$. May couple to $G_{12/13}$	Located in the predominantly in the stomach fundus, also located in the gastrointestinal tract, heart, kidneys, lungs. Possibly present in the brain. Also found in vascular tissues.
$5HT_{2C}$	GPCR - $G_{q/11}$. May couple to $G_{12/13}$	Located exclusively in the CNS, predominantly in the choroid plexi, but also expressed in limbic structures. Large potential for extensive RNA editing, with different edits linked to various neurological disorders.
$5HT_{3A}$	Ligand-gated ion channel	Expressed in the CNS, but displays low levels of expression in the forebrain. Linked to the dorsal motor nucleus of the vagus nerve, with $5HT_{3A}$ antagonists displaying antiemetic effects. Also present in the gastrointestinal tract and peripheral nervous system.
$5HT_{3B}$	Ligand-gated ion channel	Similar expression to $5HT_{3A}$ receptors, unkown function.
$5HT_{3C}$	Ligand-gated ion channel	Not currently known.
$5HT_4$	GPCR - G_S	Promotes cAMP production. Located

		in the CNS, gastrointestinal tract, heart and peripheral nervous system. Precise function is unknown, but some influence on hippocampal LTP and LTD in the CNS.
$5ht_{5A}$	GPCR – $G_{i/o}$	Not currently defined, some evidence of expression within the CNS.
$5ht_{5B}$	GPCR - Unknown	Not currently defined.
$5HT_6$	GPCR - G_S	Only currently identified in the CNS, seemingly linked to cholinergic neurotransmission.
$5HT_7$	GPCR – G_S	Seemingly expressed in the CNS and vascular smooth muscle.

As can be seen, the $5HT_2$ receptors are predominantly neuronal, with $5HT_{2A}$ receptors and $5HT_{2C}$ receptors being expressed in the CNS, the latter exclusively (Abramowski et al. 1995, Backstrom et al. 1997).

The interactions between $5HT_2$ receptors and AMPA receptors in the CNS as a whole however, are poorly documented, but there is emerging accumulation of evidence of functional interactions in at least some brain regions, regulating specific neurological and physiological processes. The bulk of this work has so far focused upon the AMPA receptor mediation of $5HT_{2A}$ receptors (Zhang and Marek 2008) and 5HT release in the forebrain (Pittaluga et al. 2007).

There is also evidence of the reverse – mediation of AMPA receptor activity by 5HT receptors (Pinilla et al. 2001, Bouryi and Lewis 2003), with this modulation of AMPA receptor activity seemingly occuring throughout a diverse range of CNS regions, but predominantly involves particularly $5HT_{2A}$ receptors, which have been shown to co-localise with the GluR2 AMPA receptor subunit (Peddie et al. 2008).

One such system where evidence of interplay between serotonergic and glutamatergic neurotransmission has been suggested but is increasingly becoming evident is in locomotor pathways, including the sensory transmission to reticulospinal neurones within the brainstem, where 5HT activity depresses the transmission at glutamatergic synapses (Antri et al. 2008).

Other evidence identifies a direct link between decreased AMPA receptor density and depleted 5HT expression during development, with a potential implication upon autism (Boylan et al. 2007).

Both of the CNS-based $5HT_2$ receptors - the $5HT_{2A}$ and the $5HT_{2C}$ receptors are predominantly involved in the stimulation of phospholipase C and subsequent increase in inositol 1, 2, 3 triphosphate (IP_3), which ultimately leads to an increase in intracellular Ca^{2+} (Lucaites et al. 1996). Whereas $5HT_{2A}$ receptors frequently have excitatory effects on neurotransmission, the predominant influence of $5HT_{2C}$ receptors appears to be inhibitory, via the excitation of GABAergic interneurones (Liu et al. 2007, Boothman et al. 2008), with some excitatory effects in specific brain regions (Gajendiran 2008).

This study focuses on the $5HT_{2C}$ receptor, a subtype of 5HT receptor that is exclusively expressed within the CNS and is important in the serotinergic-based treatments of depression, with $5HT_{2C}$ receptor agonists alleviating depressive effects in animal models (Moreau et al. 1996). Conversely, fluoxetine, a well established SSRI, displays antagonism of the $5HT_{2C}$ receptor (Giorgetti and Tecott 2004). Regardless of the precise mechanism though, this receptor subclass appears to possess significance in depression in humans as signified by the behavioural differences induced by polymorphisms (Lerer et al 2001). It is this clinical relevance that supports the investigation of the $5HT_{2C}$ receptor subtype with the overall aim of investigating the possibility of a link with AMPA receptors that could identify suitable targets for future antidepressants.

Unusually, $5HT_{2C}$ receptor knockout mice have not been investigated for any effects of their phenotype on depression, but have been shown to demonstrate enhanced exacerbation of diet induced obesity (Wang and Chehab 2006), indeed, there seems to be an association between $5HT_{2C}$ receptors and weight regulation especially following anti-psychotic treatment, with polymorphisms in the $5HT_{2C}$ receptor gene, and indeed, knockouts, displaying obesity (Buckland et al. 2005, De Luca et al. 2007).

There is also evidence of $5HT_{2C}$ receptor regulation of sleep, with $5HT_{2C}$ receptor knockouts exhibiting enhanced responses to sleep deprivation and other sleep defects, including increased wakefulness (Frank et al. 2002).

Gavarini et al. (2004) speculated upon the possibility of $5HT_{2A/2C}$ receptors interacting with AMPA receptors to promote AMPA receptor recruitment to silent synapses within nociceptive pathways within the spinal cord; the recruitment process most likely incorporating interactions between $5HT_{2A/2C}$ receptors and a PDZ protein – such as PSD-95 – facilitating functional interactions with AMPA receptors via TARPs.

This information enabled the generation of three primary hypotheses to be investigated by this project:

- $5HT_{2C}$ receptors possess a physical interaction with AMPA receptors via TARPs and an intermediate PDZ protein such as PSD-95.
- $5HT_{2C}$ receptors possess a functional interaction with AMPA receptors that incorporates TARPs
- TARPs have a number of potential interacting protein partners within the CNS and a more multifaceted role than previously supposed.

To test these hypotheses, a series of experimental techniques, including but not limited to generation of novel immunological probes to investigate and immunopurify TARPs and

their interacting proteins from native CNS tissues with an intention to classify the distribution of TARPs and identify previously unknown interacting protein partners.
In parallel will be studies using experimental animals possessing altered $5HT_{2C}$ expression within the forebrain, where the novel immunological probes will enable the physiological consequences of these experimental conditions upon AMPA receptor and TARP expression can be identified.

Ultimately these studies will provide some evidence regarding the nature of the interaction between $5HT_{2C}$ receptors and TARPs, but will also provide evidence of the role of TARPs in the context of other interacting proteins other than AMPA receptors.

Chapter 2: Materials and methods

Please note that unless otherwise stated all solutions mentioned in this chapter are detailed in Appendix A

2.1 Animals

Wild-type (C3B6Fe+, +/+) and heterozygous (C3B6Fe+ , +/stg) were derived from heterozygous breeding pairs originally obtained from The Jackson Laboratory (Bar Harbor, Maine, USA) but were the culmination of a breeding/maintenance programme at the Durham University that has continued in excess of 5 years. Both the homozygous wild-type and heterozygous derived brain tissue was combined and subsequently referred to as control material.

Stargazer mutant mouse material (C3B6Fe+, stg/stg) was obtained from the same animal populations as the control material.

These mice were maintained in the Life Sciences Support Unit (LSSU), University of Durham. All animals had unlimited access to food and water and were maintained on a 12 hour light/dark cycle.

For the $5HT_{2C}$ receptor over-expression and knock-down data, C57/Bl6 background strain mice were used. The mice were maintained at the University of Edinburgh Animal House. The $5HT_{2C}$ receptor over-expressing mice were transgenic, with the $5HT_{2C}$ receptor cDNA being co-inserted with a CAMKII promoter, causing confirmed increased expression of $5HT_{2C}$ mRNA in the frontal cortex as well as some locomotor and other phenotypic effects associated with abnormal $5HT_{2C}$ receptor expression.

The $5HT_{2C}$ receptor knockdown mice were derived from several generations subsequent to an original C57/B6 cross with mice containing a forebrain-specific TetA binding site containing $5HT_{2C}$ receptor gene. This enabled inactivation of $5HT_{2C}$ receptor expression

within the forebrain via the addition of doxycycline in the drinking water, causing decreased $5HT_{2C}$ receptor mRNA expression in the forebrain and phenotypic effects.

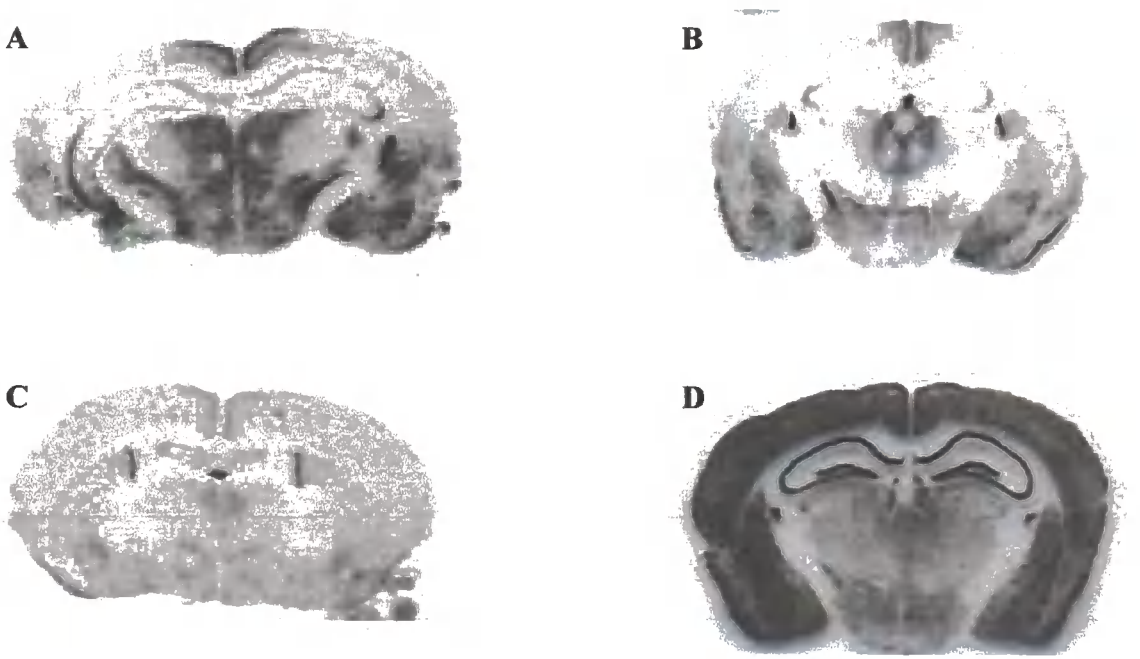

Figure 2.1 *In situ* hybridisation data showing $5HT_{2C}$ mRNA levels within the forebrain of mice with altered $5HT_{2C}$ receptor expression and their relevant controls. *Provided by Megan Holmes*

Images A and B show the $5HT_{2C}$ receptor mRNA levels in the control mice, with A being the relevant control for the $5HT_{2C}$ receptor knockdown mice and B being the relevant control for the $5HT_{2C}$ receptor over-expressing mice.

Images C and D show the $5HT_{2C}$ receptor mRNA levels in the mice with altered $5HT_{2C}$ receptor expression. C shows the $5HT_{2C}$ receptor mRNA levels in the knockdown mice, whilst D shows $5HT_{2C}$ receptor mRNA levels in the $5HT_{2C}$ receptor over-expressing mouse.

Male New Zealand white rabbits were obtained from Charles Rivers (UK)
The rabbits were maintained in the Animal Unit at the University of Sunderland

All animal husbandry, breeding and experimental procedures, at all sites, was performed in accordance with the Animals (Scientific Procedures) Act 1986.

2.2 Generation of TARP isoform-specific antibodies

It was initially decided that at least one antibody should be generated for each of the TARP isoforms currently known, namely; γ2, γ3, γ4, and γ8.

Antibody generation utilised the generation of an antigenic peptide sequence taken from each of the individual TARP isoforms, with the exception of the TARP γ2 sequence (as used in Ives et al 2004), all of the TARP peptide sequences selected were novel in the generation of antibodies. The antigenicity of the whole peptide sequence was analysed by the ANTHEPROT package designed to predict protein antigenic properties (Parker et al. 1986), with these data being contrasted to the peptide sequence to find regions that were not within a transmembrane domain and not conserved between TARP isoforms, yet displayed antigenic properties.

TARP γ3: Peptide Sequence C-HSELLKKSTFARL
TARP γ4: Peptide sequence MHDFFQQLKEGFHVS-C
TARP γ8: Two antibodies were generated – one directed to the N-terminus, the other to a region of the proximal C-terminal domain (hereafter referred to as TARP γ8N and TARP γ8C respectively). N-Terminal sequence MESLKRWNEERGLW-C
Proximal C-terminal sequence RGSSAGFLTLHNAFP-C

All of the peptide sequences were subjected to the addition of a terminal cysteine residue for utilisation of sulphide bonding in the subsequent coupling of the peptide to the carrier protein, Keyhole Limpet Haemocyanin (KLH).

2.3 Rabbit immunisation protocol.

2.3.1 Peptide conjugation

Imject® Malemide activated mcKLH kit. For each of the peptides five mg of appropriate peptide was dissolved in 300µl of the conjugation buffer supplied in the kit. This dissolved peptide solution was immediately mixed with the 10mg/ml mcKLH provided in the kit (i.e one vial of mcKLH dissolved in 200µl of dH_2O), and left to incubate for two hours at room temperature.

After the two hour incubation, EDTA was premoved from the peptide/mcKLH solution using the desalting columns provided in the kit using the following protocol:

- Initially one bottle of purification buffer salts was dissolved in 60 ml dH_2O, with each desalting column being washed with 15 ml (three column volumes) of the reconstituted purification buffer.
- Following the washes, the conjugated peptide solution was added to the desalting column.
- The conjugated peptide solution was then pushed through the column by 10 aliquots of purification buffer, added in 0.5ml volumes, with each 0.5ml fraction passing through the column being kept individually.
- The absorbance at 280nm of each collected fraction was measured, with the conjugated peptide being located in fraction with the first absorbance peak, plus any subsequent fractions tied in to that peak.
- The peak fractions containing the conjugated peptide were kept at -20°C for long-term storage.

2.3.2 Immunisation protocol

The conjugated peptides were used for the inoculation procedure. For the initial inoculation 300µl of conjugated peptide was mixed with 300µl of Freund's complete adjuvant, giving a 1:1 ratio. The mixture was then forcibly expelled and repeatedly taken

up into a glass syringe until an emulsion was formed. The emulsions were stored at 4^0C overnight to determine whether the peptide and adjuvant remained in emulsion, and if suitable, were used that morning for inoculation.
Two male New Zealand rabbits were selected and inoculated intra muscularly with 100µl of their specific peptide/adjuvant, and then monitored by the animal unit staff in case of an adverse reaction.

Subsequent inoculations occurred four weeks after the previous inoculation, but with the exception of the initial inoculation, utilised Freund's incomplete adjuvant. This was prepared in the same manner as the complete adjuvant – namely 300µl of conjugated peptide being emulsified with 300µl of incomplete adjuvant, left over night, and then 100µl of the emulsion being administered.

The only notable difference in the procedure was the subsequent inoculations being administered to alternate hind legs, ensuring the animal never received an injection into the same limb as the injection both previous and subsequent to it.

2.3.3 Collection of blood from rabbits

Immediately prior to the initial inoculation 10 ml of blood was collected from each rabbit using an ear-bleed procedure. This blood was used as a pre-immune control sample in future ELISAs.

Subsequent collection of blood was conducted 10 days post inoculation, again via an ear bleed procedure, allowing collection of up to 10ml of blood.

One from each pair of rabbits was subjected to terminal exsanguination instead of the usual ear bleed after the fourth inoculation, with the blood being collected using a cardiac puncture protocol conducted by the animal unit staff at the University of Sunderland.

The remaining rabbits were subjected to terminal exsanguination following the fifth inoculation.

Blood samples collected were stored at 4°C for transport.

2.3.4 Isolation of sera

Blood samples were incubated at 37°C for 30 minutes, before having the inside of their falcon tubes scraped with a glass Pasteur pipette to promote detachment of any formed clot, and also to ensure that any further clotting would not adhere to the tubing. The samples were then stored over night at 4°C.

The following day the blood clots were removed from their respective tubes and discarded. The sera was aliquoted into 1.5ml eppendorf tubes and centrifuged at 14,000 G for 5 minutes using a micro-centrifuge, to ensure any remaining red blood corpuscles, and other detritus could be separated from the serum.

Following centrifugation, the supernatant sera was carefully collected and aliquoted to fresh 1.5ml eppendorf tubes, a 500µl aliquot of each was prepared for use in ELISA's, but like all the samples, was flash-frozen in liquid nitrogen and stored at -20°C.

2.4 Purification of antibodies from inoculated rabbits.

2.4.1 Generation of peptide columns for purification of antibodies from serum.

The equipment used to generate the peptide columns was the PIERCE sulfolink kit (product number 44895 – now discontinued) purchased from PIERCE Biotechnology. The kit is a self-contained source of all the materials required to perform five immobilization reactions using terminal sulfhydryl groups on the proteins/peptides of choice.

The protocol used, was exactly as described in the instruction booklet provided. Outlined below in relation to how the kit was used for this project (unless stated otherwise, all buffers/items were taken from the kit). Peptides were coupled individually with the protocol being completed for a single peptide before commencing the next peptide;

- 5mg of each of the TARP isoform peptides were dissolved in separate 1.5ml eppendorf tubes containing 1ml of the sample buffer provided by the kit.
- This peptide solution was then added to the vial containing the reducing agent to produce a final concentration of 50mM MEA in the mixture and incubated for 1.5 hours at 37°C
- Towards the end of the incubation the top and bottom caps were removed from the desalting columns provided, and the column was equilibrated with 20ml of coupling buffer equivalent to 4 column volumes.
- The peptide/reducing agent mixture was allowed to cool to room temperature then applied to the equilibrated desalting column to remove excess reducing agent.
- After the mixture had been added to the desalting column, 3ml of coupling buffer was applied, with the 3ml of solution that flowed through the column being collected in 1ml fractions, with the fraction with the peak absorbance at 280nm being used for production of the peptide column.
- Equilibrate the sulfolink column with four column volumes of coupling buffer.
- Replacing the caps, add the reduced peptide, and incubate at RT for 45 minutes, mixing gently for the first 15 minutes.
- Drain solution (absorbance of which can be read to determine coupling efficiency) and wash column with three column volumes of coupling buffer.
- Block by incubation for 45 minutes with 2ml of coupling buffer containing 0.05M L-Cysteine, again with agitation for the first 15 minutes of the incubation.
- Column was then washed with 6 column volumes of wash solution, and subsequently equilibrated using the lab stock of phosphate buffered saline (PBS), with the storage solution being PBS 0.05% (w/v) sodium azide.

2.4.2 Serum purification

The purification of sera from each rabbit was conducted in a manner based upon the protocol outlined by Ives et al (2002).

Using the peptide columns generated, 3ml of isolated serum was thawed and added to the peptide column generated using the same peptide. The column itself was connected to a peristaltic pump to ensure continual circulation of the serum, and also to prevent the column from drying. This was conducted overnight at 4°C.

The following day, the pump was disconnected and the flow-through collected and flash-frozen before being stored at -20°C. The peptide column itself was washed with 6 column volumes of PBS and after the wash had passed through the column, the purified antibody was eluted by the addition of 8ml of Glycine buffer pH 2.5, and collected in 1ml fractions that were neutralised by 1M Tris. The absorbance of each fraction was measured at 280nm, and the fractions with the highest absorbance were pooled for dialysis.

2.4.3 Preparation of dialysis membrane.

The dialysis membrane used for the dialysis of the generated antibodies possessed a 12,000 - 14,000 dalton molecular weight cut off point. It was prepared for use by placing into a solution of 1mM EDTA, 2% (w/v) $NaHCO_3$ and brought to boil for 10 minutes. After these initial 10 minutes, the tubing was removed from the first solution, rinsed briefly in de-ionised water, and transferred to a second beaker containing 1mM EDTA, 2% (w/v) $NaHCO_3$ and brought to boil for another 10 minutes.

Once these 10 minutes had elapsed, the tubing was rinsed thoroughly in de-ionised water and placed into a beaker of dH_2O 0.05% $NaNO_3$ for storage at 4°C.

When used to dialyse the antibody samples, the dialysis tubing was removed from its storage solution, rinsed in de-ioinsed water, and then, once sample had been added, tied and clamped at both ends. The solution used for dialysis, which is what ultimately the antibodies were stored in, consisted of PBS 0.05% $NaNO_3$.

2.4.4 ELISA protocol

ELISA's were used to determine the antibody titre of each bleed from each rabbit, to provide some form of indication as to the quality of the antibody production, but also to aid with determining at which time point the rabbits should be terminated. The generalised protocol was the same for each of the bleeds/rabbits.

Half of a 96 well plate was incubated overnight at 4°C containing 100µl of sodium bicarbonate buffer pH 9.5 containing peptide at 1 µg/µl. The other lanes were incubated overnight at 4°C with just the bicarbonate buffer without the peptide to serve as the blank for each bleed concentration.

On the second day, each well was washed three times with 200µl of PBS/0.25% (w/v) gelatin, with each wash being removed immediately after it had been added to every well on the plate. A fourth wash was then added and left to block the wells whilst the plate wash incubated at 37°C for 45 minutes.

Following the 45 minutes blocking step, the wells were aspirated and the appropriate sera/purified antibody was added, in semi-log dilutions down each column, with row A being the most concentrated, right down to row H with the most dilute samples. The plate was then incubated overnight at 4°C to facilitate antibody binding.

Following overnight incubation with the primary antibody each well was washed three times with 200µl of PBS/0.25% (w/v) gelatin (as per the previous day), with a fourth wash being left incubating in the wells for 10 minutes.

Once the 10 minutes were over, the wellplate was aspirated and 100µl of HRP-conjugated secondary antibody (in the case of every experiment described in this thesis anti-rabbit IgG) diluted in the PBS/0.25% (w/v) gelatine was incubated in each well for 90 minutes at 37°C.

Following the 90 minute incubation with the secondary antibody the well plate was aspirated and then washed four times with 200µl of PBS/0.25% (w/v) gelatine, before a fifth wash of 200µl of PBS.

After the PBS wash, each well was incubated with 100µl of substrate (4mM O-phenylanine diamine, 0.02M citric acid, 25mM di-sodium hydrogen orthophosphate, at pH 5, with 10µl of hydrogen peroxide being added to the substrate solution immediately prior to its addition to the wellplate.

The wellplate was then stored in the dark for five minutes, or until any wells in the blank half started to turn yellow.

Reaction was stopped by adding 50µl of dH_2O/20% (v/v) sulphuric acid, with the absorbance of each well being measured at 490nm.

2.4.5 Cardiac perfusion

Mice were terminally anaesthatised with pentobarbitone and tested for hindleg reactions, blinking reflexes. Once unresponsive the animals were placed on a dissectiong tray and the fur of the abdomen and thorax removed. A small incision was made in the abdominal wall, enabling access to the chest cavity, which was opened by incision across the rib cage exposing the heart and lungs. The front of the chest was clamped open and away from the main body, whilst a hyperdermic needle attached to a peristaltic pump inserted into the left ventricle. A small incision was made to cut the right atrium, then the peristaltic pump activated, initially pumping ice-cold PBS 0.01% (w/v) Sodium nitrite into the circulatory system for at least 10 minutes, during which time the liver, lungs and

internal vasculature was observed to determine clearance of the blood. This technique was used both for preparing tissue for dissection with a vibromicrotome, but also for perfusion-fixation for immunohistochemistry.

2.5 TARP distribution mapping

2.5.1 Tissue dissection for subsequent solubilisation

Age and gender-matched C3B6Fe^{+} wild-type (both +/+ and +/stg) and stargazer (stg/stg) mice were selected in batches of three and individually injected with a terminal dose of anaesthetic before being subjected to cardiac perfusion with ice cold PBS/0.1% sodium nitrite (w/v) containing the following protease inhibitors; Aprotinin (2 μg/ml), Leupeptin (1 μg/ml), and Pepstatin A (1 μg/ml).

The brain was then extracted from the skull and stored in ice, whilst the cerebellum from each mouse was dissected out and flash frozen. Also the spinal column was extracted from each mouse and stored in ice until the spinal cord could be readily extracted. The brains themselves were cut into 200 μm coronal sections using a vibrotome containing a bath ice-cold of PBS/0.1% (w/v) sodium nitrite and were subsequently dissected using a light microscope at 4°C.

From each of the sections the cerebral cortex, hippocampus proper, dentate gyrus, striatum, and thalamus were dissected individually. Samples from each of the three mice were pooled together because the dissections occurred simultaneously, with the pooled tissues, in addition to the cerebella and spinal cords, flash frozen and stored at -80°C until solubilisation.

2.5.2 Tissue solubilisation for TARP distribution mapping.

Tissues collected were homogenised and solubilised for 30 minutes at room temperature in 500 µl of solubilising buffer (2% (w/v) SDS, 50 mM Tris, 2 mM EDTA). All solutions contained protease inhibitors; Aprotinin (2µg/ml), Leupeptin (1 µg/ml) and Pepstatin A (1 µg/ml). After solubilisation the tissues were centrifuged at 14,000 G for 10 minutes, following which the supernatant was collected, aliquoted, and flash frozen for storage at -80°C.

2.6 Generic techniques common for all immunoblotting preparations

2.6.1 Chloroform-methanol precipitation

The chloroform-methanol precipitation used for the preparation of samples for SDS-PAGE in this thesis was the standard protocol established in the literature (Wessel D, Flügge UI 1984, Duggan *et al.*, 1991).

To summarise: Up to 100µl (one volume) of sample was placed into a 1.5ml eppendorf tube, to which four volumes of methanol was added and the mixture vortexed briefly. Following vortexing, one volume of chloroform was added to the sample/methanol mixture, and again, this mixture was vortexed briefly. Immediately after, three volumes of dH_2O were added to the mixture, the sample was vortexed briefly then subjected to centrifugation on a table-top centrifuge at 14,000 G for two minutes.

Following centrifugation, three layers were detectable. Using a pipette, the uppermost layer was largely aspirated, and discarded. To the remainder of the mix, three volumes of methanol was added, and the sample gently tapped to mix the layers, before being subjected to centrifugation, again at 14,000 G for two minutes.

After this second period of centrifugation, all of the supernatant was aspirated and discarded, and the pellet was dried in a vacuum desiccator.

Once dry, the pellet was re-suspended in 2X SDS-PAGE sample buffer and heated to 95°C for five minutes, before being centrifuged at 14,000 G and either loaded onto an SDS-PAGE gel, or frozen for storage at -20°C.

2.6.2 Immunoblotting

Samples for immunoblotting were subjected to SDS-PAGE (Summers et al. 1965, revised as outlined Thompson et al. 1998) using 10% (v/v) acrylamide resolving gels prepared between alumina and glass plates suitable for use in a Hoefer Mighty Small II vertical slab gel electrophoresis unit. The plates and the spacers used were pre-rinsed with 100% ethanol and subsequently acetone prior to use, with the resolving gels prepared in batches of 1 l and stored at 4°C in running gel buffer diluted 1:3 with dH_2O.

For sample loading a 3.5% acrylamide stacking gel was prepared and set above the resolving gel with a 0.75mm 10 well comb being placed into the mixture prior to it setting. Once the stacking gel had set, the gels were immersed in 1X electrode buffer and the samples loaded into the wells using a $1cm^3$ Hamilton syringe. Pre-stained protein standards of known molecular weights (range 10-250 kDa) were also loaded.

For CNS tissues 10µg of protein was loaded in a volume of 10µl of 2X SDS-PAGE sample buffer effectively at 1µg/µl final concentration. The protein concentration was calculated using the Lowry Protein Assay (Lowry et al 1951).

For all controls and antibody characterisation where TARP transfected HEK293 cells were used HEK293 samples were of an unknown final protein concentration, with 100µl of cells taken from stock and resuspended in 100µl of 2X SDS-PAGE sample buffer making their final concentration much higher than 1µg/µl

For the immunoblots where $5HT_{2C}$ receptor expressing cells or their respective controls CHO cells transfected with either empty vector (M) were provided by Servier and were prepared by initially diluting 1 in 4 with PBS. 100µl of these diluted cells were then

subjected to Chloroform-methanol precipitation and subsequent re-suspension in 100µl of 2X SDS-PAGE sample buffer, of which 10µl was loaded per lane.

Once all samples were loaded, electrophoresis was conducted at 80V until the samples entered the resolving gel, and at 100V subsequent.

The completed SDS-PAGE gel was subjected to protein transfer onto nitrocellulose using a Hoefer TE series transphor unit set at 50V for two hours, whilst suspended in 1X transfer buffer. Cassette set-up was as recommended for the equipment, with care taken to eliminate any air bubbles.

2.6.3 Antibody labelling of immunoblots

Nitrocellulose containing the protein samples was blocked for 1 hour at room temperature in ~50ml of blocking buffer prior to overnight incubation in a 50ml Falcon tube containing primary antibody in 3ml of incubation buffer.

Antibody concentrations used for immunoblots:

- TARP γ2 = 0.5 µg/ml
- TARP γ4 = 2 µg/ml
- TARP γ8C = 0.5 µg/ml
- GluR1 = 1 µg/ml commercial antibody from Cambridge Research Biochemicals
- GluR2 = 1 in 500 dilution of commercial antibody purchased from Santa Cruz Laboratories
- $5HT_{2C}$ = Mouse and goat raised antibodies were used at a 1 in 250 dilution of the stock solution, again both were commercial antibodies purchased from Santa Cruz Laboratories
- PSD-95 = 1 in 1000 dilution of stock solution, commercial antibody purchased from Abcam

- β-Actin = 1 in 5000 dilution of commercial mouse monoclonal antibody, purchased from Sigma

Subsequent to overnight incubation the nitrocellulose was washed three times with 15-20ml of wash buffer in five minute wash steps, before being incubated with the appropriate horse radish peroxidase-linked secondary antibody for 1 hour at room temperature on rollers.

Secondary antibody concentrations

- Rabbit = 1 in 1000 dilution of commercial antibody, purchased from Amersham Life Sciences
- Mouse = 1 in 1000 dilution of commercial antibody, purchased from Amersham Life Sciences
- Goat = 1 in 5000 dilution of commercial antibody, purchased from Amersham Life Sciences

After incubation with the secondary antibody, nitrocellulose was washed five more times; the initial three times with wash buffer and the final two with PBS.
After washes the nitrocellulose was dried and labelled with diluted HRP-linked antibody to identify the protein standards and consequently the molecular weights.

The nitrocellulose itself was subjected to enhanced chemiluminescence utilising incubation in 1.25M luminol, 68mM p-coumaric acid (dissolved in DMSO) and hydrogen peroxidase for one minute, with subsequent exposure to ECL hyperfilm (Amersham) being of variable timings determined by the primary antibody. Film was developed manually using Kodak GBX fixer and developer solutions.

The subsequent bands on the film were analysed using Image J to quantify the intensity of labelling compared to the background.

2.7 Immunohistochemistry

2.7.1 Perfusion of tissue for immunohistochemistry

Protocol followed the cardiac perfusion as outlined earlier, however, after clearance with the PBS 0.01% (w/v) sodium nitrite, the tissue was perfused with ice-cold fixative solution. The needle was held in place for 10 minutes until the heart was sufficiently fixed to clamp the needle in place and left for 20 minutes post-clamping, for a total fix time of 30 minutes.

2.7.2 Fixing of tissue and preparation for immunohistochemistry

Samples were subjected to perfusion fixation and left in fixative containing 4% (w/v) paraformaldehyde overnight at 4°C. Where this was not possible, as in the case with the Edinburgh material, samples were post-fixed for 48 hours in fixative solution, which was changed at the 24 hour interval. Samples were dehydrated using sucrose infiltration, before being sliced into 30μm sections using a crystoat at -30°C. Brains were sectioned coronally, horizontally, or sagitally, whereas spinal cord was only sectioned sagitally. To prepare the spinal cord, the entire spinal column was extracted from the animal and left for overnight in fixative solution, after which the vertebrae were removed by careful dissection prior to sucrose infiltration – dehydrating the tissue so that ice crystals will not form during freezing.

Following sucrose infiltration, the samples were frozen in iso-pentane at -70°C for 1 minute and sectioned in a Cryostat at -26°C into 30μm thick sections.
Sections were transferred into a 24 well dish, with each well containing PBS 0.05% (w/v) sodium azide and stored at 4°C until use.

With the $5HT_{2C}$ receptor over-expressing and knockdown mice and their respective controls perfusion-fixation was not possible; Brains were dissected quickly and placed in 4% paraformaldehyde-based fixative and stored at 4°C, with daily changes of fixative.

2.7.3 Immunohistochemistry/Immunocytochemistry

Samples were transferred from their storage solution and placed into 300µl of Tris-buffered saline (TBS)/10% (v/v) methanol/3% (v/v) Hydrogen Peroxide, and incubated with mild agitation at room temperature for 30 minutes. This step was to inhibit any endogenous peroxidase activity present in the sample, for example, any residual red blood corpuscles.

Following this incubation the samples were washed three times with TBS 0.2% (v/v) Triton X-100™ (Hereafter referred to as TBS-T), with each wash lasting five minutes. After the wash stages, samples were incubated in TBS 0.2% (w/v) glycine for 30 minutes at room temperature to quench excess paraformaldehyde.

After incubation with TBS-glycine, the samples were incubated for one hour at room temperature with TBS-T/10% blocking serum (either horse if goat primary antibodies were to be used; goat if rabbit primary antibodies were to be used; or rabbit if mouse primary antibodies were to be used). After which the samples were incubated in primary antibody diluted in TBS/1% blocking serum over night at 4°C.

The following day the samples were allowed to equilibrate to room temperature for one hour before being washed with the TBS-T as per the previous day, prior to being incubated in the appropriate biotinylated secondary antibody (From the Vectastain ABC kit) diluted in TBS/1% blocking serum (one drop in 10ml of TBS/serum).

Incubation with the secondary antibody was for two hours at room temperature, before another wash stage, and incubation with ABC reagent diluted in TBS for one hour at room temperature.

After incubation with the ABC reagent, the samples were subjected to one wash stage (3X5 minute washes with TBS-T) and two further washes of TBS before being incubated in TBS 0.5mg/ml 3'3'-Diaminobenzidine (DAB) to which 0.00067% (v/v) hydrogen peroxide was added.

Samples were allowed to develop until an optimal signal had been achieved, without compromising the control sections.

After staining, the DAB mixture was aspirated and the samples washed twice with dH_2O before being dehydration mounted onto glass slides and set with DPX mountant.

In the case of immunocytochemisty, the HEK293 cells that had been transfected with individual TARP isoforms using the Lipofectamine 2000 (Invitrogen) protocol (transfections performed by Dr V Hann) were cultured on glass cover-slips and stored individually in wells in a 24 well-dish.

2.7.4 Concentrations of primary antibodies used in immunohistochemistry/immunocytochemistry

- TARP γ4 = 0.5μg/ml
- TARP γ8C = 0.0626μg/ml
- GluR1 = 0.5μg/ml dilution of source antibody (commercially obtained as mentioned in section 2.6.3).
- GluR2 = 1 in 1000 dilution of source antibody (commercially obtained as mentioned in section 2.6.3).

2.7.5 Peptide block (Only conducted using the generated TARP isoform-specific antibodies)

2.7.5.1 Immunohistochemisty

To screen the antibodies and determine the specificity of antibody binding to its antigenic peptide, the primary antibody was pre-incubated overnight at 4°C with a 5-fold excess of its respective peptide before being used as standard in the immunohistochemical protocol.

2.7.5.2 Immunoblotting

Again, for the purposes of determining antibody specificity to the antigenic peptide, the primary antibody used to probe the immunoblots was incubated for 30 minutes at room temperature with its respective peptide, before the antibody-peptide mixture was used in the afore-mentioned immunoblotting protocol.

2.7.5.3 Immunocytochemistry

Cells were prepared as standard for immunocytochemistry. Peptide block was conducted using an antibody-peptide pre-incubation identical to that used for the immunohistochemistry.

2.8 Immuopurifications

2.8.1 Tissue solubilisation for immunoaffinity purification

The preparation of tissue for immunopurification was based upon the protocol outlined by Kannenberg et al. (1997):

Eight cortices of tissue were initially homogenised in 50ml ice cold Sigel's buffer (NaCl-based) plus containing protease inhibitors; aproprotein (2 μg/ml), leupeptin (1 μg/ml), pepstatin A (1 μg/ml), and PMSF (1mM). Homogenate was centrifuged at 18,500 G for 30 minutes at 4°C. Supernatant was discarded and the pellet resuspended in Sigel's buffer (as above) with 1% Triton X-100™, and incubated at 4°C for 30 minutes on rollers. The

mixture was then subjected to centrifugation at 23,000 G for 30 minutes at 4°C, with the supernatant being collected and subjected to ultra-centrifugation at 40,000 G at 4°C for 75 minutes. The supernatant from this centrifugation was then passed onto a pre-equilibrated immunoaffinity column (equilibration with 60ml ice cold sigels buffer/1% Triton X-100™), and left to incubate overnight at 4°C. The following morning the column was washed (with 60ml ice cold sigels buffer/1% Triton X-100™) and subjected to acid elution with 100mM glycine pH 2.5 – neutralised in 1M Tris. The immunoaffinity purification process was repeated for a second night in an attempt to ensure all TARP γ8 protein complexes were purified. Eluted fractions were flash-frozen immediately after collection, as were the Triton X-100™ insoluble pellets from centrifugation.

2.8.2 Immunopurification of Triton X-100™ Soluble Material

The protocol for immunopurification of the Triton X-100™ material was based upon the protocol used by Ives et al (2004), and essentially the same as that outlined by section 2.4.2, with the material circulated through the immunoaffinity column derived from the TARP isoform-specific antibody of choice, overnight at 4°C. The following morning, the bound proteins were eluted using glycine buffer pH 2.5.

2.9 Proteomics

2.9.1 Clean-up of purified samples

The purified fractions containing the highest amount of eluted material (peak fractions), as determined from immunoblotting (data not shown), were initially pooled into 2ml samples and concentrated into ~100µl samples using microcon centrifuge tubes at 14,000 G at 4°C for four hours. Samples were then subjected to clean up using a 2D clean up kit (GE Healthcare). This was because of previous problems in proteomic identification caused by the buffers used in immunopurification and subsequent elution.neutralisation (personal communication, Dr H Payne). The protocol was exactly as outlined in the kit, to outline;

- Samples were incubated on ice for 15 minutes with 300µl of the precipitant (provided by kit recipe not given). Before addition of 300µl of co-precipitant (again as supplied), and subsequent centrifugation at 12000 G for five minutes at 4°C.
- Supernatant was then aspirated, with samples pulse centrifuged to ensure all supernatant could be accessed. Once aspiration was complete 40µl of co-precipitant was added and samples were incubated on ice for five minutes.
- Samples were then centrifuged for five minutes identical to that mentioned in the first step, with the supernatant being removed and replaced by 25µl of ultrapure water. The sample/water mixture was then gently vortexed for 10 seconds before addition of 1ml of wash buffer (at -20°C, again from kit) and 5µl of wash additive (supplied in kit), with the resultant sample mixture then incubated at -20°C for 30 minutes with occasional mixing.
- After the incubation step, samples were centrifuged as in the previous step, with the bulk of the supernatant aspirated, the pellet being allowed to dry and subsequently re-suspended in 100µl lysis buffer (Appendix A).

The cleaned samples were then subjected to chloroform-methanol precipitation and resuspended in 15µl of 1X Proteomic sample buffer for loading onto pre-cast NuPAGE™ gels for electrophoresis at 200V for one hour. For all proteomic gels concentrated peak samples from the Non-specific IgG, TARP γ8N IgG and TARP γ8C IgG immunoaffinity were used, with 12 µl of the sample/1X proteomic sample buffer being loaded per well. During electrophoresis, gels were immersed in 1X NuPAGE running buffer diluted from the 20X concentrated stock.

2.9.2 Silver stained gels: Protocol for use with MALDI-TOF

Following electrophoresis, the NuPAGE gels were subjected to silver-staining using the following protocol: Standard pre-cast NuPAGE gels (10% acrylamide) were initially subjected to 30 minutes fixation using a 10% (v/v) acetic acid, 40% (v/v) methanol, 50% (v/v) dH_2O mixture, with fresh fix being substituted after 15 minutes.

After fixation the gels were sensitized using a solution containing 30% methanol (v/v) and 4% (w/v) sodiumthiosulphate plus 6.8% (w/v) sodium acetate for 30 minutes. Following sensitization, the gel was washed three times with dH_2O for five minutes per wash before staining in 0.25% (w/v) silver nitrite for 20 minutes.

Subsequent to staining, the gels were briefly washed twice with dH_2O before being developed using 2.5% (w/v) sodium carbonate plus 0.04% (v/v) formaldehyde until the bands were detectable at a suitable intensity. Developing was stopped using 1.46% (w/v) EDTA for 10 minutes.

After stopping development, the gel was washed several times with dH_2O and any bands specific to either of the TARP γ8 IgG samples were cut out and subjected to MALDI-TOF or MALDI-TOF/TOF analysis.

2.9.3 MALDI-TOF/MALDI-TOF/TOF analysis

The protein bands were transferred to a 96-well microtitre plate and then subjected to the ProGest long trypsin digestion protocol at a ProGest workstation (Genomic Solutions Ltd):

- Initially the bands were equilibrated in 50µl of 50mM ammonium bicarbonate before subsequent reductive alkylation with 10mM DTT and 100mM iodoacetamide.
- The reductively alkylated bands were then destained and desiccated using acetonitrile.
- Bands were subsequently re-hydrated with 50mM ammonium bicarbonate containing 6.6% (w/v) trypsin (Promega) and digested overnight.
- The following morning, peptides were extracted using 50% (v/v) acetonitrile, 0.1% (v/v) TFA into a final volume of 50µl (2 x 25µl extractions)
- The resulting extracts were then freeze-dried and re-suspended in 10 µl of 0.1% formic acid.

For MALDI-TOFAnalysis

- Using the 'thin-film' method: Approx. 0.2 µl of matrix (α-cyano-4-hydroxy-cinnamic acid in nitrocellulose/acetone) was spotted to the target plate, with 1 µl of digested sample was applied to the thin film & allowed to dry.
- The samples were then washed in-situ with 0.1% TFA and left to dry before performing MALDI-TOF using a Voyager-DE™ STR BioSpectrometry™ Workstation (Applied Biosystems).
- De-isotoped & calibrated spectra were then used to generate peak lists which were searched using MASCOT (www.matrixscience.com) mass spectrometry database search software.

For MALDI-TOF/TOF Analysis

- Matrix is α-cyano-4-hydroxy-cinnamic acid / in 50% acetonitrile.1 µl of matrix was spotted and 1 µl of digested sample on top and allowed to dry.
- MALDI-TOF/TOF was performed using a 4800 Plus MALDI TOF/TOF Analyzer (Applied Biosystems) – From the initial MS spectra, the top 10 precursor peptides are selected for subsequent MS/MS sequencing.
- De-isotoped & calibrated spectra were then used to generate peak lists. Peak lists and accompanying MS/MS spectra were used to search against MASCOT (www.matrixscience.com) database search software.

All MALDI-TOF and MALDI-TOF/TOF analysis was completed by Joanne Robson.

2.10 Receptor autoradiography

2.10.1 Collection and preparation of tissue

Whole brains were collected from terminally anaesthatised $5HT_{2C}$ receptor over-expressing and knockdown mice, and their respective controls, and stored in PBS/20% sucrose at 4°C until use.

For sectioning, the brains were subjected to hemisectemy and one hemisphere, selected for autoradiography and flash-frozen in isopentane at -40°C for 3 minutes prior to being sectioned on a cryostat into sections 16μm thick.

The sections were thaw-mounted onto polysine coated glass slides and stored at -20°C until their use in autoradiography.

2.10.2 Autoradiography of mice possessing altered $5HT_{2C}$ receptor expression

- Sections were pre-incubated for 20 minutes in pre-incubation buffer containing 30mM Tris at pH 7.4 on ice.
- Following preincubation, sections were transferred to buffer that was identical to the pre-incubation buffer with the addition of the radio-ligand, in this instance [^{3}H] AMPA at a 20nM and 100mM KSCN; on ice for 1 hour.
- After incubation with the ligand containing buffer, sections were subjected to a series of staggered immersion washes of 15 seconds each, with the first three washes being wash buffer (30mM Tris, pH 7.4, 100mM KSCN, and the final being dH_2O; all conducted on ice.
- After washes, sections were left overnight to dry before being placed in an autoradiography cassette exposed to [^{3}H] Hyperfilm (Amersham), prepared in a darkroom and left for 5 weeks before manual developing using the Kodak GBX fixer solutions as per immunoblots.
- For non-specific binding samples were incubated in radio-ligand buffer to which 1mM glutamate had been added and left for one hour on ice.

The film was analysed using Image J and the relative intensities of the cortical labelling calculated between the experimental samples and their controls.

2.11 Statistical analysis of immunoblots and autoradiography.

This was conducted using Microsoft Excel and GraphPad software in an un-paired *t* test, with $p<0.05$ considered statistically significant.

Chapter 3: Generation of novel TARP isoform-specific antibodies and their use in determining TARP isoform distribution in the CNS.

Introduction

The initial aim of this project was to develop and validate a panel of antibodies specific to the known TARP isoforms. There are several TARPs expressed in the mammalian brain, with the information regarding their distribution based largely upon in situ hybridisation. However, a lack of suitable probes has resulted in limited information regarding the distribution of the TARP isoforms at the protein level. The panel of new probes will be used to not only define the distribution of the TARP isoforms throughout the CNS, but will also help both identify the most relevant TARP to investigate for an interaction with $5HT_{2C}$ within the forebrain and enable investigations regarding the nature of this interaction. As such, these antibodies will be vital to define the anatomical framework for this project, not only in the determination of the relevant TARP for study, but also for use in generating immunoaffinity columns for identifying specific TARP interacting partners by immunopurification.

To that end, the peptide sequences of each of the known TARP isoforms were studied, with peptide sequences from each TARP isoform selected to try to maximize antigenicity, but primarily to maximize TARP isoform specificity by minimizing the similarities between the sequence chosen and its analogous counterparts in the other TARP isoforms. The resultant sequences were then used to generate novel peptides used as antigens to generate polyclonal antibodies specific to each of the TARP isoforms. There was alsot he consideration of potential binding sites to consider, so where possible, sequences in domains similar to successful TARP γ2 antibodies already in use in the lab were selected.

Once the probes were generated and validated using recombinant TARPs expressed in HEK293 cells, they were used to map the distribution of each of the TARP isoforms throughout the CNS to both compare with, and expand upon the TARP distribution data already in the literature, with the specific goal of identifying which TARP isoforms were prevalent in the regions of interest.

Results

Initially, for generation of the TARP isoform-specific antibodies for use in this project, the peptide sequence for each of the TARPs had to be examined for suitable regions to use in the generation of isoform-specific antibodies. Regions had to be highly specific to the TARP isoform of choice, but also within regions unlikely to undergo epitope masking by other proteins. Ideally, the regions also displayed high antigenicity.

Gamma 2	•	•	•	•	•	•	•	•	•	•	•	M	G	L	F	D	R	G	V	Q	M	L	L	T	T	V	G	A	F	A
Gamma 3	•	•	•	•	•	•	•	•	•	•	•	M	R	M	C	D	R	G	I	Q	M	L	T	T	T	V	G	A	F	A
Gamma 4	•	•	•	•	•	•	•	•	•	•	•	M	V	R	C	D	R	G	L	Q	M	L	L	T	T	A	G	A	F	A
Gamma 8	M	E	S	L	K	R	W	N	E	E	R	G	L	W	C	E	K	G	V	Q	V	L	L	T	T	I	G	A	F	S

Gamma 2	A	F	S	L	M	T	I	A	V	G	T	D	Y	W	L	Y	S	R	G	•	•	V	C	K	T	K	S	V	S	E
Gamma 3	A	F	S	L	M	T	I	A	V	G	T	D	Y	W	L	Y	S	R	G	•	•	V	C	R	T	K	S	T	S	D
Gamma 4	A	F	S	L	M	A	I	A	I	G	T	D	Y	W	L	Y	S	S	A	H	•	I	C	N	G	T	N	L	T	M
Gamma 8	A	F	G	L	M	T	I	A	I	S	T	D	Y	W	L	Y	T	R	A	L	•	I	C	N	T	T	N	L	T	A

Gamma 2	N	•	•	•	•	•	E	T	S	K	K	N	E	E	•	•	•	•	•	•	•	•	V	M	T	H	S	G	L	W
Gamma 3	N	•	•	•	•	•	E	T	S	R	K	N	E	E	•	•	•	•	•	•	•	•	V	M	T	H	F	G	L	W
Gamma 4	D	•	•	D	G	•	P	P	P	R	R	A	R	G	•	•	•	•	•	•	•	•	D	L	T	H	S	G	L	W
Gamma 8	G	•	D	D	G	•	P	P	H	R	G	G	S	G	S	S	E	K	K	D	P	G	G	L	T	H	S	G	L	W

Gamma 2	R	T	C	C	L	E	G	N	F	K	G	•	•	•	•	•	•	•	•	•	•	•	•	•	•	•	•	•	L	C
Gamma 3	R	T	C	C	L	E	G	A	F	R	G	•	•	•	•	•	•	•	•	•	•	•	•	•	•	•	•	•	V	C
Gamma 4	R	V	C	C	I	E	G	I	Y	R	G	•	•	•	•	•	•	•	•	•	•	•	•	•	•	•	•	•	H	C
Gamma 8	R	I	C	C	L	E	G	L	K	R	G	•	•	•	•	•	•	•	•	•	•	•	•	•	•	•	•	•	V	C

Gamma 2	K	Q	I	D	H	F	P	E	•	D	A	D	Y	E	A	D	T	A	E	Y	F	L	R	A	V	R	A	S	S	I
Gamma 3	K	K	I	D	H	F	P	E	•	D	A	D	Y	E	Q	D	T	A	E	Y	L	L	R	A	V	R	A	S	S	V
Gamma 4	F	R	I	N	H	F	P	E	•	D	N	D	Y	D	H	D	S	S	E	Y	L	L	R	I	V	R	A	S	S	V
Gamma 8	V	K	I	N	H	F	P	E	•	D	T	D	Y	D	H	D	S	A	E	Y	L	L	R	V	V	R	A	S	S	I

Gamma 2	F	P	I	L	S	V	I	L	L	F	M	G	G	L	C	I	A	A	S	E	F	Y	K	T	R	H	N	I	I	L
Gamma 3	F	P	I	L	S	V	T	L	I	F	F	G	G	L	C	V	A	A	S	E	F	H	R	S	R	H	S	V	I	L
Gamma 4	F	P	I	L	S	T	I	L	L	L	L	G	G	L	C	I	G	A	G	R	I	Y	S	R	K	N	N	I	V	L
Gamma 8	F	P	I	L	S	A	I	L	L	L	L	G	G	V	C	V	A	A	S	R	V	Y	K	S	K	R	N	I	I	L

Gamma 2	S	A	G	I	F	F	V	S	A	G	L	S	N	I	I	G	I	I	V	Y	I	S	A	N	A	G	D	P	S	•
Gamma 3	S	A	G	I	F	F	V	S	A	G	L	S	N	I	I	G	I	I	V	Y	I	S	A	N	A	G	D	P	G	•
Gamma 4	S	A	G	I	L	F	V	A	A	G	L	S	N	I	I	G	I	I	V	Y	I	S	S	N	T	G	D	P	S	D
Gamma 8	G	A	G	I	L	F	V	A	A	G	L	S	N	I	I	G	V	I	V	Y	I	S	A	N	A	G	E	P	G	P

Gamma 2	•	•	•	K	S	D	S	•	K	K	N	S	Y	S	Y	G	W	S	F	Y	F	G	A	L	S	F	I	T	A	E
Gamma 3	•	•	•	Q	R	D	S	•	K	K	•	S	Y	S	Y	G	W	S	F	Y	F	G	A	F	S	F	I	I	A	E
Gamma 4	•	•	•	K	R	D	E	D	K	K	N	H	Y	N	Y	G	W	S	F	Y	F	G	A	L	S	F	I	V	A	E
Gamma 8	•	•	•	K	R	D	E	E	K	K	N	H	Y	S	Y	G	W	S	F	Y	F	G	G	L	S	F	I	L	A	E

Gamma 2	M	V	G	V	L	A	V	H	M	F	I	D	R	H	K	Q	L	R	A	T	A	R	A	T	D	Y	L	Q	A	•
Gamma 3	I	V	G	V	V	A	V	H	I	Y	I	E	K	H	Q	Q	L	R	A	R	S	•	H	S	E	L	L	K	K	•
Gamma 4	T	V	G	V	L	A	V	N	I	Y	I	E	K	N	K	E	L	R	F	K	T	•	K	R	E	F	L	K	S	•
Gamma 8	V	I	G	V	L	A	V	N	I	Y	I	E	R	S	R	E	A	H	C	Q	S	•	R	S	D	L	L	K	A	G

Gamma 2	•	•	•	•	•	•	•	•	•	•	•	S	A	I	T	R	I	P	S	Y	R	Y	R	Y	Q	R	R	S	R	S
Gamma 3	•	•	•	•	•	•	•	•	•	•	•	S	T	F	A	R	L	P	P	Y	R	Y	R	F	R	R	R	S	•	•
Gamma 4	•	•	•	•	•	•	•	•	S	S	S	S	P	Y	A	R	M	P	S	Y	R	Y	R	•	R	R	R	S	R	S
Gamma 8	G	G	A	G	G	S	G	G	S	G	P	S	A	I	L	R	L	P	S	Y	R	F	R	Y	R	R	R	S	R	S

Gamma 2	S	S	R	•	S	T	E	P	S	H	S	R	D	A	S	P	V	G	V	K	G	F	N	T	L	P	S	T	E	I
Gamma 3	S	S	R	•	S	T	E	P	•	R	S	R	D	L	S	P	I	S	•	K	G	F	H	T	I	P	S	T	D	I
Gamma 4	S	S	R	•	S	T	E	A	S	P	S	R	D	A	S	P	V	G	L	K	I	T	G	A	I	P	M	G	E	L
Gamma 8	S	S	R	G	S	S	E	A	S	P	S	R	D	A	S	P	G	G	P	G	G	P	G	F	A	S	T	•	D	I

Gamma 2	S	M	Y	T	L	S	R	D	P	L	K	A	A	T	T	P	•	•	•	•	•	•	•	•	•	•	•	•	•	T
Gamma 3	S	M	F	T	L	S	R	D	P	S	K	L	T	M	G	•	•	•	•	•	•	•	•	•	•	•	•	•	•	•
Gamma 4	S	M	Y	T	L	S	R	E	P	L	K	V	T	T	A	A	•	•	•	•	•	•	•	•	•	•	•	•	•	•
Gamma 8	S	M	Y	T	L	S	R	D	P	S	K	G	S	V	A	A	G	L	A	S	A	G	G	G	G	S	G	A	G	V

Gamma 2	A	T	Y	N	•	•	•	•	•	•	•	•	•	•	•	•	•	•	•	•	•	•	S	D	R	D	•	•	•	N
Gamma 3	T	L	L	N	•	•	•	•	•	•	•	•	•	•	•	•	•	•	•	•	•	•	S	D	R	D	•	•	•	H
Gamma 4	•	S	Y	S	•	•	•	•	•	•	•	•	•	•	•	•	•	•	•	•	•	•	P	D	Q	D	•	•	•	A
Gamma 8	G	A	Y	G	G	A	A	G	A	A	G	G	G	G	•	•	•	•	•	A	G	S	E	R	D	R	G	S	S	A

Gamma 2	S	F	L	Q	V	H	N	C	I	Q	K	D	S	K	D	S	L	H	A	N	T	•	•	•	•	•	•	•	•	•
Gamma 3	A	F	L	Q	F	H	N	S	T	P	K	E	F	K	E	S	L	H	N	N	P	•	•	•	•	•	•	•	•	•
Gamma 4	G	F	L	Q	M	H	D	F	F	Q	Q	D	L	K	E	G	F	H	V	S	M	•	•	•	•	•	•	•	•	•
Gamma 8	G	F	L	T	L	H	N	A	F	P	K	E	A	A	S	G	V	T	V	T	V	T	G	P	P	A	A	P	A	P

Gamma 2	•	•	•	•	•	•	•	•	•	•	•	•	•	•	•	•	•	•	•	•	•	•	•	•	•	A	N	R	R			
Gamma 3	•	•	•	•	•	•	•	•	•	•	•	•	•	•	•	•	•	•	•	•	•	•	•	•	•	A	N	R	R			
Gamma 4	•	•	•	•	•	•	•	•	•	•	•	•	•	•	•	•	•	•	•	•	•	•	•	•	•	L	N	R	R			
Gamma 8	A	P	A	P	P	A	P	A	A	P	A	P	G	T	L	S	K	E	A	A	A	S	N	T	N	T	L	N	R	K		

Gamma 2	T	T	P	V
Gamma 3	T	T	P	V
Gamma 4	T	T	P	V
Gamma 8	T	T	P	V

Figure 3.1.1 Amino acid sequences for each of the TARP isoforms

Aligned amino acid sequences for each of the TARP isoforms. Transmembrane domains are underlined, the peptide sequences used to generate each antibody are green. The black dots correspond to empty stretches of sequence.

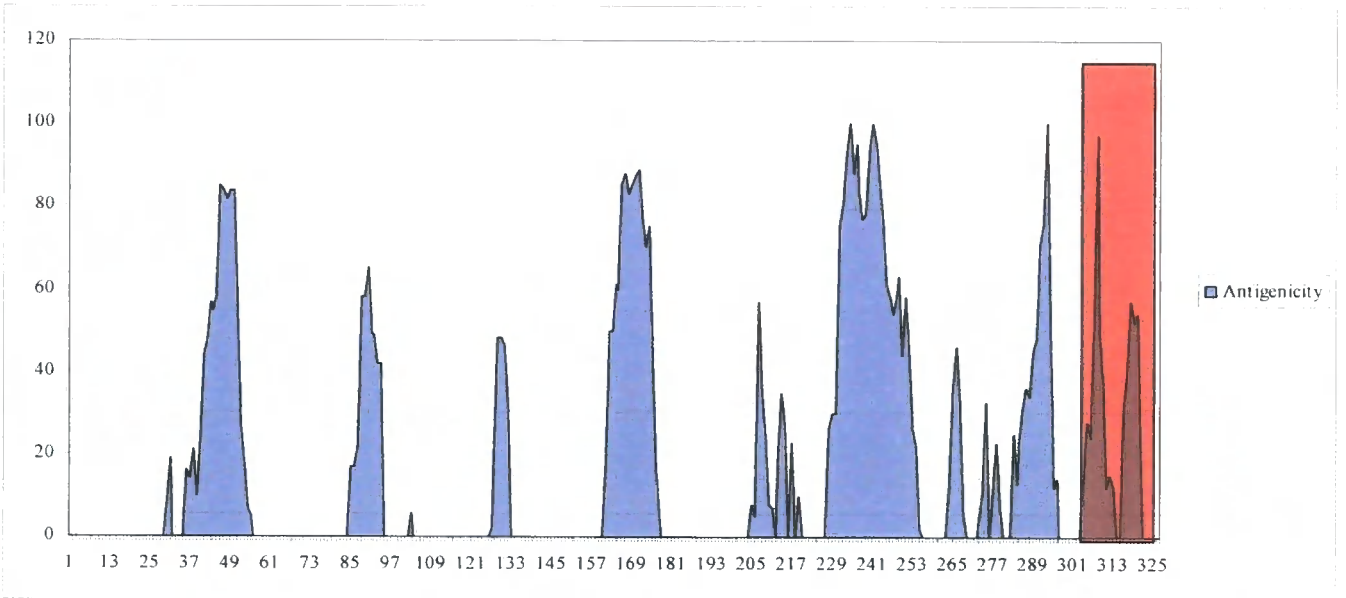

Figure 3.1.2 Graph showing peak regions of antigenicity in the TARP γ2 isoform peptide sequence

The antigenicity of the TARP γ2 isoform as shown using the ANTHEPROT package, with the region corresponding to the site of peptide sequence selected for antibody generation highlighted in red.

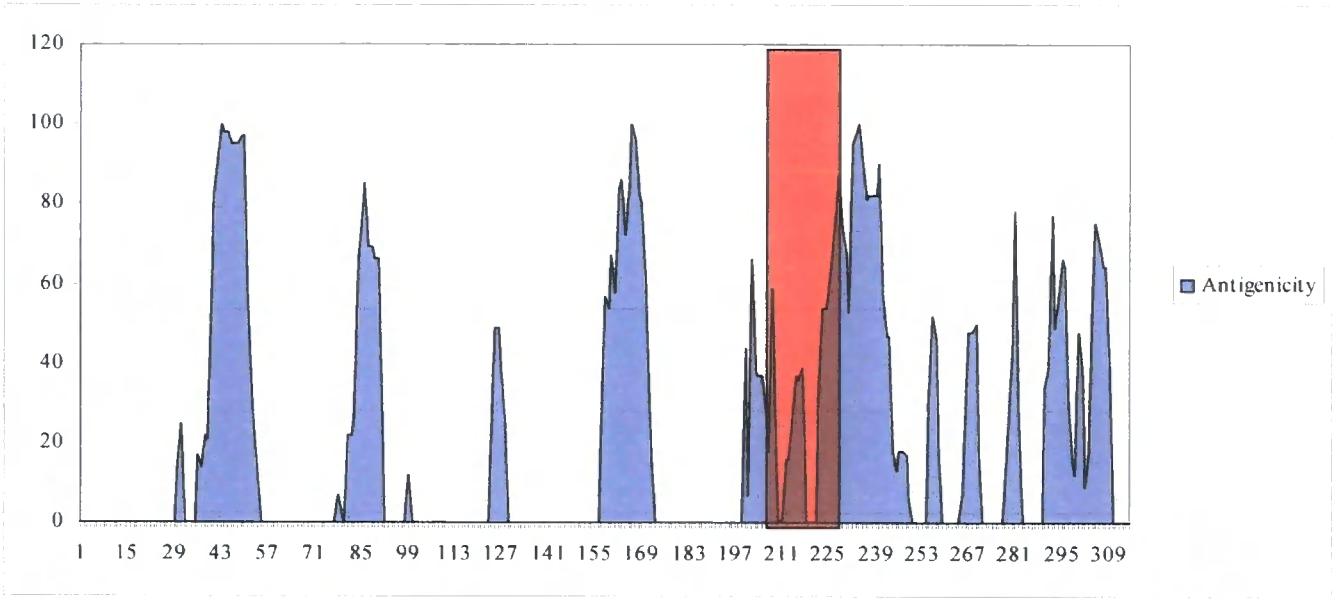

Figure 3.1.3 Graph showing peak regions of antigenicity in the TARP γ3 isoform peptide sequence

The antigenicity of the TARP γ3 isoform as shown using the ANTHEPROT package, with the region corresponding to the site of peptide sequence selected for antibody generation highlighted in red.

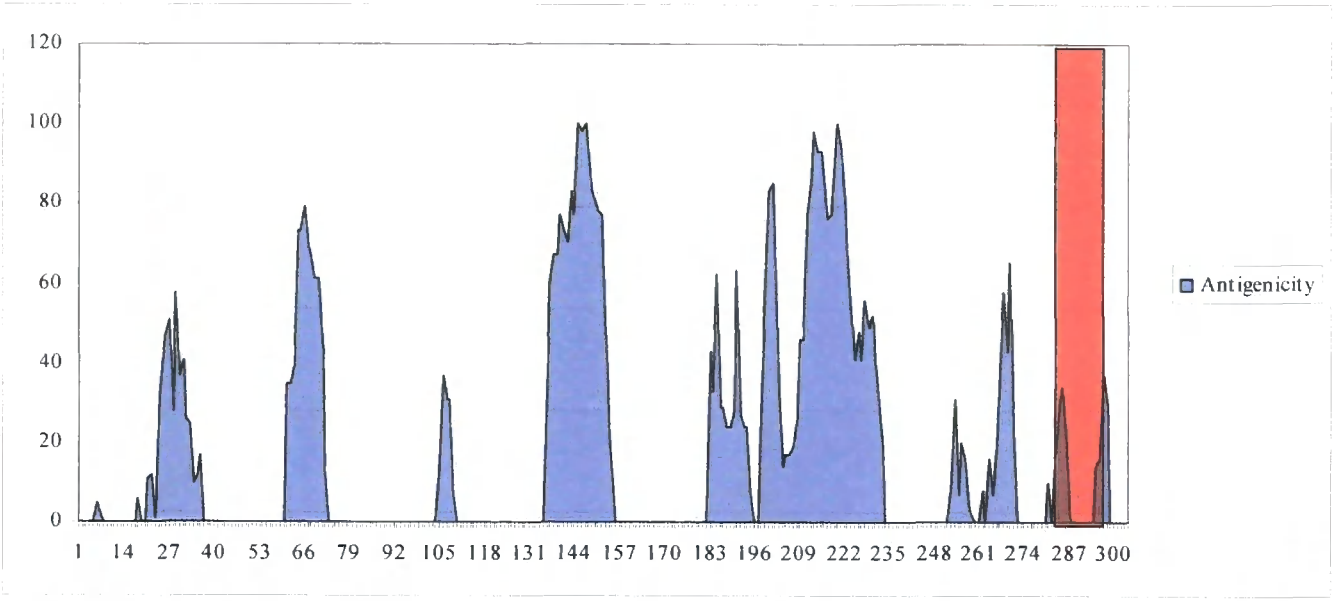

Figure 3.1.3 Graph showing peak regions of antigenicity in the TARP γ4 isoform peptide sequence

The antigenicity of the TARP γ4 isoform as shown using the ANTHEPROT package, with the region corresponding to the site of peptide sequence selected for antibody generation highlighted in red. The regions chosen for this antibody weren't the most antigenic because of the possibility of epitope masking and lack of isoform-specific peptide sequence within the most antigenic sites.

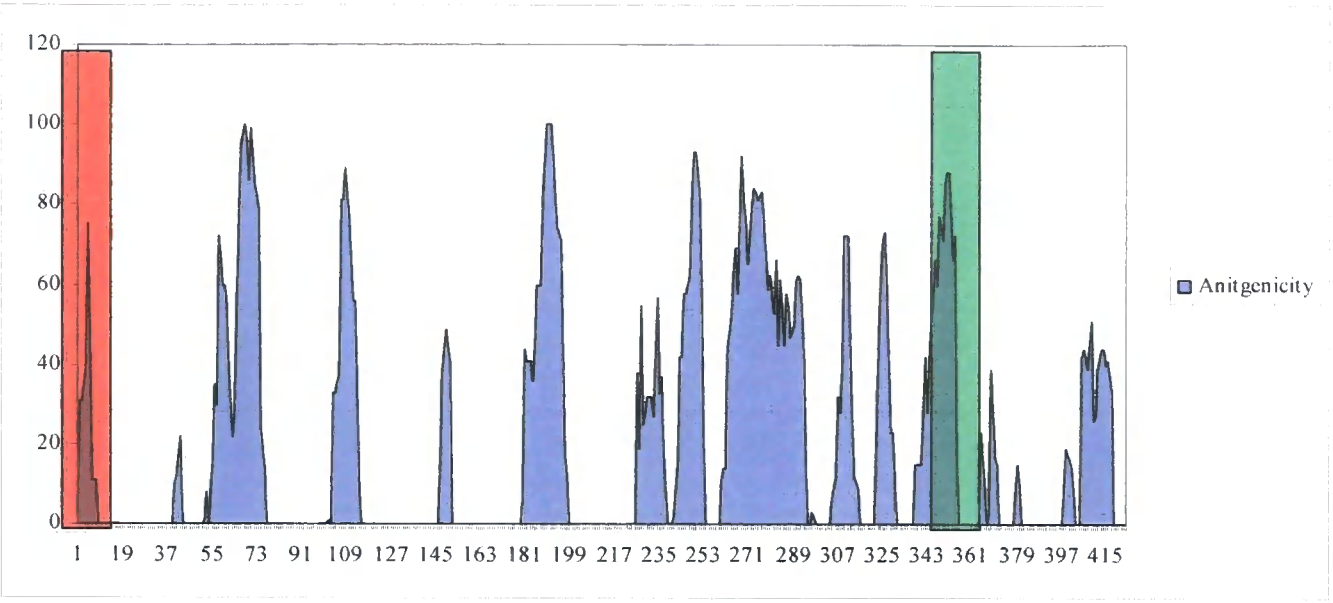

Figure 3.1.4 Graph showing peak regions of antigenicity in the TARP γ8 isoform peptide sequence

The antigenicity of the TARP γ8 isoform as shown using the ANTHEPROT package, with the region corresponding to the site of peptide sequence selected for generation of the TARP γ8 N-terminal directed antibody is highlighted in red, whilst the site of peptide sequence selected for the generation of the C-terminal directed antibody is in green.

The peptide sequences selected for each of the TARP isoform-specific antibodies generated are specific to their TARP isoform.

From examining Figure 1.1 it is obvious that there is a low sequence homology between each of the peptide sequences chosen for antibody generation when compared with the comparable peptide sequences of the other TARP isoforms. The sequences themselves also possessed reasonable antigenic properties as shown in Figure 1.2.

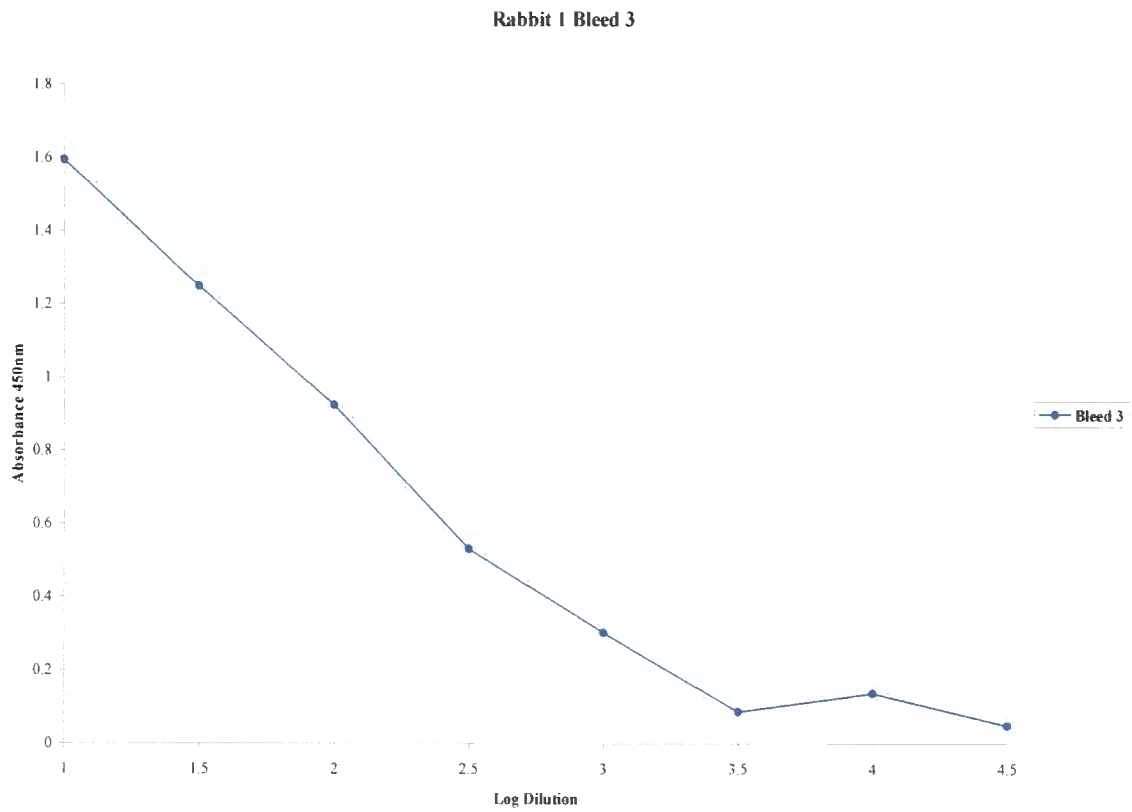

Figure 3.2.1.1 Graphical representation of ELISA data obtained for Rabbit 1 bleed 3.

Graph shows the absorbance @450nm of each dilution of serum from rabbit 1 bleed 3. Serum was incubated in semi-log dilution factors up to a maximal dilution factor of 1/31600 overnight at 4°C in wells containing bound peptide.

Titre of the antibody was determined as the dilution factor where the peak absorbance recorded had diminished 50%.

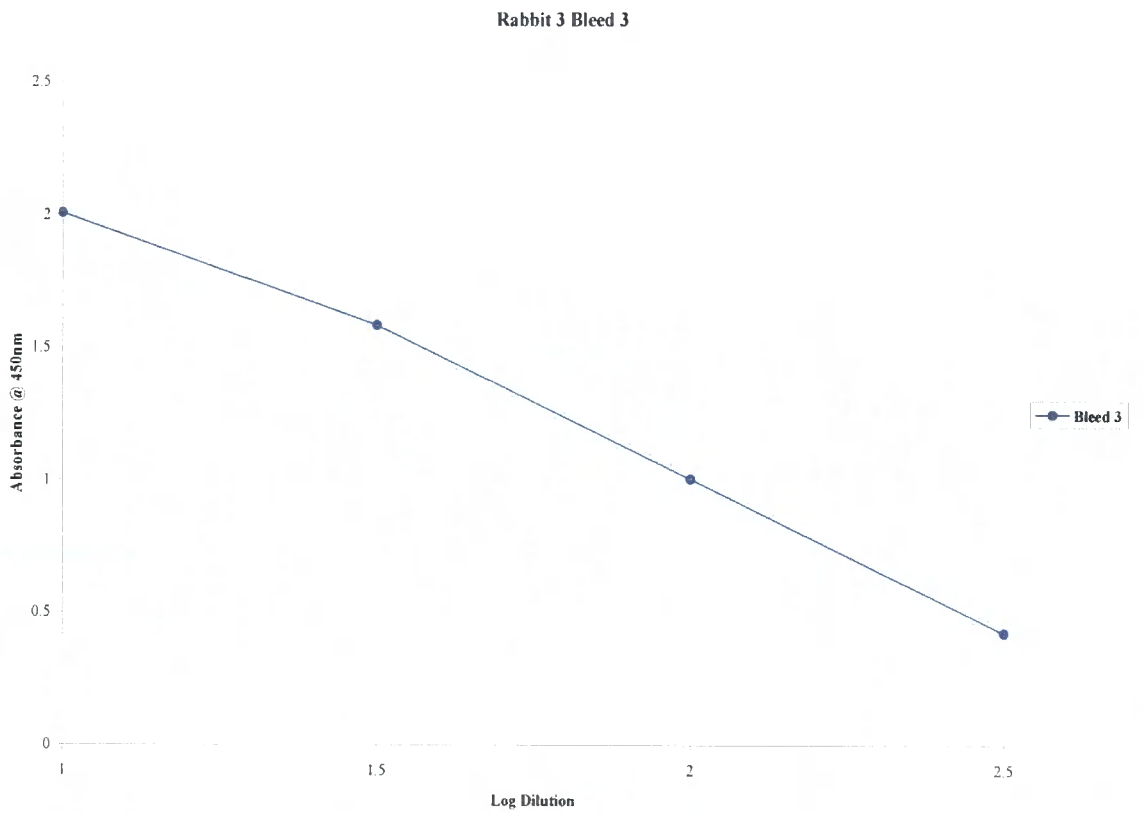

Figure 3.2.1.2 Graphical representation of ELISA data obtained for Rabbit 3 bleed 3.

Graph shows the absorbance @450nm of each dilution of serum from rabbit 3 bleed 3. Serum was incubated in semi-log dilution factors up to a maximal dilution factor of 1/31600 overnight at 4°C in wells containing bound peptide.

Titre of the antibody was determined as the dilution factor where the peak absorbance recorded had diminished 50%.

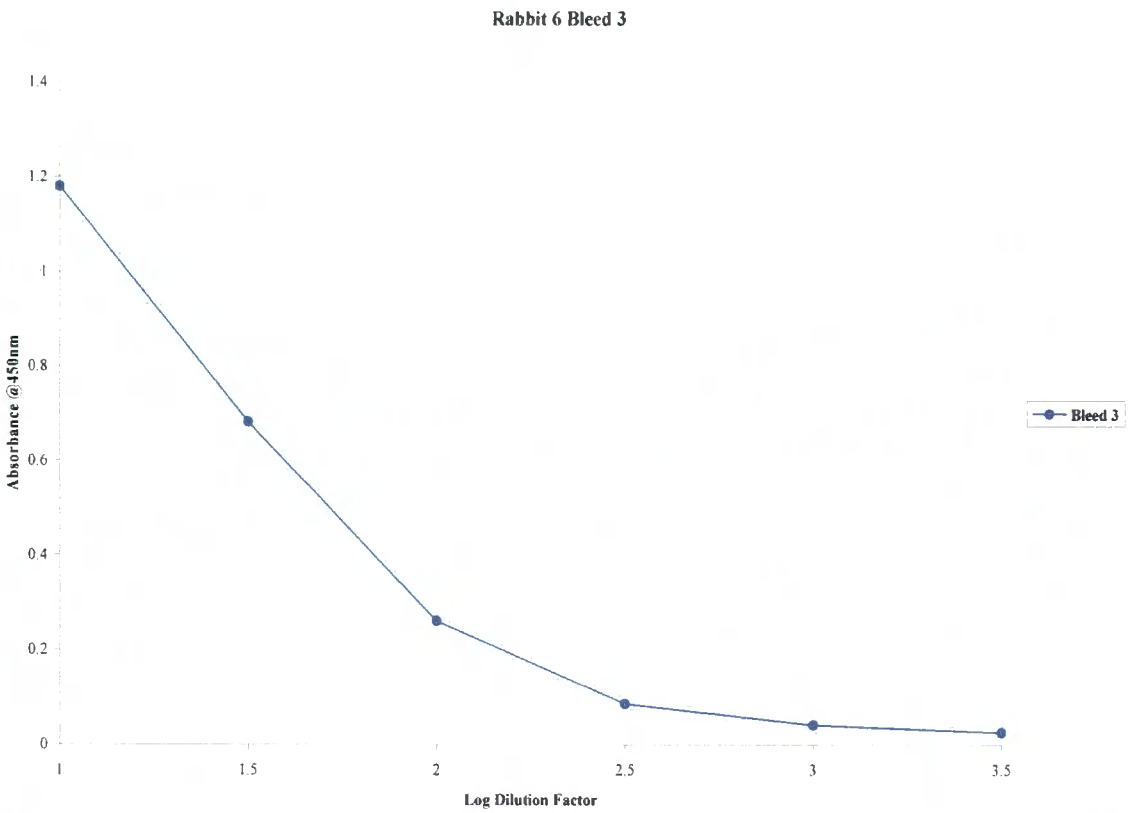

Figure 3.2.1.3 Graphical representation of ELISA data obtained for Rabbit 6 bleed 3.

Graph shows the absorbance @450nm of each dilution of serum from rabbit 6 bleed 3. Serum was incubated in semi-log dilution factors up to a maximal dilution factor of 1/31600 overnight at 4°C in wells containing bound peptide.

Titre of the antibody was determined as the dilution factor where the peak absorbance recorded had diminished 50%.

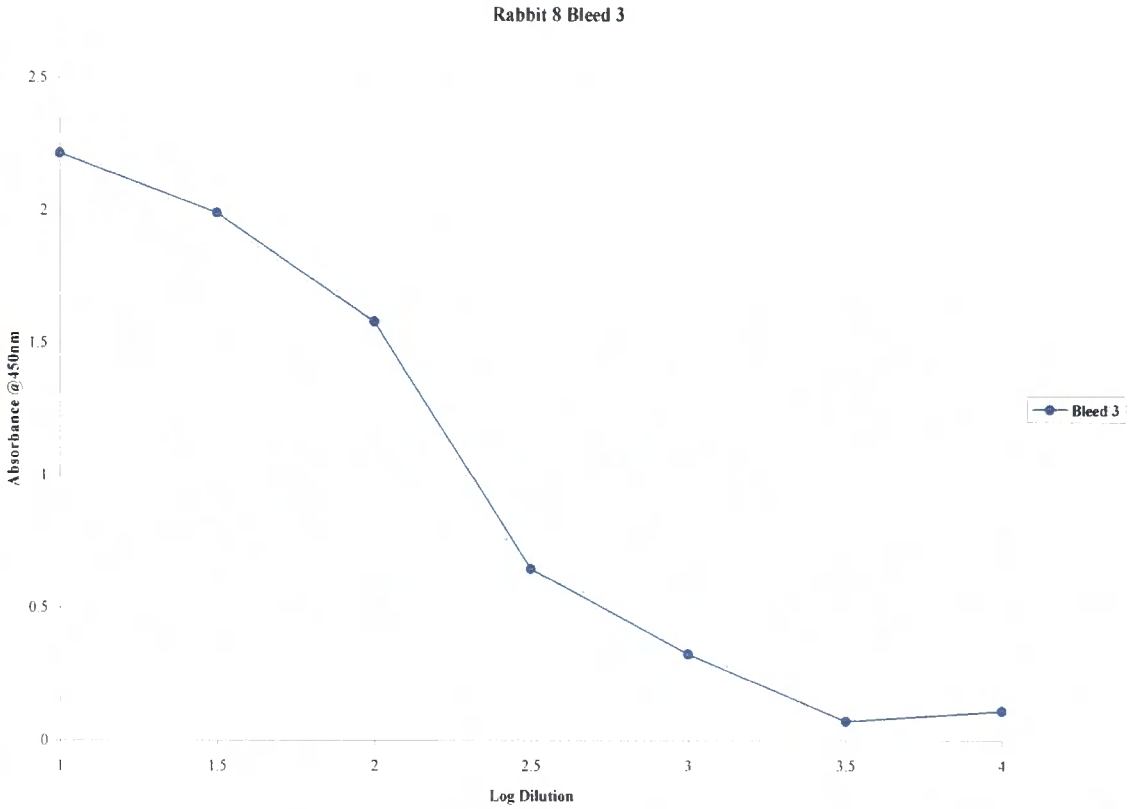

Figure 3.2.1.4 Graphical representation of ELISA data obtained for Rabbit 8 bleed 3.

Graph shows the absorbance @450nm of each dilution of serum from rabbit 8 bleed 3. Serum was incubated in semi-log dilution factors up to a maximal dilution factor of 1/31600 overnight at 4°C in wells containing bound peptide.

Titre of the antibody was determined as the dilution factor where the peak absorbance recorded had diminished 50%.

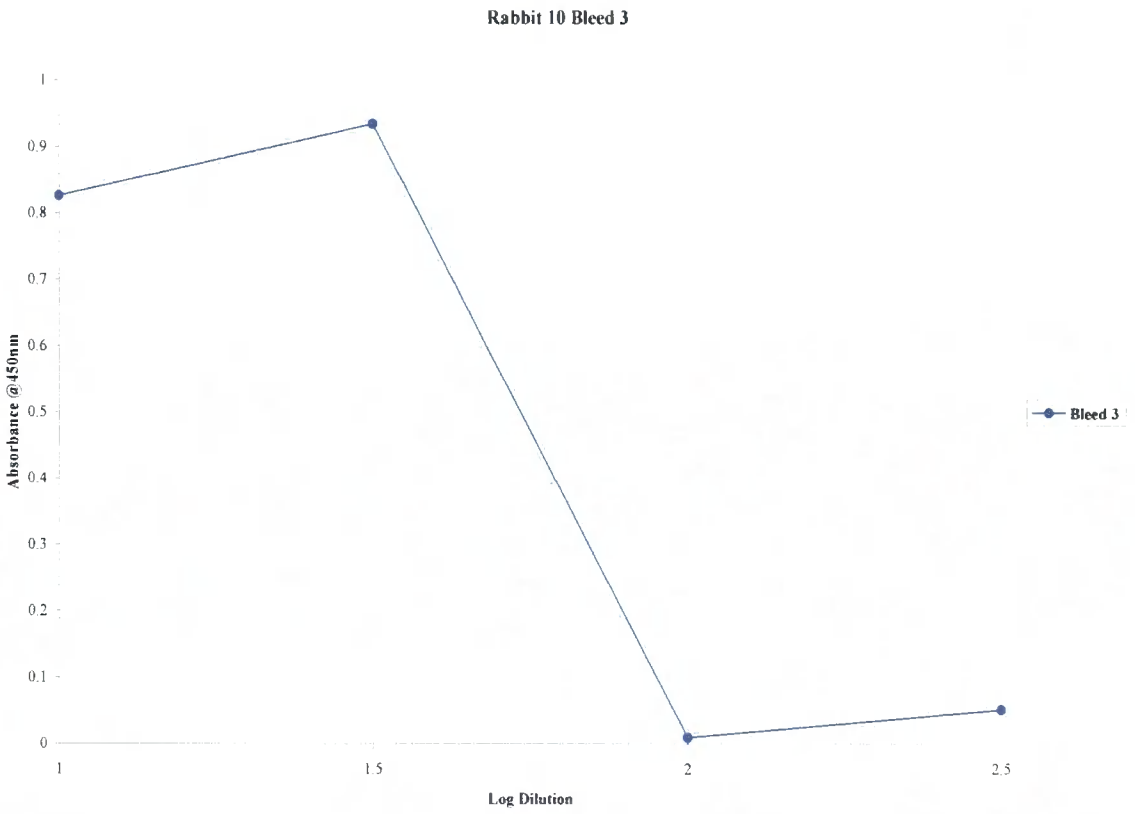

Figure 3.2.1.5 Graphical representation of ELISA data obtained for Rabbit 10 bleed 3.

Graph shows the absorbance @450nm of each dilution of serum from rabbit 10 bleed 3. Serum was incubated in semi-log dilution factors up to a maximal dilution factor of 1/31600 overnight at 4°C in wells containing bound peptide.

Titre of the antibody was determined as the dilution factor where the peak absorbance recorded had diminished 50%.

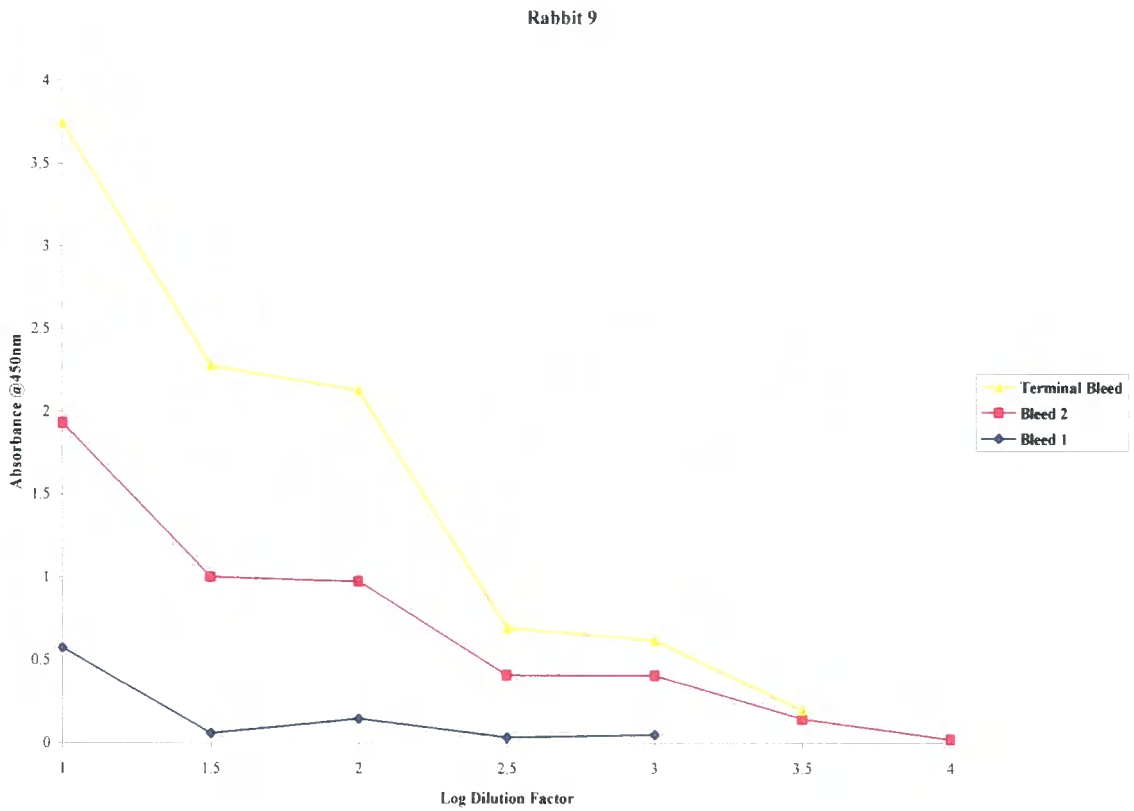

Figure 3.2.2 Graphical representation of ELISA data obtained for Rabbit 9 over the entire innoculation protocol.

Graph shows the absorbance @450nm of each dilution of serum from each bleed for a single antibody, in this case the TARP γ8 C-terminal directed antibody being generated by rabbit 9. Serum was incubated in semi-log dilution factors up to a maximal dilution factor of 1/31600 overnight at 4°C in wells containing bound peptide.

Titre of the antibody was determined as the dilution factor where the peak absorbance recorded had diminished 50%.

Figure 3.2.2 Summary table of approximate ELISA titres for each of the bleeds obtained from each rabbit.

Rabbit	TARP isoform	Bleed Number			
		1	2	3	4
		Titre (Approx)			
1	TARP γ2	1/200	1/200	1/200	1/500
2	TARP γ2	1/500	1/10000	1/5000	-
3	TARP γ3	1/10	1/10	1/200	1/1000
4	TARP γ3	1/20	1/200	1/100	-
5	TARP γ4	1/150	1/175	1/1500	-
6	TARP γ4	0	1/100	1/10	1/30
7	TARP γ8N	1/100	1/1000	1/1500	-
8	TARP γ8N	1/200	1/200	1/200	1/100
9	TARP γ8C	1/10	1/200	1/200	-
10	TARP γ8C	1/20	1/100	1/200	1/10

Table shows the approximate Titre obtained for each bleed taken from each rabbit. Titre was calculated using the graphical presentation of absorbance Vs dilution factor, as mentioned in Figure 3.2.1.1-10.

The ELISA data was used to indicate immune response in the rabbits and determine duration of the inoculation protocol.

The purpose of the ELISAs was to identify the level of immune response in each of the rabbits following inoculation with the peptide-adjuvant combination.

When the ELISA titre recorded remained static, or began to diminish, it was decided to administer the terminal bleed subsequent to the next inoculation, with one rabbit for each of the TARP isoform-specific antibodies being subjected to one further inoculation prior to terminal exsanguination.

As can be seen in Figures 3.2.1.1-10. 3.2.2, the titres recorded for each antibody were quite variable, with little comparison between the different TARP isoforms.

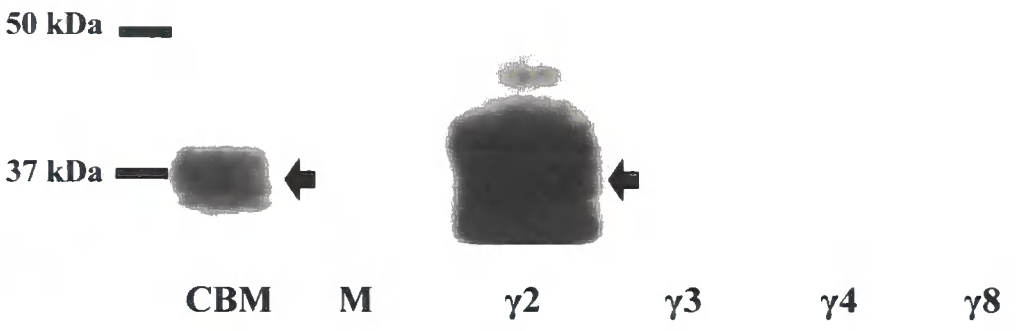

Figure 3.3.1 Screening the anti TARP γ2 antibody by Immunoblotting

Figure shows an immunoblot of a 10% SDS-PAGE gel loaded with 10 μg SDS-solubilised mouse cerebellum (CBM) and HEK293 cells transfected with either empty vector (M), or one of the four TARP isoforms; γ2, γ3, γ4 or γ8, then screened using the anti TARP γ2 antibody at 0.5μg/ml. The immunoreactive species of interest is indicated by the black arrows either in the native tissue sample (CBM) or the transfected HEK293 cells. The slightly higher molecular weight immunoreactive species in the γ2 transfected HEK293 cells is TARP γ2 subsequent to some form of post translational modification, which is has not been investigated in the context of this thesis.

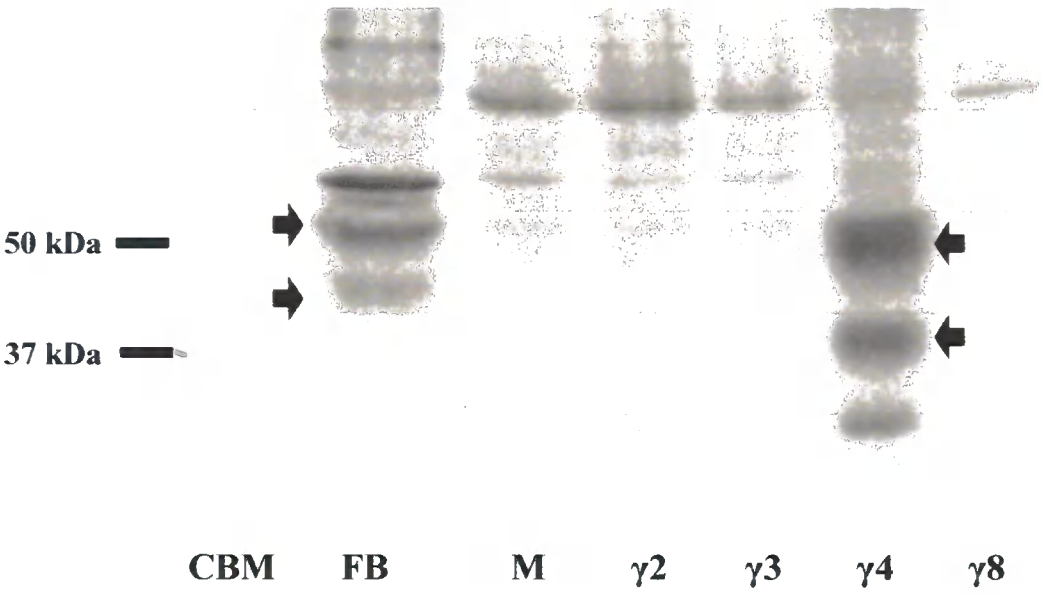

Figure 3.3.2 Screening the anti TARP γ4 antibody by Immunoblotting

Figure shows an immunoblot of a 10% SDS-PAGE gel loaded with 10 µg SDS-solubilised mouse cerebellum (CBM), forebrain (FB) and HEK293 cells transfected with either empty vector (M), or one of the four TARP isoforms; γ2, γ3, γ4 or γ8, then screened using the anti TARP γ4 antibody at 2µg/ml. Immunoreactive species of interest, corresponding to TARP γ4 can be seen, as indicated by the red arrows, in the FB and TARP γ4 transfected HEK293 cells.

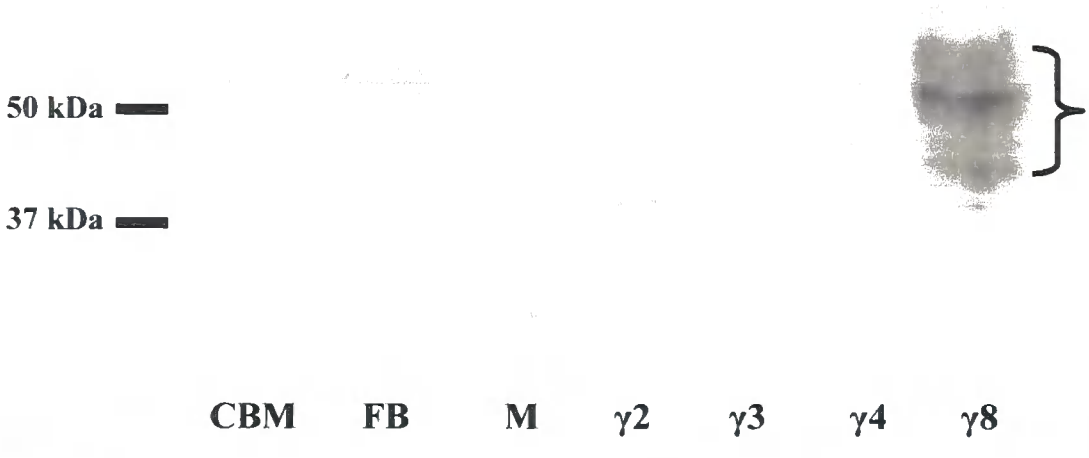

Figure 3.3.3 Screening the anti TARP γ8 N-terminal directed antibody by Immunoblotting

Figure shows an immunoblot of a 10% SDS-PAGE gel loaded with 10 µg SDS-solubilised mouse cerebellum (CBM), forebrain (FB) and HEK293 cells transfected with either empty vector (M), or one of the four TARP isoforms; γ2, γ3, γ4 or γ8, then screened using the anti TARP γ8 N-terminal directed antibody at 4µg/ml. Three diffuse bands, most likely corresponding to various post-translational states of TARP γ8, can be detected, as indicated by the bracket, in the TARP γ8 transfected HEK293 cells and very weakly within the FB sample.

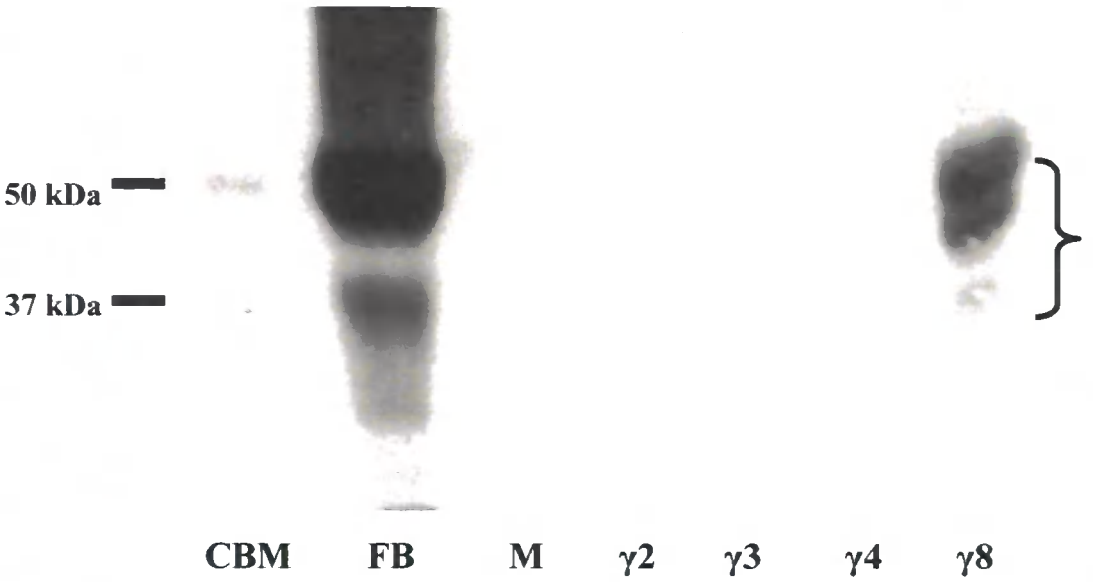

Figure 3.3.4 Screening the anti TARP γ8 C-terminal directed antibody by Immunoblotting

Figure shows an immunoblot of a 10% SDS-PAGE gel loaded with 10 µg mouse SDS-solubilised cerebellum (CBM), forebrain (FB) and HEK293 cells transfected with either empty vector (M), or one of the four TARP isoforms; γ2, γ3, γ4 or γ8, then screened using the anti TARP γ8 C-terminal directed antibody at 1µg/ml. Immunoreactive species corresponding to TARP γ8, within the region indicated by the bracket, but possessing different molecular weights – most likely as a consequence of post translational modification – can be detected within the CBM, FB and TARP γ8 transfected HEK293 cells.

The TARP isoform-specific antibodies were specific to the TARP isoform to which they were raised (Figure 3).

Figure 3.3.1 shows the TARP γ2 isoform-specific antibody generated when screened against recombinant cells expressing one of the TARP isoforms in addition to native CNS

tissue taken from the cerebellum of C3B6Fe+ mice. As this was the peptide used previously to generate a TARP γ2 specific antibody, it is little surprise that it appears to be highly specific, with detectable bands appearing at approximately 36-38 kDa in the CBM and 34-39 kDa in the recombinant TARP γ2 expressing cells. Most important is the absence of any detectable bands in the cells transfected with other TARP isoforms.

Figure 3.3.2 shows the TARP γ4 isoform-specific antibody generated when screened against recombinant cells expressing one of the TARP isoforms in addition to material taken from both the forebrain and cerebellum of C3B6 mice. Forebrain was included as a native CNS tissue in this screen due to the published evidence suggesting TARP γ4 is diffuse throughout the mouse brain, at least at the mRNA level (Tomita et al. 2004).
As can be seen, three major, specific immunoreactive species can be seen (20, 37 and 50 kDa) in the TARP γ4 transfected recombinant cells, with the 50kDa band also being detectable in the forebrain sample.

The abnormal nature of expression within HEK293 cells, a cell type where mouse TARP γ4 shouldn't typically be expressed, might also explain the multiple immunoreactive species detected, with the high levels of TARP γ4 being expressed, potentially activating cellular defences against protein aggregation. The non-specific binding displayed in the HEK293 cells appears to correspond to proteins not typically found within the mouse CNS, but further investigation would be required to determine their identity. In mouse CNS the TARP γ4 immunoreactive species do not fully align with those detected in the TARP γ4 transfected HEK293 cells, speculatively due to post-translational modification of the protein, the precise nature of which is currently unknown but would likely include different phosporylation states (H Payne, unpublished).

Figure 3.3.3 shows the antibody generated using TARP γ8 N-terminal peptide. As with the TARP γ4, it displays some low-level non-specific labelling detectable in the recombinant cell samples. Three major, specific immunoreactive species are detected (molecular weights ranging from 40-60 kDa) in the TARP γ8 expressing cells. The single

immunoreactive band detected in the CNS tissues corresponds in molecular weight (~55 kDa) to the strongest labelled band in the TARP γ8 expressing cells. Again reference can be made to the multiple immunoreactive species present being due to possible phosphorylation states, a common feature with the various TARP isoforms studied in the lab (H Payne, unpublished).

Figure 3.3.4 Shows the antibody generated using the TARP γ8 C-terminal peptide. As can be clearly seen, of the recombinant cells, only the TARP γ8 expressing cells show any labelling, a band of approximately 55 kDa being prevalent, which corresponds to the bands detected in the CNS tissues. As with the other TARP antibodies, this immunoblot demonstrates that the antibody generated is highly specific to the TARP isoform it was generated towards.

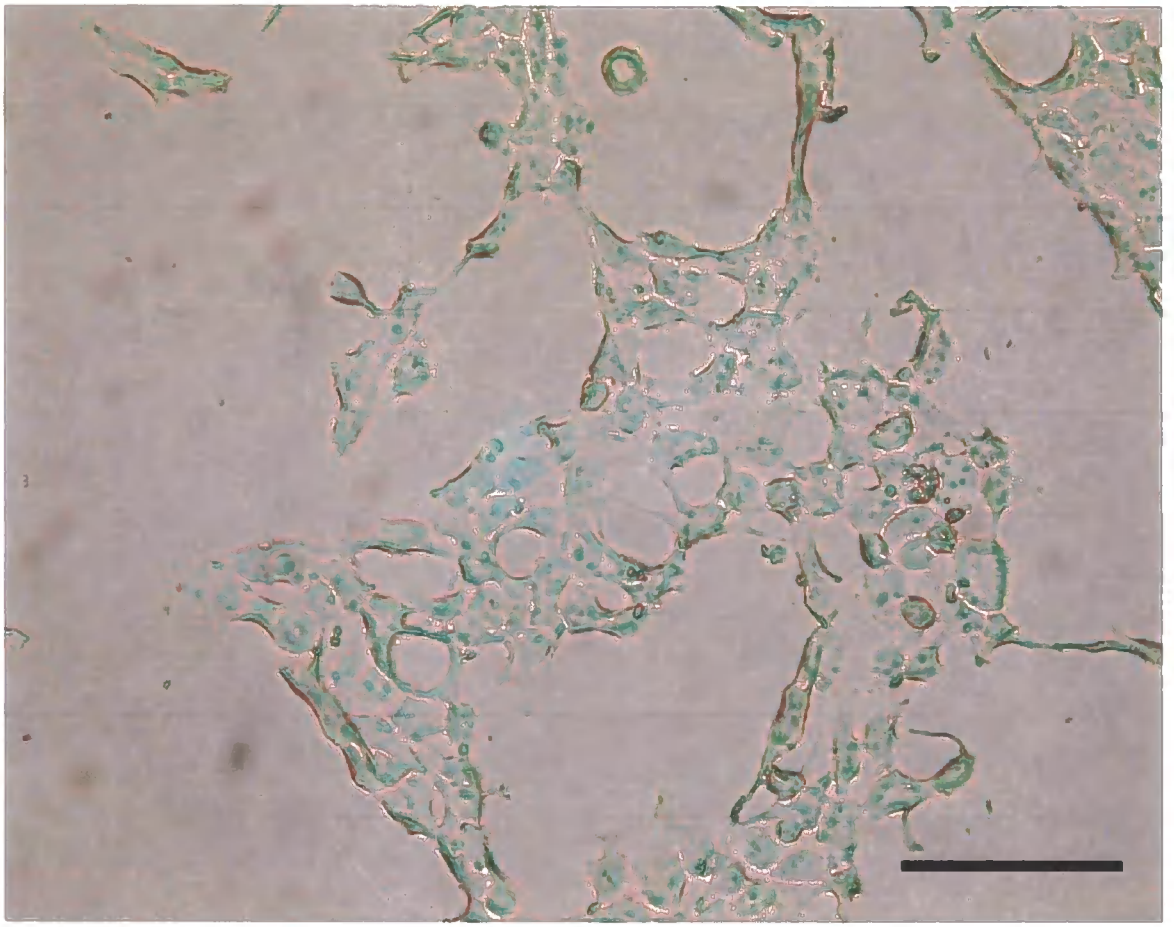

Figure 3.4.1 Screening the anti-TARP γ4 antibody using heterologous cells transfected with an empty vector.

HEK293 cells transfected with an empty vector – effectively a mock transfection. Cells were cultured on a glass coverslip for two weeks before being fixed with 4% paraformaldehyde and subjected to immunocytochemistry. Cells were probed with the anti-TARP γ4 antibody at a dilution of 0.5μg/ml, shown at 200X magnification. Scale bar = 100 μm.

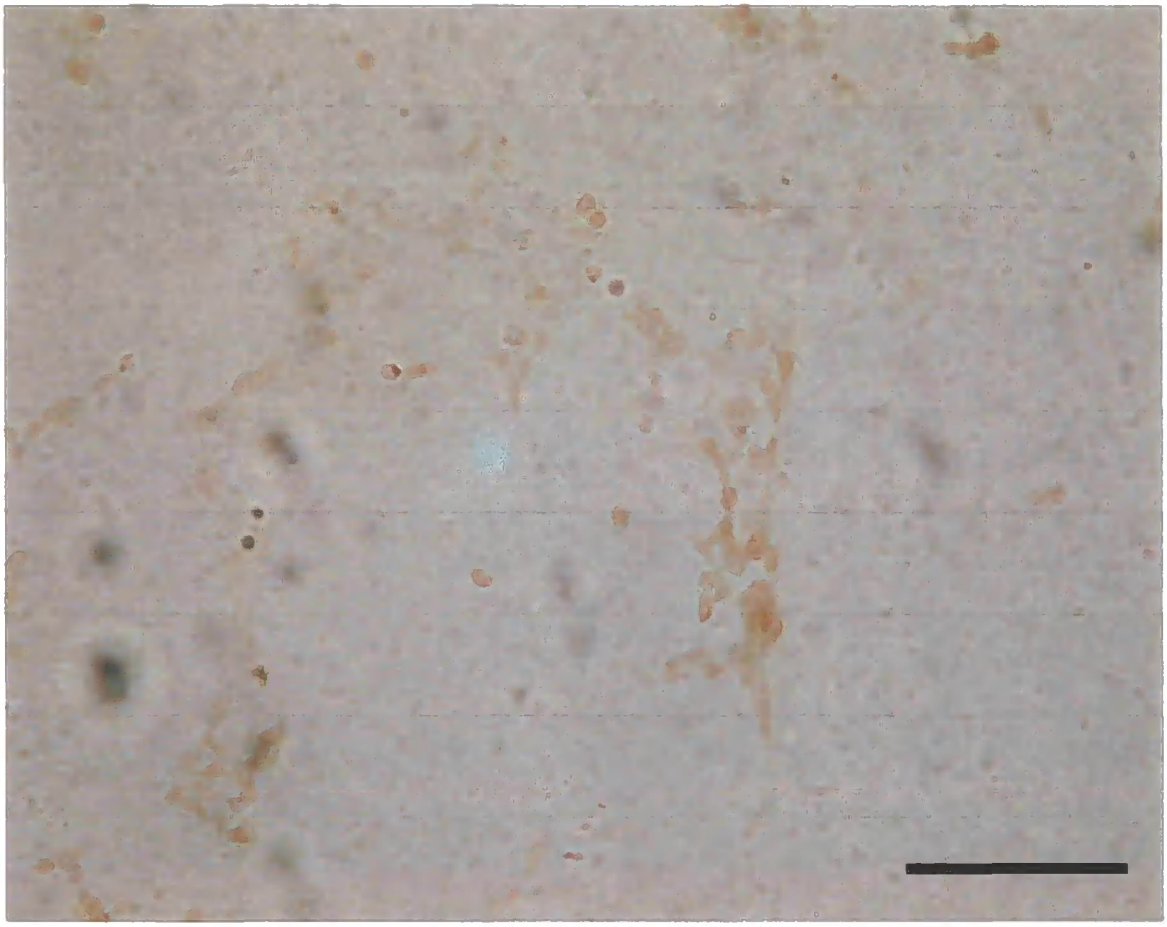

Figure 3.4.2 Screening the anti-TARP γ4 antibody using heterologous cells transfected with the TARP γ2 isoform.

HEK293 cells transfected with the TARP γ2 isoform. Cells were cultured on a glass coverslip for two weeks before being fixed with 4% paraformaldehyde and subjected to immunocytochemistry. Cells were probed with the anti-TARP γ4 antibody at a dilution of 0.5μg/ml, shown at 200X magnification. Scale bar = 100 μm.

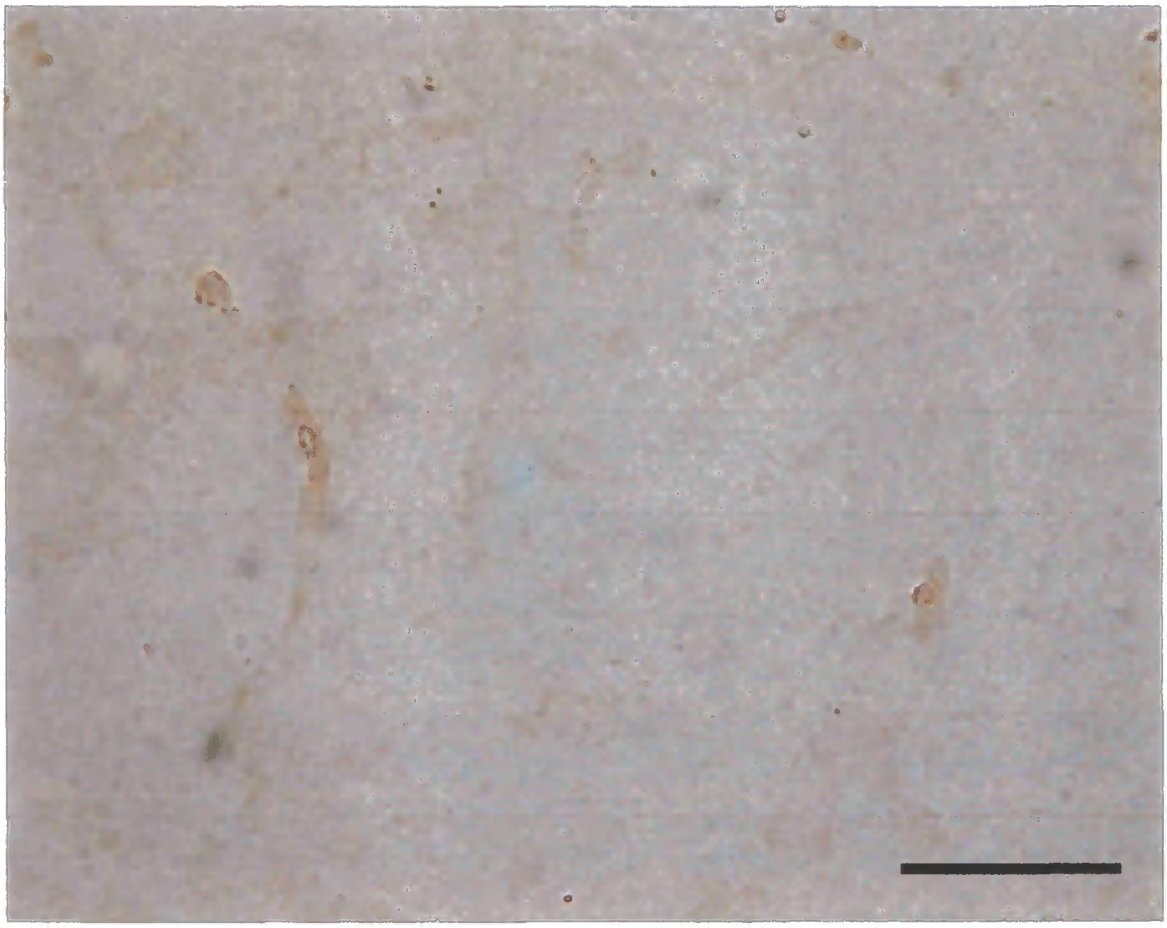

Figure 3.4.3 Screening the anti-TARP γ4 antibody using heterologous cells transfected with the TARP γ3 isoform.

HEK293 cells transfected with the TARP γ3 isoform. Cells were cultured on a glass coverslip for two weeks before being fixed with 4% paraformaldehyde and subjected to immunocytochemistry. Cells were probed with the anti-TARP γ4 antibody at a dilution of 0.5μg/ml, shown at 200X magnification. Scale bar = 100 μm.

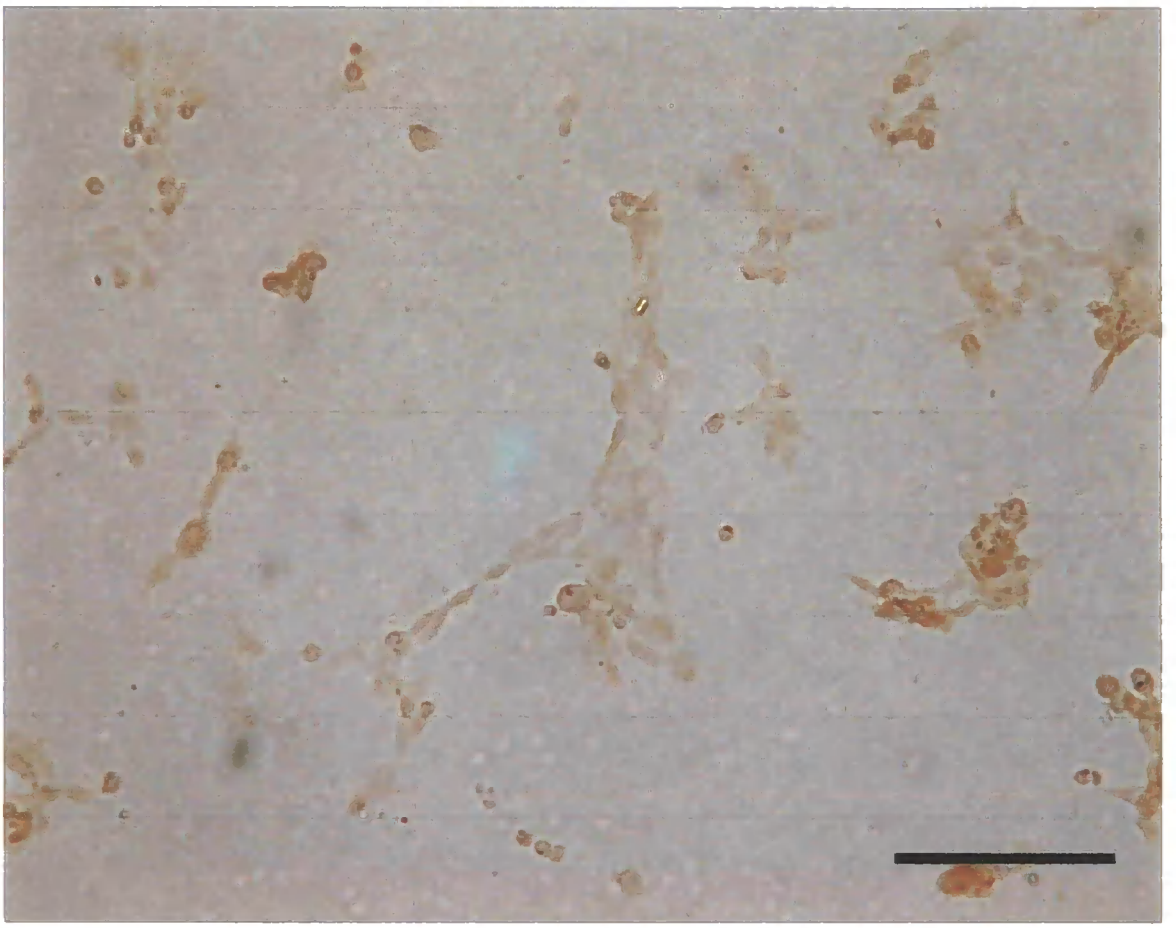

Figure 3.4.4 Screening the anti-TARP γ4 antibody using heterologous cells transfected with the TARP γ8 isoform.

HEK293 cells transfected with the TARP γ8 isoform. Cells were cultured on a glass coverslip for two weeks before being fixed with 4% paraformaldehyde and subjected to immunocytochemistry. Cells were probed with the anti-TARP γ4 antibody at a dilution of 0.5μg/ml, shown at 200X magnification. Scale bar = 100 μm.

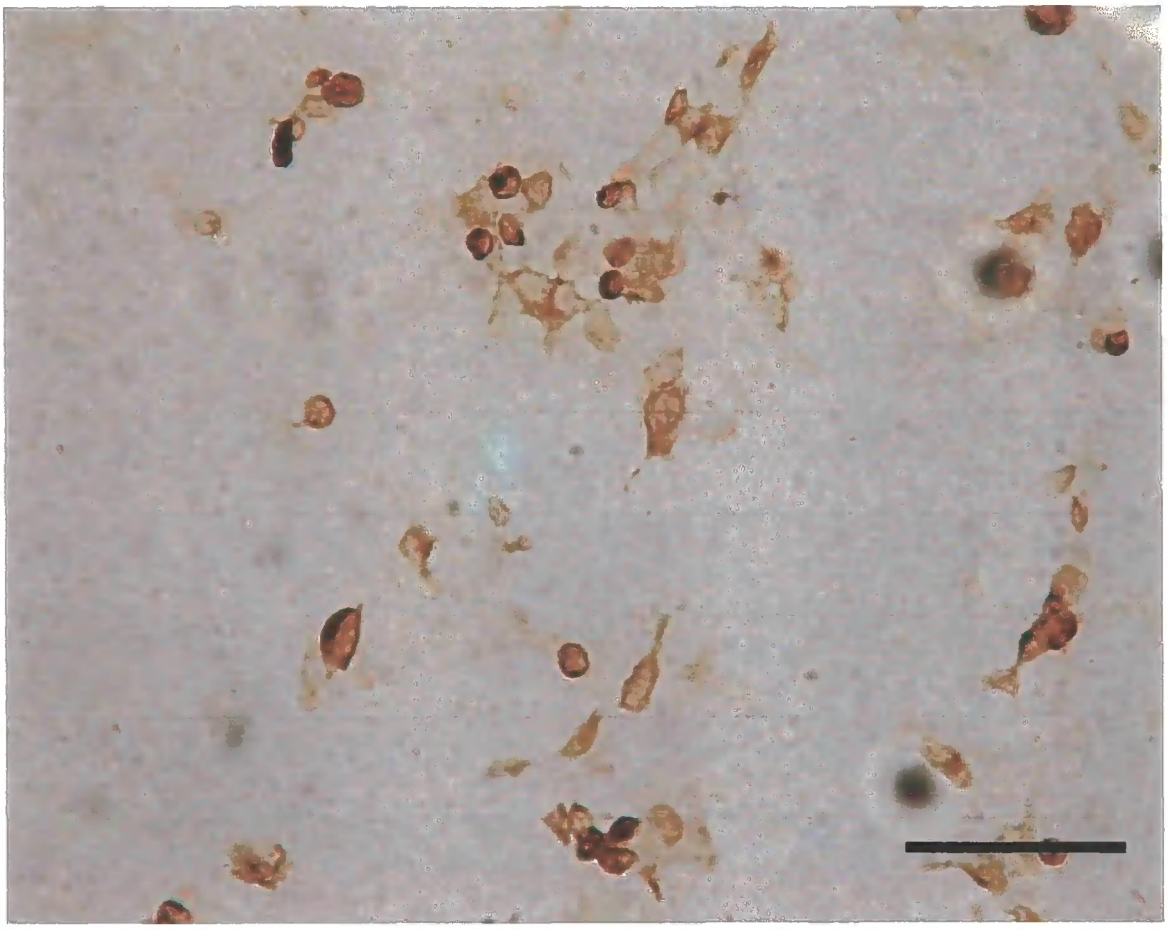

Figure 3.4.5 Screening the anti-TARP γ4 antibody using heterologous cells transfected with the TARP γ4 isoform.

HEK293 cells transfected with the TARP γ4 isoform. Cells were cultured on a glass coverslip for two weeks before being fixed with 4% paraformaldehyde and subjected to immunocytochemistry. Cells were probed with the anti-TARP γ4 antibody at a dilution of 0.5μg/ml, shown at 200X magnification. Scale bar = 100 μm.

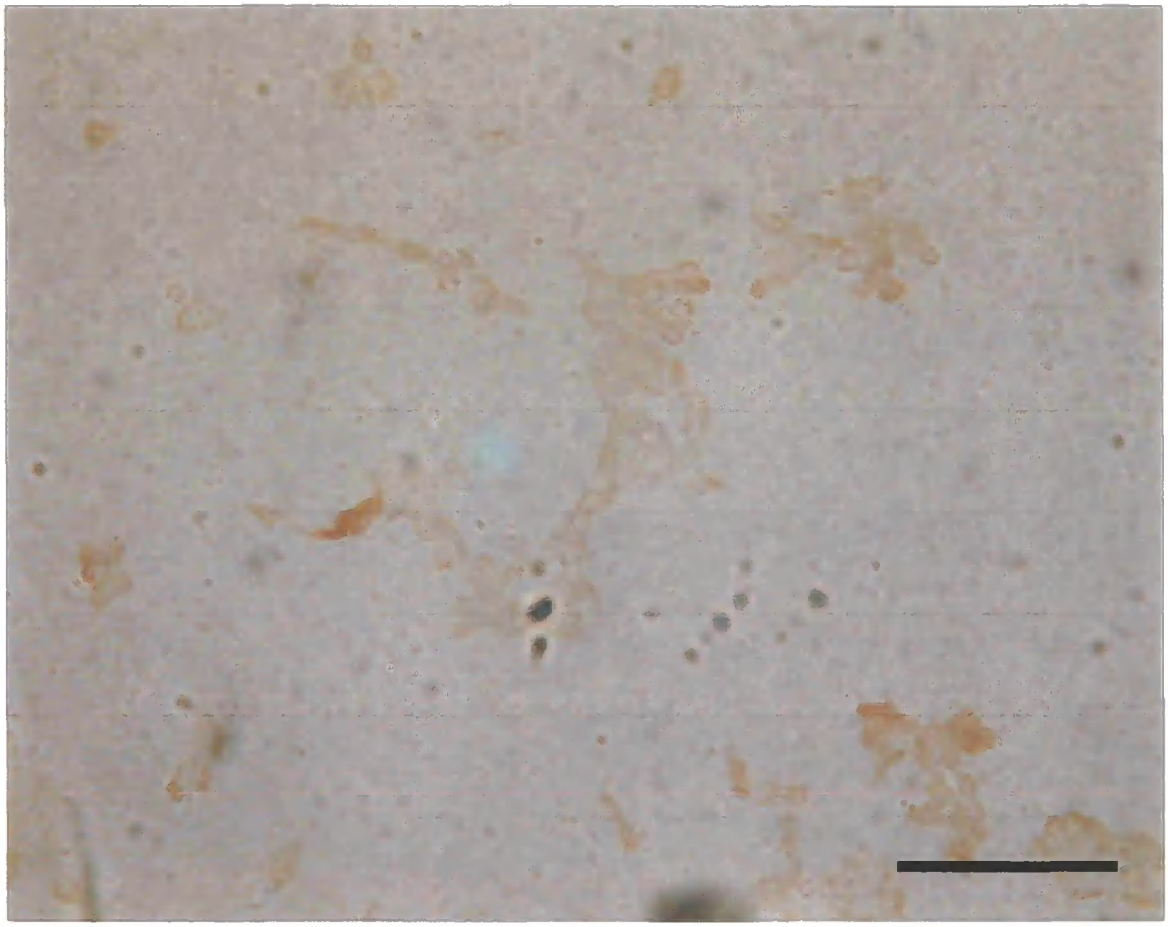

Figure 3.4.6 Screening the anti-TARP γ4 antibody using TARP γ4 expressing heterologous cells, following peptide block.

HEK293 cells transfected with the TARP γ4 isoform. Cells were cultured on a glass coverslip for two weeks before being fixed with 4% paraformaldehyde and subjected to immunocytochemistry. Cells were probed with the anti-TARP γ4 antibody at a dilution of 0.5μg/ml that had been incubated overnight with 1.25μg/ml of the TARP γ4 peptide, shown at 200X magnification. Scale bar = 100 μm.

The antibody generated using the TARP γ4 shows suitability for use in immunocytochemistry, with demonstrable specificity for recombinant cells expressing the TARP γ4 isoform but not recombinant cells expressing other TARP isoforms or empty vector (Figure 4).

Figure 3.4.1 shows recombinant cells expressing empty vector probed using the antibody generated using the TARP γ4 peptide. The absence of any detectable labelling, indicates that the weak non-specific labelling detected by immunoblotting is not detectable in immunocytochemisty.

Figures 3.4.2-4.4 show recombinant cells expressing TARP isoforms γ2, γ3 and γ8 respectively, display very low background labelling. This is easily distinguished with Figure 3.4.5 showing the TARP γ4 expressing recombinant cells labelled with the anti TARP γ4 antibody, these cells displaying noticeably intense labelling, which is abolished when pre-blocked using the TARP γ4 peptide as shown in Figure 3.4.6, indicating that the antibody is specific not only for the TARP, but also to the peptide used in its generation.

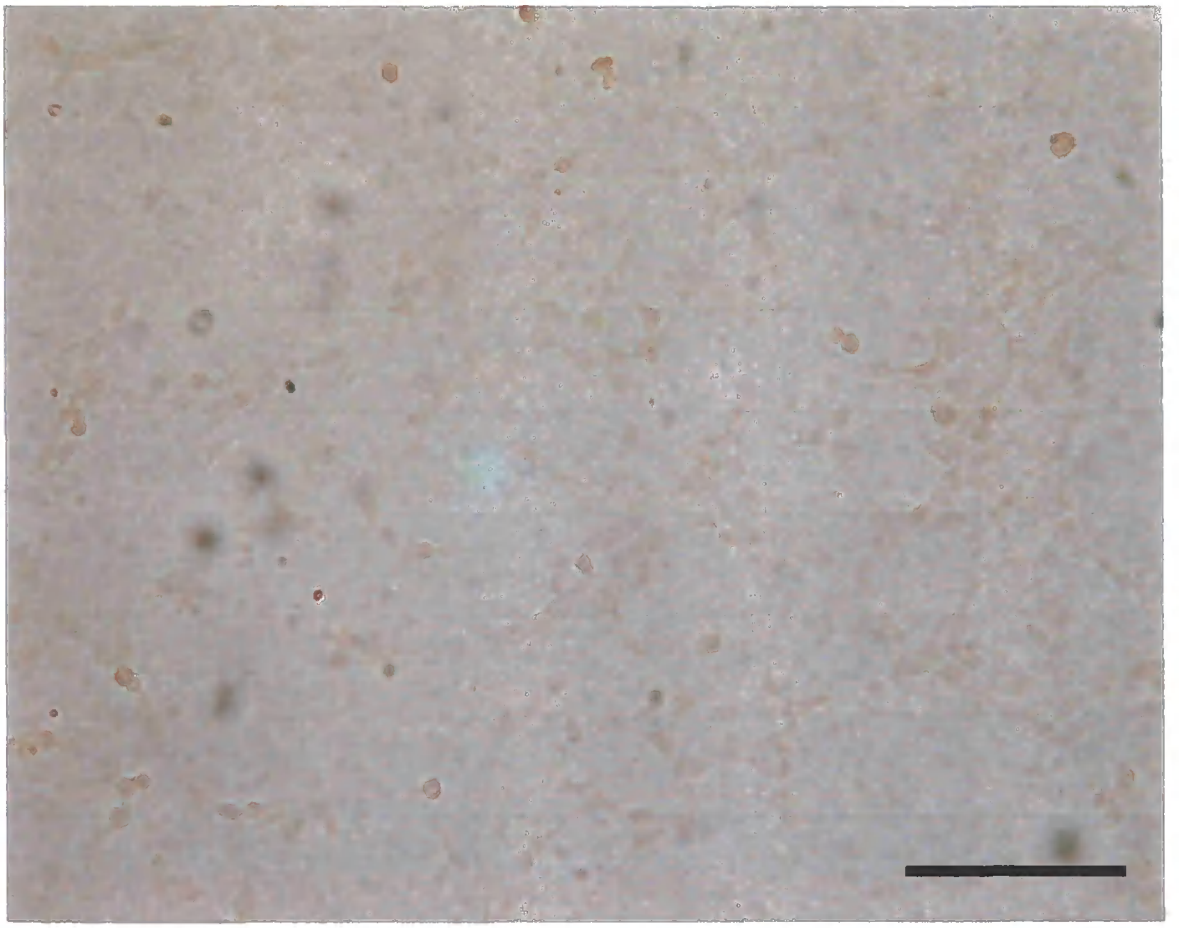

Figure 3.5.1 Screening the anti-TARP γ8 C-terminal directed antibody using heterologous cells transfected with an empty vector.

HEK293 cells transfected with an empty vector – effectively a mock transfection. Cells were cultured on a glass coverslip for two weeks before being fixed with 4% paraformaldehyde and subjected to immunocytochemistry. Cells were probed with the anti-TARP γ8 C-terminal directed antibody at a dilution of 0.0625μg/ml, shown at 200X magnification. Scale bar = 100 μm.

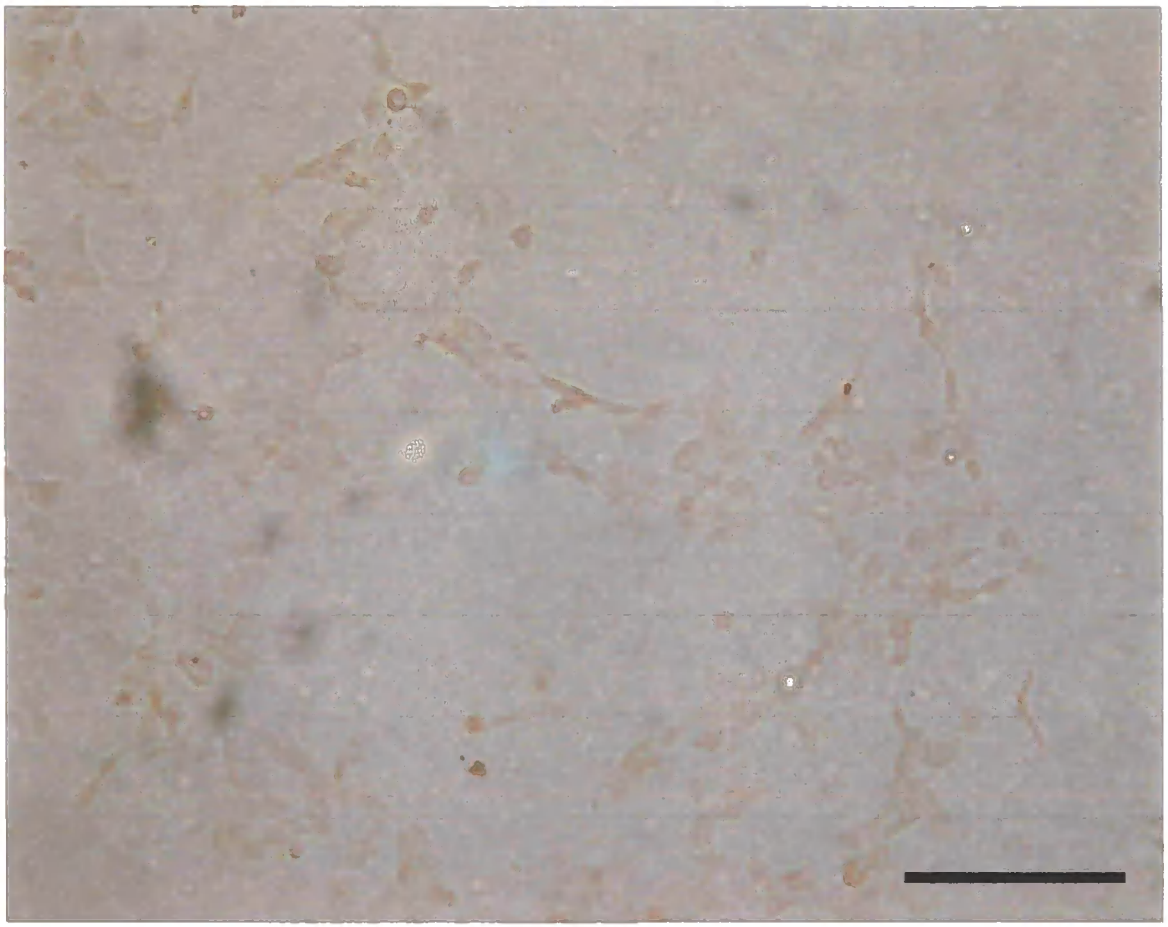

Figure 3.5.2 Screening the anti-TARP γ8 C-terminal directed antibody using TARP γ2 expressing heterologous cells.

HEK293 cells transfected with the TARP γ2 isoform. Cells were cultured on a glass coverslip for two weeks before being fixed with 4% paraformaldehyde and subjected to immunocytochemistry. Cells were probed with the anti-TARP γ8 C-terminal directed antibody at a dilution of 0.0625μg/ml, shown at 200X magnification. Scale bar = 100 μm.

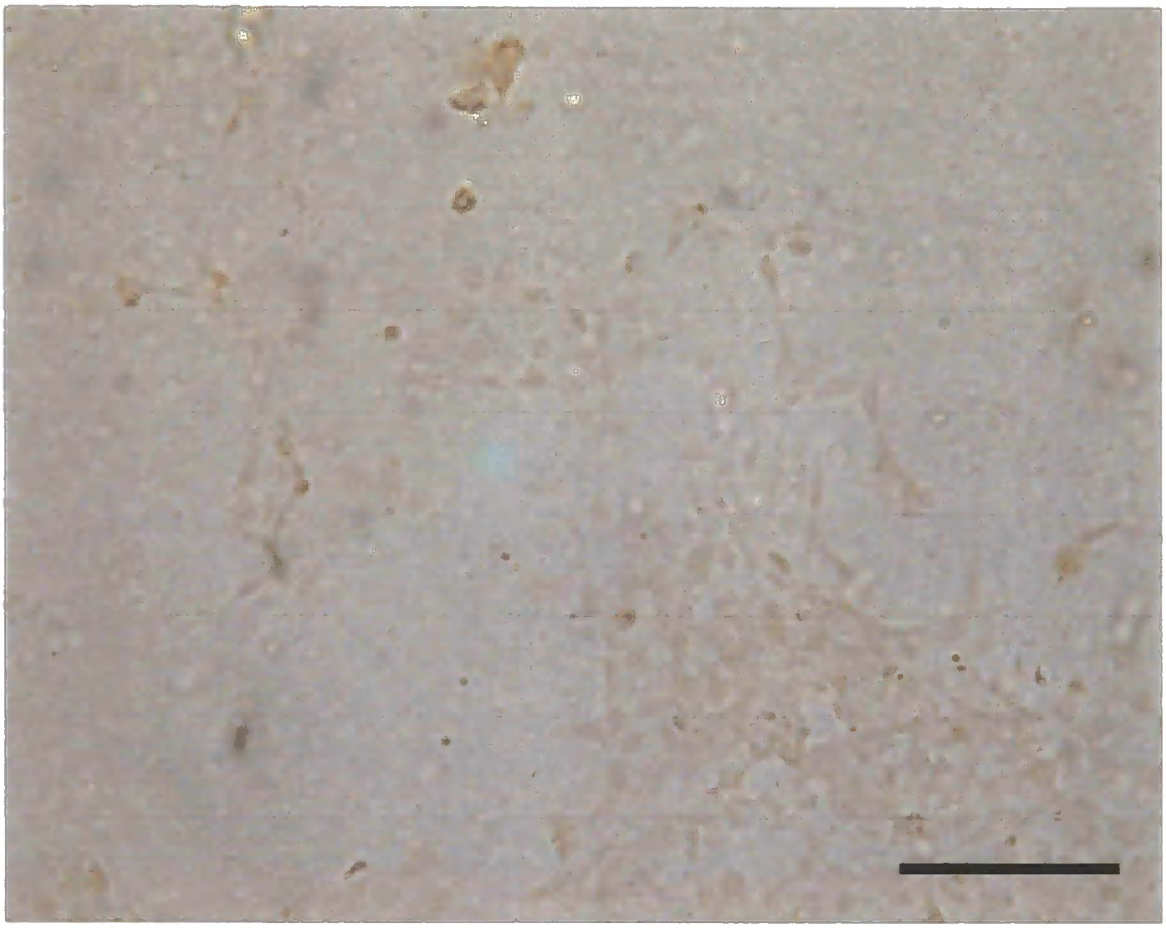

Figure 3.5.3 Screening the anti-TARP γ8 C-terminal directed antibody using TARP γ3 expressing heterologous cells.

HEK293 cells transfected with the TARP γ3 isoform. Cells were cultured on a glass coverslip for two weeks before being fixed with 4% paraformaldehyde and subjected to immunocytochemistry. Cells were probed with the anti-TARP γ8 C-terminal directed antibody at a dilution of 0.0625μg/m, shown at 200X magnification. Scale bar = 100 μm.

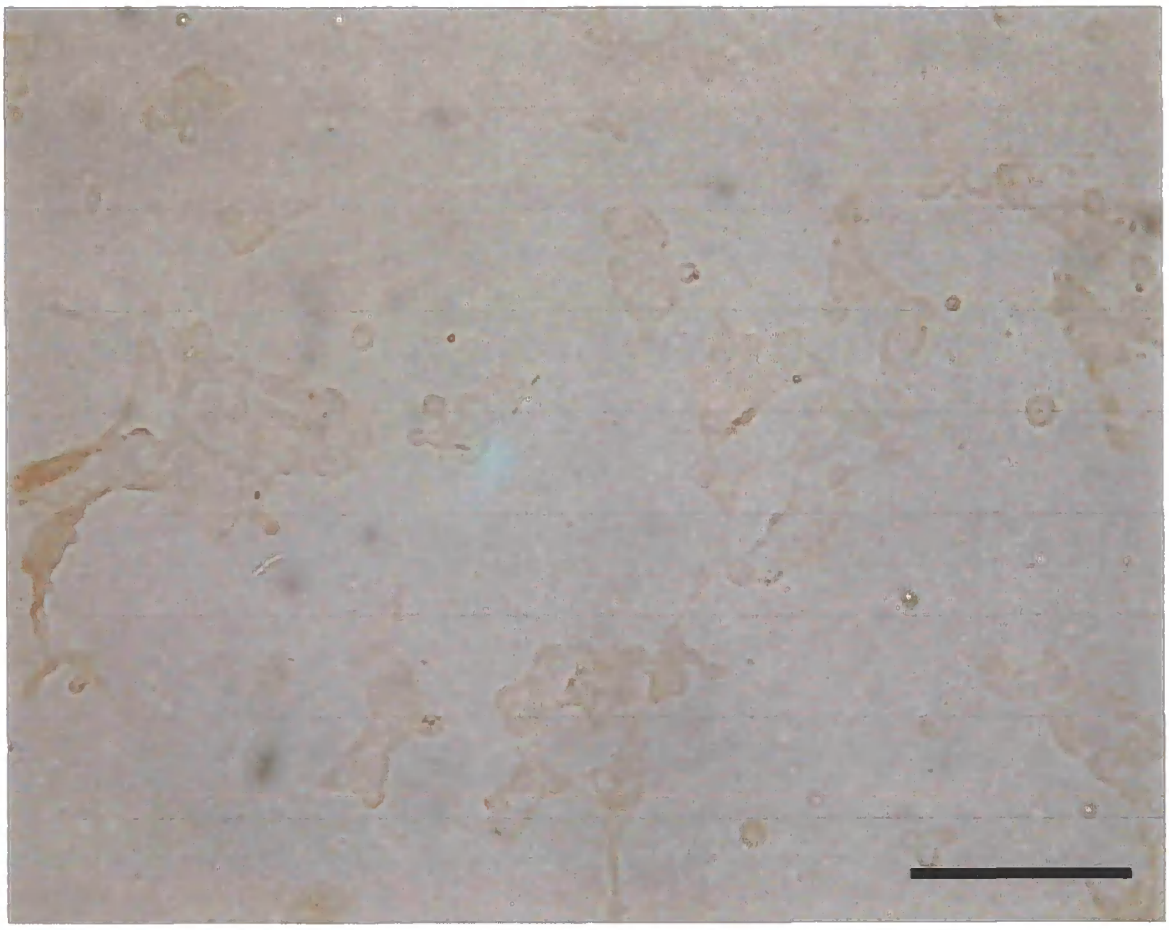

Figure 3.5.4 Screening the anti-TARP γ8 C-terminal directed antibody using TARP γ4 expressing heterologous cells.

HEK293 cells transfected with the TARP γ4 isoform. Cells were cultured on a glass coverslip for two weeks before being fixed with 4% paraformaldehyde and subjected to immunocytochemistry. Cells were probed with the anti-TARP γ8 C-terminal directed antibody at a dilution of 0.0625μg/ml, shown at 200X magnification. Scale bar = 100 μm.

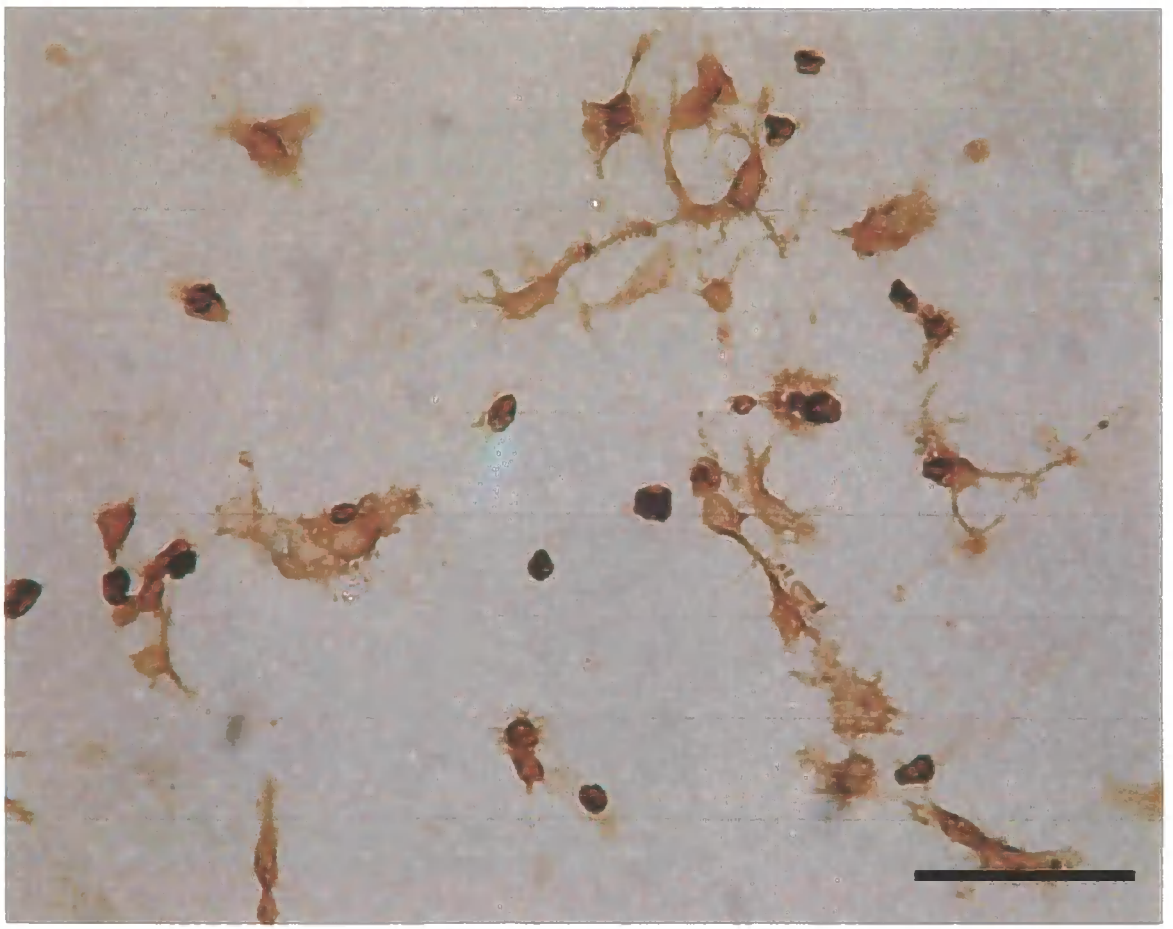

Figure 3.5.5 Screening the anti-TARP γ8 C-terminal directed antibody using TARP γ8 expressing heterologous cells.

HEK293 cells transfected with the TARP γ8 isoform. Cells were cultured on a glass coverslip for two weeks before being fixed with 4% paraformaldehyde and subjected to immunocytochemistry. Cells were probed with the anti-TARP γ8 C-terminal directed antibody at a dilution of 0.0625μg/ml, shown at 200X magnification. Scale bar = 100 μm.

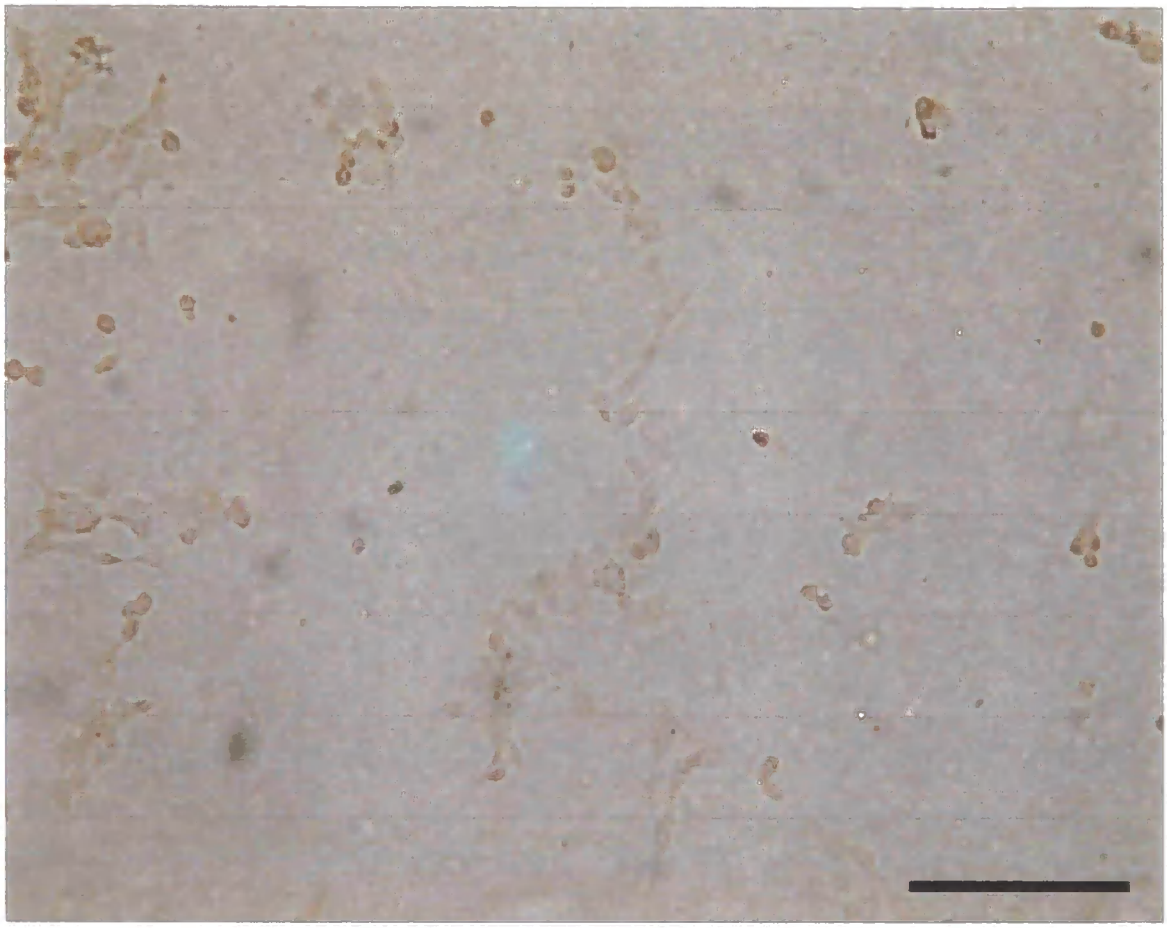

Figure 3.5.6 Screening the anti-TARP γ8 C-terminal directed antibody using TARP γ8 expressing heterologous cells, following peptide block.

HEK293 cells transfected with the TARP γ8 isoform. Cells were cultured on a glass coverslip for two weeks before being fixed with 4% paraformaldehyde and subjected to immunocytochemistry. Cells were probed with the anti-TARP γ8 C-terminal directed antibody at a dilution of 0.0625μg/ml that had been incubated overnight with 0.3125μg/ml of the TARP γ8 C-terminal peptide, shown at 200X magnification. Scale bar = 100 μm.

Figures 3.5.1-5.6

These Figures show the immunocytochemical screening of the TARP γ8 C-terminal directed antibody against HEK293 cells transfected with either empty vector (3.5.1) or one of the following four TARP isoforms; γ2 (3.5.2), γ3 (3.5.3), γ4 (3.5.4), γ8 (3.5.5). As can be seen, the TARP γ8 C-terminal directed antibody demonstrates a high degree of specificity for the HEK293 cells expressing the TARP γ8 isoform, with no significant labelling of the HEK cell expressing any of the other TARP isoforms or the empty vector, further supporting the data provided by immunoblotting to screen the antibody.

To confirm specificity, the antibody was also subjected to a peptide block protocol, whereby the working concentration of the TARP γ8 C-terminal directed antibody was incubated with a concentration of the TARP γ8 C-terminal peptide that was effectively five times the working concentration of antibody, overnight at 4°C. This peptide blocked antibody was then used in immunocytochemistry alongside the non-peptide blocked TARP γ8 C-terminal directed antibody.

As can be seen in the TARP γ8 transfected HEK293 cells probed with the peptide blocked antibody (3.5.6) there is no discernable labelling compared with the mock transfected (3.5.1) HEK293 cells, confirming that this labelling is specific both to the peptide the antibody was raised to, but also to the TARP isoform that the peptide was derived from.

The TARP γ8 C-terminal directed antibody shows suitability for immunocytochemistry with highly specific labelling of recombinant cells expressing the TARP γ8 isoform compared with recombinant cells expressing other TARP isoforms (Figure 3.5).

As with the TARP γ4 specific antibody, the antibody generated using the C-terminal peptide of the TARP γ8 isoform demonstrates very low background labelling of recombinant cells expressing either empty vector, or other TARP isoforms, as shown in Figures 3.5.1-5.4. Figure 5.5 shows a clearly apparent specific labelling of the TARP γ8 expressing recombinant cells which when coupled with the Figure 3.5.6 peptide block

data indicates that the TARP γ8 c-terminal directed antibody is highly specific to the TARP γ8 C-terminal peptide to which it was generated.

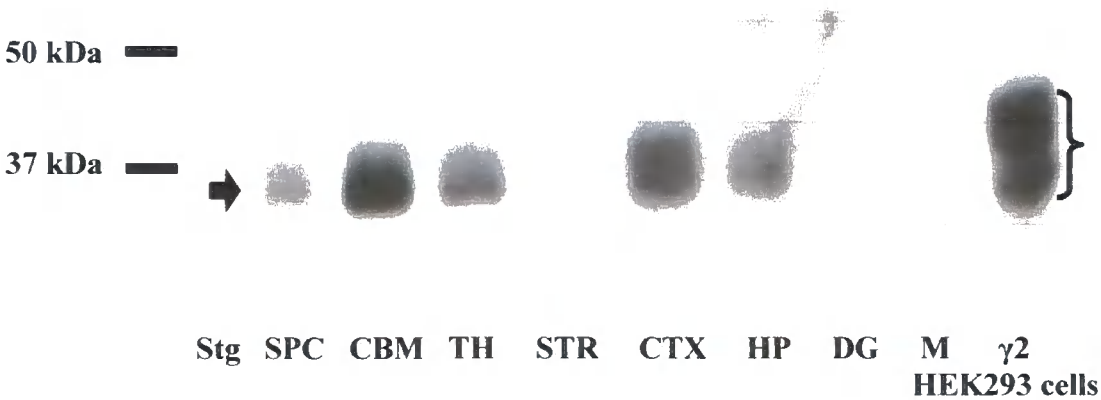

Figure 3.6.1 Immunoblot showing distribution of the TARP γ2 isoform across a range of dissected CNS tissue probed with the anti TARP γ2 isoform specific antibody.

All tissues were solubilised in SDS-solubilising buffer (see methods) before being precipitated using chloroform-methanol precipitation into 150μl 2X SDS-PAGE sample buffer, with 10μg of each were loaded onto a 10% SDS-PAGE gel. *Stargazer* cerebellum (stg) was used as a negative control. Wild type tissues loaded; Spinal cord (SPC); Cerebellum (CBM); Thalamus (TH); Striatum (STR); Cerebral cortex (CTX); Hippocampus (HP); Dentate gyrus (DG). HEK293 cells transfected with either empty vector (M) or the TARP γ2 isoform were also loaded. Immunoreactive bands corresponding to TARP γ2 are indicated by the black arrows, or the bracket in the TARP γ2 transfected HEK293 cells.

CNS Region	SPC	CBM	TH	STR	CTX	HP	DG
Relative amount of TARP γ2	++	++++	++	+	+++	++	-

Figure 3.6.2 Table showing relative TARP γ2 amounts across the range of dissected tissues.

Samples were SDS-solubilised, with relative amounts being determined by the intensity of bands detected by immunoblotting in relation to one another.

TARP γ2 is detectable in a range of CNS tissues.

As shown by Figure 3.6.1, TARP γ2 is detectable by immunoblotting in all of the CNS tissues dissected, except for the dentate gyrus, and is most concentrated in the cerebellum, but also detectable at high levels in the cerebral cortex and thalamus. It is also detectable at modest levels in the spinal cord and hippocampal formation.

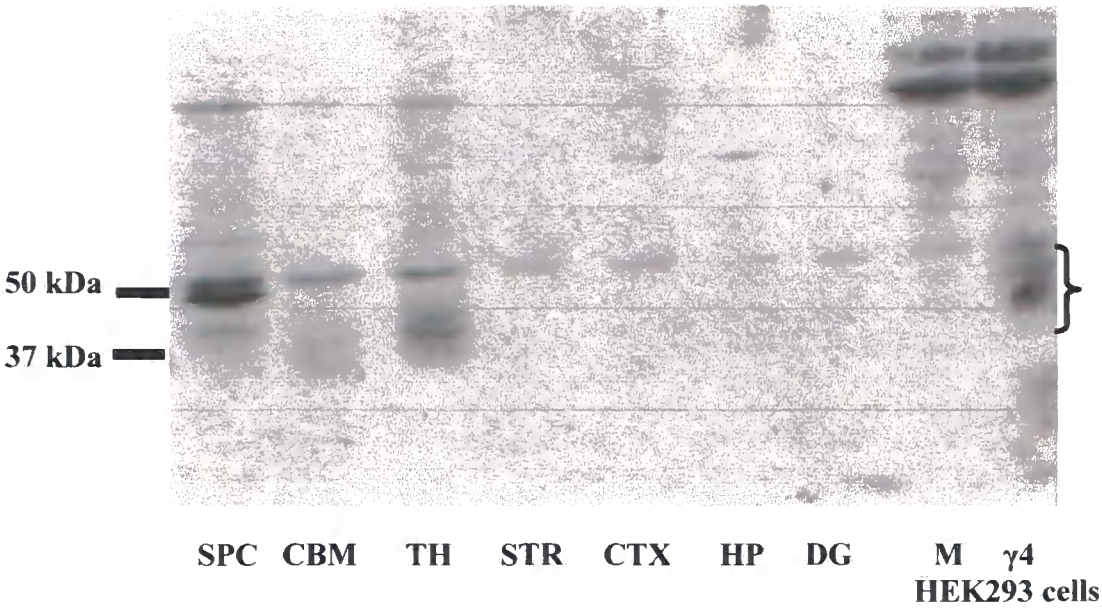

Figure 3.7.1 Immunoblot showing distribution of the TARP γ4 isoform across a range of dissected CNS tissue when probed with the anti TARP γ4 isoform specific antibody.

All tissues were solubilised in SDS-solubilising buffer (see methods) before being precipitated into 150µl 2X SDS-PAGE sample buffer, with 10µg of each were loaded onto a 10% SDS-PAGE gel. Wild type tissues loaded; Spinal cord (SPC); Cerebellum (CBM); Thalamus (TH); Striatum (STR); Cerebral cortex (CTX); Hippocampus (HP); Dentate gyrus (DG). HEK293 cells transfected with either empty vector (M) or the TARP γ4 isoform were also loaded. Anti TARP γ4 antibody used was from an earlier bleed to that used in Figure 3.3.2 (That bleed was used for generation of a TARP γ4 immunoaffinity column), so there are some differences in affinity and appearance of immunoreactive species. Immunoreactive species corresponding to TARP γ4 are indicated by the brackets.

CNS Region	SPC	CBM	TH	STR	CTX	HP	DG
Relative amount of TARP γ4	+	+	++	-	+/-	+/-	-

Figure 3.7.2 Table showing relative TARP γ4 amounts across the range of dissected tissues.

Samples were SDS-solubilised, with relative amounts being determined by the intensity of bands detected by immunoblotting in relation to one another.

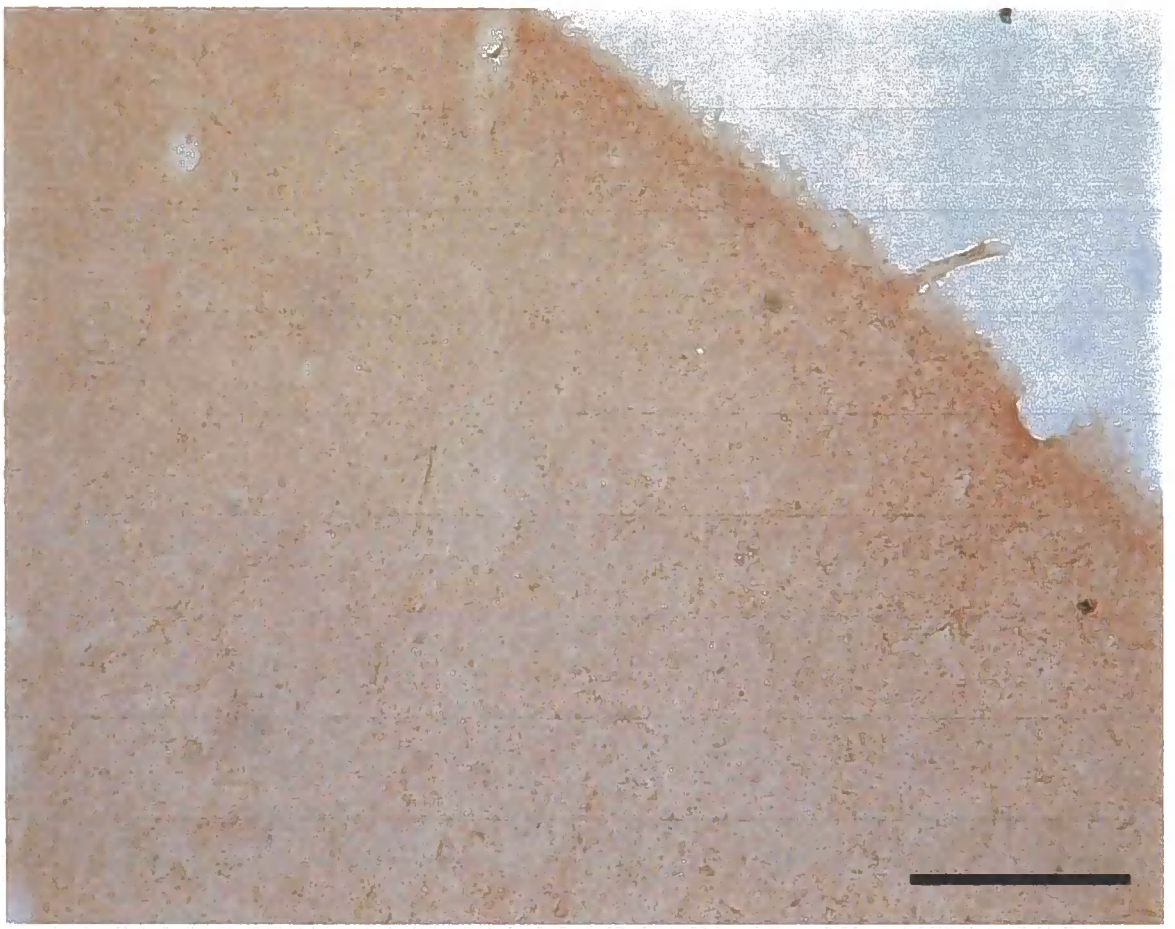

Figure 3.7.3.1 Immunohistochemical mapping of the TARP γ4 isoform in the cerebral cortex.

Brain was fixed with 4% (w/v) paraformaldehyde and subsequently cut into 30μm sections. Tissue is labelled with the anti-TARP γ4 antibody at 0.5μg/ml working concentration.

Image shows cerebral cortex at 200X magnification, taken from the approximate location of frontal cortex area 3. Scale bar = 100 μm.

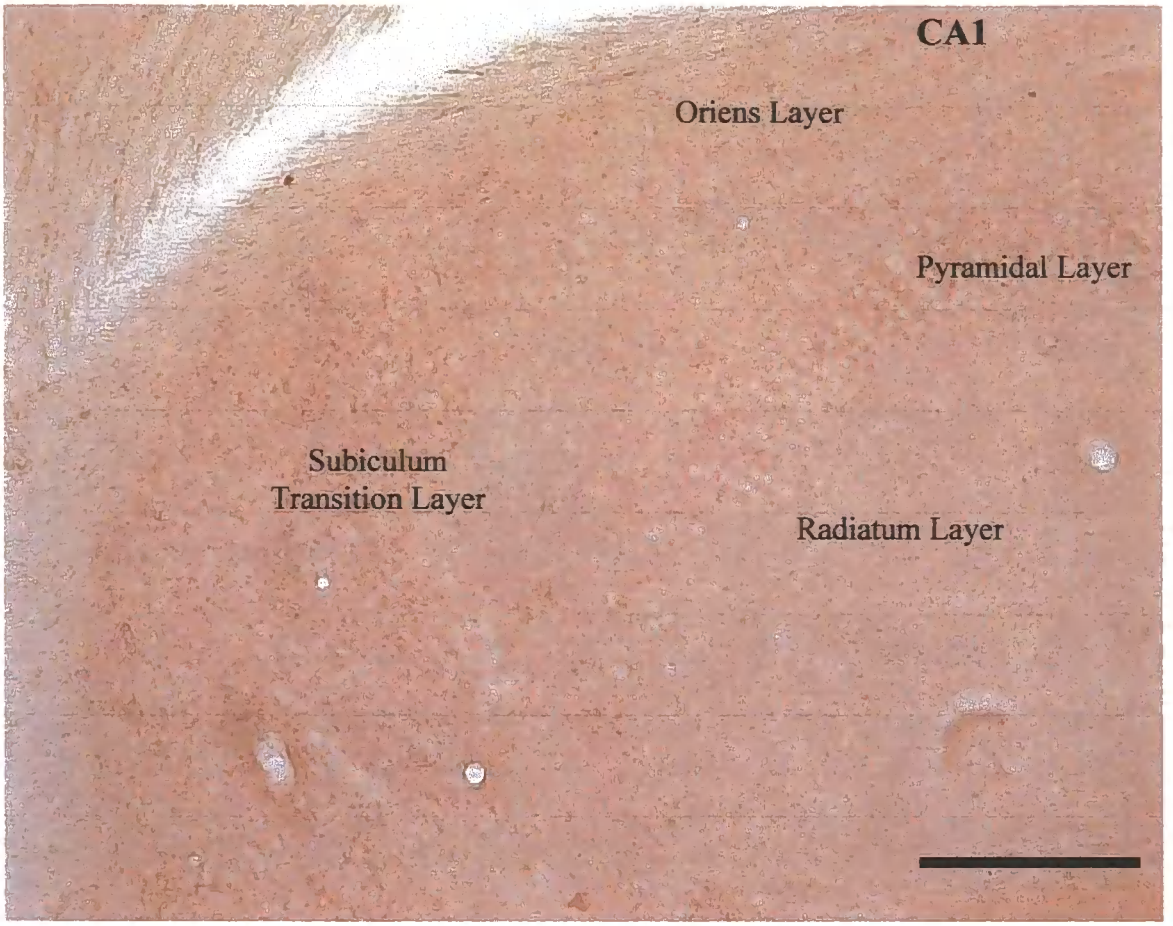

Figure 3.7.3.2 Immunohistochemical mapping of the TARP γ4 isoform in the hippocampal formation (1).

Tissue was fixed in 4% (w/v) paraformaldehyde and probed with the anti-TARP γ4 antibody at a 0.5μg/ml working concentration.

Image shows the hippocampus at the CA1 location at 200X magnification. Scale bar = 100 μm.

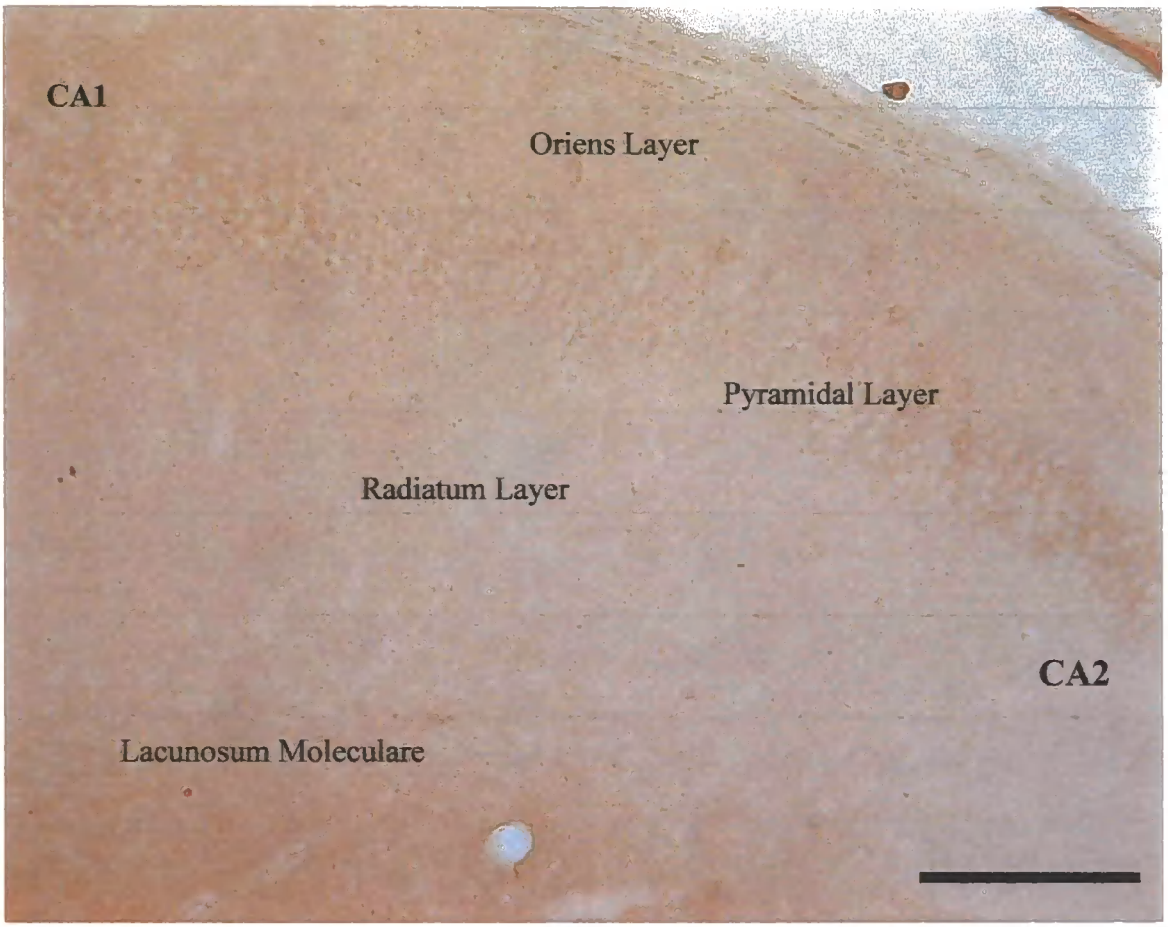

Figure 3.7.3.3 Immunohistochemical mapping of the TARP γ4 isoform in the hippocampal formation (2).

Tissue was fixed in 4% (w/v) paraformaldehyde and probed with the anti-TARP γ4 antibody at a 0.5μg/ml working concentration.

Image shows the hippocampus at the CA1 – CA2 location at 200X magnification. Scale bar = 100 μm.

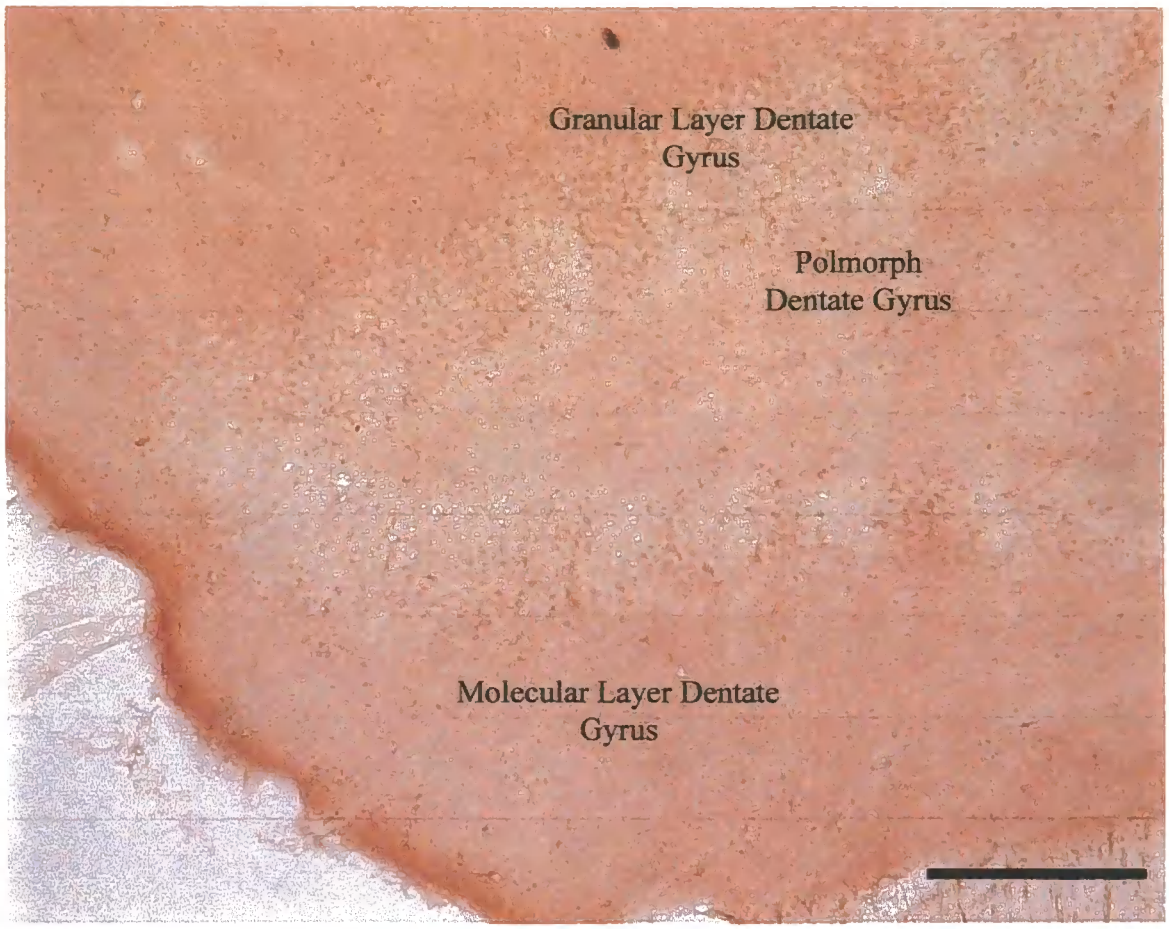

Figure 3.7.3.4 Immunohistochemical mapping of the TARP γ4 isoform in the dentate gyrus.

Tissue was fixed in 4% (w/v) paraformaldehyde and probed with the anti-TARP γ4 antibody at a 0.5μg/ml working concentration.

Image shows the dentate gyrus at 200X magnification. Scale bar = 100 μm.

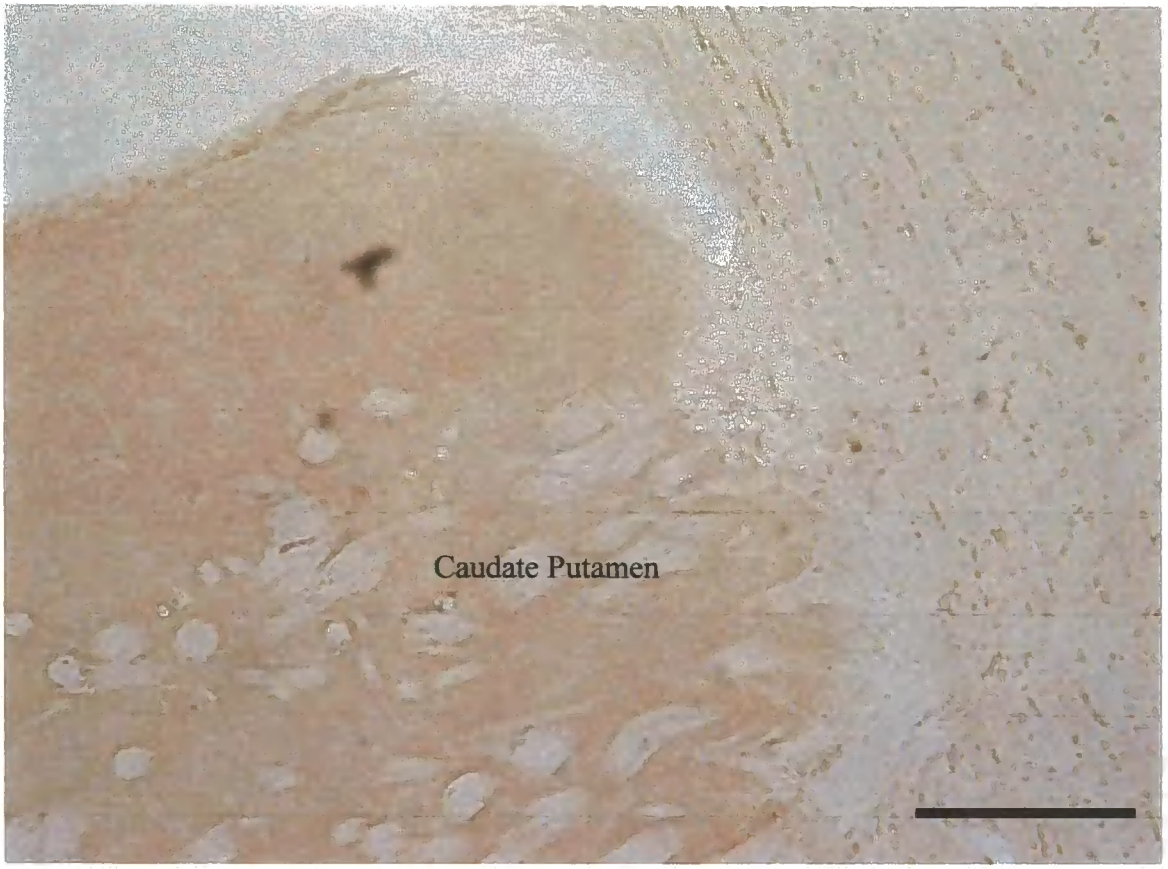

Figure 3.7.3.5 Immunohistochemical mapping of the TARP γ4 isoform in the Striatum.

Tissue was fixed in 4% (w/v) paraformaldehyde and probed with the anti-TARP γ4 antibody at a 0.5μg/ml working concentration.

Image shows the caudate putamen at 200X magnification. Scale bar = 100 μm.

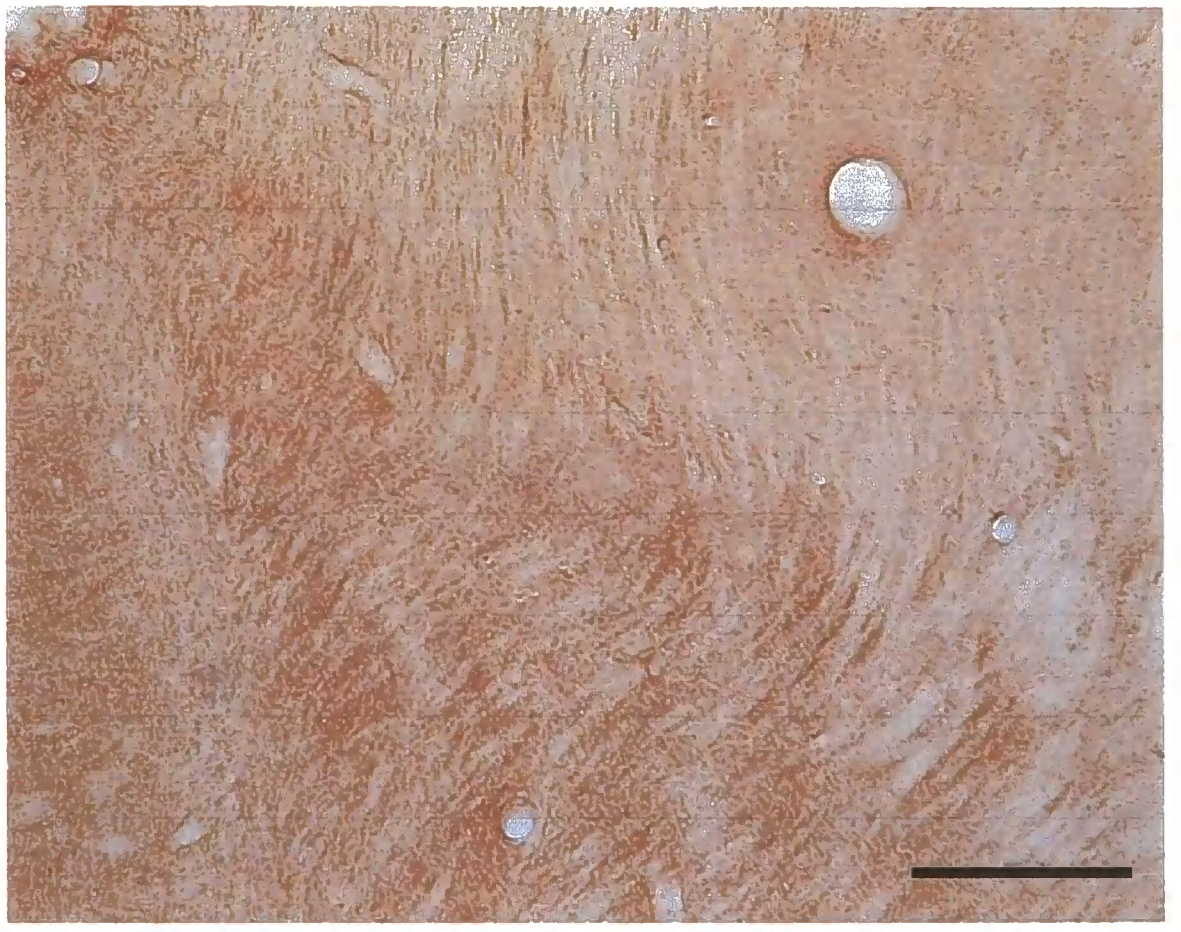

Figure 3.7.3.6 Immunohistochemical mapping of the TARP γ4 isoform in the Thalamic Region.

Tissue was fixed in 4% (w/v) paraformaldehyde and probed with the anti-TARP γ4 antibody at a 0.5μg/ml working concentration.

Image shows the thalamic region at the CA1 location at 200X magnification. Scale bar = 100 μm.

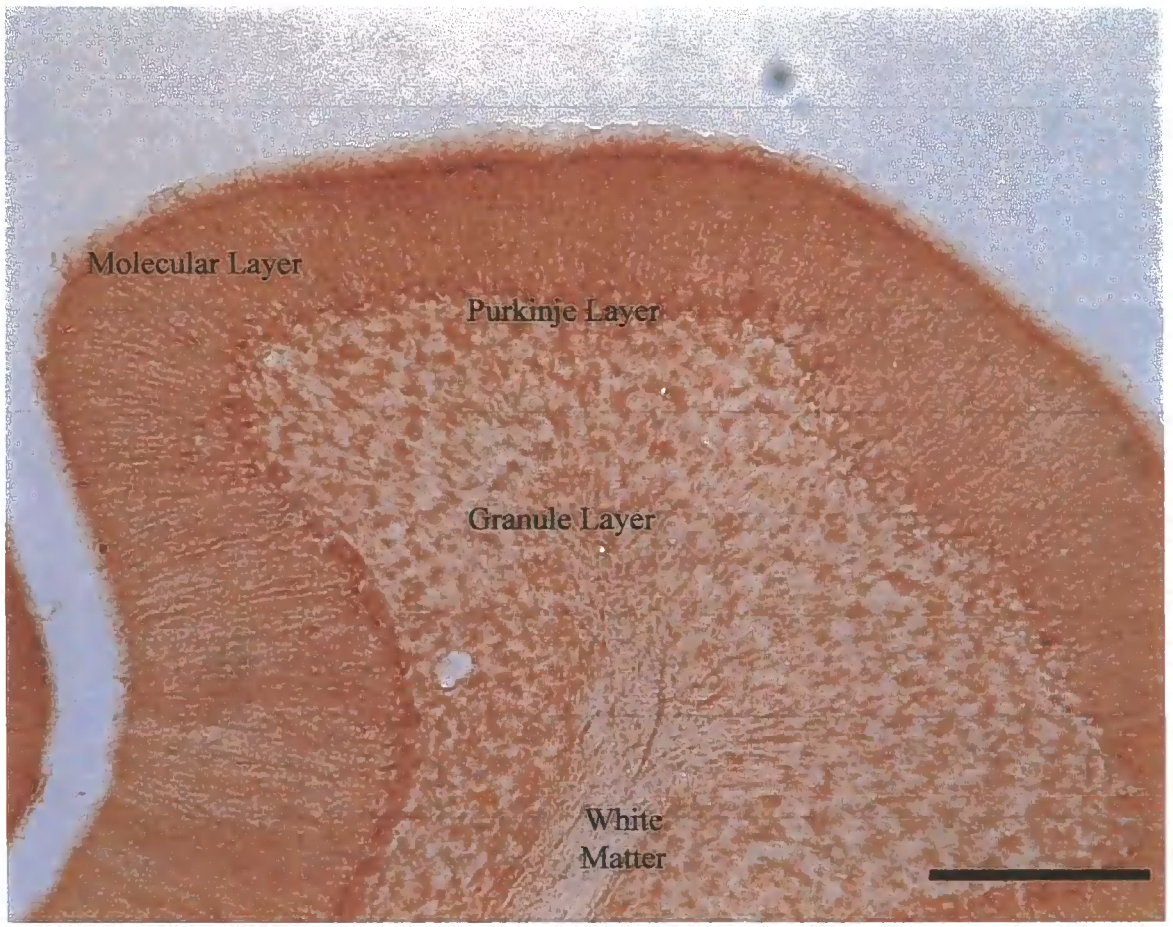

Figure 3.7.3.7 Immunohistochemical distribution of the TARP γ4 isoform in cerebellum.

Tissue was fixed in 4% (w/v) paraformaldehyde and probed with the anti-TARP γ4 antibody at a 0.5μg/ml working concentration.

Image shows the cerebellum at 200X magnification. Scale bar = 100 μm.

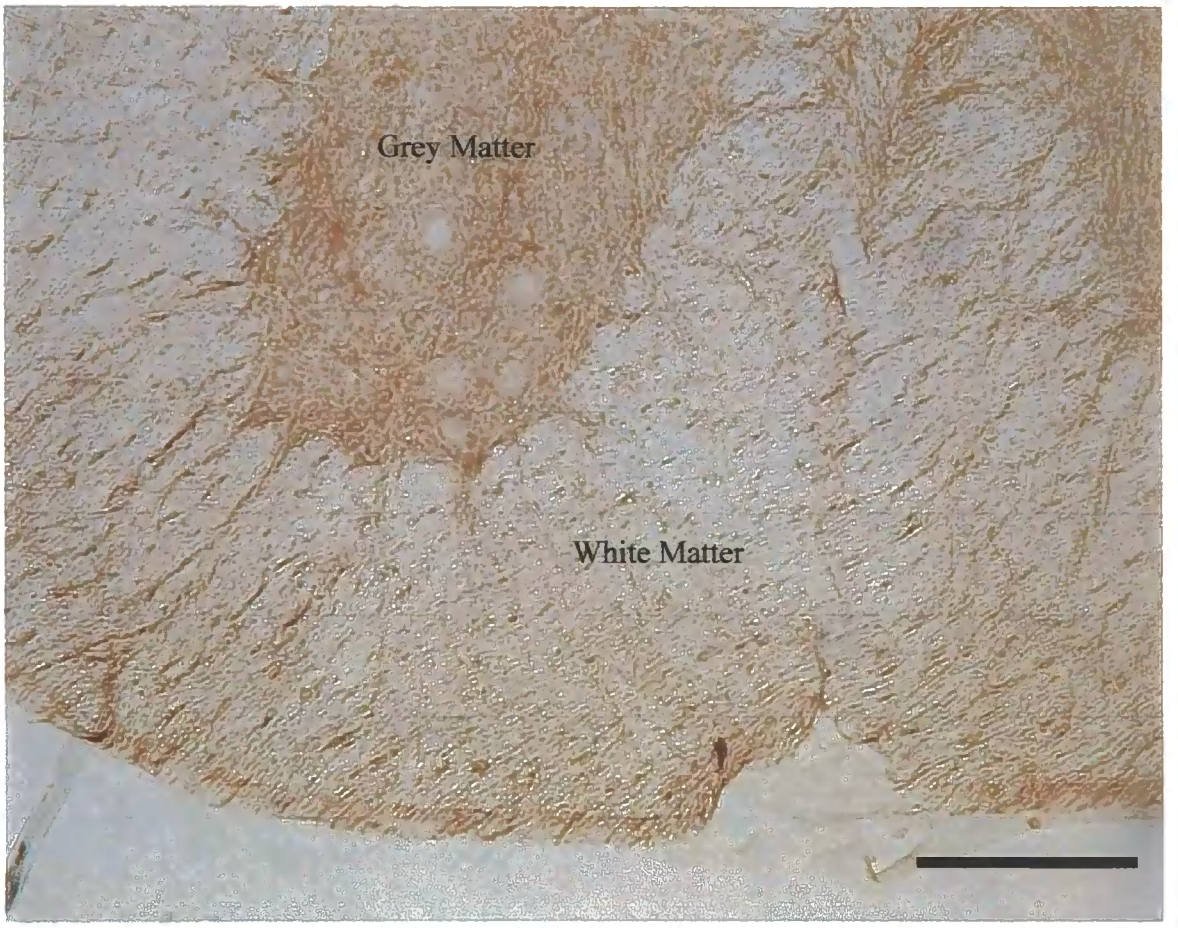

Figure 3.7.3.8 Immunohistochemical distribution of the TARP γ4 isoform in the spinal cord.

Tissue was fixed in 4% (w/v) paraformaldehyde and probed with the anti-TARP γ4 antibody at a 0.5μg/ml working concentration.

Image shows the ventral horn of the spinal cord at 200X magnification. Scale bar = 100 μm.

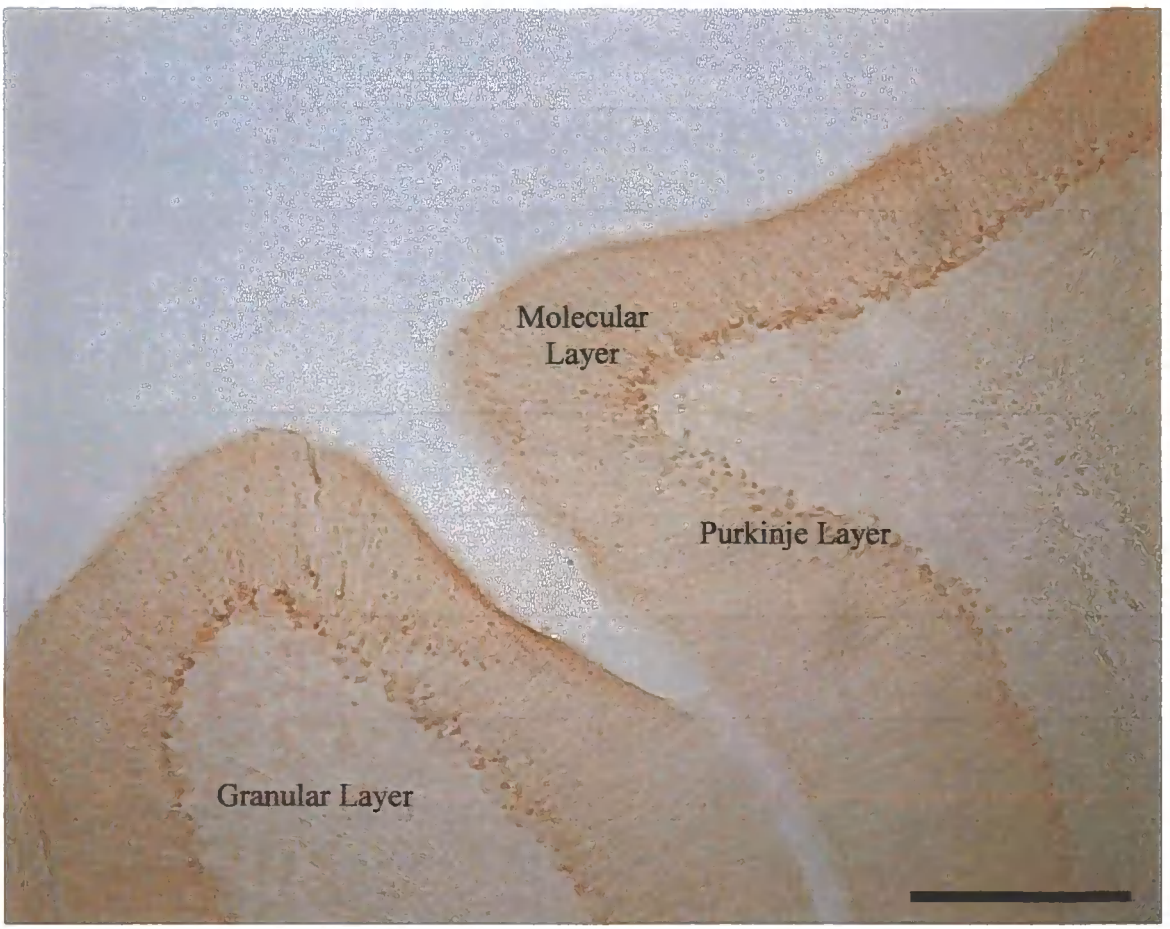

Figure 3.7.3.9 Confirming the TARP γ4 immunohistochemical distribution data with peptide block.

Tissue was fixed in 4% (w/v) paraformaldehyde and dissected into 30μm thick sections. Tissue was subsequently probed with the anti-TARP γ4 antibody at 0.5μg/ml working concentration, that had been pre-incubated with 1.25mg/ml of the TARP γ4 peptide.

Image shows the cerebellum at 200X magnification. Scale bar = 100 μm.

TARP γ4 is distributed at low levels throughout the CNS, but is concentrated in the deep brain structures.

Figure 3.7.1 shows the distribution of TARP γ4 by immunoblotting, with the most concentrated and readily detectable levels of TARP γ4 being present in the thalamus. This is confirmed by the IHC shown in Figure 3.7.3, where, despite some region-specific concentrated levels of TARP γ4 being present in the hippocampus, the most intense levels of TARP γ4 are detectable in both the thalamus, and the cerebellum.

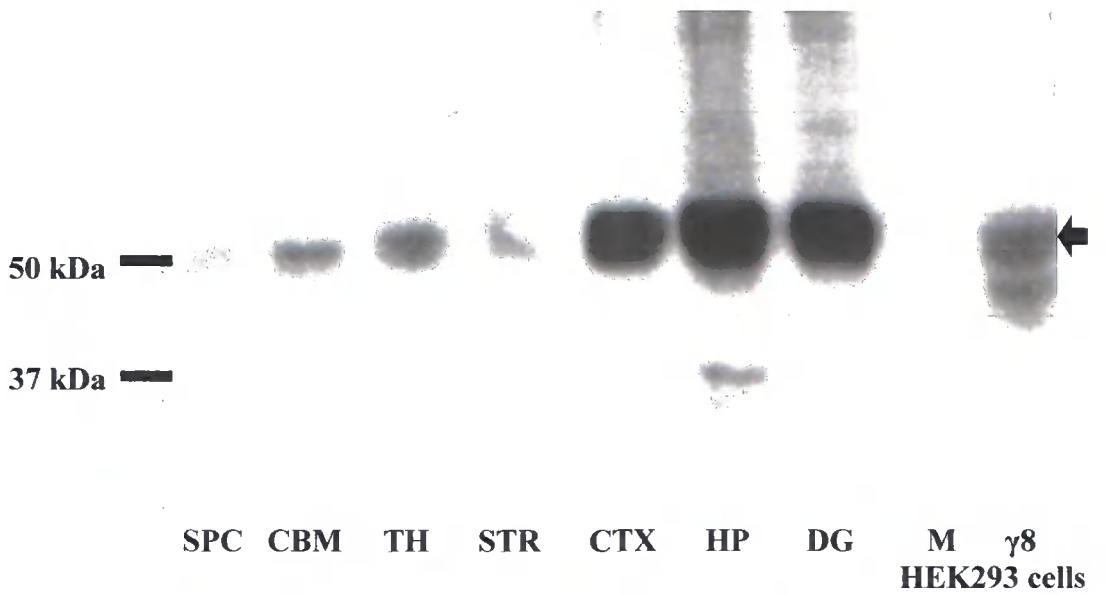

Figure 3.8.1 Immunoblot showing distribution of the TARP γ8 isoform across a range of dissected CNS tissue when probed with the anti TARP γ8 C terminal directed antibody.

All tissues were solubilised in SDS-solubilising buffer (see methods) before being precipitated into 150µl 2X SDS-PAGE sample buffer, with 10µg of each were loaded onto a 10% SDS-PAGE gel. Wild type tissues loaded; Spinal cord (SPC); Cerebellum (CBM); Thalamus (TH); Striatum (STR); Cerebral cortex (CTX); Hippocampus (HP); Dentate gyrus (DG). HEK293 cells transfected with either empty vector (M) or the TARP γ8 isoform were also loaded. All immunoreactive species correspond with TARP γ8, the bands corresponding to mature TARP γ8, expressed as a doublet in CTX, HP and DG, are indicated by the black arrow.

CNS Region	SPC	CBM	TH	STR	CTX	HP	DG
Relative amount of TARP γ8	+	++	++	+	++++	+++++	+++++

Figure 3.8.2 Table showing relative TARP γ8 amounts across the range of dissected tissues.

Samples were SDS-solubilised, with relative amounts being determined by the intensity of bands detected by immunoblotting in relation to one another.

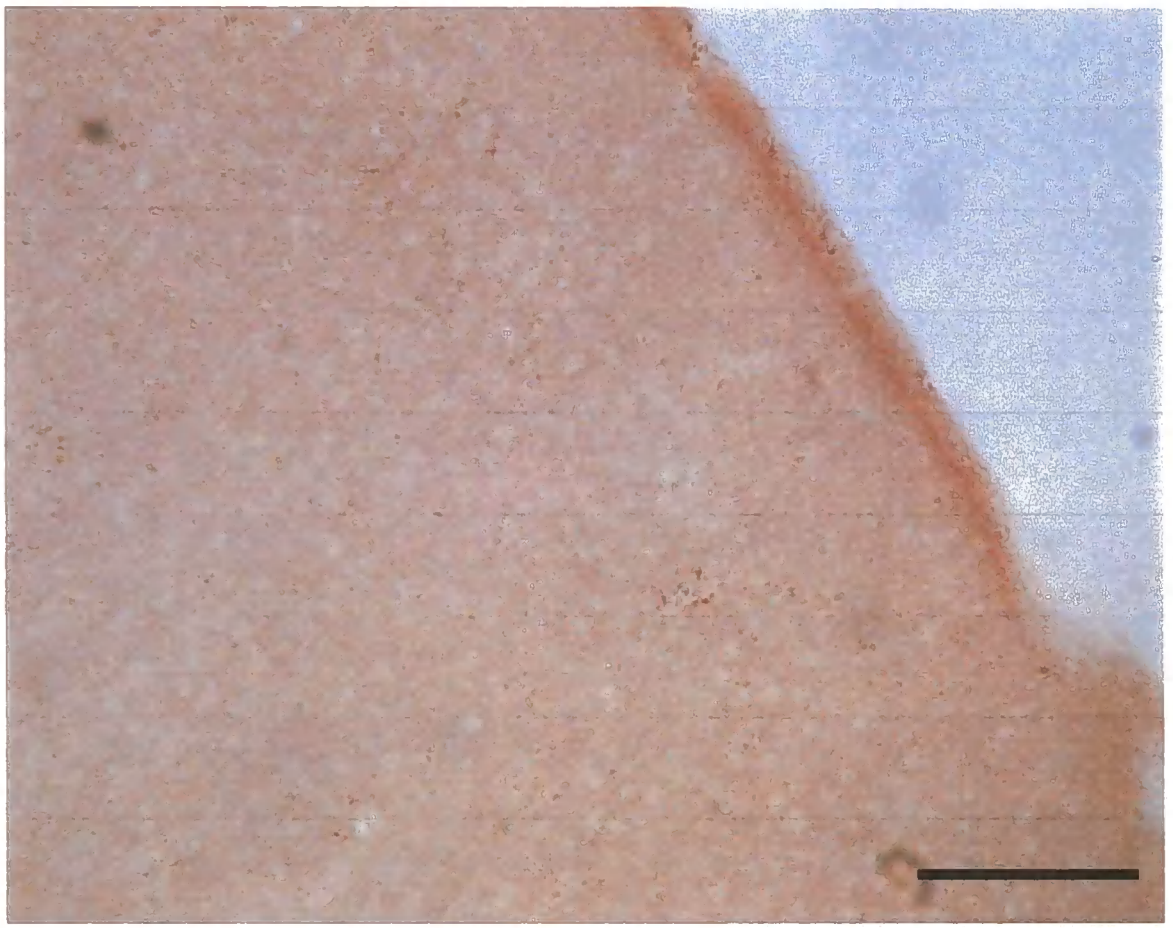

Figure 3.8.3.1 Immunohistochemical mapping of the TARP γ8 isoform in the cerebral cortex.

Brain was fixed with 4% (w/v) paraformaldehyde and subsequently cut into 30μm sections. Tissue is labelled with the anti-TARP γ8C antibody at 0.0625μg/ml working concentration.

Image shows cerebral cortex at 200X magnification, taken from the approximate location of frontal cortex area 3. Scale bar = 100 μm.

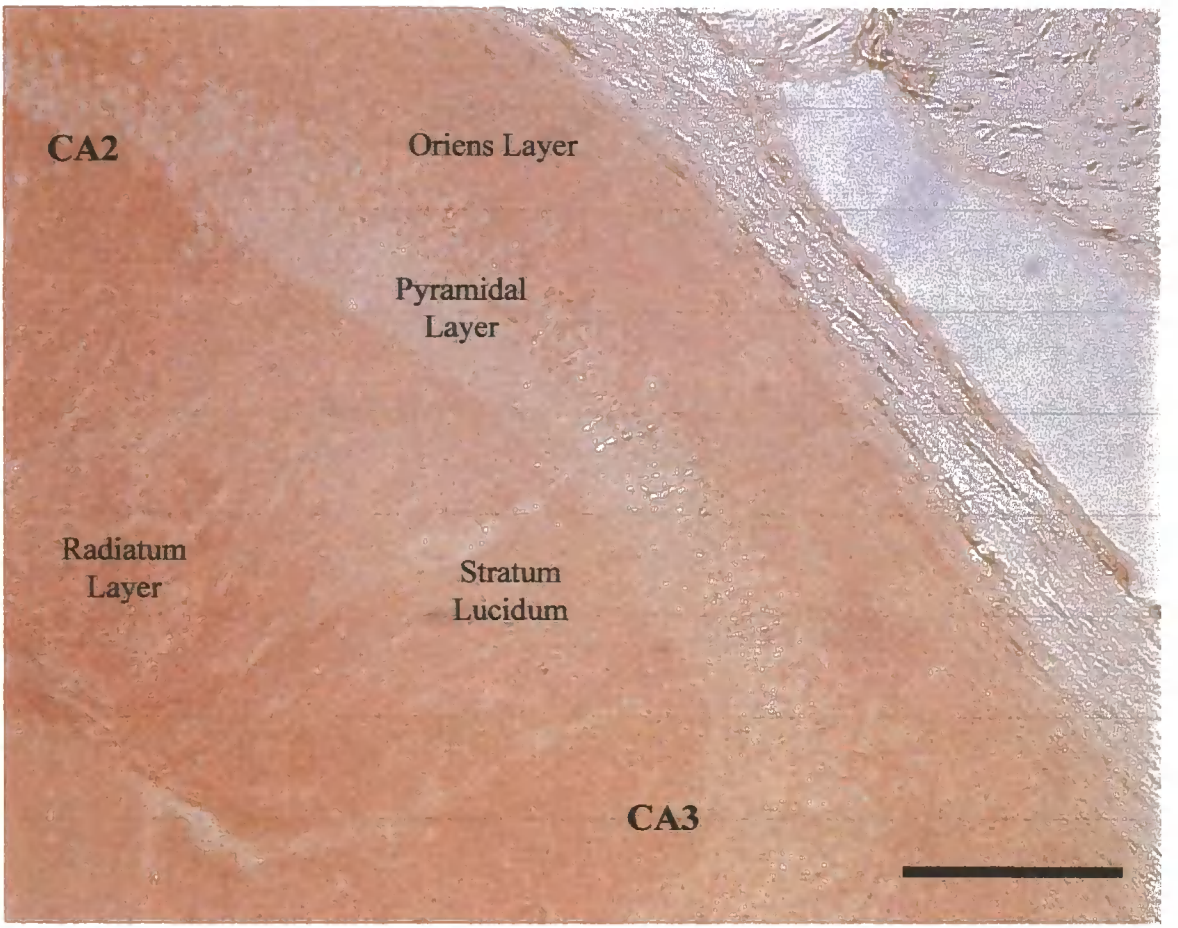

Figure 3.8.3.2 Immunohistochemical mapping of the TARP γ8 isoform in the hippocampal formation.

Brain was fixed with 4% (w/v) paraformaldehyde and subsequently cut into 30μm sections. Tissue is labelled with the anti-TARP γ8C antibody at 0.0625μg/ml working concentration.

Image shows the hippocampus at the CA2 – CA3 location, taken at 200X magnification. Scale bar = 100 μm.

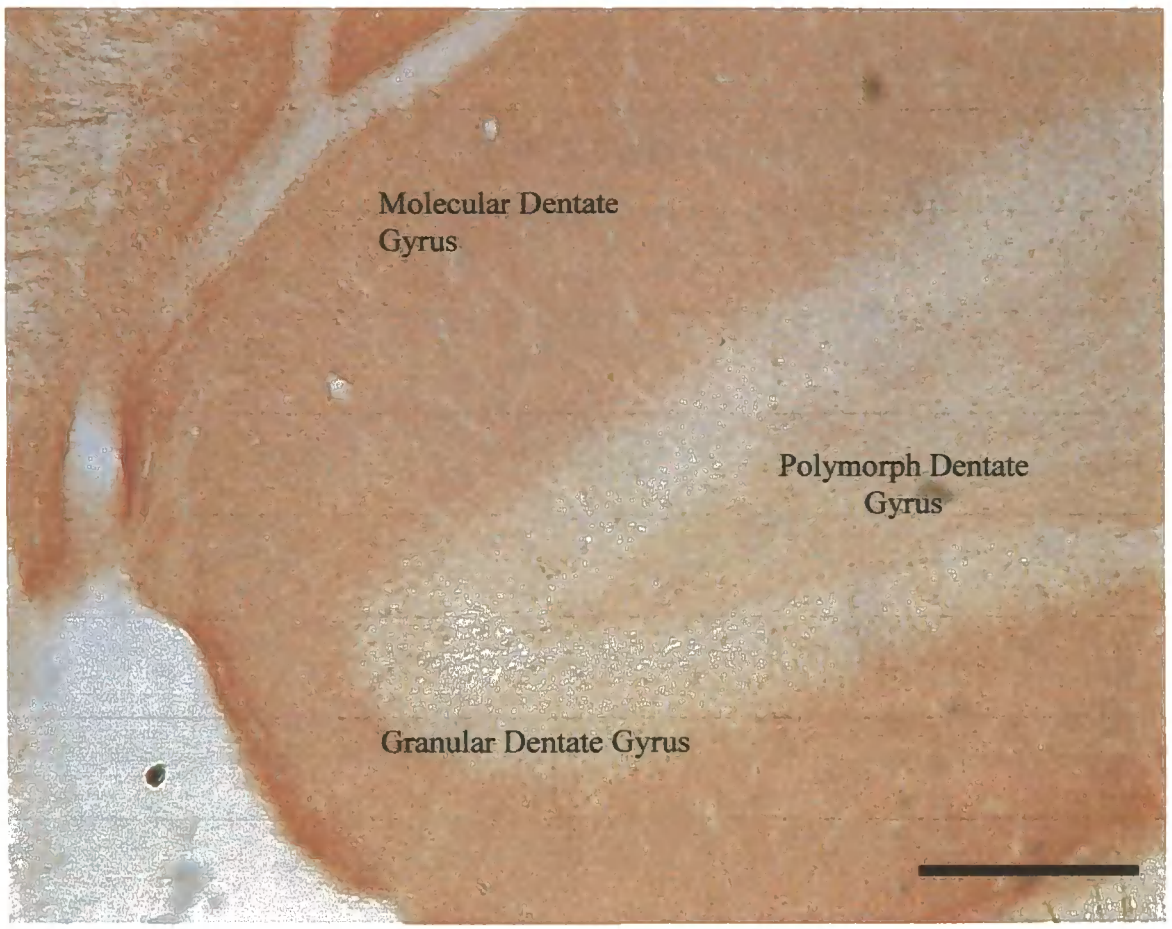

Figure 3.8.3.3 Immunohistochemical mapping of the TARP γ8 isoform in the dentate gyrus.

Brain was fixed with 4% (w/v) paraformaldehyde and subsequently cut into 30μm sections. Tissue is labelled with the anti-TARP γ8C antibody at 0.0625μg/ml working concentration.

Image shows the dentate gyrus at 200X magnification. Scale bar = 100 μm.

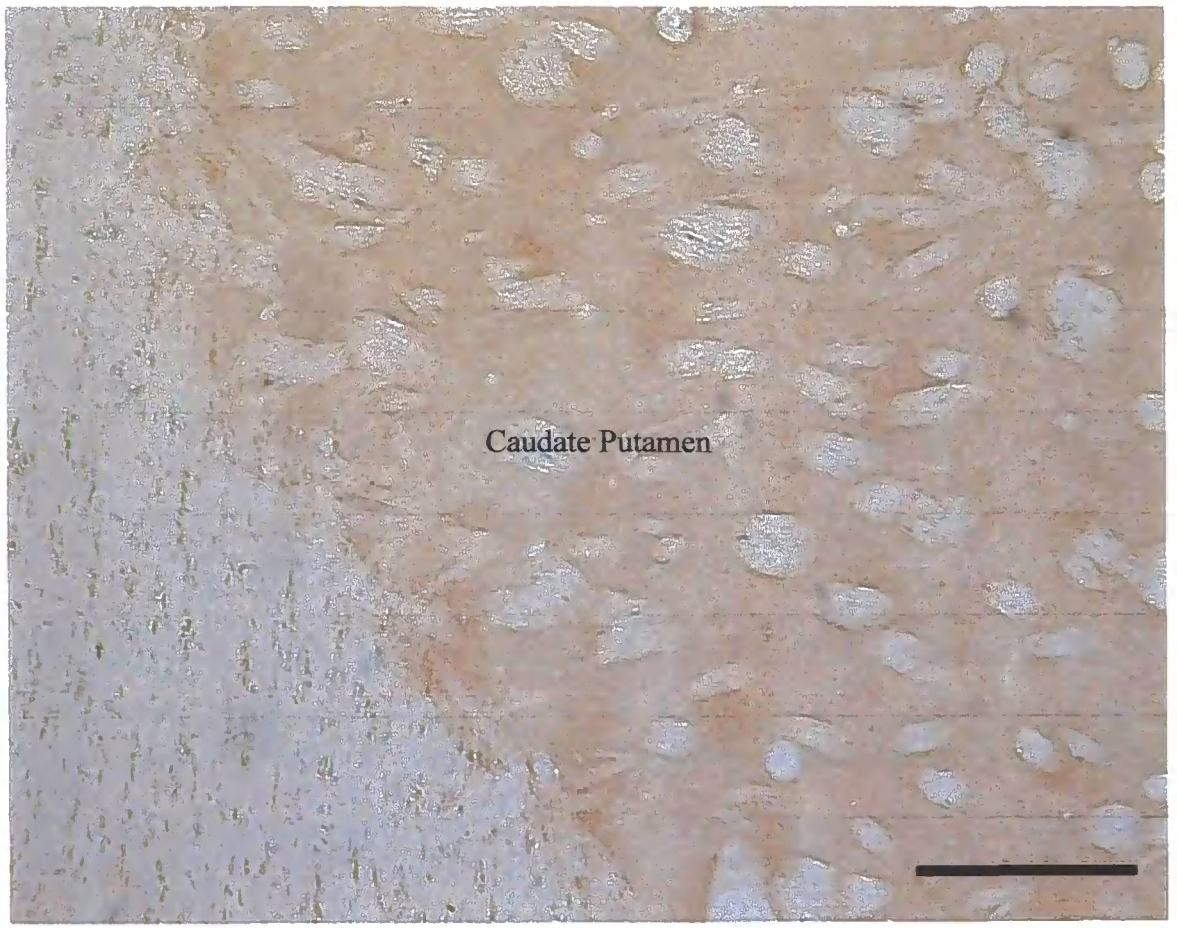

Figure 3.8.3.4 Immunohistochemical mapping of the TARP γ8 isoform in the striatum.

Brain was fixed with 4% (w/v) paraformaldehyde and subsequently cut into 30μm sections. Tissue is labelled with the anti-TARP γ8C antibody at 0.0625μg/ml working concentration.

Image shows the striatum, more specifically the caudate putamen, at 200X magnification. Scale bar = 100 μm.

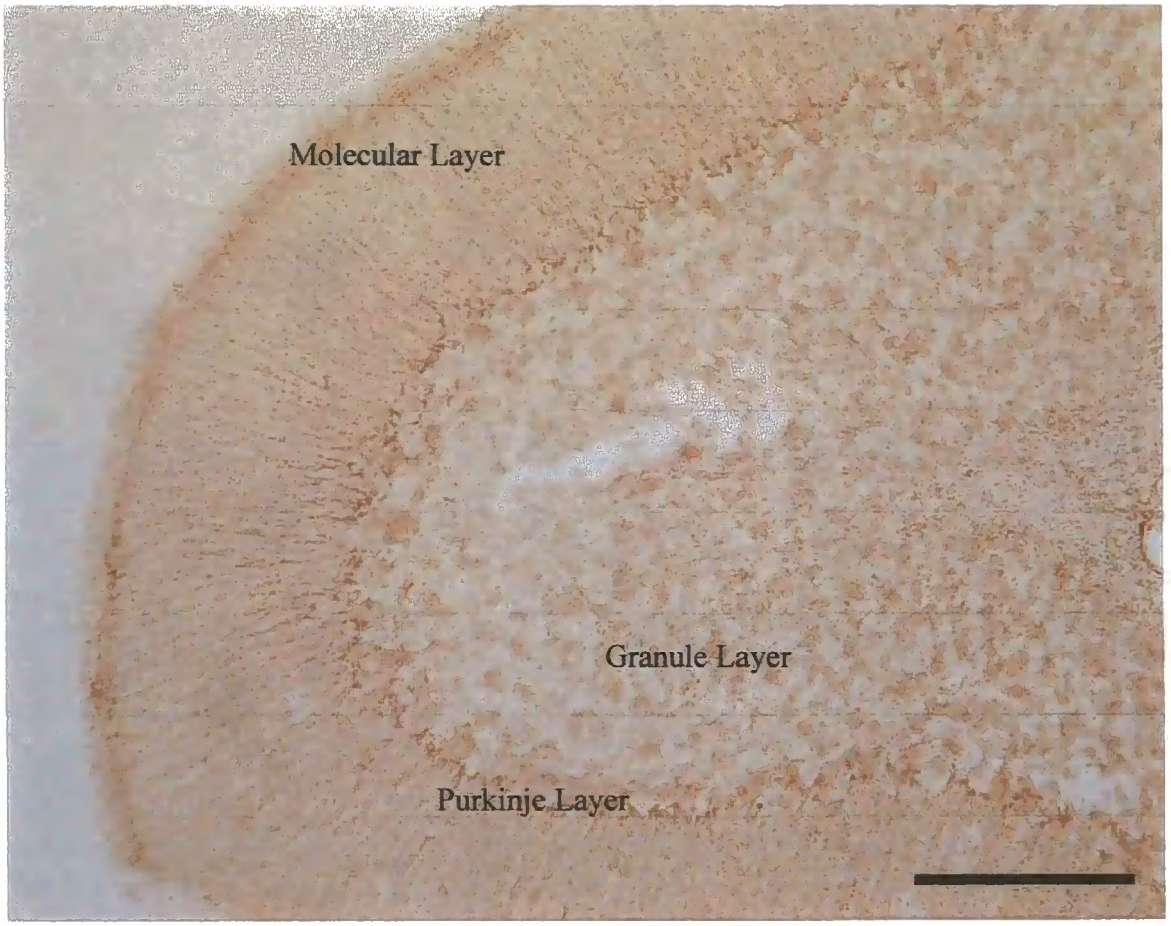

Figure 3.8.3.5 Immunohistochemical mapping of the TARP γ8 isoform in the cerebellum.

Brain was fixed with 4% (w/v) paraformaldehyde and subsequently cut into 30μm sections. Tissue is labelled with the anti-TARP γ8C antibody at 0.0625μg/ml working concentration.

Image shows the cerebellum at 200X magnification. Scale bar = 100 μm.

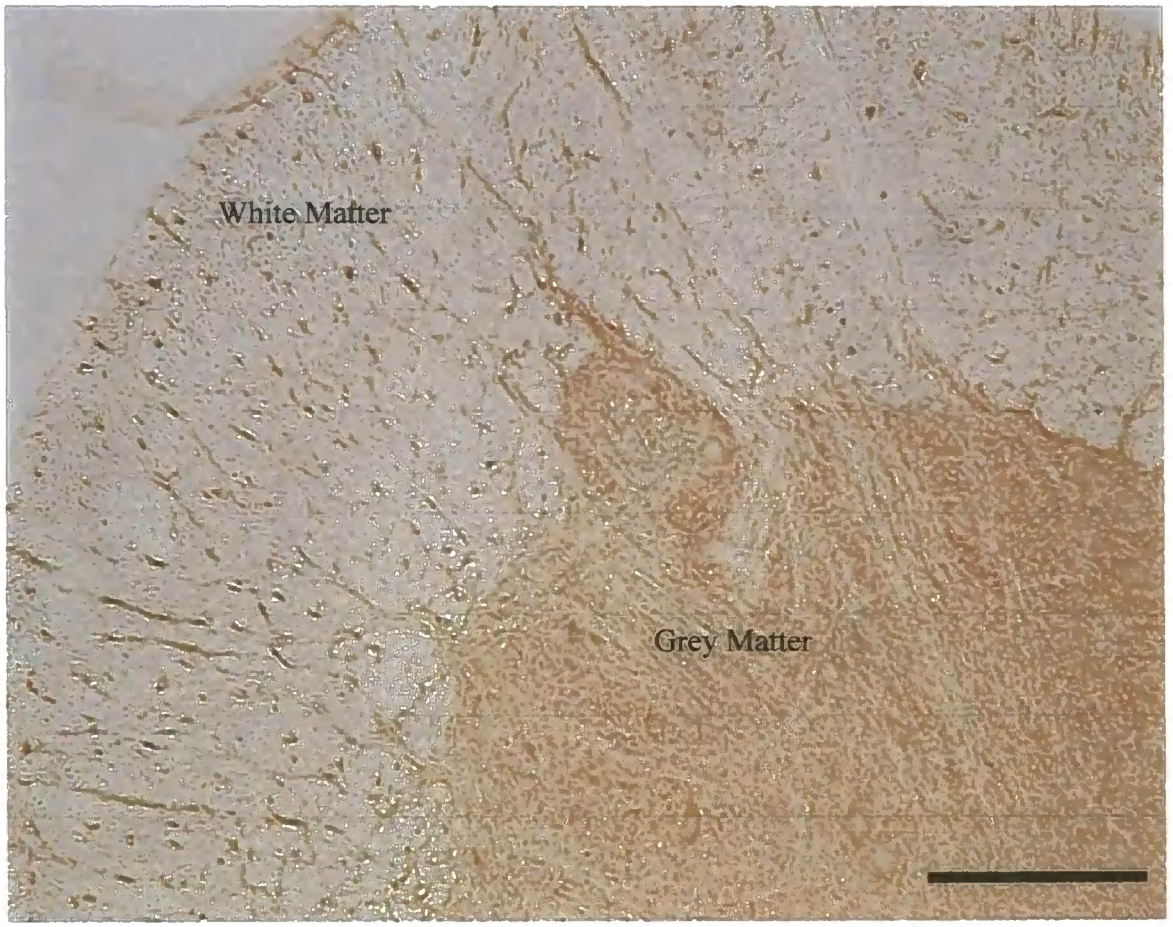

Figure 3.8.3.6 Immunohistochemical mapping of the TARP γ8 isoform in the spinal cord (1).

Tissue was fixed with 4% (w/v) paraformaldehyde and subsequently cut into 30μm sections. Tissue is labelled with the anti-TARP γ8C antibody at 0.0625μg/ml working concentration.

Image shows the dorsal horn of the spinal cord at 200X magnification. Scale bar = 100 μm.

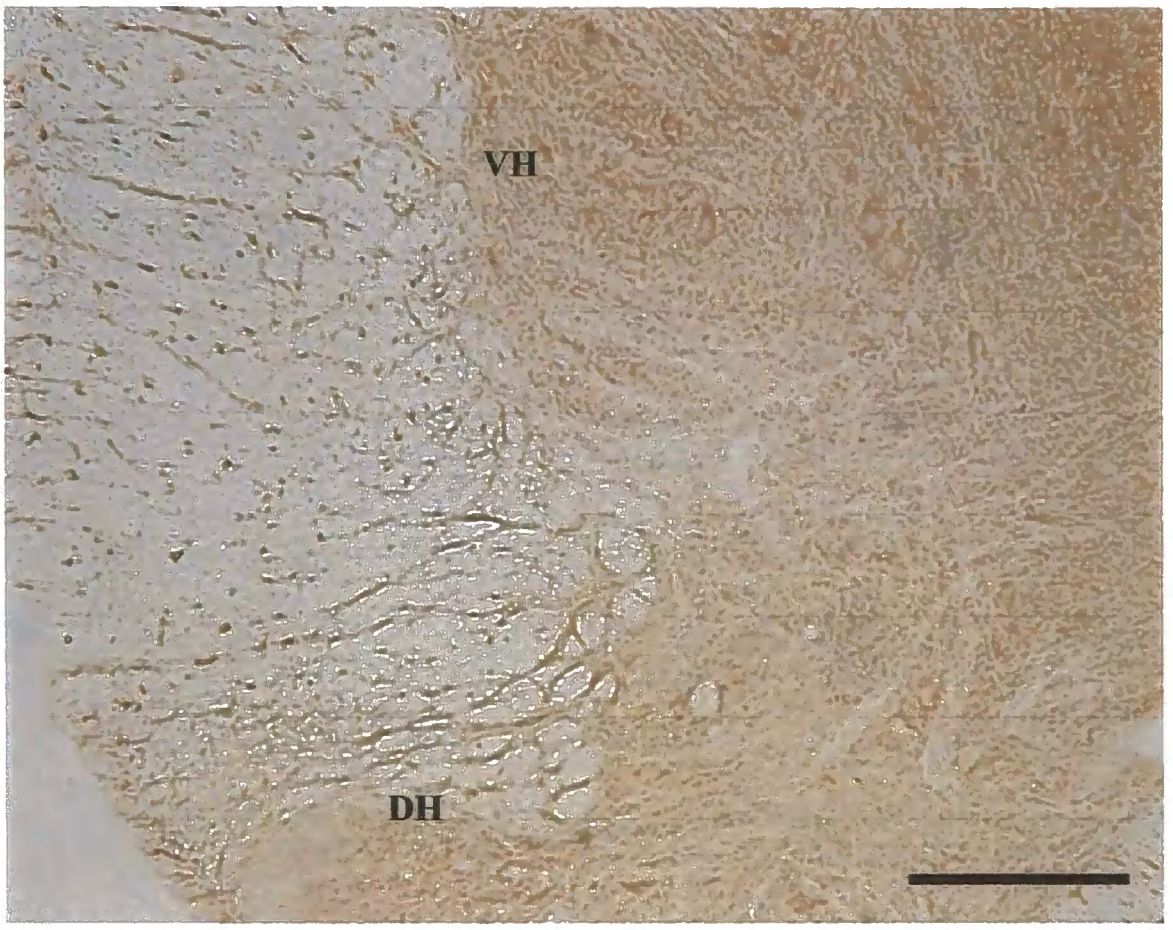

Figure 3.8.3.7 Immunohistochemical mapping of the TARP γ8 isoform in the spinal cord (2).

Tissue was fixed with 4% (w/v) paraformaldehyde and subsequently cut into 30μm sections. Tissue is labelled with the anti-TARP γ8C antibody at 0.0625μg/ml working concentration.

Image shows the both the dorsal (DH) and ventral horn (VH) at 200X magnification. Scale bar = 100 μm.

TARP γ8 is distributed throughout the CNS, at highest levels in the forebrain.

Figure 3.8.1 shows that TARP γ8 is present in all of the regions of the CNS that were probed by immunoblotting, including the spinal cord and cerebellum. As was expected the highest levels of TARP γ8 were detected in the dentate gyrus and hippocampal formation. The cerebral cortex also showed high levels of TARP γ8 expression.

Figure 3.8.3 confirms and expands on this information, demonstrating that TARP γ8 is detectable in each of the tissues by immunohistochemistry, and displays some cell-specific labelling, particularly in the hippocampal formation, where it is not expressed in the cell bodies of the granule cell layer of the dentate gyrus.

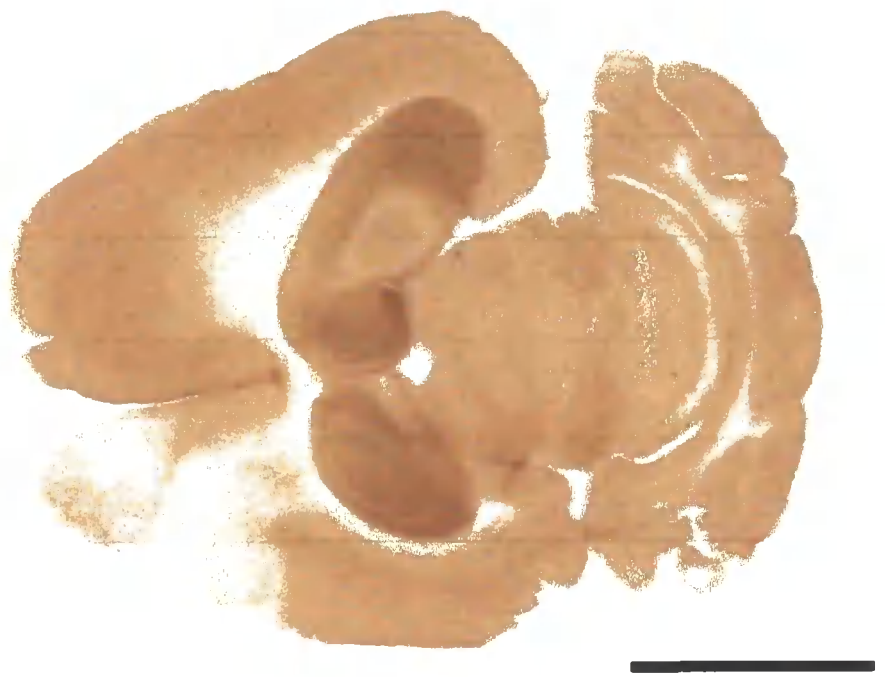

Figure 3.9.1 Immunohistochemically screened horizontal section of brain probed for TARP γ8 using the anti-TARP γ8C antibody.

Brain was fixed in 4% (w/v) paraformaldehyde and cut into 30μm thick sections. Probed with anti-TARP γ8C antibody at 0.0625μg/ml working concentration. Scale bar = 5 mm.

Figure 3.9.2 Immunohistochemically screened horizontal section of brain probed for GluR1.

Brain was fixed in 4% (w/v) paraformaldehyde and cut into 30μm thick sections. Probed with anti-GluR1 antibody at a 1μg/ml working concentration. Scale bar = 5 mm.

Figure 3.10.1 Sagittal section of brain probed with the anti-TARP γ8 C antibody.

Brain was fixed in 4% (w/v) paraformaldehyde and cut into 30μm thick sections, which were probed using the anti TARP γ8 C-terminal directed antibody at 0.0625μg/ml working concentration. Notable regions of labelling include the hippocampal formation (HP), Layer IV of the cerebral cortex (CTX). Scale bar = 5 mm.

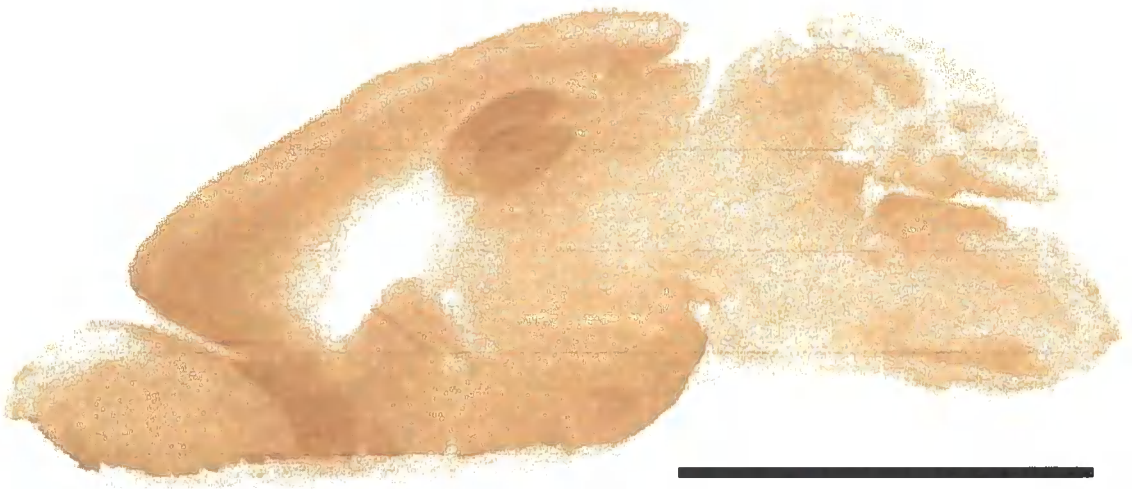

Figure 3.10.2 Sagittal section of brain probed with the anti-GluR2 antibody.

Brain was fixed in 4% (w/v) paraformaldehyde and cut into 30μm thick sections, which were probed using a commercial anti-GluR2 antibody at 1μg/ml working concentration. Scale bar 5 mm. Scale bar = 5 mm.

Figure 3.10.3 Immunohistochemically screened horizontal section of brain probed for TARP γ8 using the anti-TARP γ8C antibody.

Brain was fixed in 4% (w/v) paraformaldehyde and cut into 30μm thick sections. Probed with anti-TARP γ8C antibody at 0.0625μg/ml working concentration. Scale bar = 5 mm.

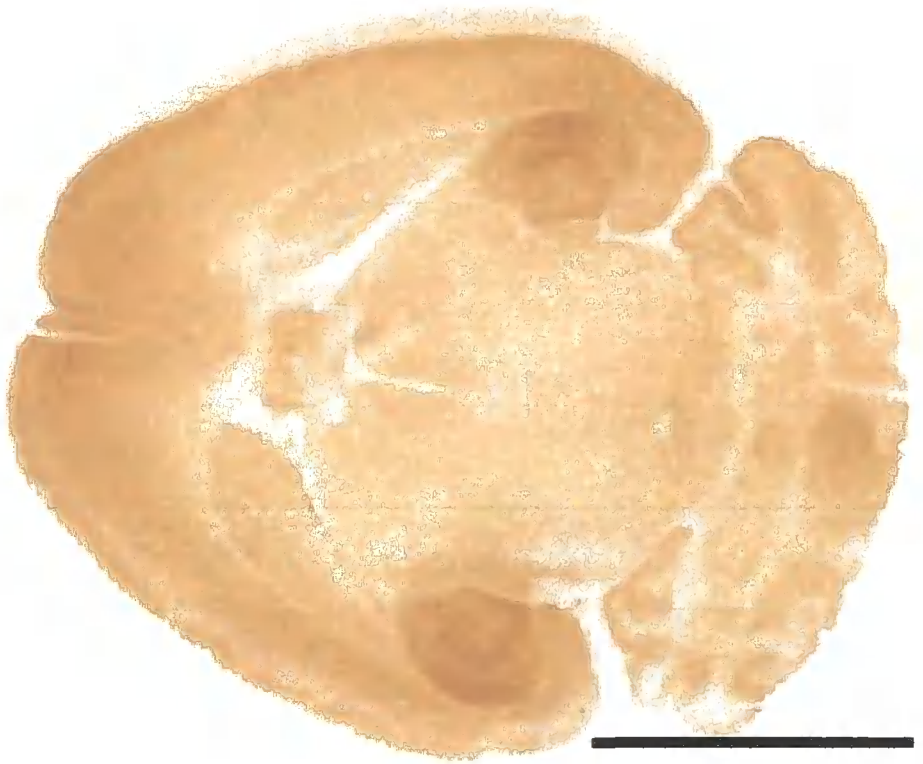

Figure 3.10.4 Immunohistochemically screened horizontal section of brain probed for GluR2.

Brain was fixed in 4% (w/v) paraformaldehyde and cut into 30μm thick sections. Probed with anti-GluR2 1μg/ml working concentration. Scale bar = 5 mm.

The GluR1 and GluR2 AMPA receptor subunits show some similarity in regional distribution with the TARP γ8 isoform.

Figures 3.9 and 3.10 show the distribution of the GluR1 and GluR2 AMPA receptor subunits, with the distribution of both, particularly the GluR2 subunit, showing striking similarities to the distribution of TARP γ8 seen immunohistochemically. This is most detectable in the cerebral cortex and hippocampal formation.

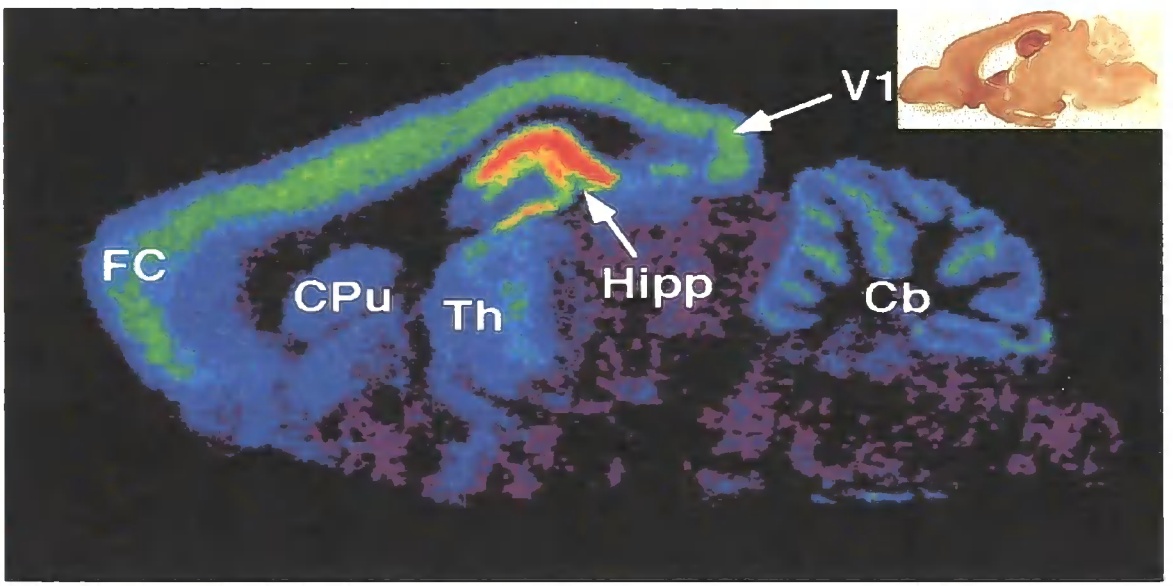

Figure 3.11. Distribution of a [^{3}H] positive allosteric AMPA receptor modulator in the mouse brain *(Provided by Servier, c/o Michael Spedding).*

Main image shows the distribution of binding of a [^{3}H] positive allosteric AMPA receptor modulator developed by Servier, specific for GluR *flop* isoforms.
Inset shows Figure 10.1 – TARP γ8 distribution in the mouse brain probed using the TARP γ8C antibody.

Binding of a positive allosteric modulator of AMPA receptors (AMPAkine) displays a very similar regional distribution to the TARP γ8 isoform.

Figure 3.11 shows binding data provided by Servier regarding an AMPAkine compound, specific for GluR *flop* isoforms. Its binding distribution in the mouse CNS is very similar to the distribution of TARP γ8 with the AMPAkine displaying slightly less binding in the

CA3 region of the hippocampus due to the prevalence of GluR *flip* isoforms in this region.

Discussion

Novel antibodies to each of the known TARP isoforms were designed and subsequently generated, with the finished antibodies screened against both native tissue and recombinant cells transfected with the TARP isoforms using several immunological techniques. Of these, antibodies specific to the TARP γ2, γ4 and TARP γ8 isoforms were successfully generated, with the finished antibodies demonstrating suitability for a range of techniques, with the focal point being on the generation of immunopurification columns.

Regrettably, the lack of suitable available immunological probes for immunohistochemical labelling of the $5HT_{2C}$ receptor distribution, combined with its low expression levels in the CNS, make analysis of $5HT_{2C}$ receptor at the protein level, extremely difficult using these techniques, and insufficient time was available to try an alternative approach.

TARP γ2

As can be seen, the generation of an antibody specific to the TARP γ2 isoform was successful, especially with its earlier bleeds, which showed no cross-reactivity with any of the other TARP isoforms, the latter bleeds detecting TARP γ8 as well as TARP γ2. The antibody is suitable for use in immunoblotting, and the later bleeds were also used to generate an immunoaffinity column capable of purifying TARP γ2.

Unfortunately, the antibody did demonstrate its unsuitability for use in immunohistochemistry, with the early bleeds displaying no discernable labelling on paraformaldehyde-fixed sections. The later bleeds, which displayed some cross-reactivity with TARP γ8, only labelled what appeared to be TARP γ8 and even then only in the

regions where TARP γ8 was most concentrated. A similar problem with the cross-reactivity was also encountered with the TARP γ2 immunoaffinity column, limiting the number of uses for this antibody.

Screening the dissected tissues for TARP γ2 (Figure 3.6.1) demonstrated a variable distribution of TARP γ2 throughout the tissues investigated, with low levels of TARP γ2 being detected in the striatum, reasonable levels of TARP γ2 being detectable in the spinal cord, thalamus, cerebral cortex and the hippocampal formation, and the highest level of expression of TARP γ2 is detectable in the cerebellum. This is consistent with data obtained from the investigation of the *stargazer* mutant mouse phenotype, which suggests that TARP γ2 is the predominant TARP isoform detectable in the cerebellum.

Extensive testing of the dentate gyrus however, revealed no detectable TARP γ2, and in this respect, is unique with regard to the tissues investigated.

TARP γ4

The anti TARP γ4 antibody developed demonstrated suitability for a wide variety of techniques, including both immunoblotting and immunohistochemistry, with no cross-reactivity to any of the other TARP isoforms, despite some very minor non-specific labelling being detected in the immunoblotting.

The anti TARP γ4 antibody also displayed the most variance in affinity between bleeds, with the earlier bleeds, whilst specific, displayed less affinity for TARP γ4 than subsequent bleeds.

When used to screen dissected tissues for TARP γ4 expression, the antibody was consistent with the mRNA data for TARP γ4 distribution in the CNS as described by Tomita et al. (2003), with TARP γ4 being expressed at low levels seemingly throughout the CNS, with its highest levels of expression being in the thalamus, seen by both immunoblotting (Figure 3.7.1) and immunohistochemistry (Figure 3.7.3.6). A key difference with the mRNA distribution in the literature, is the absence of detectable

TARP γ4 in the striatum (Figure 3.7.1; Figure 3.7.3.5), indicating a difference between the mRNA distribution of TARP γ4 when compared with the protein distribution.

This may potentially be explained by the possibility of TARP γ4 protein being expressed within a different region of its parent neurone to its mRNA, with the protein being detectable in the processes extending from the neurones, whilst the mRNA is localised to the neurones origin. Another plausible explanation for the differences observed, and one which shall be also discussed with regard to the TARP γ8 isoform both in this chapter and in chapter 5, is the possibilities of variation between the mice strains used both in this thesis, and those in the literature.

TARP γ8

The development of the two antibodies specific to the TARP γ8 isoform was highly successful, with both antibodies displaying no cross-reactivity with any of the other TARP isoforms (Figures 3.3.3 and 3.3.4). Only the antibody generated using the TARP γ8 C-terminal (anti TARP γ8C) domain sequence was suitable for use in immunohistochemistry, the anti TARP γ8 N-terminal antibody (anti TARP γ8 N) demonstrated no ability to label either recombinant cells or native tissue (data not shown). In immunocytochemisty and immunohistochemistry the anti TARP γ8 C-terminal antibody displayed a high degree of specificity (Figures 3.5.1-5.5) that could be blocked by incubation with the peptide used to generate the antibody (Figure 3.5.6).

Due to the fact that the anti TARP γ8C antibody demonstrated a higher affinity for the TARP γ8 isoform than the anti TARP γ8N counterpart, combined with the lack of any non-specific binding detected with the TARP γ8C antibody, the TARP γ8C antibody was selected as the antibody for use in the distribution mapping of TARP γ8 (Figures 3.8.1, 3.8.3).

The immunoblot of the dissected tissues probed with the anti TARP γ8C antibody revealed that the TARP γ8 isoform was present in all of the tissues examined, with the

highest levels of expression in the forebrain structures, particularly the hippocampus, which correlates to the data in the literature (Rouach et al. 2005), but also expands upon it, with evidence of TARP γ8 expression in the cerebellum, but also the spinal cord.

Of potential interest in the cerebral cortex and hippocampal formation, a closely-spaced doublet species pattern can be detected with the anti TARP γ8C antibody. This has been previously observed in our laboratory with TARP γ2 and has correlated to the activity-dependant phosphorylation state of the TARP (Payne et al., unpublished), with this being the most likely explanation for observation with TARP γ8. This does beg the question as to why only a single band is detectable in the cerebellum and spinal cord, and would be a potential avenue for further investigation.

The immunohistochemical data observed with the anti TARP γ8C antibody further supports the immunoblotting data, with the most immediately apparent staining being detectable in the hippocampal formation. However, when the whole section is examined (Figures 3.9.1 and 3.10.1), a much more extensive labelling distribution can be seen, with a distribution, particularly in the cerebral cortical laminae being mirrored by the AMPA receptor GluR2, subunit, but also to a lesser extent by the GluR1 subunit (Figure 3.10.2).

Again, supporting the information obtained by immunoblotting, TARP γ8 was detectable within the spinal cord, a region not previously described as expressing TARP γ8, possibly implying a less-specialised role than would have been considered if TARP γ8 was expressed exclusively in the hippocampal formation.

The importance of this TARP distribution data as stand-alone evidence is minimal, the full significance only being apparent once the roles of the TARP isoforms within each of these CNS regions have been determined. To allude to these roles and indeed what neurological processes these TARPs, and the AMPA receptors they traffic, are contributing to, it is important to isolate the TARP isoforms and their interacting proteins using the isoform specific probes generated, characterised, and validated in this chapter to develop immunoaffinity columns capable of purifying the individual TARP isoforms.

Chapter 4: Immunoaffinity purification of TARPs and their interacting proteins analysed by immunoblotting and proteomic methodologies.

Introduction

In the last chapter, a panel of antibodies specific to each of the TARP isoforms were generated and validated. The TARP γ8 isoform was selected specifically for further study in this chapter for two key reasons; Firstly from a scientific and information perspective, as the prevalent TARP in the hippocampal formation it possess vast implications in such neurological phenomena as LTP; Secondly, from a methodological perspective, TARP γ8s distinction at the time as the prevalent TARP isoform in the hippocampal formation – and the only TARP isoform expressed in the dentate gyrus (Payne et al. 2006) – offered a valuable environment for looking at the potential interaction with $5HT_{2C}R$ of an individual TARP isoform, potentially in a culture environment, but crucially as an effectively isolated system that needed no further experimental isolation from the other TARP isoforms, somewhat similar to the possibilities offered by the cerebellum with regard to TARP γ2. Based on the distribution pattern, it is clear that the TARP γ8 most closely matches AMPA receptor topology in the mouse forebrain, with high levels of expression in the cortex and hippocampal formation. Clearly as predicted from mRNA studies, TARP γ8, and not TARP γ2 is the major isoform expressed in the hippocampus as shown in Chapter 3.

The intent of generating two TARP γ8 antibodies, one to the extreme N-terminus and one to the C-terminal domain, was to ensure that potential epitope masking by interacting proteins would not be a problem. Using the TARP isoform-specific antibodies generated to test the hypothesis that $5HT_{2C}$ receptors interact with TARP/AMPA receptors via a physical interaction, immunoaffinity columns were generated with the intent to purify the individual TARP isoforms. In addition to the TARP isoforms, any interacting proteins associated to the TARP of interest would be purified, ideally in large, multi-protein

complexes. The subsequent screening of these complexes, many of which potentially could contain previously unknown interacting partners, would utilise both immunological and proteomic methodologies, immunological using antibodies specific to individual proteins of interest with regard to the hypothesis, most notably the $5HT_{2C}$ receptor, and proteomic to identify novel interacting partners that had not been considered previously.

Known interacting proteins for the TARP isoforms obviously include AMPA receptors, of which GluR1 and GluR2 are the prevalent subunits expressed in the CNS. Another known TARP interacting protein is Microtubule associated protein 1A (MAP-1A), originally shown to interact with the TARP γ2 isoform (Ives et al. 2004), but subsequently identified in our laboratory as an interacting partner with other TARP isoforms (Hann et al., unpublished). These known TARP interacting proteins were to be investigated immunologically and could be used to as a criterion in determining whether the immunoaffinity columns were successfully purifying intact TARP-interacting protein complexes.

Potential TARP interacting proteins, to be identified utilising proteomic tools, in this case MALDI-TOF and possibly MALDI-TOF/TOF could be any protein from a vast and diverse range of functional families. The most likely candidates being proteins that are related to the functional roles of the TARPs such as those proteins that are located within the synapse, those that are involved either in trafficking, or the cytoarchitecture, or the ER.

Results

Immunopurifications of TARP γ8 and its interacting proteins using the immunoaffinity columns generated using the N and C terminal directed antibodies.

Utilising the immunoaffinity columns generated using the Promega kit and the two TARP γ8 specific antibodies, a series of immunopurifications of Triton X-100™ soluble frontal cortex was conducted, with the resultant purified material being screened by

immunoblotting for TARP γ8 and potential interacting proteins. In all instances TX Insol refers to the Triton X-100™ insoluble fraction; Input/TX Sol refers to the Triton X-100™ soluble fraction that was loaded onto the columns; F1-F5 refers to the eluted fraction in the sequential order they were eluted from the column; FT refers to the Flow-Through, essentially the unbound material that had passed through the column (Input minus purified fractions).

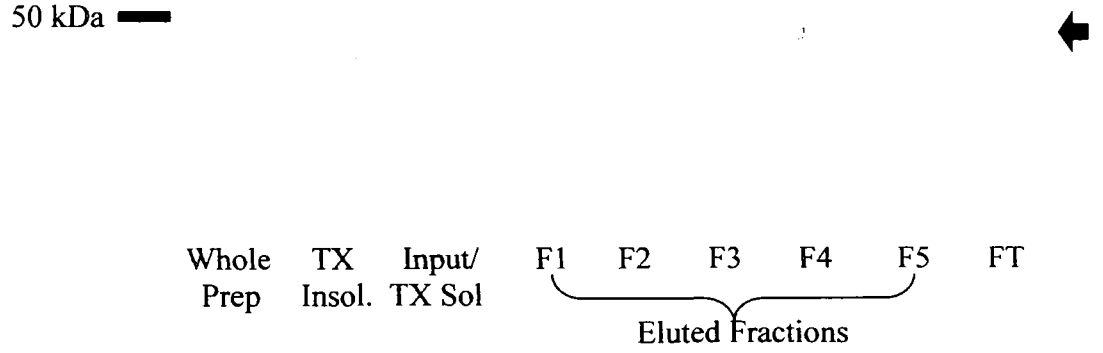

Figure 4.1: Immunoblot of Triton X-100™ soluble frontal cortex fractions purified using the immunoffinity column generated using the TARP γ8 N-terminal antibody probed for TARP γ8 using the anti-TARP anti-TARP γ8C antibody.

For eluted fractions 150µl of sample was chloroform-methanol precipitated and resuspended in 25µl 2X SDS-PAGE sample buffer, of which 10µl of sample was loaded per lane. Immunoblot was probed with the anti TARP γ8C antibody at a working concentration of 0.5µg/ml. The immunoreactive species of interest, corresponding to TARP γ8 is indicated by the black arrow.

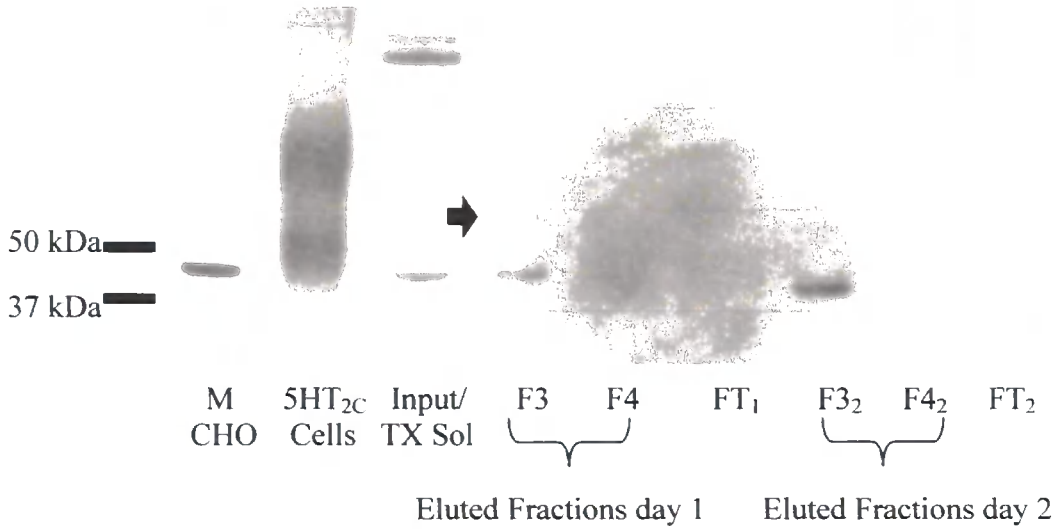

Figure 4.2: Immunoblot of Triton X-100™ soluble frontal cortex fractions purified using the immunoffinity column generated using the TARP γ8 N-terminal antibody probed for $5HT_{2C}$R using the Santa Cruz mouse monoclonal antibody.

For eluted fractions 150µl of sample was chloroform-methanol precipitated and resuspended in 25µl 2X SDS-PAGE sample buffer, of which 10µl of sample was loaded per lane. Immunoblot was probed with the Santa Cruz mouse monoclonal anti-$5HT_{2C}$R antibody at a 1 in 250 dilution.The immunoreactive species of interest, corresponding to the $5HT_{2C}$ receptor is indicated by the black arrow.

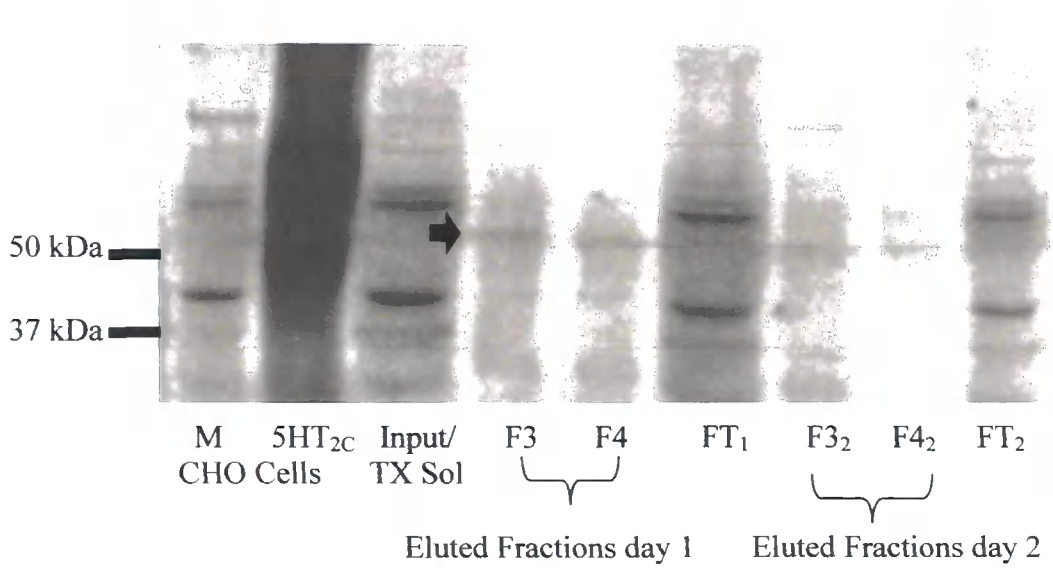

Figure 4.3: Immunoblot of Triton X-100™ soluble frontal cortex fractions purified using the immunoffinity column generated using the TARP γ8 N-terminal antibody probed for $5HT_{2C}$R using the Santa Cruz mouse monoclonal antibody.

For eluted fractions 150µl of sample was chloroform-methanol precipitated and resuspended in 25µl 2X SDS-PAGE sample buffer, of which 10µl of sample was loaded per lane. Immunoblot was probed with the Santa Cruz mouse monoclonal anti-$5HT_{2C}$R antibody at a 1 in 250 dilution. The immunoreactive species of interest, corresponding to the $5HT_{2C}$ receptor is indicated by the black arrow and detectable in the F3 and F4 eluted fractions from day 1.

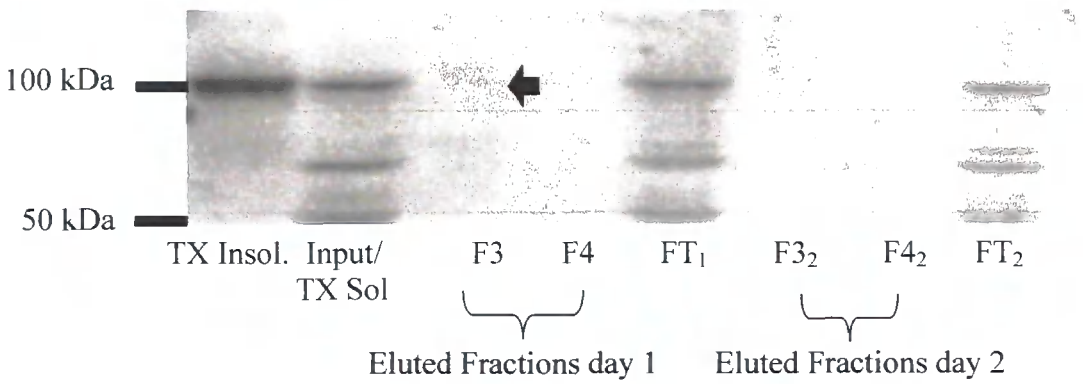

Figure 4.4: Immunoblot of Triton X-100™ soluble frontal cortex fractions purified using the immunoffinity column generated using the TARP γ8 N-terminal antibody probed for PSD-95.

For eluted fractions 150µl of sample was chloroform-methanol precipitated and resuspended in 25µl 2X SDS-PAGE sample buffer, of which 10µl of sample was loaded per lane. Immunoblot was probed with the Abcam anti-PSD-95 antibody at a 1 in 500 dilution. The immunoreactive species of interest, corresponding to PSD-95 are indicated by the black arrow, which has been placed to emphasise the presence of PSD-95 in the purified fractions.

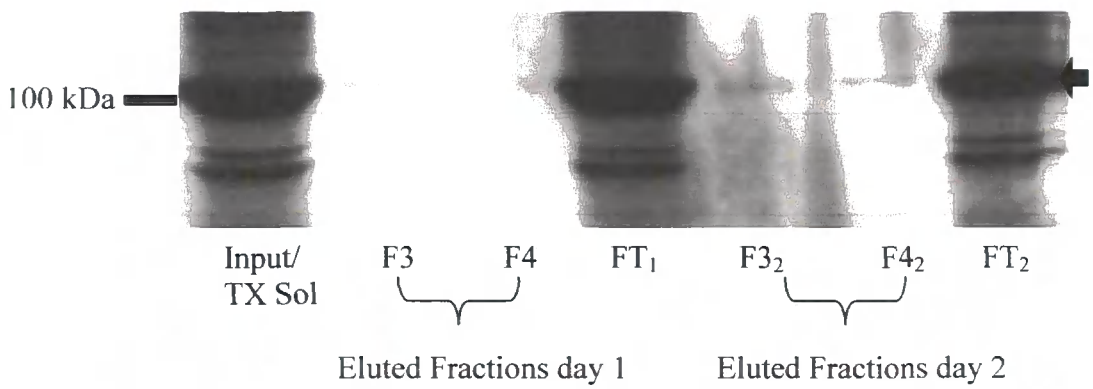

Figure 4.5: Immunoblot of Triton X-100™ soluble frontal cortex fractions purified using the immunoffinity column generated using the TARP γ8 N-terminal antibody probed for the GluR1 AMPAR subunit.

For eluted fractions 150µl of sample was chloroform-methanol precipitated and resuspended in 25µl 2X SDS-PAGE sample buffer, of which 10µl of sample was loaded per lane. Immunoblot was probed with the Cambridge Research Biochemicals anti GluR1 antibody at a 1 in 500 dilution. The immunoreactive species of interest, corresponding to GluR1 are indicated by the black arrow.

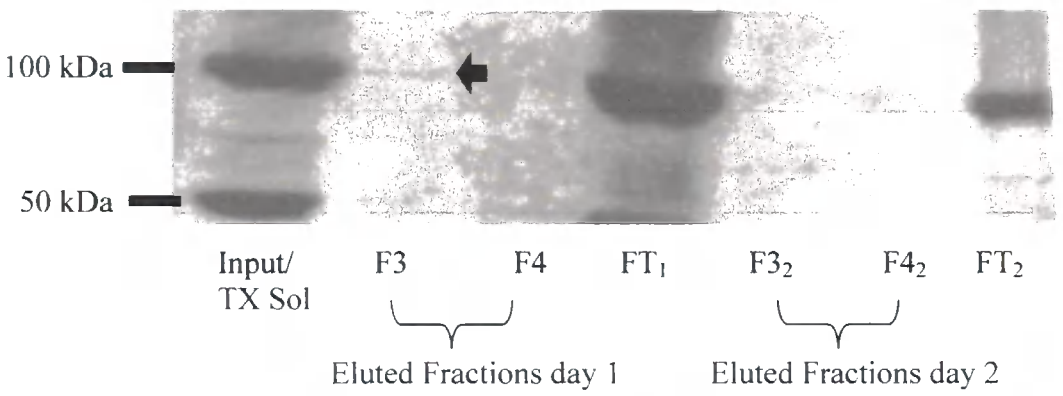

Figure 4.6: Immunoblot of Triton X-100™ soluble frontal cortex fractions purified using the immunoffinity column generated using the TARP γ8 N-terminal antibody probed for the GluR2 AMPAR subunit.

For eluted fractions 150µl of sample was chloroform-methanol precipitated and resuspended in 25µl 2X SDS-PAGE sample buffer, of which 10µl of sample was loaded per lane. Immunoblot was probed with the Santa Cruz anti GluR1 antibody at a 1 in 500 dilution. A weak signal from the immunoreactive species of interest, corresponding to GluR2 is detectable in F3. All immunoreactive species of interest are indicated by the black arrow, which emphasises the weak signal in F3.

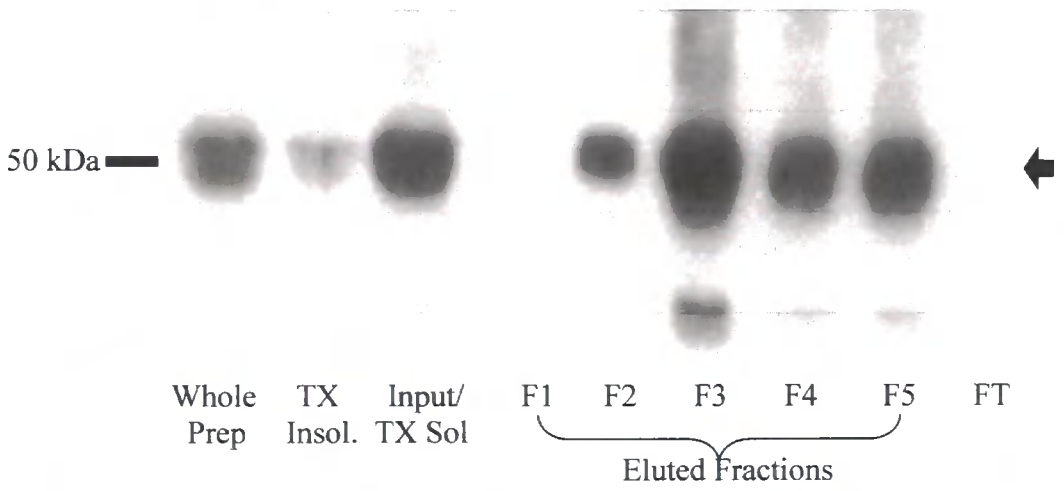

Figure 4.7: Immunoblot of Triton X-100 ™ soluble frontal cortex fractions purified using the immunoffinity column generated using the TARP γ8 C-terminal antibody probed for TARP γ8 using the anti-TARP anti-TARP γ8C antibody.

For eluted fractions 150µl of sample was chloroform-methanol precipitated and resuspended in 25µl 2X SDS-PAGE sample buffer, of which 10µl of sample was loaded per lane. Immunoblot was probed with the anti TARP γ8C antibody at a working concentration of 0.5µg/ml. The immunoreactive species of interest, corresponding to TARP γ8 are indicated by the black arrow.

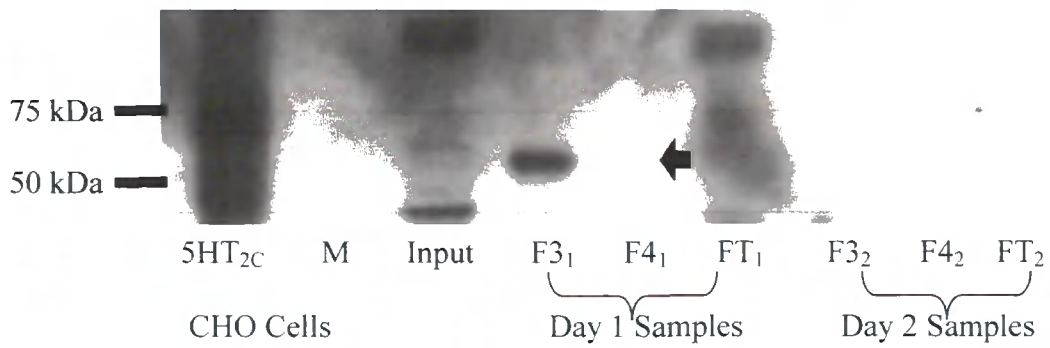

Figure 4.8: Immunoblot of Triton X-100™ soluble frontal cortex fractions purified using the immunoffinity column generated using the TARP γ8 C-terminal antibody probed for $5HT_{2C}$R using the Santa Cruz mouse monoclonal antibody.

For eluted fractions 150µl of sample was chloroform-methanol precipitated and resuspended in 25µl 2X SDS-PAGE sample buffer, of which 10µl of sample was loaded per lane. Immunoblot was probed with the Santa Cruz mouse monoclonal anti-$5HT_{2C}$R antibody at a 1 in 250 dilution. The immunoreactive species of interest, corresponding to the $5HT_{2C}$ receptor is in samples $F3_1$ and $F3_2$, indicated by the black arrow.

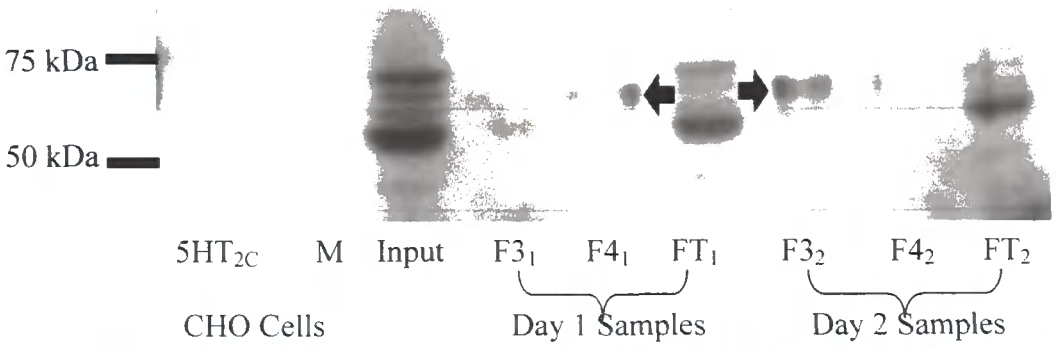

Figure 4.9: Immunoblot of Triton X-100™ soluble frontal cortex fractions purified using the immunoffinity column generated using the TARP γ8 C-terminal antibody probed for $5HT_{2C}$R using the Abcam rabbit polyclonal antibody.

For eluted fractions 150µl of sample was chloroform-methanol precipitated and resuspended in 25µl 2X SDS-PAGE sample buffer, of which 10µl of sample was loaded per lane. Immunoblot was probed with the Abcam rabbit anti-$5HT_{2C}$R polyclonal antibody at a 1 in 500 dilution. Species variations between the $5HT_{2C}$ Receptor expressed by the CHO cells compared with species used to generate the Abcam anti $5HT_{2C}$ receptor antibody resulted in the Abcam antibody not detecting $5HT_{2C}$ receptor in the CHO cells. The immunoreactive species of interest, corresponding to the $5HT_{2C}$ receptor are most easily detectable in samples $F3_{1-2}$ and $F4_{1-2}$ and are indicated by the black arrow.

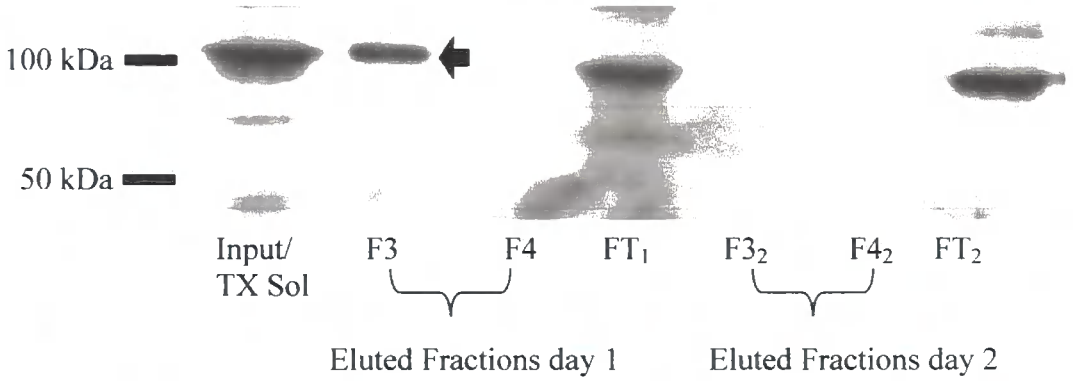

Figure 4.10: Immunoblot of Triton X-100™ soluble frontal cortex fractions purified using the immunoffinity column generated using the TARP γ8 C-terminal antibody probed for the GluR1 AMPAR subunit.

For eluted fractions 150µl of sample was chloroform-methanol precipitated and resuspended in 25µl 2X SDS-PAGE sample buffer, of which 10µl of sample was loaded per lane. Immunoblot was probed with the Cambridge Research Biochemicals anti GluR1 antibody at a 1 in 500 dilution. The immunoreactive species of interest, corresponding to GluR1 is indicated by the black arrow and emphasised in the F3 eluted fractions from day1.

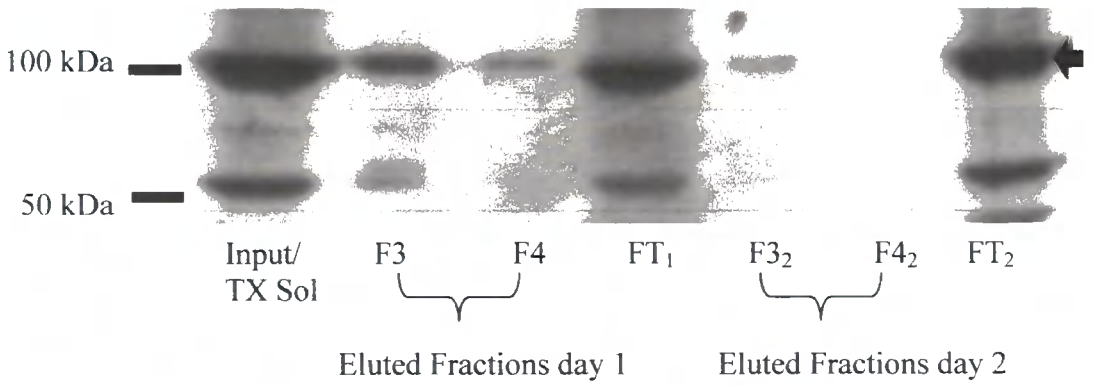

Figure 4.11: Immunoblot of Triton X-100™ soluble frontal cortex fractions purified using the immunoffinity column generated using the TARP γ8 C-terminal antibody probed for the GluR2 AMPAR subunit.

For eluted fractions 150µl of sample was chloroform-methanol precipitated and resuspended in 25µl 2X SDS-PAGE sample buffer, of which 10µl of sample was loaded per lane. Immunoblot was probed with the Santa Cruz anti GluR2 antibody at a 1 in 250 dilution. The immunoreactive species of interest, corresponding to GluR2 is indicated by the black arrow.

The immunoaffinity column generated using the TARP γ8 isoform specific antibodies are capable of purifying intact TARP γ8 interacting complexes.

Figures 4.1 and 4.7 demonstrate that both of the immunoaffinity columns generated with either the N-terminal directed or C-terminal directed TARP γ8 specific antibodies are capable of purifying TARP γ8 from a Triton-X100^{TM} solubilised cerebral cortex preparation, with the presence of known TARP interacting proteins, namely the AMPA receptor subunits GluR1 and GluR2 being co-purified, demonstrating the ability of the column to purify TARP γ8 interacting partners successfully (Figures 4.5, 4.6, 4.10 and 4.11).

The immunoaffinity column generated using the TARP γ8C antibody demonstrated the greatest efficiency of the two columns at purifying TARP γ8 and the interacting AMPA receptors from the tissue preparation. All the TARP γ8 that was detectable in the input was purified by the TARP γ8 C-terminal directed column, whereas the N-terminal directed TARP γ8 immunoaffinity column demonstrates approximately 50% efficiency at purifying TARP γ8. This potentially suggests that the N-terminal domain, particularly the site of the antigenic epitope, is partially masked or occluded by interacting proteins or structural properties of TARP γ8 that are not present in the C-terminal epitope.

Differences in the amounts of AMPA receptor subunits purified using each of the columns is most likely attributable to the lower purification levels obtained using the anti TARP γ8N column as such it will purify significantly less TARP γ8 that is potentially interacting with AMPA receptor subunits.

A $5HT_{2C}$ receptor-like species is purified as a protein interacting with TARP γ8.

Both immunoaffinity columns purified a protein of approximately 60 kDa in the peak fraction of the TARP γ8 purified material, which was detectable using three different antibodies raised to the $5HT_{2C}$ receptor (Figures 4.2, 4.3, 4.8 and 4.9). This protein was not discernable in the input or flow-through material, indicating that the protein was concentrated by the immunopurification to a detectable level as a consequence of purifying TARP γ8 and its interacting partners. The use of multiple antibodies, whilst not

confirming the proteins identity fully, gives strong indication that the protein is the $5HT_{2C}$ receptor.

PSD-95 is co-purified with TARP γ8 in Triton X-100™ soluble material.

Despite the majority of PSD-95 being present in the Triton X-100™ insoluble material, as was expected with a synaptic protein, a modest amount of PSD-95 was also detectable in the Triton X-100 ™ soluble input, of which a small, but detectable amount was co-purified using the TARP γ8 antibodies (Figure 4.4), indicating that some PSD-95 is located non-synaptically and is interacting with TARP γ8.

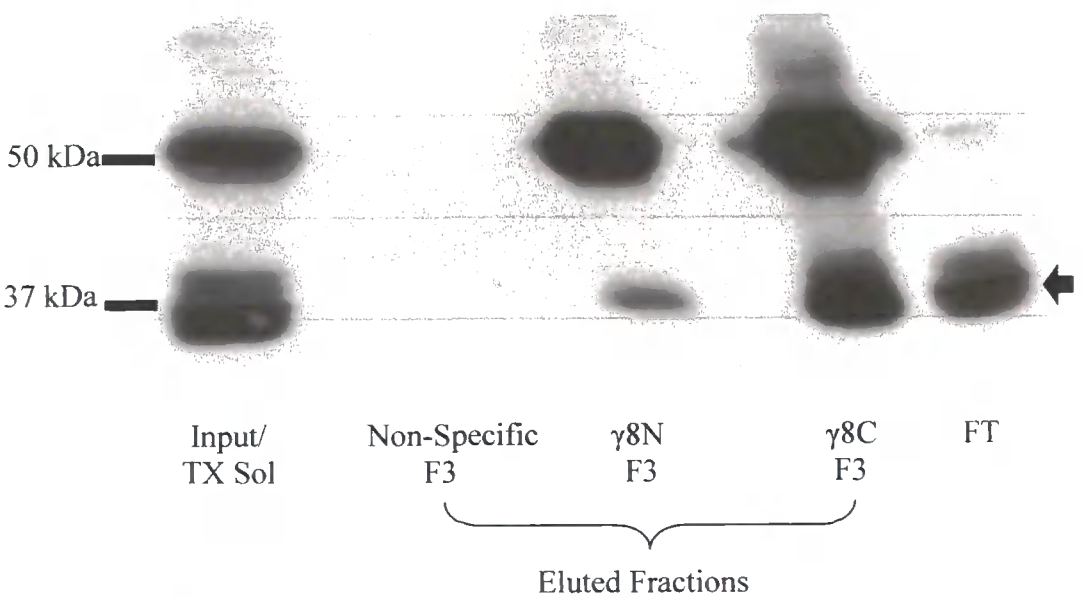

Figure 4.12: Immunoblot of Triton X-100™ soluble and immunopurified frontal cortex fractions using control IgG, or the anti TARP γ8 N-terminal antibody, or the anti TARP γ8 C-terminal antibody column, probed for TARP γ2.

For eluted fractions 150µl of sample was chloroform-methanol precipitated and resuspended in 25µl 2X SDS-PAGE sample buffer, of which 10µl of sample was loaded per lane. Immunoblot was probed with the anti TARP γ2 antibody at a working concentration of 1µg/ml. Fractions containing the highest concentrations of purified protein were selected. The immunoreactive species of interest, corresponding to TARP γ2, are indicated by the black arrow.

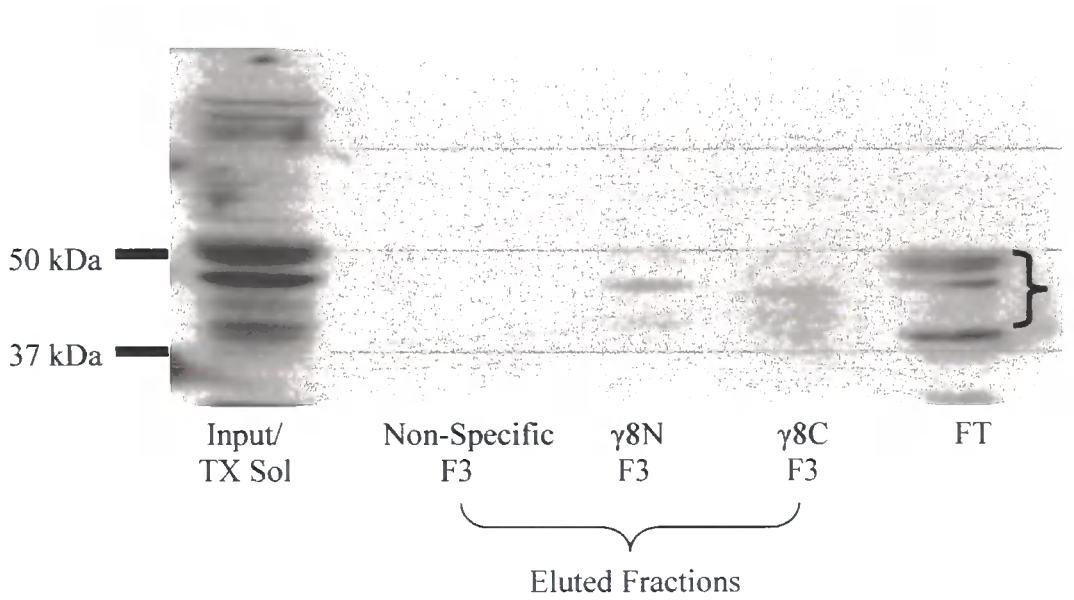

Figure 4.13: Immunoblot of Triton X-100™ soluble and immunopurified frontal cortex fractions using the immunoffinity column generated using control IgG, or the anti TARP γ8 N-terminal antibody, or the anti TARP γ8 C-terminal antibody column, probed for TARP γ4.

For eluted fractions 150µl of sample was chloroform-methanol precipitated and resuspended in 25µl 2X SDS-PAGE sample buffer, of which 10µl of sample was loaded per lane. Immunoblot was probed with the anti TARP γ4 antibody at a working concentration of 2µg/ml. Again the immunopurified fractions containing the peak amounts of protein were used. The immunoreactive species of interest, corresponding to TARP γ4 are indicated by the brackets and detectable in the Input, γ8N and γ8C columns.

TARP γ8 associates with other TARP isoforms within an interacting complex.

Figures 4.12 and 4.13 demonstrate the presence of TARPs γ2 and γ4 within the TARP γ8 purified material. Due to the specificity of the antibody, it is not due to cross-reactivity of the TARP γ8 antibodies with the other TARP isoforms, but rather, that TARP γ2 and γ4 interact with TARP γ8, either directly, or via an intermediate protein such as PSD-95, or more likely AMPA receptor subunit(s).

Proteomic analysis of TARP γ8 interacting proteins.

Using the immunoaffinity columns generated with the TARP γ8 specific N and C terminal directed antibodies, a series of immunopurifications was conducted on Triton X-100™ soluble frontal cortex, with the peak eluted fractions being pooled and prepared for proteomic analysis using MALDI-TOF and MALDI-TOF/TOF.

NS γ8N γ8C Mol. wt

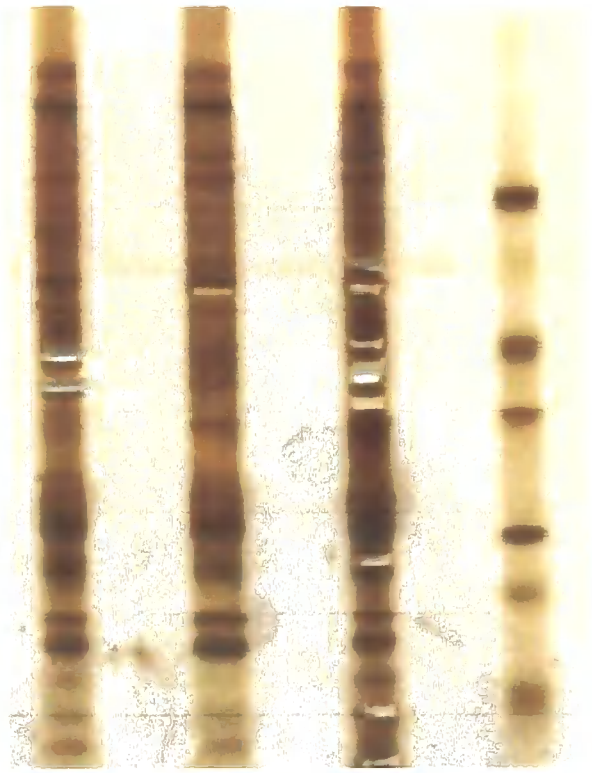

NS γ8N γ8C Mol. wt

Figure 4.14: Representative examples of the 1-Dimensional gels used for proteomics.

On the left is the Nu-PAGE 10% SDS gel loaded with the peak eluted fractions from the immunoaffinity columns generated using non-specific IgG (NS), TARP γ8 N-terminal (γ8N), and TARP γ8 C-terminal (γ8C) antibodies prior to extraction of the bands of interest. The image on the right, shows the same gel subsequent to band extraction. To identify banding pattern, the gels were silver stained, with this being the most suitable method of labelling the protein when compared with RubyPro staining with regard to being able to detect the proteins and extract them manually. Unfortunately, the scanner used to record the image on the left, means that its resolution cannot be enhanced to show the bands selected on the gel itself. Not all bands extracted from the gels were identified successfully.

Proteins purified by the N-terminal TARP γ8 immunoaffinity column	Proteins purified by the C-terminal TARP γ8 immunoaffinity column
Vesicle-fusing ATPase (Vesicular-fusion protein NSF) (N-ethylmaleimide sensitive fusion protein) [Mus musculus] – Identified by MALDI-TOF/TOF	2',3'-cyclic-nucleotide 3'-phosphodiesterase I [Mus musculus] – Identified by both MALDI-TOF and MALDI-TOF/TOF on separate samples.
Na+/K+ -ATPase beta 1 subunit [Mus musculus] – Identified using MALDI-TOF/TOF	Myelin basic protein – Identified by both MALDI-TOF and MALDI-TOF/TOF on separate samples.
2',3'-cyclic-nucleotide 3'-phosphodiesterase I [Mus musculus] – Identified by MALDI-TOF/TOF	Gamma-actin [Mus musculus] – Identified by MALDI-TOF
	Purine rich element binding protein B [Mus musculus] – Identified by MALDI-TOF
	Na+/K+ -ATPase beta 1 subunit [Mus musculus] – Identified by MALDI-TOF/TOF

Figure 4.15: Summary table showing the different proteins purified using the TARP γ8 immunoaffinity columns that were subsequently identified by proteomic analysis of the extracted bands.

For the immunoaffinity columns generated using the anti TARP γ8 antibodies, only protein bands detectable using silver staining that were completely distinct from any existing bands in the material purified using the non-specific IgG immunoaffinity column

were analysed. Some bands unique to the non-specific material were also analysed, but no positive identification was possible. Six interacting proteins were identified using proteomics, with two of those proteins being identified in material purified by both the N and C terminal directed TARP γ8 immunoaffinity columns (blue). The raw data generated from the MALDI-TOF analysis can be located in Appendix B (Pages 187-196). The proteomic analysis of the bands was conducted, as mentioned in the materials and methods, page 50, by Joanne Robson (University of Durham).

The TARP γ8 immunoaffinity columns both demonstrate the ability to purify previously unknown TARP γ8 interacting proteins

The diverse range of proteins selectively purified by the TARP γ8 specific immunoaffinity columns, including myelination-related proteins and those related to the cytoarchitecture highlight the suitability of these columns and the proteomic methodology for identifying unknown TARP γ8 interacting proteins. The presence of N-ethylmaleimide sensitive fusion protein (NSF) provides reassurance regarding the specificity of the proteomic analysis by virtue of its already described interactions with AMPA receptors.

Discussion

The immunoaffinity columns generated, whilst both successful at purifying TARP γ8 and its interacting proteins, display different levels of immunopurification of the TARP γ8 isoform. The γ8C immunoaffinity column purified TARP γ8 to the extent that none was detectable in the flow-through after a single immunopurification, indicating that the immunoaffinity column has a high affinity and binding capacity for TARP γ8 that was not saturated by the amount of material added to the column. Consequentially, the γ8C immunoaffinity column also successfully purified the highest concentration of interacting proteins, particularly the AMPA receptor subunits, when compared with the γ8N immunoaffinity column. Whilst explicable by the relative affinity of the antibodies for

TARP γ8, the possibility of epitope masking in the N-terminus, which is an issue due to the purification method retaining intact protein complexes, cannot be dismissed. Regardless of the explanation and whether or not a sub-population of TARP γ8 defined by its interacting partners is being undetected by the γ8N immunoaffinity column, the γ8C immunoaffinity column is purifying all the detectable TARP γ8 from the sample, so the eluted fractions obtained from that column are not lacking any detectable functional sub-population of TARP γ8.

Both immunoaffinity columns also successfully purified a protein of approximately 60 kDa that was recognised with multiple commercial anti-$5HT_{2C}$ receptor antibodies. The molecular weight of this protein corresponds with the molecular weight of a glycosylated $5HT_{2C}$ receptor (Abramowski et al. 1995, Backstrom et al. 1999, Parker et al. 2003), providing some reassurance that this is $5HT_{2C}$ receptor. Due to the antibodies lack of congruent specificity in native tissue where $5HT_{2C}$ receptor appears to be expressed at sufficiently low levels to avoid detection, the commonality of this band is reassuring, providing yet more support that this protein is $5HT_{2C}$ receptor. At the current time the identity cannot be fully confirmed because of the absence of demonstrable $5HT_{2C}$ receptor protein expression in the native tissue due to physiologically low concentrations of the protein in most CNS regions and the absence of choroid plexi material as a positive control.

The presence of PSD-95 in the TARP γ8 purified material, offers further support to the original hypothesis in that it may be the intermediate protein interacting with $5HT_{2C}$ receptors and TARPs/AMPA receptors. However, it may not be the only intermediate protein or even in the same complex as both TARPs/AMPA receptors and $5HT_{2C}$ receptors.

As such, whilst the columns and methodology does demonstrate the capacity to purify proteins interacting with TARP γ8, it does not provide evidence that they are all interacting with TARP γ8 in the same complex or at the same time, with the likely

possibility existing that multiple protein complexes exist within the TARP γ8 purified material.

To further complicate the number of potential protein complexes being purified by the columns, is the presence of both TARP γ2 and TARP γ4 in the TARP γ8 immunopurified material. Due to the specificity of the TARP γ8 antibodies, that showed no cross-reactivity with the other TARP isoforms, this interaction has to be believed to be genuine, and somewhat unprecedented with nothing in the literature indicating multiple TARP isoforms being present within the same complex. Indeed, at the current time, there is still speculation as to the precise number of TARPs present within an AMPA receptor complex at any one time, so the functional significance of multiple TARP isoforms within the same complex is purely speculative. It is most likely that the assortment of TARPs within an AMPA receptor complex, combined with the combinations of AMPA receptor subunits, would be responsible for targeting specific populations of AMPA receptors to different cellular locations, via interactions with different key proteins.

One final observation from the data is that TARP γ8 appears to be predominantly non-synaptic, with the vast majority being present in the Triton X-100™ soluble material. This does not imply however, that TARP γ8 is mostly extra-synaptic, because the solubilised material contains both extra-synaptic membrane proteins and intracellular proteins. As such, it is possible that the interactions of TARP γ8 with not only the other TARP isoforms, but also the $5HT_{2C}$ receptor-like species occur intracellularly, and no information is given as to what cellular processes these interactions occur in.

The data obtained from the material purified using the TARP γ8 immunoaffinity columns and subsequently analysed via proteomic techniques offers a novel and in some cases, previously unconsidered set of interacting proteins to those detected by immunoblotting. Of the two proteomic techniques used for analysis; MALDI-TOF and MALDI-TOF/TOF, one of the only common proteins identified was myelin basic protein, a protein that is, as its name would suggest, extensively associated with myelin (Kornguth et al. 1965, Boggs 2006). This is an unusual and novel finding, for whilst myelin is an integral component in

the nervous system architecture, it wouldn't obviously be associated with a protein such as TARP γ8; a protein whose role in the myelin sheath has not even been considered, but may have implications in conditions such as multiple sclerosis (Sarchielli et al. 2007).

The other protein common to both proteomic techniques and both TARP γ8 immunoaffinity columns was 2',3' cyclic-nucleotide 3' phosphodiesterase 1 (CNPase), again another protein exclusive to myelinated regions of the CNS, predominantly expressed in oligodendrocytes as opposed to neurones (Nishizawa et al. 1981, Brunner et al. 1989). Significantly, CNPase has been implicated in schizophrenia and other neurological conditions where incorrect myelination has been identified as a potentially important component, although the specific role of CNPase in these conditions is unclear (Yin et al. 2006, McCullumsmith et al. 2007). CNPase is known to have a role in mictrotubule assembly and subsequent linkage to cellular membranes (Lee et al. 2005), suggesting that its most likely interaction with TARP γ8 is in the trafficking/targeting stages of the TARP γ8 functional role, possibly in a complex with MAP-1A, a mictrotubule associating protein demonstrated to interact with both TARPs and AMPA receptors (Ives et al. 2004 Seog 2004).

These results essentially facilitate the possibility that TARP γ8 is present in other cells in the central nervous system, most likely with a basic functional role similar to that in neuronal cells, but in different processes, a possibility that, due to the presence of ionotropic glutamate receptors on non-neuronal cells in the CNS, is a logical consideration, but a poorly investigated one (Patneau 1994, Chew et al. 1997, Káradóttir et al. 2005).

The implications for this have the potential to be considerable, with the role of AMPA receptors in oligodendrocytes believed to potentially promote development from progenitors into mature oligodendrocytes and myelination (Pende et al. 1994); but also includes the mediation of excitotoxic cell death following injury, particularly in the spinal cord (Sánchez-Gómez and Matute 1999, Li and Stys 2000, Park et al. 2003).

Perhaps the most significant of the proteins purified with regard to confirming the practical functionality of the immunoaffinity columns, and an established AMPA receptor interacting protein, was N-ethylmaleimide sensitive fusion protein (NSF). NSF has been shown to interact with GluR2 containing AMPA receptors in a range of brain regions; promoting their cycling at the synapse, most likely to and from intracellular pools, via NMDA-activated disruption of PICK1 binding (Lee et al. 2002, Sossa et al. 2006, 2007, Steinberg et al. 2004).

The presence of this protein provides strong positive evidence of intact interacting complexes being purified by the immunoaffinity columns as well as increasing confidence in the identification techniques. The inability of the proteomic methodology to identify either TARPs or AMPA receptor subunits is not a cause for concern due to the number of interacting proteins purified coupled with the large quantity of proteins at similar molecular weights being present in the sample. As such further separation of the protein bands, possibly by 2-D gel electorphoresis may be required in future studies.

Other notable proteins identified by either MALDI-TOF or MALDI-TOF/TOF as interacting with TARP γ8 include subunits of both beta and gamma actin, suggesting that the TARP γ8 purified material contains at least some TARP γ8 interacting in a complex with elements of the cytoarchitecture, possibly in trafficking, or in anchoring at the cell surface. This interaction between TARP γ8 and elements of the cytoarchitecture again raises the possibility of MAP-1A and components of the microtubule network being present in this interaction, contributing to its functional significance.

Chapter 5: An investigation of the functional significance of the interactions between TARPs and $5HT_{2C}$ receptors using mice with altered forebrain expression of $5HT_{2C}$ receptors.

Introduction

One of the most potentially significant results of the immunoaffinity purifications in the previous chapter was the presence of a band detectable with multiple commercial $5HT_{2C}$ receptor antibodies that was co-purified with TARP γ8. This provides evidence supporting the hypothesis of $5HT_{2C}$ receptors physically interacting with TARPs and potentially AMPA receptors within a protein complex.

The $5HT_{2C}$ receptor is a G-protein coupled receptor involved in the stimulation of phospholipase C and subsequent increase in inositol 1, 2, 3 triphosphate (IP_3), leading to an increase in intracellular Ca^{2+}.

The $5HT_{2C}$ receptor also possesses five adenosine sites, labelled as A, B, C, D and E, located in the amino acids at positions 156-160 (5'-3') that undergo mRNA editing. This property means that there are potentially 32 $5HT_{2C}$ receptor mRNA variants, from which 24 different protein splice variants are possible (Burns et al. 1997, Nakae et al. 2008). From these potential 24 variants, 22 have been seen to be expressed in the CNS. The unedited variant of the receptor displays the highest levels of constitutive activity and G protein coupling, and the fully edited variant displays neither, with the partially edited variants displaying differing degrees of both; Editing at either the C and E sites appears to have the greatest effect on these properties (Herrick-Davis et al. 1999, Niswender et al. 1999, Wang et al. 2000, Berg et al. 2001, Flomen et al. 2004).

The splice variants also display specific regional distributions, with further evidence indicating that they frequently form functional conformational heteromeric dimers at the cell surface (Mancia et al. 2008).

There is also evidence that changes in the editing of $5HT_{2C}$ receptor mRNA can occur as a consequence of chronic treatment with some pharmacological agents, or as a consequence of chronic changes brought about by a neurological condition, within certain brain regions, indicating that the specific splice variants may play individual roles in $5HT_{2C}$ receptor pharmacology in the CNS as a whole. A good example of this are the enhanced levels of editing at site A in the post-mortem samples of frontal cortex obtained from clinically depressed individuals who had successfully committed suicide (Niswinder et al. 2001).

Functionally, the $5HT_{2C}$ receptor displays multiple roles in the central nervous system, with evidence of $5HT_{2C}$ receptors having a role in appetite, locomotion, anxiety, schizophrenia and depression (Pandey et al. 1995, Moreau et al. 1996, Jenck et al. 1998, Clenet et al. 2001, Frank et al. 2002, Nunes-de-Souza et al. 2008). It is the latter of these roles that is of interest in this study, due to the increasing prevalence of evidence for an AMPA receptor component in depression, and more specifically, the pharmacological treatment of depression, then the possibility of a functional interaction between $5HT_{2C}$ receptors and AMPA receptors could be a key component in understanding depression and developing future treatments.

The $5HT_{2C}$ receptor is also unusual in the fact that it undergoes internalisation in both the presence of agonists and antagonists (Van Oekelen et al 2003).

Unfortunately, due to the inherent limitations of both the proteomic technique and the versatility of the $5HT_{2C}$ receptor antibodies, the band identified following immunopurification was lacking positive confirmation, so an alternative approach to investigate a potential interaction between $5HT_{2C}$ receptors and AMPA receptors via TARP $\gamma 8$ was required. Dr Megan Holmes, based at Edinburgh University, had developed mice both over-expressing $5HT_{2C}$ receptors and mice exhibiting $5HT_{2C}$ receptor knockdown within the frontal cortex, and kindly provided access to these resources so that any physiological consequences of these two experimental phenotypes upon the levels of TARPs and AMPA receptors could be investigated.

Results

Hemispheres from the mice possessing altered $5HT_{2C}$ receptor expression were contrasted with their relevant controls, with the differences in TARP and AMPA receptor subunit expression levels measured by quantitative immunoblotting. Further differences in protein expression were recorded by immunohistochemical and autoradiographical methodologies, with the observations providing data regarding the presence of a functional interaction between $5HT_{2C}$ receptors and TARPs/AMPA receptors.

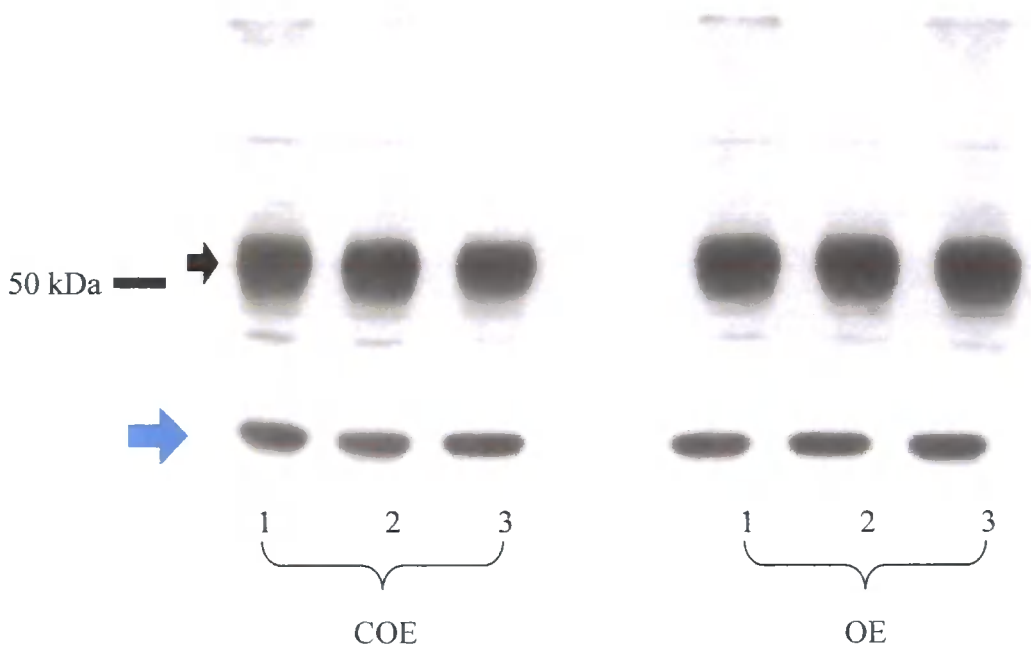

Figure 5.1.1: Representative immunoblot of $5HT_{2C}$ receptor overexpressing forebrain Vs control probed with the TARP γ8C antibody.

One cerebral hemisphere, minus the cerebellum, from either control (COE) or $5HT_{2C}$ receptor over-expressing (OE) mice was loaded onto a 10% SDS-PAGE gel. Three separate control mice and their over-expressing equivalents were used for a total *n* of 3. Protein amounts calculated by Lowry protein assay allowed 10 µg of protein to be loaded per lane. Immunoblot was probed with the TARP γ8C antibody and band intensity calculated using ImageJ.

The immunoreactive species indicated by the black arrow is TARP γ8. The immunoreactive species indicated by the blue arrow, and not shown at actual molecular weight, is a representative example of the β-actin loading control. The immunoblot was repeated in triplicate with the mean TARP γ8/β-actin intensities for the knockdown condition and the controls were calculated, with these values being used as described in Section 2.11 on page 50.

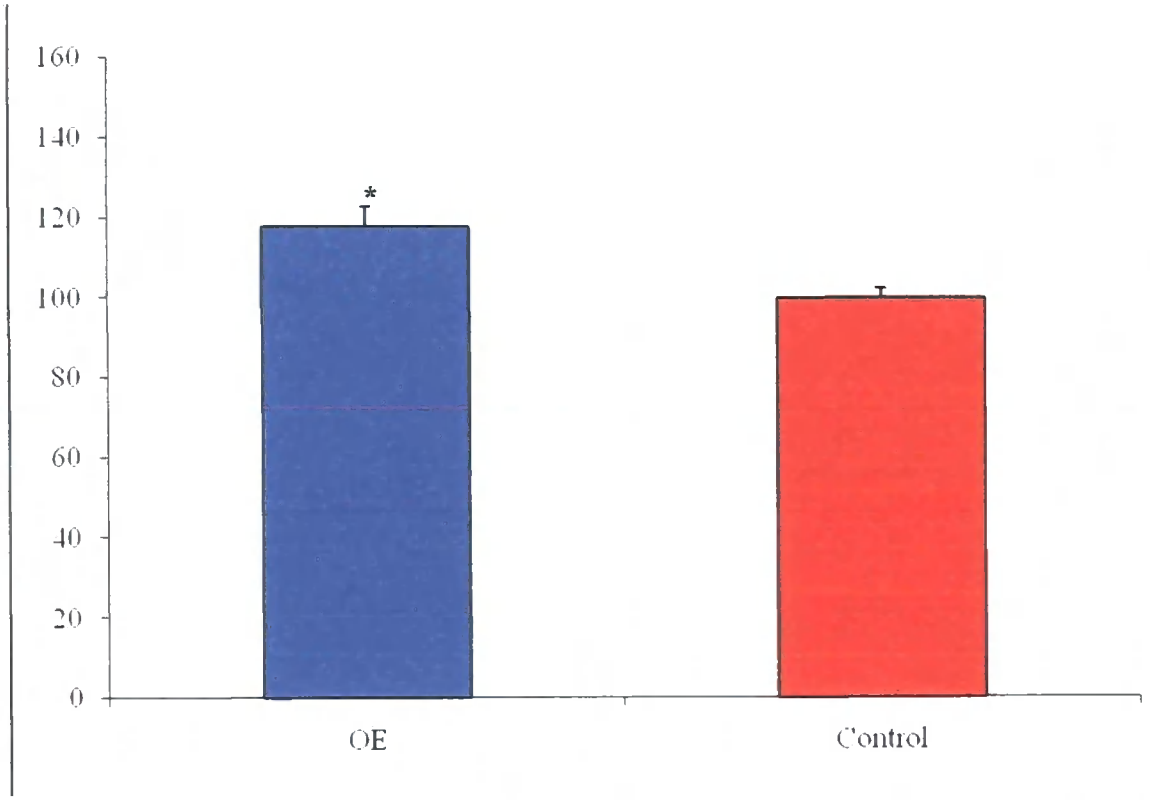

Figure 5.1.2: Graph showing the mean percentage expression of TARP γ8 in the forebrain of the $5HT_{2C}$ receptor over-expressing mice compared with controls.

Shows the mean percentage difference in forebrain expression of TARP γ8 between the $5HT_{2C}$ receptor over-expressing mice and their controls calculated using triplicate samples from an *n* of 3. For the Control the mean percentage was set as 100%. The asterisk signifies that this percentage difference corresponds to a statistically significant (at the <0.05 probability level) difference between the expression of TARP γ8 in the $5HT_{2C}$ receptor over-expressing mice compared with controls.

Total levels of TARP γ8 are significantly increased in the forebrain $5HT_{2C}$ receptor over-expressing mice.

The total levels of TARP γ8 in $5HT_{2C}$ receptor over-expressing mice demonstrated a statistically significant increase in total TARP γ8 expression of 17% compared to the control. Results were significant at the probability of <0.05, P = 0.0328 based upon an *n* of 3.

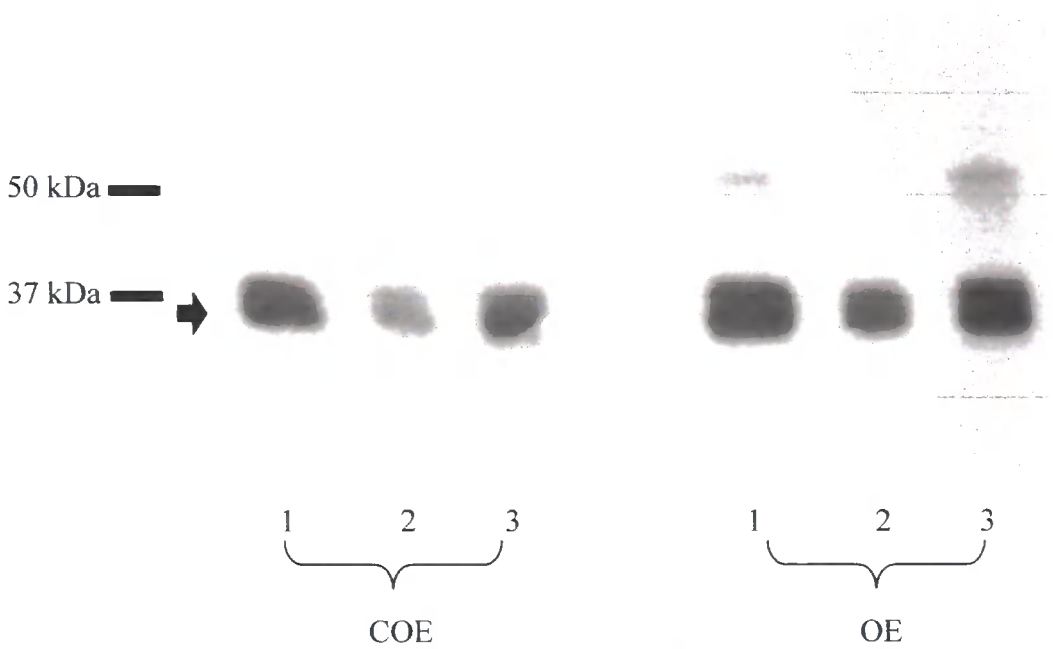

Figure 5.2.1: Representative immunoblot of $5HT_{2C}$ receptor overexpressing forebrain Vs control probed with the TARP γ2 antibody.

One cerebral hemisphere, minus the cerebellum, from either control (COE) or $5HT_{2C}$ receptor over-expressing (OE) mice was loaded onto a 10% SDS-PAGE gel. Three separate control mice and their over-expressing equivalents were used for a total *n* of 3. Protein amounts calculated by Lowry protein assay allowed 10 μg of protein to be loaded per lane. Immunoblot was probed with the TARP γ2 antibody and band intensity calculated using ImageJ. The immunoblot was repeated in triplicate with the mean TARP

γ2/β-actin intensities for the knockdown condition and the controls were calculated, with these values being used as described in Section 2.11 on page 50. The immunoreactive species corresponding to TARP γ2 is indicated by the black arrow.

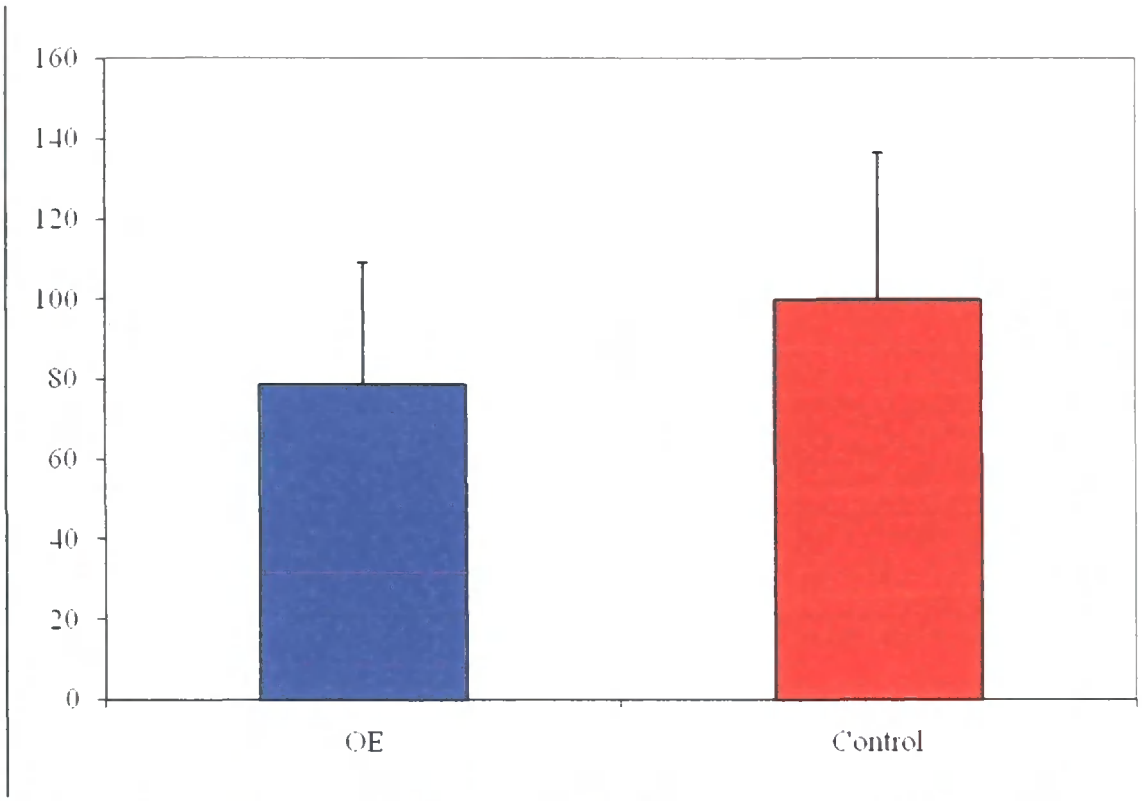

Figure 5.2.2: Graph showing the mean percentage expression of TARP γ2 in the forebrain of the $5HT_{2C}$ receptor over-expressing mice compared with controls.

Shows the mean percentage difference in forebrain expression of TARP γ2 in $5HT_{2C}$ receptor over-expressing mice compared with their controls calculated using triplicate samples from an *n* of 3. For the Control the average was set as 100%

Total levels of TARP γ2 appear to be lower in the forebrain of $5HT_{2C}$ receptor over-expressing mice.

All repeats of the TARP γ2 analysis displayed a trend towards a decrease in the levels of TARP γ2 expression, however, this decrease was not seen to be significantly significant, P = 0.5345, based on an *n* of 3.

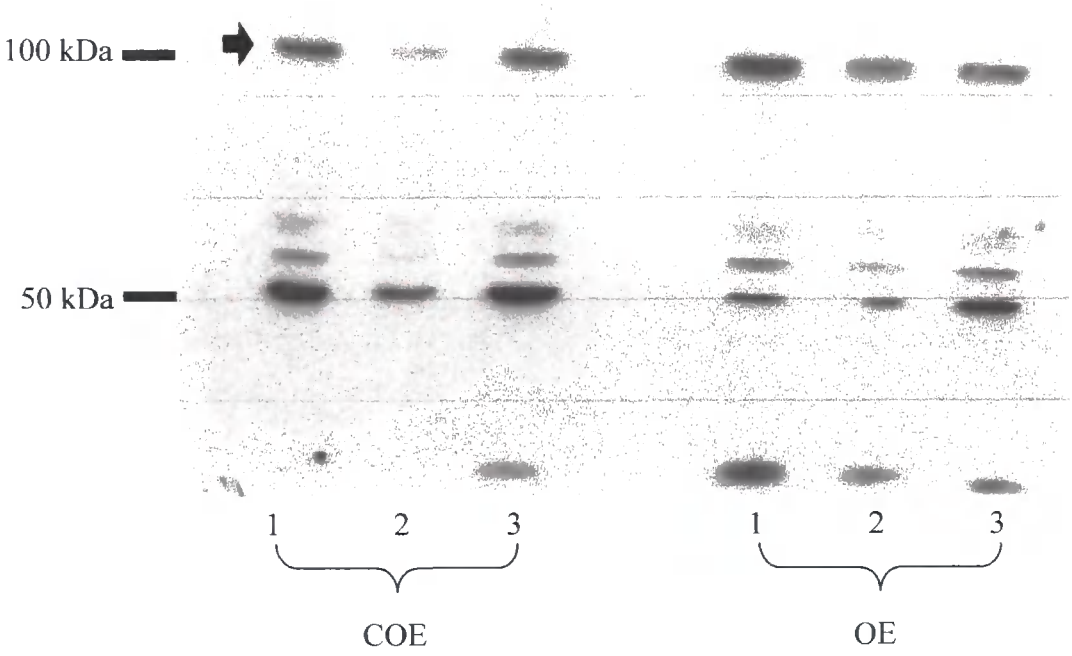

Figure 5.3.1: Representative immunoblot of $5HT_{2C}$ receptor overexpressing forebrain Vs control probed with the GluR1 antibody.

One cerebral hemisphere, minus the cerebellum, from either control (COE) or $5HT_{2C}$ receptor over-expressing (OE) mice was loaded onto a 10% SDS-PAGE gel. Three separate control mice and their over-expressing equivalents were used for a total *n* of 3. Protein amounts calculated by Lowry protein assay allowed 10 μg of protein to be loaded per lane. Immunoblot was probed with the GluR1 antibody and band intensity calculated using ImageJ. The immunoblot was repeated in triplicate with the mean GluR1/β-actin intensities for the knockdown condition and the controls were calculated, with these values being used as described in Section 2.11 on page 50. The immunoreactive species corresponding to GluR1 is indicated by the black arrow.

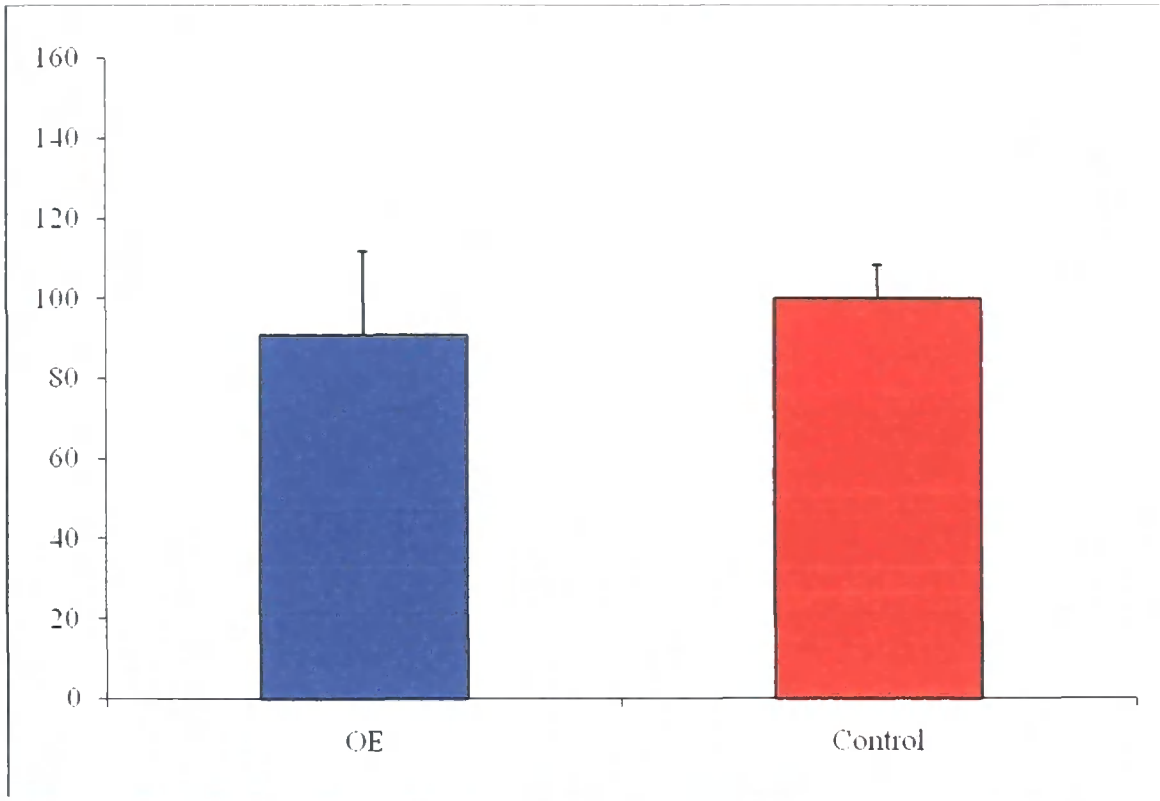

Figure 5.3.2: Graph showing the mean total levels of GluR1 in the forebrain of the $5HT_{2C}$ receptor over-expressing mice.

Shows the mean percentage difference in forbrain expression of GluR 1 in the $5HT_{2C}$ receptor over-expressing mice compared with their controls calculated using triplicate samples from an *n* of 3. For the Control the average was set as 100%.

Total levels of GluR1 appear to be unaffected in the forebrain or $5HT_{2C}$ receptor over-expressing mice.

A trend towards a slight (less than 10%) decrease in total GluR1 expression was noticed in the $5HT_{2C}$ receptor over-expressing mice forebrains, however, this was not statistically significant, P = 0.2657, based upon an *n* of 3.

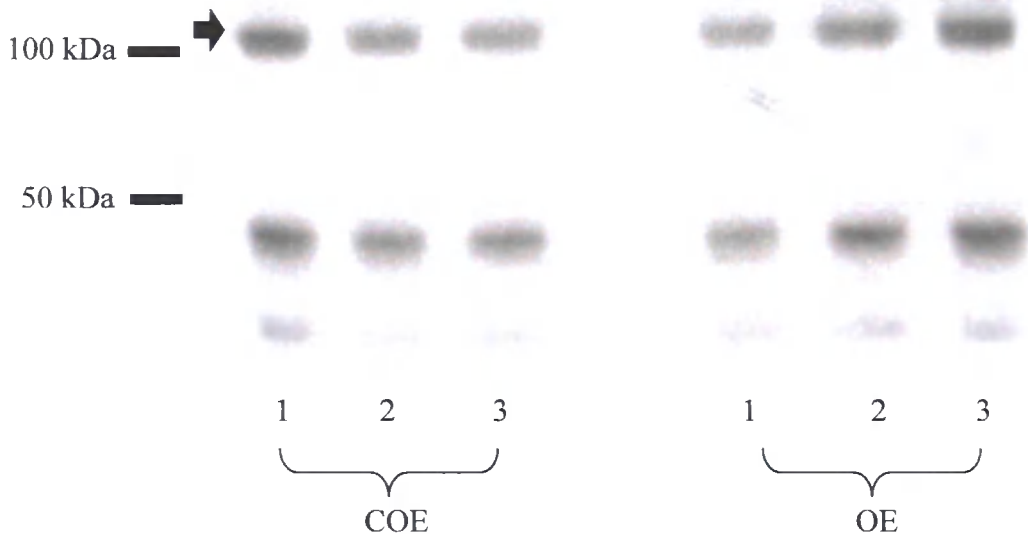

Figure 5.4.1: Representative immunoblot of $5HT_{2C}$ receptor overexpressing forebrain Vs control probed with the GluR2 antibody.

One cerebral hemisphere, minus the cerebellum, from either control (COE) or $5HT_{2C}$ receptor over-expressing (OE) mice was loaded onto a 10% SDS-PAGE gel. Three separate control mice and their over-expressing equivalents were used for a total *n* of 3. Protein amounts calculated by Lowry protein assay allowed 10 μg of protein to be loaded per lane. Immunoblot was probed with the GluR2 antibody and band intensity calculated using ImageJ. The immunoblot was repeated in triplicate with the mean GluR2/β-actin intensities for the knockdown condition and the controls were calculated, with these values being used as described in Section 2.11 on page 50. The immunoreactive species corresponding to GluR2 is indicated by the black arrow

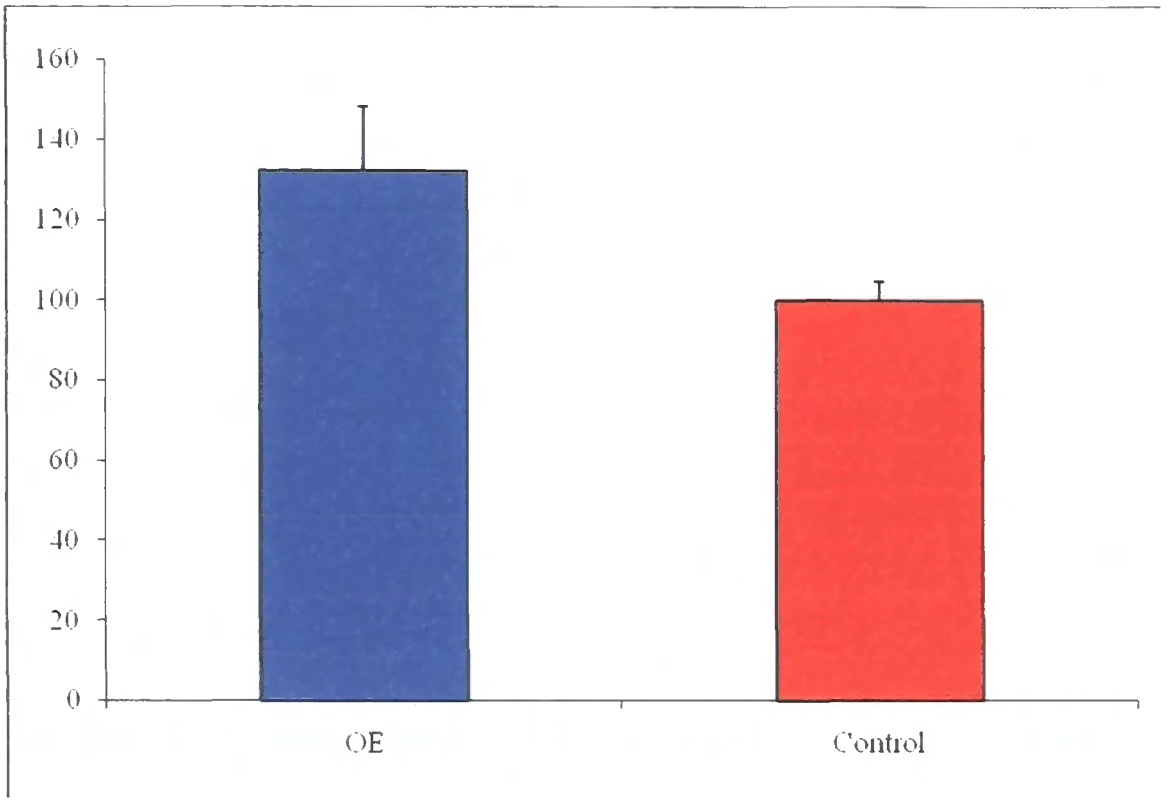

Figure 5.4.2: Graph showing the mean percentage expression of GluR2 in the forebrain of the $5HT_{2C}$ receptor over-expressing mice.

Shows the mean percentage difference in GluR2 expression in the forbrains of $5HT_{2C}$ receptor over-expressing mice calculated using triplicate samples from an *n* of 3. For the Control the average was taken as 100%.

Total levels of GluR2 appear to be elevated in the forebrain of $5HT_{2C}$ receptor over-expressing mice.

All repeats of the GluR2 analysis showed a trend towards an increase in the levels of GluR2 expression. However, this increase was not seen to be significantly significant, P = 0.1215, based on an *n* of 3..

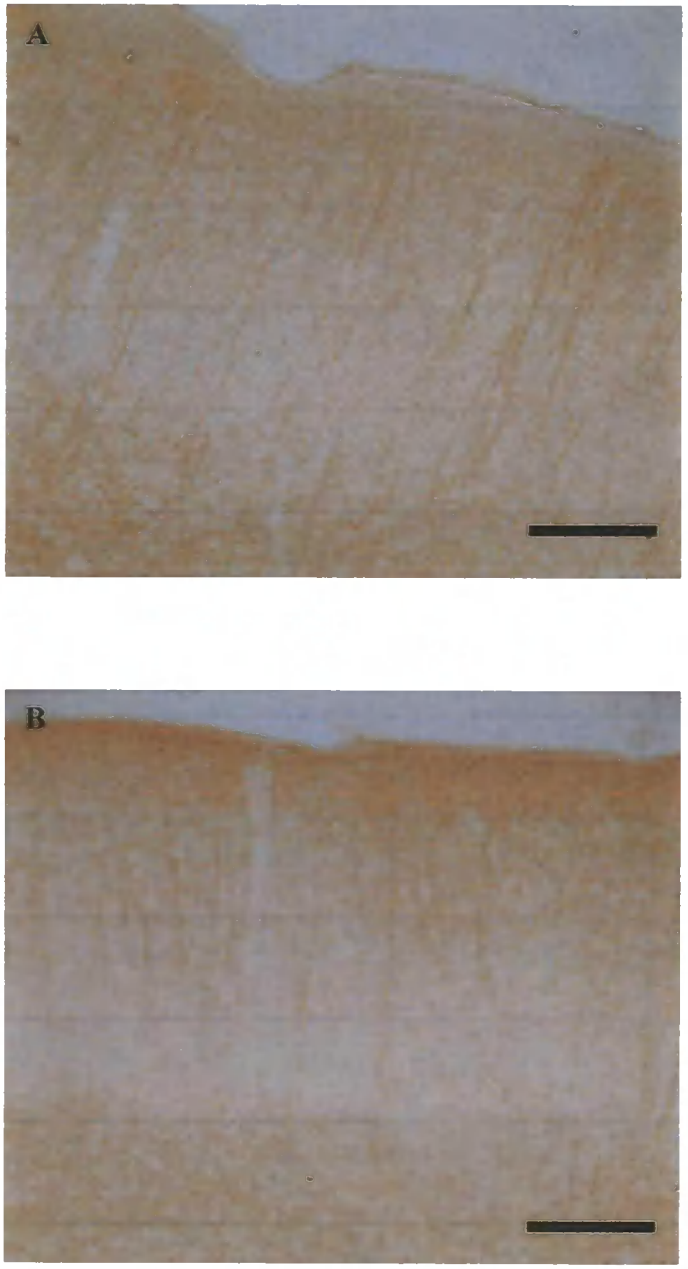

Figure 5.5: Immunohistochemical sections of $5HT_{2C}$ over-expressing (A) and control (B) mice frontal cortex probed with the TARP γ8C. Magnification X200. Scale bars = 100 μm.

The $5HT_{2C}$ receptor over-expressing mouse shows a greater level of TARP γ8 immunoreactivity compared to the control, with subtle differences in the labelling distribution detectable.

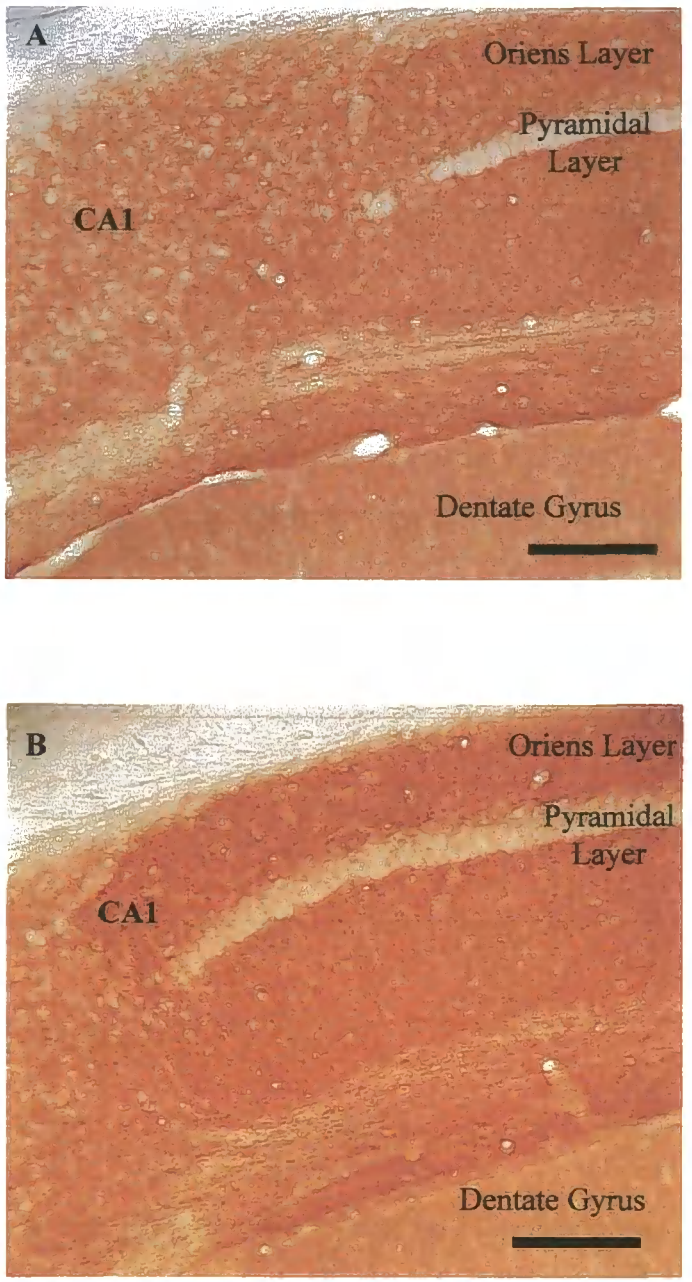

Figure 5.6: Immunohistochemical sections of $5HT_{2C}$ over-expressing (A) and control (B) mice hippocampal formation probed with the TARP γ8C. Magnification X200. Scale bars = 100 μm.

As can be seen, there is no detectable differences in hippocampal TARP γ8 expression between the $5HT_{2C}$ receptor over-expressing mouse and the control.

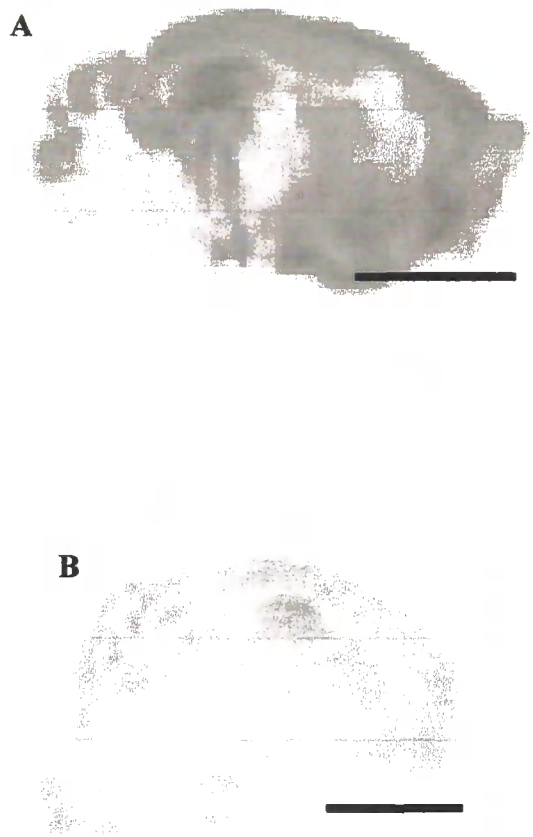

Figure 5.7.1: Autoradiography showing $^{[3]}$H AMPA binding in the $5HT_{2C}$ receptor Over-expressing mouse (A) and control (B). Scale bars = 5mm.

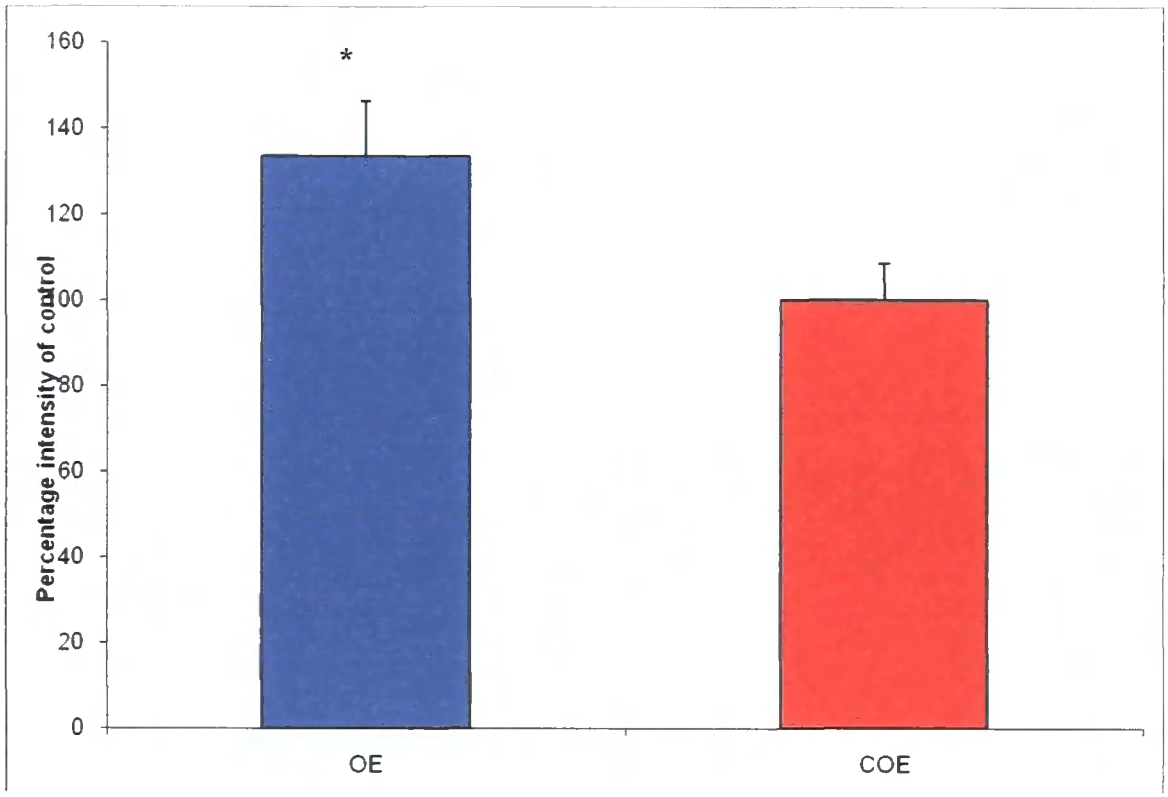

Figure 5.7.2: Graph showing the percentage of $^{[3]}$H labelled AMPA binding in the cerebral cortex of $5HT_{2C}$ receptor over-expressing mice compared with control.

Results are measured as a comparable percentage, taking the control percentage as 100%. The asterisk signifies that the percentage of $^{[3]}$H AMPA binding in the cerebral cortex of the $5HT_{2C}$ receptor over-expressing mice corresponds to a statistically significant (at the <0.05 probability level) difference (a mean increase of 67%) compared with the controls.

$5HT_{2C}$ receptor over-expressing mice display elevated levels of AMPA binding in the frontal cortex.

The results show an increase in AMPA binding in the $5HT_{2C}$ receptor over-expressing mice of 67%, a result taken as statistically significant at the <0.05 level, P = 0.0085,

based on an *n* of 3. Results were calculated from the mean of 5 measured sections taken from 5 separate brain slices from 3 individual mice.

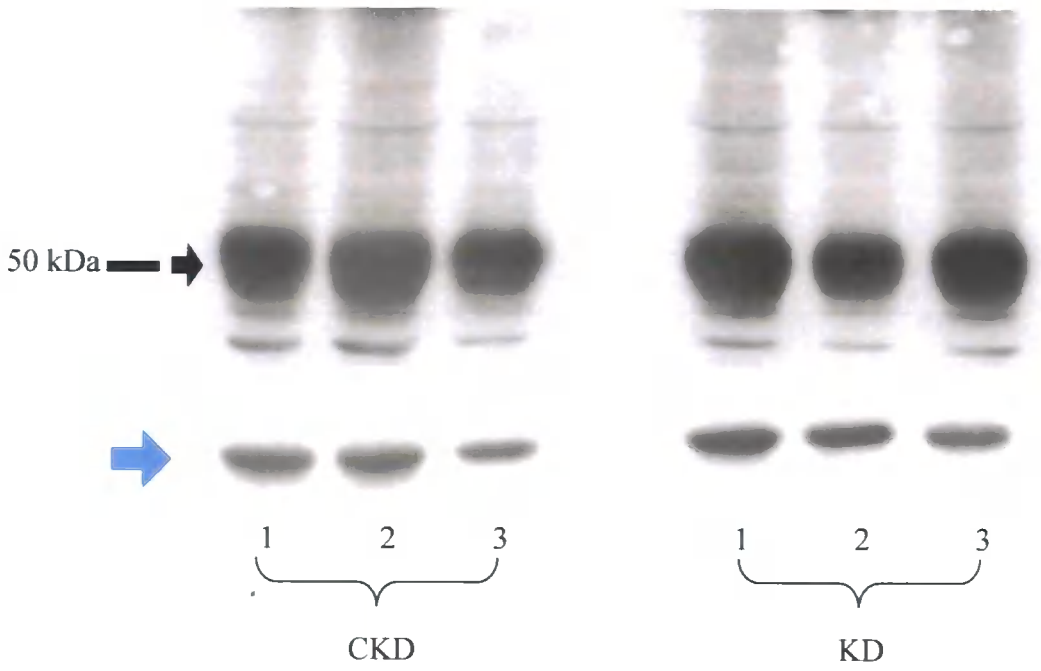

Figure 5.8.1: Representative immunoblot of $5HT_{2C}$ receptor knockdown forebrain Vs control probed with the TARP γ8C antibody.

One cerebral hemisphere, minus the cerebellum, from either control (CKD) or $5HT_{2C}$ receptor knockdown (KD) mice was loaded onto a 10% SDS-PAGE gel. Three separate control mice and their knockdown equivalents were used for a total *n* of 3. Protein amounts calculated by Lowry protein assay allowed 10 μg of protein to be loaded per lane. Immunoblot was probed with the TARP γ8C antibody and band intensity calculated using ImageJ. The immunoblot was repeated in triplicate and the mean TARP γ8/β-actin intensities for the knockdown condition and the controls were calculated, with these values being used as described in Section 2.11 on page 50.

The immunoreactive species indicated by the black arrow is TARP γ8. The immunoreactive species indicated by the blue arrow, and not shown at actual molecular weight, is a representative example of the β-actin loading control.

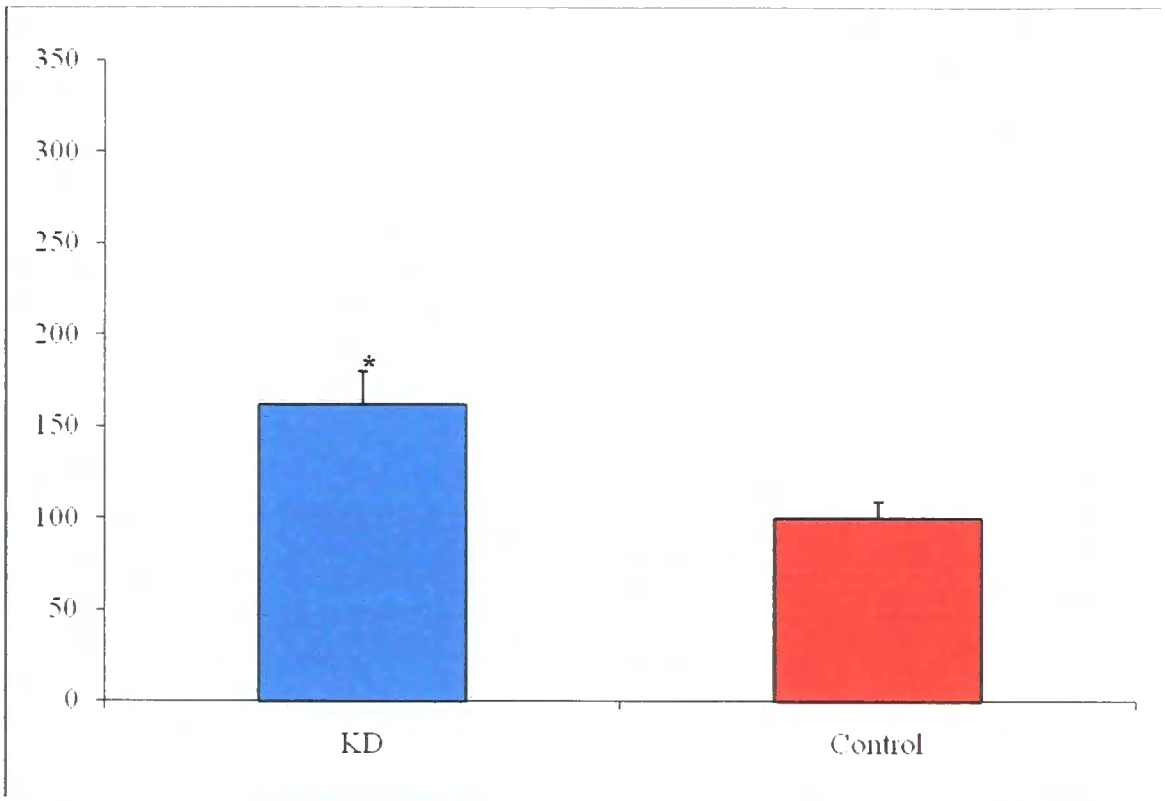

Figure 5.8.2: Graph showing the mean percentage expression of TARP γ8 in the forebrain of the $5HT_{2C}$ receptor knockdown mice compared with controls.

Shows the mean difference in percentage expression of TARP γ8 between the $5HT_{2C}$ receptor knockdown mice and their respective controls using triplicate samples from an *n* of 3. For the Control the mean percentage expression was set as 100%. The asterisk signifies that the difference in percentage of mean TARP γ8 expression between the $5HT_{2C}$ receptor knockdown mice compared with their controls, as shown in this graph, represents a difference that is statistically significant at the <0.05 probability level.

Total levels of TARP γ8 are significantly increased in the forebrain $5HT_{2C}$ receptor knock-down mice.

The total levels of TARP γ8 in $5HT_{2C}$ receptor knockdown mice demonstrated a significant increase of approximately 66% on average compared with the controls. Results were significant at the probability of <0.05 (P = 0.0030) based upon an *n* of 3.

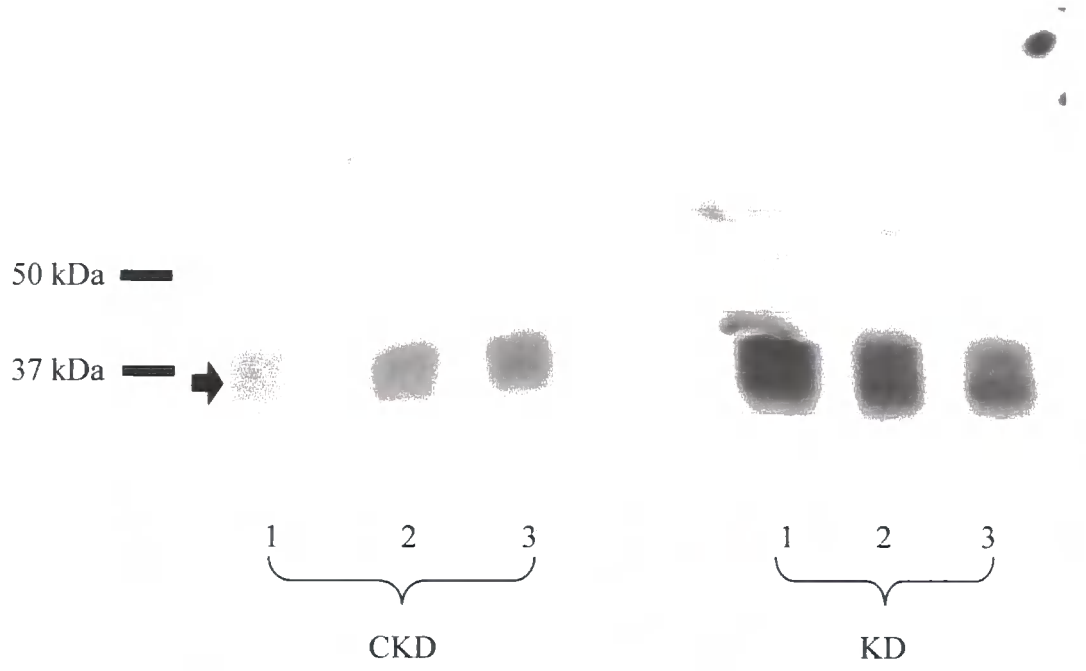

Figure 5.9.1: Representative immunoblot of $5HT_{2C}$ receptor knockdown forebrain Vs control probed with the TARP γ2 antibody.

One cerebral hemisphere, minus the cerebellum, from either control (CKD) or $5HT_{2C}$ receptor knockdown (KD) mice was loaded onto a 10% SDS-PAGE gel. Three separate control mice and their knockdown equivalents were used for a total *n* of 3. Protein amounts calculated by Lowry protein assay allowed 10 μg of protein to be loaded per lane. Immunoblot was probed with the TARP γ2 antibody and band intensity calculated using ImageJ. The immunoblot was repeated in triplicate and the mean TARP γ2/β-actin intensities for the knockdown condition and the controls were calculated, with these values being used as described in Section 2.11 on page 50. The immunoreactive species corresponding to TARP γ2 is indicated by the black arrow.

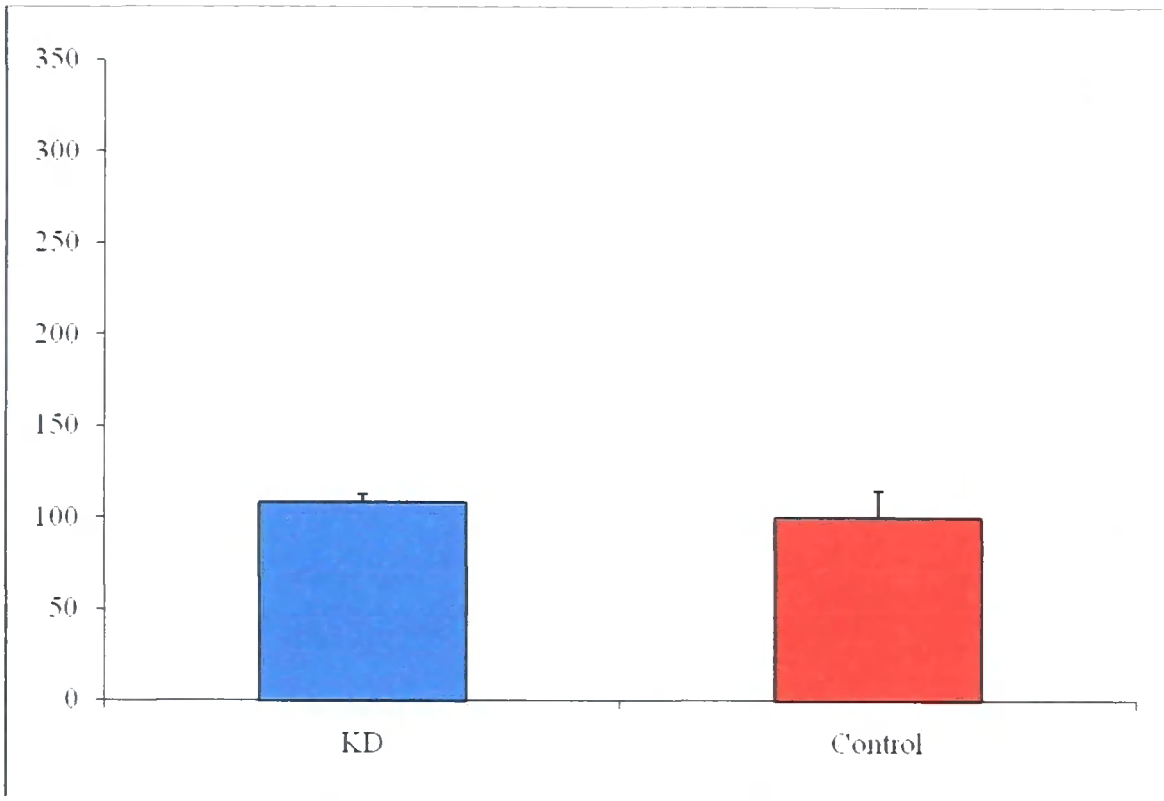

Figure 5.9.2: Graph showing the mean percentage of TARP γ2 expression in the forebrain of the $5HT_{2C}$ receptor knockdown mice relative to controls.

Shows the mean percentage difference of TARP γ2 expression in the $5HT_{2C}$ receptor knockdown mice compared with the controls calculated using triplicate samples with an *n* of 3. For the Control the average was taken as 100%.

Total levels of TARP γ2 appear to be unchanged in the forebrain of $5HT_{2C}$ receptor knockdown mice.

All repeats of the TARP γ2 analysis displayed a trend towards a minimal increase in the levels of TARP γ2 expression. However, this increase was not seen to be significantly significant, P = 0.7374, based upon an *n* of 3. The immunoblot shown is misleading in appearance, the higher intensity in TARP γ2 expression being due predominantly to a higher total level of protein loaded in the sample.

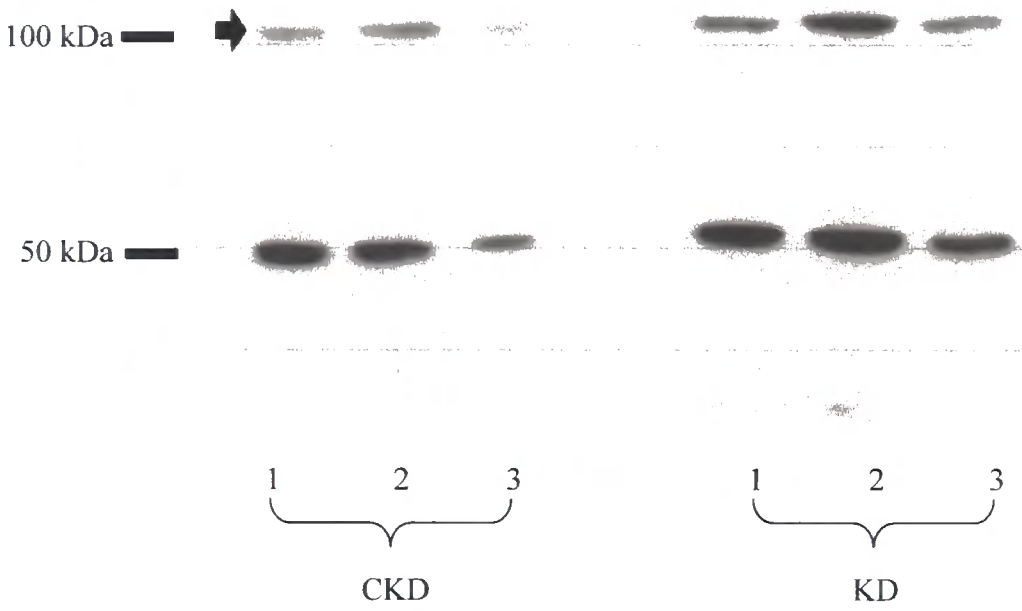

Figure 5.10.1: Representative immunoblot of $5HT_{2C}$ receptor knockdown forebrain Vs control probed with the GluR1 antibody.

One cerebral hemisphere, minus the cerebellum, from either control (CKD) or $5HT_{2C}$ receptor knockdown (KD) mice was loaded onto a 10% SDS-PAGE gel. Three separate control mice and their knockdown equivalents were used for a total *n* of 3. Protein amounts calculated by Lowry protein assay allowed 10 µg of protein to be loaded per lane. Immunoblot was probed with the GluR1 antibody and band intensity calculated using ImageJ. The immunoblot was repeated in triplicate with the mean GluR1/β-actin intensities for the knockdown condition and the controls calculated and used as described in Section 2.11 on page 50. Differences in the immunoreactive species detected with this antibody (primarily the losses of multiple bands at 50-70 kDa), compared with Figure 5.3.1 are due to a change in the anti GluR1 antibody used in this project, with the original batch no longer being an option for use in this project. The immunoreactive species corresponding to GluR1 is indicated by the black arrow.

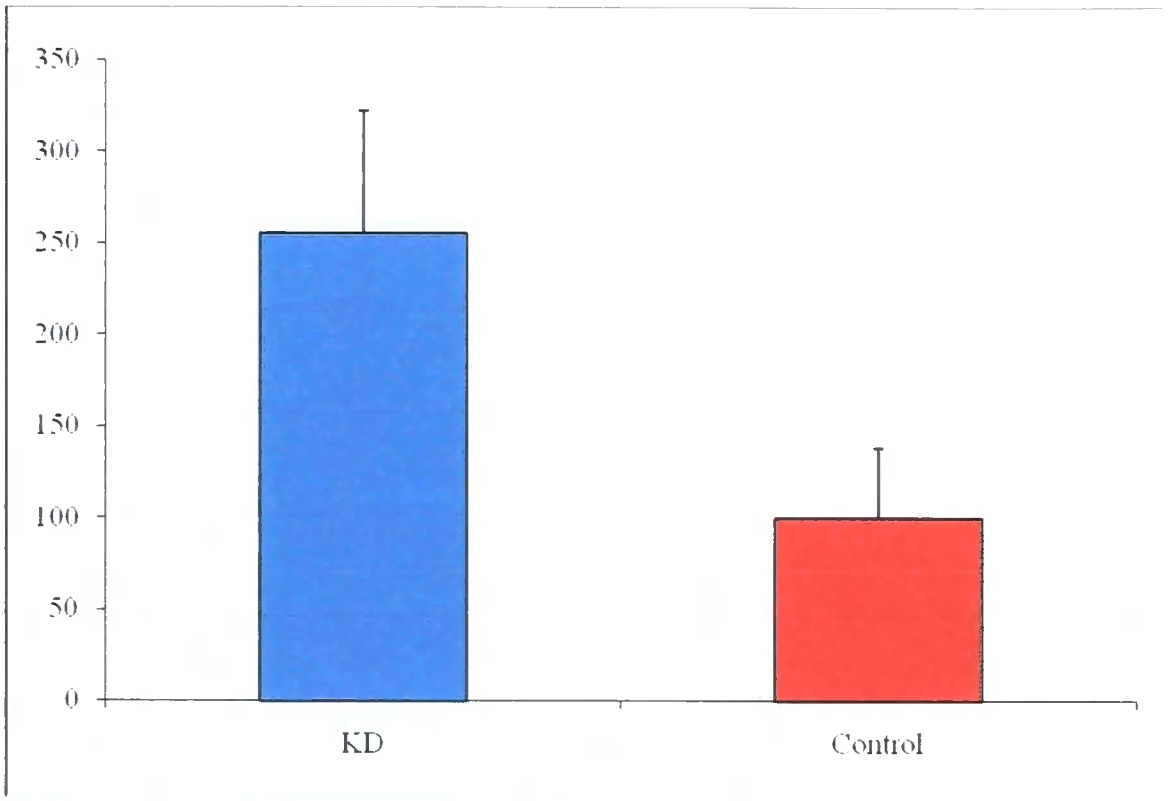

Figure 5.10.2: Graph showing the mean percentage of GluR1 expression in the forebrain of the $5HT_{2C}$ receptor knockdown mice relative to the controls.

Shows the mean percentage difference in GluR1 expression between the $5HT_{2C}$ receptor knockdown mice and the controls taken from triplicate samples with an *n* of 3. For the Control the mean percentage expression was set as 100%.

Total levels of GluR1 appear to be increased in the forebrain or $5HT_{2C}$ receptor knockdown mice.

An trend towards an increase in total GluR1 expression was noticed in the $5HT_{2C}$ receptor knockdown mice forebrains, however, this was not calculated as statistically significant, only reaching a P = 0.113, based upon an n of 3, most likely as a consequence of high variability, and consequently large error bars, in the increased expression resulting from the change in antibody probe and their different affinities for GluR1.

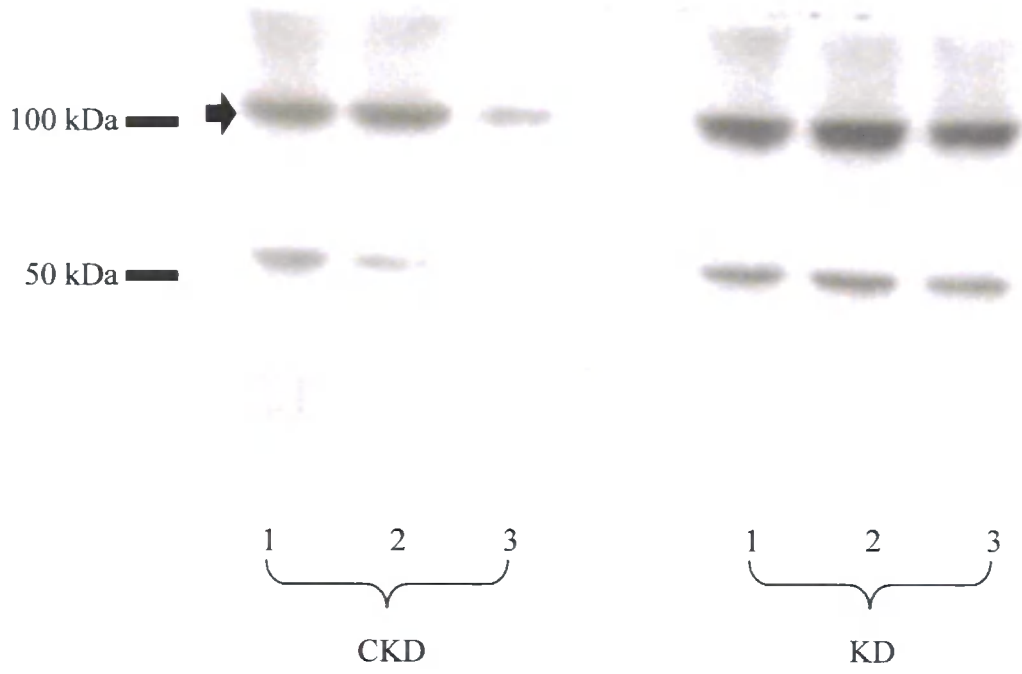

Figure 5.11.1: Representative immunoblot of $5HT_{2C}$ receptor knockdown forebrain Vs control probed with the GluR2 antibody.

One cerebral hemisphere, minus the cerebellum, from either control (CKD) or $5HT_{2C}$ receptor knockdown (KD) mice was loaded onto a 10% SDS-PAGE gel. Three separate control mice and their knockdown equivalents were used for a total *n* of 3. Protein amounts calculated by Lowry protein assay allowed 10 μg of protein to be loaded per lane. Immunoblot was probed with the GluR2 antibody and band intensity calculated using ImageJ. The immunoblot was repeated in triplicate, the mean GluR2/β-actin intensities for the knockdown condition and the controls were calculated, with these values being used as described in Section 2.11 on page 50. The immunoreactive species corresponding to GluR2 is indicated by the black arrow

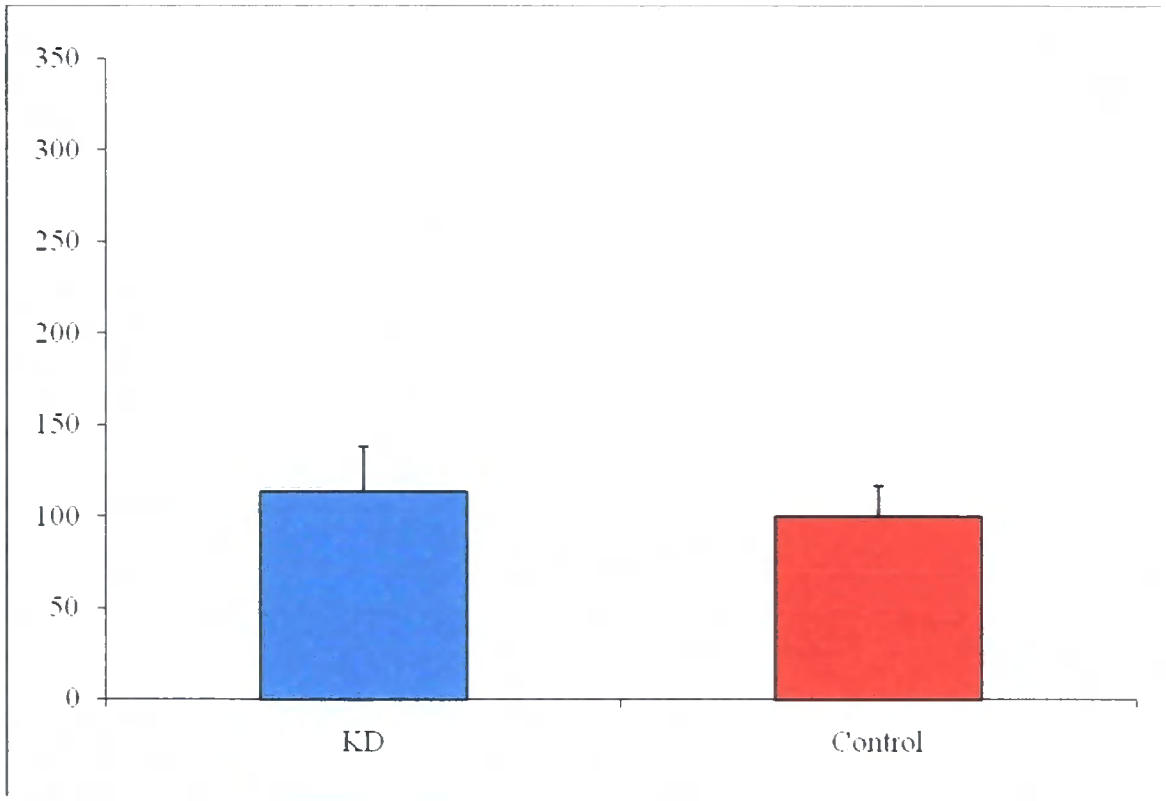

Figure 5.11.2: Graph showing the mean percentage of GluR2 expression in the forebrain of the $5HT_{2C}$ receptor knockdown mice.

Shows the mean percentage difference in the expression of GluR2 in the $5HT_{2C}$ receptor knockdown mice compared with controls, calculated using triplicate samples from an *n* of 3. For the Control the mean percentage expression was set as 100%

Total levels of GluR2 in the forebrain of $5HT_{2C}$ receptor knockdown mice show a slight, but not significant increase in expression.

The total levels of GluR2 measured in the $5HT_{2C}$ receptor knockdown mice showed no statistically significant difference once the ratio of GluR2/β-actin was calculated, P = 0.7873, based upon an n of 3, although a trend towards a slightly increased expression was observed.

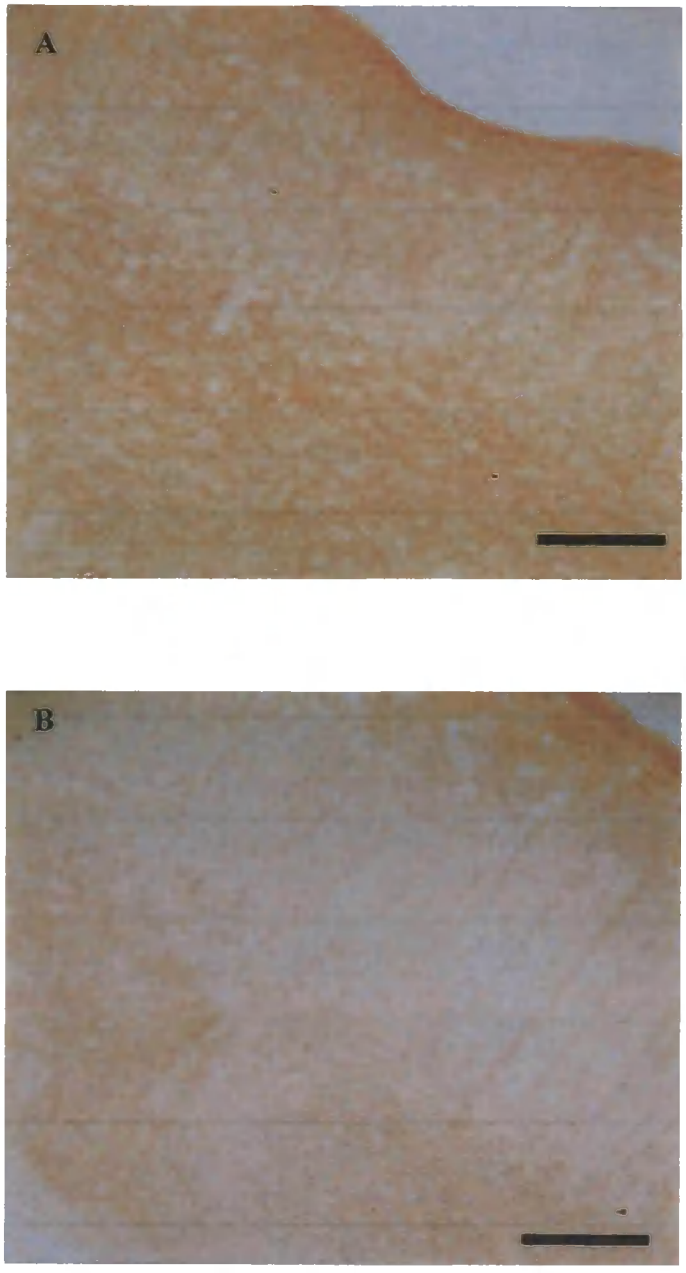

Figure 5.12: Immunohistochemical sections of $5HT_{2C}$ knockdown (A) and control (B) mice frontal cortex probed with the TARP γ8C. Magnification X200. Scale bars = 100 μm.

The $5HT_{2C}$ receptor knockdown mouse shows a much greater level of TARP γ8 immunoreactivity compared to the control, with noticeable differences in the labelling.

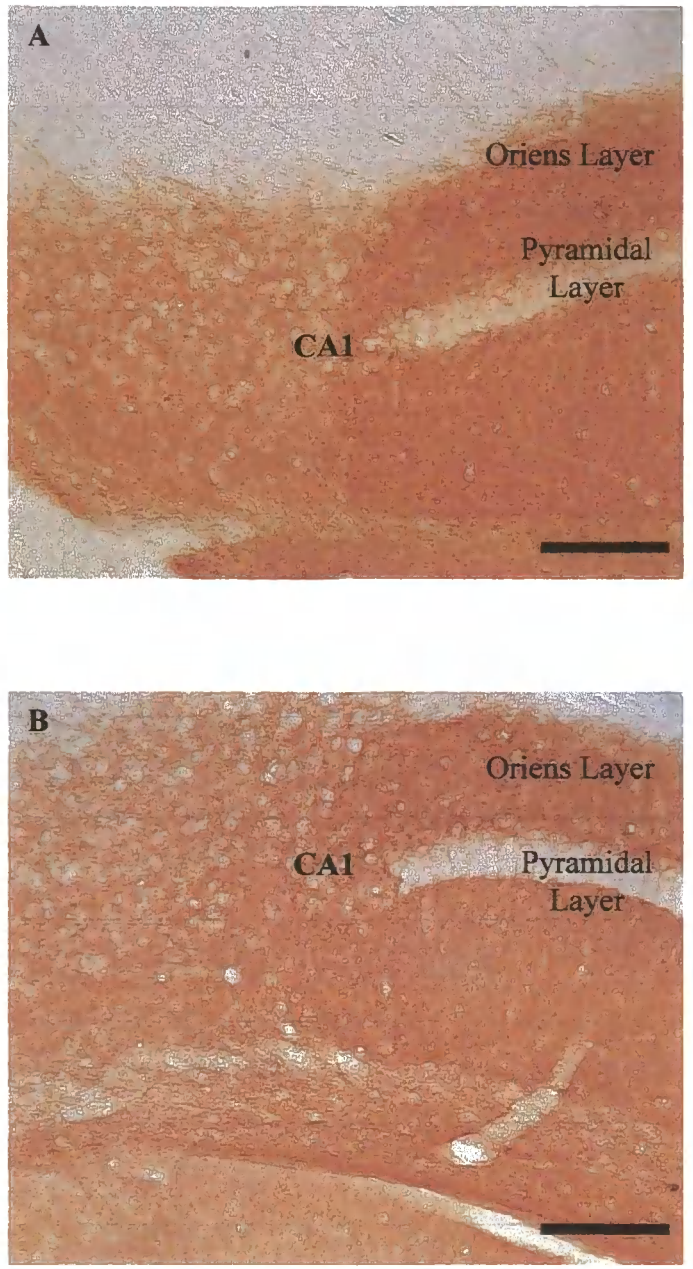

Figure 5.13: Immunohistochemical sections of $5HT_{2C}$ knockdown (A) and control (B) mice hippocampal formation probed with the TARP γ8C. Magnification X200. Scale bars = 100 μm.

As can be seen, there is no detectable differences in hippocampal TARP γ8 expression between the $5HT_{2C}$ receptor knockdown mouse and the control.

Figure 5.14.1: Autoradiography showing $^{[3]}$H AMPA binding in the $5HT_{2C}$ receptor knockdown mouse (A) and control (B). Scale bars = 5mm.

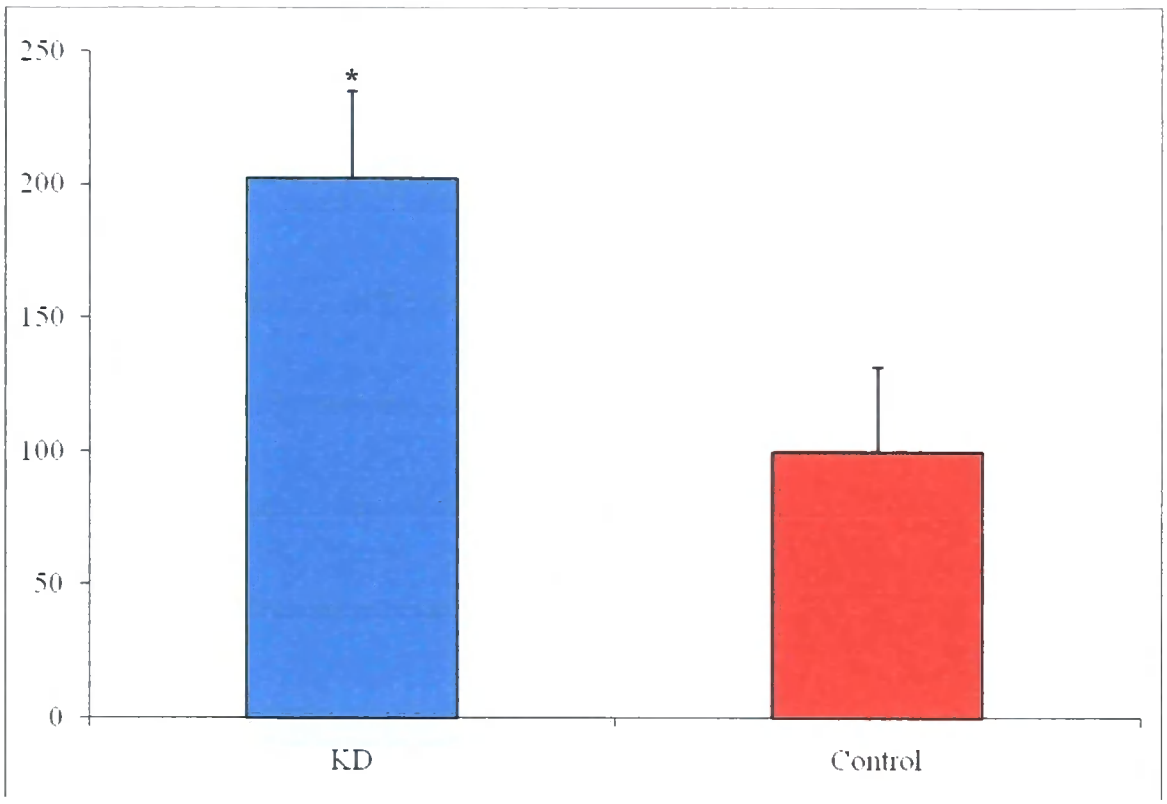

Figure 5.15.2: Graph showing percentage of $^{[3]}$H labelled AMPA binding in the cerebral cortex of $5HT_{2C}$ receptor knockdown mice compared with control.

Results are measured as a comparable percentage, taking the control percentage as 100%. The asterisk signifies that this percentage increase reflects a statistically significant (at the <0.05 probability level) difference between the $^{[3]}$H AMPA binding in the $5HT_{2C}$ receptor knockdown mice compared with their respective controls.

$5HT_{2C}$ receptor knockdown mice display elevated levels of AMPA binding in the frontal cortex.

The results show an increase in the mean percentage of total $^{[3]}$H AMPA binding in the $5HT_{2C}$ receptor knockdown mice of 100% compared with the controls, a result statistically significant at the <0.05 level, P = 0.0499, based on an *n* of 3. Results were

calculated from the mean of 5 measured sections taken from 5 seperate brain slices from 3 individual mice.

Discussion

The alteration of $5HT_{2C}$ receptor expression appeared to have somewhat similar effects upon TARP isoform expression, irrespective of the specific experimental condition.

It is certainly not without precedent for a G Protein-coupled receptor to regulate AMPA receptor trafficking and expression via interactions with GABAergic interneurones, with the influence of Dopamine receptors, such as D4 on AMPA receptors being known (Gao and Wolf 2007, Kwon et al. 2008, Yuen and Yan 2009).

This would appear to be the case here, with both the $5HT_{2C}$ receptor over-expressing mice and the $5HT_{2C}$ receptor knockdown mice both demonstrating significant increases in TARP γ8 expression within the forebrain.

In the $5HT_{2C}$ receptor over-expressing mice this statistically significant increase in the levels of TARP γ8 is associated with an observed, trend towards increased expression of GluR2, but no change in the expression GluR1 and TARP γ2.

These data suggests that the over-expression of $5HT_{2C}$ receptors induces a consequential increase in the level of TARP γ8 and GluR2 containing AMPA receptors in the forebrain. This is somewhat contradictory as, whilst the AMPA receptors present in the synapse are not exclusively, GluR2 containing AMPA receptors, the majority of GluR2 containing AMPA receptors are present within the synapse. TARP γ8 on the other hand, is primarily Triton X-100™ soluble, implying that the majority of TARP γ8 is non-synaptic.

The autoradiography data, suggests an increase in total AMPA receptor number in the frontal cortex, indicating that an enhancement of some excitatory component of the CNS is effected, if this was associated with an increase in GluR2 subunit containing AMPA

receptor expression, then this might indicate a chronic enhancement of synaptic AMPA receptor mediated currents as opposed to acute LTP (Kauer and Malenka 2006, McCormick et al. 2006). However, unlike circumstances with other types of neurotransmitter receptor, for example, the $GABA_A$ receptors, determining the specific composition of these up-regulated AMPA receptors is not possible based upon autoradiography data alone.

The $5HT_{2C}$ receptor knockdown mice also demonstrated a statistically significant increase in the levels of TARP γ8 expressed in the forebrain. These mice also displayed an observed trend in the increase in the expression of TARP γ2. With regard to the AMPA receptor subunits screened, there was a trend towards increased expression of the GluR1 subunit, and slight trend of increased expression level of GluR2.

This observation appears to be the reverse of the AMPA receptor effects induced by the over-expression of $5HT_{2C}$ receptors, despite having the same effect of increasing total TARP γ8 expression levels. The increase in expression of the GluR1 subunit in preference to the GluR2 subunit, which by comparison only displays a very slight and non-significant observable increase, implies that the predominant AMPA receptors being expressed in the forebrain as a consequence of $5HT_{2C}$ receptor knockdown are those that contain GluR1, quite possibly as the predominant subunit. A logical speculation on this would be that the upregulated AMPA receptors are lacking the GluR2 subunit, similar to the AMPA receptors that are upregulated following LTP.

Indeed, this may well be the case, as it has been observed repeatedly with other neural circuits in other CNS regions that the activation of one type of neurotransmitter receptor has knock-on effects upon AMPA receptor subunit expression, particularly the GluR1 subunit. This can most readily be observed by the activity of dopaminergic neurones within the Nucleus Accumbans (NAc), as a consequence of reward seeking behaviour, where the activation of D_1 dopaminergic receptors, results in an increase in synaptic GluR1 expression (Bespalov et al. 2007). Similar interactions, whereby dopaminergic activity at the D_1 receptor regulates both synaptic and surface GluR1 expression, often

within dopaminergic neurones, can be observed in the ventral tegmental area (VTA) and dorsal striatum, and are of particular importance with regard to addictive substances of abuse such as cocaine (Bachtell and Self 2008, Bachtell et al. 2008, Kim et al. 2008), morphine (Lane et al. 2008), and heroin (LaLuimiere and Kalivas 2008). However, the fundamental difference here would be the implication that as it is the *loss* of $5HT_{2C}$ receptor activation, that the increase in GluR1 expression is occurring as a result of the activation of other, currently unknown, receptors as a consequence of decreased $5HT_{2C}$ receptor mediated inhibition.

This potential decrease in an inhibitory component of the frontal cortex in the $5HT_{2C}$ receptor knockdown mice would be as a consequence of the loss of $5HT_{2C}$ receptor mediated excitation of GABAergic interneurones (Liu et al. 2007). In the $5HT_{2C}$ receptor over-expressing mice forebrains, these GABAergic neurones are most likely going to display elevated excitation levels compared to wildtype mice. When this increased excitation is taken into account with the agonist-induced down-regulation of $5HT_{2C}$ receptors, then the resulting system is most likely highly sensitive to 5HT but the consequential effects are limited by the responses of $5HT_{2C}$ receptors to activation, leading to a more pronounced display of effects upon inhibitory circuits in the frontal cortex of the $5HT_{2C}$ receptor knockdown mice.

The autoradiography data shows there is a large increase in the number of AMPA receptors in the frontal cortex, an observation that is logical considering the most likely decreased inhibitory component in that region following $5HT_{2C}$ receptor knockdown. Unfortunately, there is the same problem concerning the exact subunit identity of these AMPA receptors.

When data from both of the experimental mice is combined it implies that $5HT_{2C}$ receptor over-expression and knockdowns both have effects on enhancing AMPA receptor signalling, but most likely via different mechanisms leading to different AMPA receptor compositions and most likely different AMPA receptor functions. However, both appear to cause an increase in TARP $\gamma 8$ expression. The reasons for this could be;

- Different neuronal populations are being affected by each condition.
- TARP γ8 is primarily involved in cell surface trafficking of AMPA receptors in preference to synaptic targeting and that its increased expression is a common pathway for the mobilisation of all AMPA receptors to the cell surface in TARP γ8 expressing neurones irrespective of the mechanisms determining AMPA receptor expression and composition.

The following series of schemas attempt to explain these two points within a simplified framework.

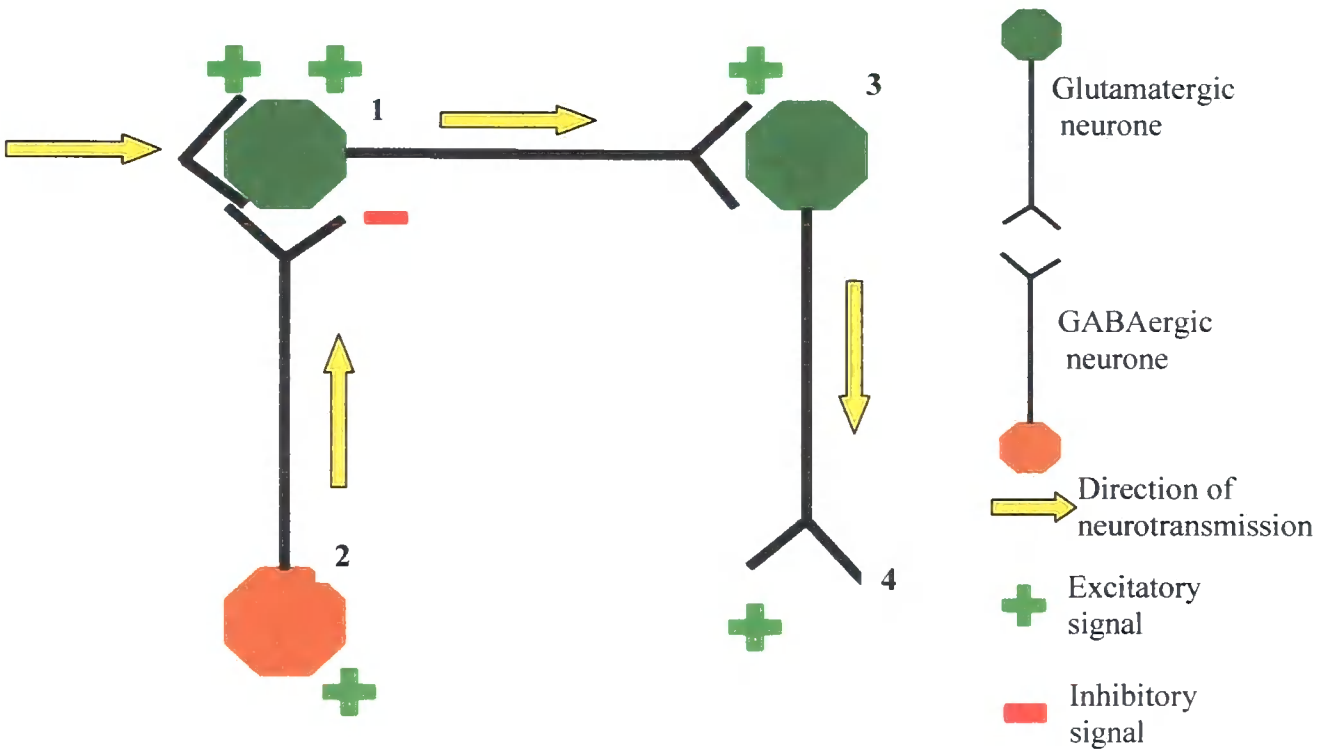

Figure 5.15.1 Simplified schema showing net neurotransmission in control mice. Excitatory input is received by the glutamatergic neurone (1). The neurone itself is also influenced by inhibitory signals received from GABAergic interneurones (2), which dampen the netexcitatory output of the neurone, reducing the excitatory signal received by neurones at its axonal terminals (3). This reduced net excitatory signal is subsequently transmitted along to interconnected neurones (4).

With the excitation of the GABAergic interneurones being regulated, at least in part, by $5HT_{2C}$ receptor activity, then alteration of $5HT_{2C}$ receptor expression can affect this neuronal network by altering the inhibitory regulation of the glutamatergic neurones. The constitutive activity of $5HT_{2C}$ receptors ensures that there is always some form of inhibitory regulation present in neuronal pathways.

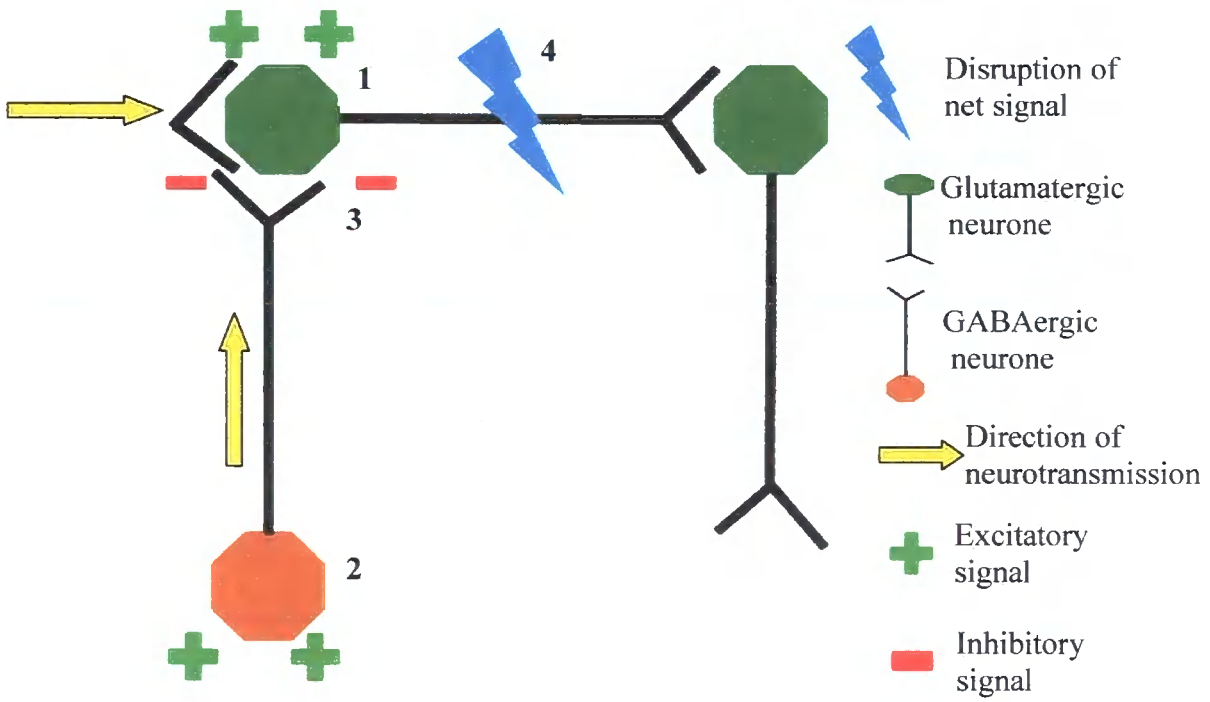

Figure 5.15.2 Simplified schema showing speculative net neurotransmission in $5HT_{2C}$ receptor over-expressing mice.

Excitatory input is received by the glutamatergic neurone (1). Enhanced constitutive activity of the GABAergic interneurone (2), in this instance as a consequence of increased expression of $5HT_{2C}$ receptors, results in an increase in the regulatory inhibition of the glutamatergic neuronal pathways (3). This increased inhibition results in a significantly reduced excitatory signal being transmitted along the neuronal pathway (4). This has the net effect of significantly reducing spontaneous excitatory activity, but also dampens induced excitatory neurotransmission which will logically alter the synaptic

composition of those neurones as this is dependent upon levels of activity. This could result in the subsequent increase in the ratio of non-synaptic:synaptic AMPA receptors, which as previously discussed, are largely dependent upon TARP isoforms for trafficking, with TARP γ8 being largely present in the non-synaptic material as observed from the Triton X-100™ solubilisations discussed in Chapter 4, then it would be a logical consequence, that there would be increased TARP γ8 expression. There is also the highly like probability that the increased inhibition of some excitatory pathways in the CNS will result in an enhancement of the activity of others. As such, the increased TARP γ8 expression in the $5HT_{2C}$ receptor mice may be occurring in neuronal networks not directly affected by the $5HT_{2C}$ receptor expression.

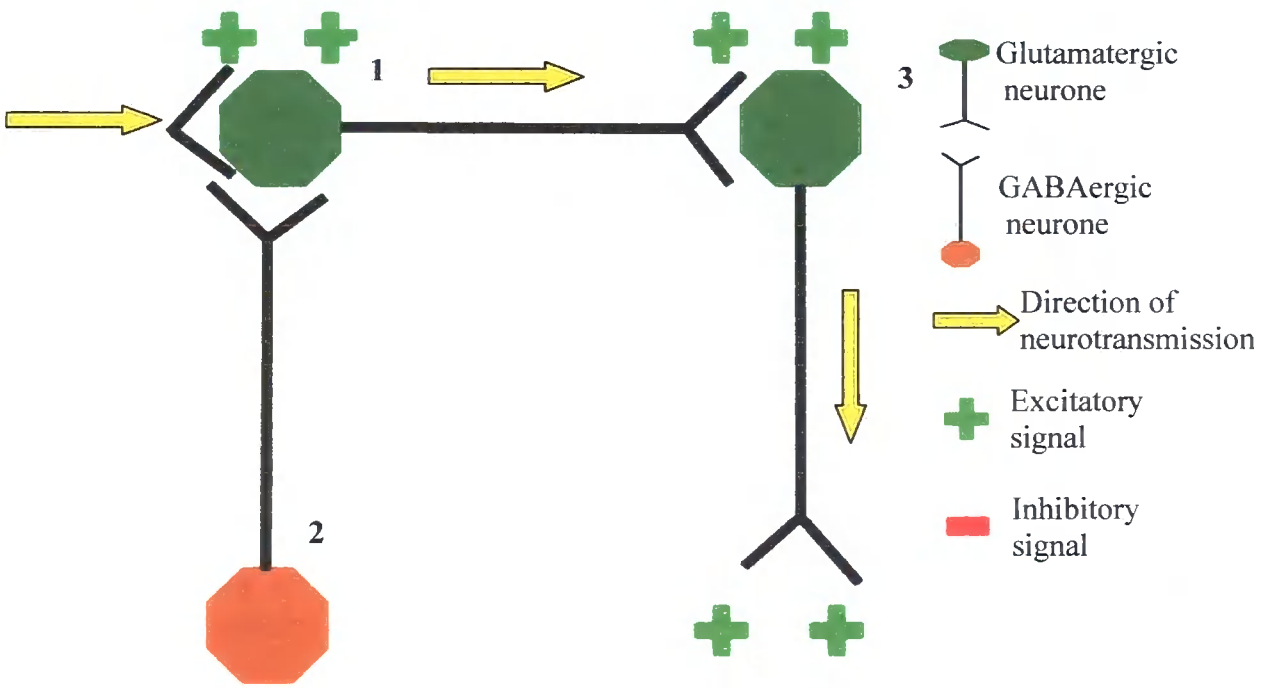

Figure 5.15.3 Simplified schema showing speculative net neurotransmission in $5HT_{2C}$ receptor knockdown mice.

Excitatory input is received by the glutamatergic neurone (1). The absence/significant decrease of $5HT_{2C}$ receptors on the GABAergic interneurones results in their decreased excitation, and a net loss of inhibitory signals on the neuronal pathway (2). This loss of inhibitory signalling results in a much larger excitatory signal being transmitted from the

primary glutamatergic neurone to subsequent neurones in the network (3) than would be transmitted if the inhibitory signals were present.

This increase in net excitatory signalling, due in this instance to a loss of inhibition, will result in profound changes in the synaptic composition of the excitatory neurones directly involved in the network affected, potentially increasing synaptic AMPA receptor number as well as total AMPA receptor expression. The increased glutamate likely being released in this model would in greater activation of peripheral synapses as a consequence of extra-synaptic AMPA receptor activation following the spill-out of glutamate from synaptic boutons. This increase in glutamatergic activity would necessitate an increase in TARP expression and whilst TARP γ2 shows no increase, other TARP isoforms, including TARP γ8, may have an increased functional role.

Looking at the results, it is extremely likely that any functional interaction between $5HT_{2C}$ receptors and AMPA receptors, and by extension TARPs, will involve other neuronal receptors. Again, returning to the increasingly well investigated area of dopamine receptors interacting with AMPA receptors, this concept of multiple mechanisms facilitating the effects of the interactions between G-protein coupled receptors and AMPA receptors has been demonstrated, with the presence of a NMDA receptor dependent component in the enhanced GluR1 containing AMPA receptor expression following cocaine administration that facilitates the dopaminergic response (Engblom et al. 2008).

Of course, the aberrant activity of the neurones in these mice, such as enhanced glutamatergic signalling, would have knock-on effects on other neuronal pathways that are influenced both directly and indirectly by the neurones described in this schema. A good example involving other 5HT receptors, would be the activity dependent modulation by AMPA receptor to 5HT afferents from the dorsal raphe nucleus and median raphe nucleus to frontal cortex. This interaction is a complex interplay known to incorporate both $5HT_{1A}$ receptors and neurokinin receptors (Gartside et al. 2007, Guiard et al. 2007). Another particularly relevant example is the regulation of dopaminergic

neurones in the NAc, which are actually inhibited by $5HT_{2C}$ receptor activation (Dremencov et al 2005). This is particularly relevant to the $5HT_{2C}$ receptor knockdown mice, with the loss of $5HT_{2C}$ receptor-mediated inhibition likely to result in enhanced reward seeking behaviour, and subsequent increases in AMPA receptor activity within the NAc, most likely explaining some of the increased TARP γ8 expression within the forebrain of these mice.

One thing regarding $5HT_{2C}$ receptor interactions that these results do suggest is that the functional effects of this potential interaction is not limited to purely physical interactions, the $5HT_{2C}$ receptor knockdown mouse suggesting a signalling component of $5HT_{2C}$ receptors that determines AMPA receptor composition, a purely physical interaction would be most likely to see opposite effects between the two conditions regarding TARP/AMPA receptor expression, but the reality is that whilst there are seemingly opposite effects, they are in AMPA receptor composition and not number.

A complication, based upon the limited amount of material available, is that the quantitative immunoblotting had to be conducted on whole forebrain hemispheres. As a consequence, there is the, quite likely possibility, that any modest altered TARP/AMPA receptor expression if confined to a specific region of the forebrain would not be detectable in a whole forebrain preparation, only dramatic changes in expression would be easily detectable. Indeed, it is not even certain whether the altered TARP γ8 expression even occurs in the same neurones between the two conditions.

Another potential factor to be taken into consideration for future work is the presence of chronobiology. The $5HT_{2C}$ receptor is intrinsically involved in the maintenance of biorhythmical processes, with specific phases of each circadian cycle correlating with specific properties of the endogenous $5HT_{2C}$ receptors (Pan and Gala 1988, Weiner et al. 1992, Holmes et al. 1997).

Of course the information obtained in this chapter is limited by the fact that with the exception of the TARP γ8 data the other data is not statistically significant and whilst

there are observed patterns, it is possible that the results are due to chance. This appears to be due to limitations in the methodology;

- The accessibility of the mice allowed only a *n* number of 3 to be used, with the quantifications repeated in triplicate.
- Experiments were only capable, due to limitations in tissue amounts, to be conducted on entire hemispheres of forebrain material, which, as seen by the immunhistochemistry and in situ hybridisation, did not display effects $5HT_{2C}$ receptor throughout across these regions in a uniform manner.

Further studies using only the frontal cortex from more source animals would most likely show statistically significant and much more readily measurable differences in the level of TARP isoform and AMPA receptor subunit expression as a consequence of altered $5HT_{2C}$ receptor expression within these tissues.

In conclusion, further investigation is necessary, possibly with more precise dissections of specific sub-regions of the forebrain, to positively identify exact changes in TARP/AMPA receptor expression in specific regions, possibly using better immunohistochemical probes, a severely limiting factor in this instance, to more successfully identify regions of interest. This could be coupled with more exact investigation using immunological probes specific to AMPA receptor phosphorylation states and confocal studies to determine exactly which neurones were being affected by these changes in $5HT_{2C}$ receptor expression.

Final Discussion and Future Work

With the original intentions of this project being to investigate the potential interactions between $5HT_{2C}$ receptors and TARPs/AMPA receptors in the mammalian frontal cortex, by designing, generating and characterising novel immunological probes specific for each individual TARP isoform – probes that are capable of immunologically isolating specific TARPs and their respective interacting proteins – some progress was made, with each of the antibodies being used to generate information regarding TARP protein distribution.

The TARP γ8 C-terminal directed antibody quickly became the focus of study, following the confirmation of the prevalence of TARP γ8 within the hippocampus, a region of importance in cognition, but also in neurological disorders, such as depression. Evidence of antidepressant enhancement of the hippocampal-medial-prefrontal cortical pathway (Ohashi et al. 2002), coupled with the effects of the SSRI and $5HT_{2C}$ receptor antagonist fluoxetine upon calcineurin and GluR1 (Crozatier et al. 2007) within the hippocampus, and the distribution of TARP γ8 within not only the hippocampus, but also throughout the frontal cortex, within a very distinct distribution, made it highly likely that any AMPA receptor involvement in depression that would inevitably affect AMPA receptor trafficking or targeting, would involve TARP γ8.

This reasoning was further supported by the evidence that the distribution of the GluR2 AMPA receptor subunit within the frontal cortex, was very similar to that of the TARP γ8 isoform. The distribution of GluR2 within the prefrontal cortex being shown to undergo decreased expression in chronic social defeat models of depression in tree shrews, with this decreased expression being reversible by the application of D_2 dopamine receptor partial agonist which possessed SSRI activity (Michael-Titus et al. 2008).

The hippocampus was also the region of the forebrain that displayed the highest levels of GluR1 expression, making it likely that TARP γ8 and GluR1 would interact within that region which is interesting in light of evidence that has recently been presented of a GluR1 knock-out mouse that demonstrates depressive behaviour, with profound

neurotransmitter deficits within the hippocampus (Chourbaji et al. 2008). With this disruption within the hippocampus of AMPA receptors as a consequence of the GluR1 knockout, a disruption of the TARP isoform expression within the hippocampus would be likely to occur, most likely affecting TARP γ8 and its interactions significantly.

With TARP γ8 being the predominant TARP isoform within the hippocampus, there is also a logical consideration that TARP γ8 has an important role in LTP.

Hippocampal LTP is believed to play a fundamental role in memory and cognition and ironically, there is another member of the 5HT receptor family that may have a role in LTP within the hippocampus, that receptor being the $5HT_{1A}$ receptor. Activation of the $5HT_{1A}$ receptor in the hippocampus prevents the activity of calmodulin-dependent protein kinase II, a protein important in delivery of AMPA receptors to silent synapses (Shi et al. 2001), in addition to reducing PP1 and protein kinase A activity (Schiaparelli et al. 2005), whereas antagonism of the $5HT_{1A}$ receptor results in enhanced surface expression of phosphorylated AMPA receptor subunits (Schiaparelli et al. 2006). Considering the aforementioned importance of CAMKII in phosphorylating TARP γ2 (Tomita et al. 2005) and, due to the sequence homology, potentially TARP γ8, and both of these proteins high expression within the hippocampus as well, it is highly likely that both proteins are affected by $5HT_{1A}$ receptor activity. However, further investigation would be required to elucidate which TARP isoforms were affected by GluR1 knockout and $5HT_{1A}$ receptors.

The relationship between $5HT_{1A}$ receptors and AMPA receptors is not limited to the hippocampus, there is also evidence of $5HT_{1A}$ in regions of the prefrontal cortex, localised with glutamatergic synapses (Kia et al. 1996). With the frontal cortex being another region of CNS with high expression of TARP γ8, it is likely that there would be at the very least some form of functional interaction between $5HT_{1A}$ receptors and AMPA receptors that would be affected by TARP γ8 expression.

The immunopurifications also enabled the purification of a protein that was identified using multiple $5HT_{2C}$ receptor antibodies and possessed a molecular weight corresponding to $5HT_{2C}$ receptors. This result provides credible evidence of a physical interaction between $5HT_{2C}$ receptors and TARPs/AMPA receptors and although it offers no further data regarding the functional purpose of this interaction, it does generate a suitable starting point for further investigation into the nature of this interaction.

This direct physical interaction may have some significance even though it is uncertain exactly how mature either the TARP γ8 or the $5HT_{2C}$ receptor is and where in the cell the interaction occurs. It has been observed that within the hypothalamic tuberlomamillary nucleus, there is evidence of expression of both AMPA receptors and $5HT_{2C}$ receptors within the same histaminergic neurone, where activation of either is capable of inducing neuronal excitation (Sergeeva et al. 2007).

The experimental work on mice with altered $5HT_{2C}$ receptor expression generated some complex data, suggesting that the functional interactions between $5HT_{2C}$ receptors and TARPs/AMPA receptors is anything but simple. Both the $5HT_{2C}$ receptor over-expressing mice and the forebrain knockdown mice display elevated levels of TARP γ8 expression, but appear to have altered AMPA receptor subunit expression, suggesting that whilst $5HT_{2C}$ receptors have a physical interaction with TARP γ8 at some point in their existence, they also possess an independent functional interaction influencing AMPA receptor composition.

This would not be the first such example of modulation of AMPA receptors by $5HT_2$ receptors, with $5HT_2$ receptor activation altering AMPA receptor conductance and activity in a signalling pathway incorporating protein kinases and phosphatases but requiring activation of Type 1 Metabotropic glutamate receptors (Bocchiaro and Feldman 2004, Neverova et al. 2007). Indeed, in the prefrontal cortex, there is even evidence of $5HT_{2A}$ and $5HT_{2C}$ receptors modulating LTD (Zhong et al. 2008), but also possessing opposing functional effects (Marek 2008) which, when considering the importance of GluR2 containing AMPA receptors in LTD and the aforementioned similarity in TARP

γ8 and GluR2 distributions, would represent a tantalising starting point for investigating the mechanisms explaining how $5HT_{2C}$ receptors when over-expressed or knocked-down both result in increased expression of TARP γ8 within the frontal cortex.

At the current time, none of the current studies of AMPA receptors in neurological dysfunction have examined the potential impact of TARP interactions, making the probes generated in this project a valuable basis for future work within this field. It has also, unfortunately, made the knowledge provided by these probes, more speculative than definitive, with the information provided by them being making intriguing starting points for further investigation, but not offering complete answers to any questions currently asked.

Using the TARP γ4 and TARP γ8 probes, this project has enabled a more accurate expansion of the existing data regarding these two TARP isoforms distributions in the CNS than what is in the literature, with TARP γ8 in particular being demonstrated to be expressed at the protein level in several tissues previously ignored by the literature, such as the spinal cord.

The antibodies have also led to the observation of differences in TARP γ8 distribution with regard to Triton X-100™ solubility, implying that TARP γ8 has a preference for non-synaptic domains. Of course, this is only an observation at this current stage, but offers up an area of potential future investigation.

The generation of immunoaffinity columns using the TARP isoform-specific antibodies has enabled proteomic analysis of material purified using a TARP antibody to identify previously unknown and unsuspected interacting partners.

Proteomic analysis of TARP γ8 interacting partners within the frontal cortex has generated a several previously unknown interacting partners, including proteins involved in neuronal myelination, as well as proteins involved in the cytoarchitecture, implying TARP γ8 is expressed in non-neuronal cells in the CNS and interacts with a host of

structural proteins whilst fulfilling its functional role. This is one of the areas that offers the most potential avenues for branched investigation, with each of the interacting partners providing links to other aspects of the CNS.

Since the completion of the practical work outlined in this thesis, all of the proteins co-purified with TARP γ8 using the anti TARP γ8 immunoaffinity columns and identified with MALDI-TOF or MALDI-TOF/TOF have since been identified by immunoblotting using antibodies specific to these proteins and providing some positive confirmation regarding these proteins respective identities.

The combination of proteins identified by proteomic analysis as a result of the TARP γ8 immunoaffinity purification, all have a stronger relationship with oligodendrocytes in the CNS and not neurones, which is an unexpected occurance. It is known that developing oligodendrocytes express functional AMPA receptors (Patneau et al. 1994, Follett et al. 2000) that, whilst poorly defined in terms of their specific functional role, they are believed to be involved in Ca^{2+} mediated signalling and regulating development (Gallo et al. 1996, Gallo and Ghiani 2000, Butt 2006). The presence of AMPA receptors within oligodendrocytes is known to be a major contributing factor in excitotoxic death following ischaemia or injury (Deng et al. 2006, McCarran and Goldberg 2007). The presence of TARP γ8 in oligodendrocytes, the first TARP knowingly identified as such, would not only set a precedent of TARP γ8 being another protein likely involved in AMPA receptor mediated excititoxic shock in oligodendrocytes, but also other TARP isoforms as well. Indeed, the selective inhibition of Na^+/K^+ ATPase, one of the proteins identified as a TARP γ8 interacting partner, is associated directly with excitotoxic damage in oligodendrocytes (Chen et al. 2007).

Furthermore, this AMPA receptor mediated excitotoxic shock may have implications in other neurological disorders such as Multiple Sclerosis, where glutamatergic activity semmingly contributes both directly to the autoimmune component of this disorder by intensifying demyelination of axons (Bannerman et al. 2007) or indirectly, by promoting

microglial secretions of other neurotoxic compounds such as tumor necrosis factor α (Matute 2007).

In addition to roles in multiple sclerosis (Musse and Harauz 2007, Stern and Keskin 2008), Myelin basic protein and CNPase both also have an implied link with schizophrenia (Dracheva et al. 2006, Martins-de-Souzaet al. 2008), a neurological condition which already has a strongly implied glutamatergic component (Hsu et al. 2008, Wiedholz et al. 2008).

All of this evidence, would indicate a strong relationship between those proteins identified by proteomic analysis and AMPA receptors, so it is not a fantastic stretch of logic to appreciate the presence of an interaction with TARP γ8, a question to be answered now would be *why, what is the specific significance of this interaction?*

Another interesting observation, not directly related to unknown interacting proteins and one that would most certainly be worth pursuing, is the possibility of strain variation of specific neuronal proteins within a species. An observation was made that TARP γ8 appeared to have a slightly different pattern of expression when the immunohistochemical data taken from the C57 background strain of mice was contrasted with the C3B6Fe+ strain.

Although, this is only an observation at this point, there are documented differences between these strains (Ennaceur et al. 2006), including, but not limited to, anxiety and other behavioural traits that could be related to this altered protein expression. At an extreme range of relevance, taking into account that this entire thesis has been investigating potential interactions of TARPs/AMPA receptors with $5HT_{2C}$ receptors, then differences between mice strains and their significance with regard to behavioural effects may have properties analogous to humans individual susceptibility to neurological disorders. Individual regions of the brain may have significantly different expression levels of TARP isoforms, which, depending on the region, may have effects on personality traits.

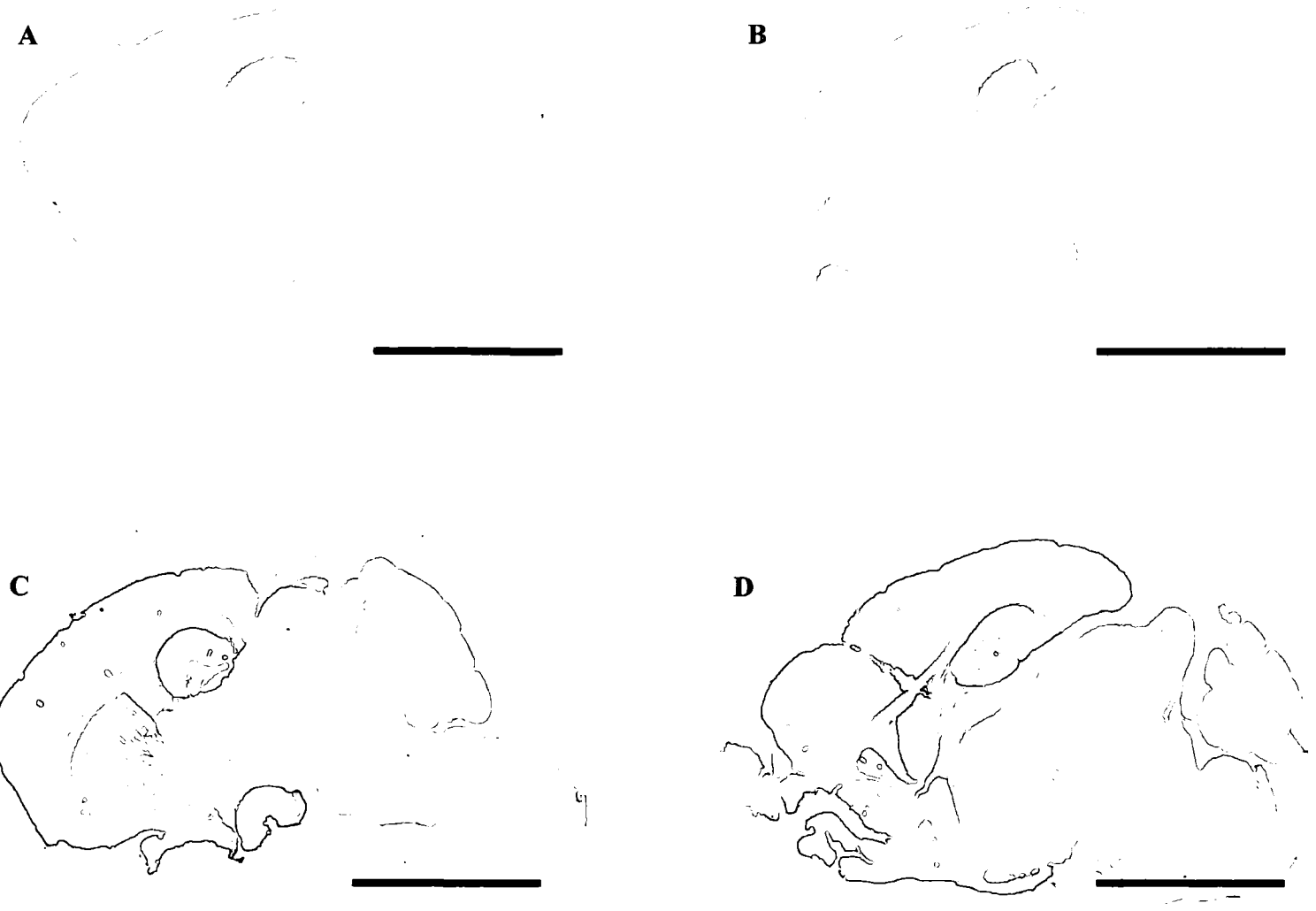

Figure 6: Images A and B show TARP γ8 distribution in C57/B6 mice. Images C and D show TARP γ8 distribution in C3/B6 mice. Whilst there are similarities, certainly within the forebrain, there appear to be noticeable differences in the olfactory bulb, cerebellum and midbrain. These differences are especially apparent when the relative intensity of the hippocampal:forebrain labelling in the C57/B6 mice is compared to that in the C3/B6. Scale bars = 5mm.

Regions such as the basal ganglia, which display differences between these two strains of mice (Figure 6), can have dramatic effects on personality if impaired (Saint-Cyr et al. 1995), so it is possible that subtle changes, but not impairment, would produce subtle differences in personality traits or the processing of emotional stimuli (Engels et al.

2007), which may have implications for treatment of disorders using compounds that effect TARPs/AMPA receptors. It would certainly support the usage of AMPAkines in treating disorders if there was a link between differential TARP expression and the development of negative personality traits/mood disorders. Indeed, cognitive enhancers, although not specifically AMPAkines, have been shown to have anti-anxiety effects even though, at the current time, the precise reasons for their effectiveness is not known (Dusseldorp et al. 2007), it would, speculatively be possible, that in the areas affected abnormal TARP expression was detectable.

As with all initial forays into avenues of science where the previous data is limited, the project has generated more potential areas of interest and more questions than answers, exposing a rich vein of complexities concerning the TARPs and their interactions in the CNS, including those with the $5HT_{2C}$ receptor. It has, however, established a basic identification of a physical interaction between $5HT_{2C}$ receptors and TARPs/AMPA receptors, in addition to identifying the basis of a functional interaction – the underlying aims behind the reasoning of this thesis. However, the full contribution can only be measured when the tools developed in this project are taken into account and used to expand upon the the initial data generated by this project. In short, the understanding provided by this project into this particular field is dwarfed by the potential this project provides for further, directed, investigation.

Work that could continue from the findings of this project:

- **Investigations into Triton X-100™ insoluble (Synaptic) Material** - All experiments so far have examined Triton X-100™ soluble, predominantly non-synaptic material. As such differences in tissue solubilisation and methods of purifying synaptic proteins could be used to investigate TARP γ8 interacting proteins within the synapse.

Investigations into the nature of the interaction between $5HT_{2C}$ receptors and TARPs/AMPA receptors:

- **Surface biotinylation assays** - Using material prior to solubilisation and subsequent immunopurification to determine the location of some of the TARP γ8 interactions, potentially providing information regarding the nature and function of some of these interactions. With specific reference to $5HT_{2C}$ receptor interactions it would help enable the determination as to where the interaction occurs, i.e. at the cell surface or in within some intracellular domain.
- **Hippocampal/cortical co-cultures or pure cultures** - Could determine the effects on AMPA receptor and TARP expression, both protein levels and phosphorylation states, following application of compounds acting upon the $5HT_{2C}$ receptor. Of course compounds, such as AMPA receptor modulators, tianeptine, etc could be investigated. By creating a system to test numerous compounds *in vitro*, cultures would provide a wealth of data on protein interactions and the effects of various compounds.
- **Investigations into splice variants of $5HT_{2C}$ receptors and their effects on TARP/AMPA receptor expression and $5HT_{2C}$ receptor interaction** – Using the abnormal $5HT_{2C}$ receptor expression mice supplied by Megan Holmes has provided evidence of a functional interaction between TARPs/AMPA receptors and $5HT_{2C}$ receptors, but no actual information regarding whether individual splice variants have specific effects. Several possible experiments would require generation of the antibodies specific to the splice variants of the $5HT_{2C}$ receptor

which, whilst problematic because of the pre-existing difficulties with generating highly specific antibodies to the $5HT_{2C}$ receptor, has been achieved with some success by at least one research group. The most simple of which would be using splice variant specific antibodies on the protein purified using the TARP γ8 immunoaffinity column. There would also be the possibility of conducting immunopurifications using these splice variant antibodies and determining which purify TARPs/AMPA receptor subunits.

Work that could expand upon this project:

- **TARP distribution differences between different strains of mice** – As an observation, this finding deserves at least some investigation and if demonstrable could be combined with behavioural studies to identify correlations between TARP isoform distribution and behavioural characteristics, with relation specifically to TARP γ8, but also potentially TARP γ4.
- **Investigation into the Triton X-100™ interacting proteins of TARPs in different regions of the CNS using proteomics** - Initially TARP γ8, but also potentially TARP γ4 s. Lab has already conducted studies into TARP γ8 interacting proteins in the cerebral cortex and cerebellum, with some data being generated.
- **Immunopurification of TARP γ4** – Identification of interacting proteins similar to that conducted for TARP γ8 with specific attention to whether the $5HT_{2C}$ receptor-like protein is present in material purified using the TARP γ4 immunoaffinity column.

- **Hippocampal/cortical co-cultures or pure cultures** – The experiments using culture systems to investigate the signalling pathways and the nature of the functional interaction between $5HT_{2C}$ receptors and TARPs/AMPA receptors could also be applied to other proteins, such as $GABA_A$ receptor modulators and their interactions with $5HT_{2C}$/TARPs/AMPA receptors.
- **Co-localisation of $5HT_{2C}$ receptors, TARPs, AMPA receptor subunits and PSD-95** – The transfection of the key players in the original hypothesis into recombinant cells. Complications even if TARP γ8 is the only TARP transfected, include the choice of vector, the diversity of AMPA receptor subunits and their *flip* or *flop* configurations, and the possibility that the interacting protein is not (just) PSD-95.

Appendix A: Laboratory Solutions

2.4.1

PBS: 0.14M NaCl, 0.0027M KCl, 0.01M Na_2HPO_4, 0.0018M KH_2PO_4 – made up in dH_2O

2.4.2

Glycine elution buffer (for antibody purification): 100mM Glycine, pH 2.5 (achieved using H_2SO_4) – made up in dH_2O

1M Tris: Literally 1M Tris in dH_2O

2.6.1

2X SDS-PAGE sample buffer: Made by diluting 3X SDS-PAGE sample buffer (30mM NaH_2PO_4, 30% (v/v) glycerol, 0.05% (w/v) Bromophenol blue, 7.5% (w/v) sodium dodecyl sulphate, made up in dH_2O) with 200mM Dithiothreitol (DTT) and dH_2O in a 10:3:2 ratio.

2.6.2

SDS-PAGE resolving gels: 49.4% (v/v) dH_2O, 25.3% (v/v) Acrylogel-3 solution (from VWR –30% acrylamide), 25.25% (v/v) running gel buffer (1.5M Tris, 8mM EDTA, 0.4% (w/v) SDS, pH 8.8 using H_2SO_4, made up in dH_2O), to which 0.06% (w/v) ammonium persulphate was added prior to degassing in a vacuum dessicater for 30 minutes. Following degassing, 24µl of TEMED was added before the mixture was allowed to set, with each gel being kept hydrated by an upper layer of H_2O-saturated iso-butanol added once the mixture was in the gel stacker.

SDS-PAGE stacking gels: 76.1% (v/v) dH_2O, 9% (v/v) Acrylogel-3 (final concentration is 3.5%), 12.5% 1M Tris-HCl (pH 6.8), 1% (w/v) SDS (from 10% (w/v) SDS stock), 1% ammonium persulphate. Mixture was degassed for 10 minutes, then 10µl of TEMED was added before the mixture was poured and allowed to set.

Electrode buffer: 0.01M Tris, 0.8M Glycine, 0.0046M EDTA, 0.2% (w/v) SDS, pH 8.8 using NaOH, made up in dH_2O. Buffer was diluted 1:1 with dH_2O prior to use.
Transfer buffer: 0.025M Tris, 0.4M Glycine, 20% (v/v) Methanol, final volume made up with dH_2O. Buffer was diluted 1:1 with dH_2O prior to use.

2.6.3

Blocking buffer for immunblotting: 5% (w/v) skimmed, dried milk, 0.2% Tween-20, made up in PBS.
Incubation buffer: 2.5% (w/v) skimmed, dried milk in PBS.
Wash buffer for immunoblotting: 2.5% (w/v) skimmed, dried milk, 0.2% Tween-20, made up in PBS.
Luminol: 1.25mM Luminol, 0.1M Tris-HCl pH 8.5, made up in dH_2O.

2.7.1

Paraformaldhyde Fixative: Made by combining Dibasic sodium phosphate buffer (0.2M Na_2HPO_4 in dH_2O) with monobasic sodium phosphate buffer (0.2M NaH_2PO_4 in dH_2O) in a 1:4 ratio. Heated up to, but not exceeding 60°C before 4% paraformaldehyde was added along with 4-10 drops of 1M NaOH until the paraformaldehyde had dissolved into solution. Fixative was stored at 4°C.

2.7.2

Sucrose infiltration of fixed tissue: Essentially PBS with either 10%, 20%, or 30% (w/v) sucrose. Increments increased on subsequent days, all conducted at 4°C.

2.7.3

TBS: 50mM Tris, 0.9% (w/v) NaCl, pH 7.2. Made up in dH_2O.

2.8.1

Sigels buffer: 100mM NaCl, 2mM $MgCl_2$, 1mM EGTA, 10mM HEPES, pH 7.5. Made up in dH_2O.

Glycine elution buffer for immunopurification of TARP interacting compounds: 50mM glycine, 10% (w/v) sucrose, 500mM KCl, 0.2% (v/v) Triton X-100^{TM}. Made up in dH_2O.

2.9.1

Loading Buffer for Proteomics (PROMEGA recipe): 10mM Tris, 50mM EDTA, 0.25% (w/v) bromophenol blue, 30% (v/v) glycerol, pH 7.5. Made up in ultra-pure dH_2O.

NuPAGE buffer: **This was bought commercially, but subjected to a 1 in 20 dilution with ultra-pure dH_2O.**

Appendix B: Proteomic Data from MALDI-TOF Analysis

12 plus-one silver stained 1D bands, from mouse brain

Spot ID	Sample ID	Best Match	MOWSE Score
E06	1	ATP synthase, H+ transporting, mitochondrial F1 complex, alpha subunit, isoform 1, isoform CRA_e [Mus musculus]	240
E07	2		
E08	3	tubulin, beta 5 [Mus musculus]	89*
E09	4		
E10	5	2',3'-cyclic-nucleotide 3'-phosphodiesterase I [Mus musculus]	194
E11	6	gamma-actin [Mus musculus]	89
E12	7	put. beta-actin (aa 27-375) [Mus musculus]	98
F01	8	purine rich element binding protein B [Mus musculus]	151
F02	9		
F03	10	myelin basic protein isoform 4 [Mus musculus]	147
F04	11		
F05	12	Chain A, Crystal Structure Of Apoenzyme Camp-Dependent Protein Kinase Catalytic Subunit [Mus musculus]	85*

NB. Scores less than 80 are not significant
Spots not in the above table gave no good database hits

CNPase proteomic analysis data.

gi|2160434 **Mass:** 45025 **Score: 194** **Expect:** 2.3e-13 **Queries matched:** 23
2',3'-cyclic-nucleotide 3'-phosphodiesterase I [Mus musculus]
gi|14193678 **Mass:** 45025 **Score: 194** **Expect:** 2.3e-13 **Queries matched:** 23
cyclic nucleotide phophodiesterase 1 [Mus musculus]
gi|148670605 **Mass:** 48562 **Score: 190** **Expect:** 5.9e-13 **Queries matched:** 23
cyclic nucleotide phosphodiesterase 1, isoform CRA_a [Mus musculus]
gi|26341378 **Mass:** 47267 **Score: 185** **Expect:** 1.9e-12 **Queries matched:** 23
unnamed protein product [Mus musculus]
gi|51338761 **Mass:** 47493 **Score: 185** **Expect:** 1.9e-12 **Queries matched:** 23
2',3'-cyclic-nucleotide 3'-phosphodiesterase (CNP) (CNPase)
gi|6753476 **Mass:** 47493 **Score: 185** **Expect:** 1.9e-12 **Queries matched:** 23
2',3'-cyclic nucleotide 3' phosphodiesterase [Mus musculus]

---

gi|149054231 **Mass:** 45227 **Score: 121** **Expect:** 4.7e-06 **Queries matched:** 17
cyclic nucleotide phosphodiesterase 1, isoform CRA_b [Rattus norvegicus]
gi|57977323 **Mass:** 47638 **Score: 115** **Expect:** 1.9e-05 **Queries matched:** 17
cyclic nucleotide phosphodiesterase 1 [Rattus norvegicus]
gi|159164662 **Mass:** 24374 **Score:** 62 **Expect:** 3.5 **Queries matched:** 9
Chain A, Solution Structure Of Catalytic Domain Of Rat 2',3'-Cyclic-
Nucleotide 3'-Phosphodiesterase (Cnp) Protein

---

gi|33303781 **Mass:** 48061 **Score:** 61 **Expect:** 4.6 **Queries matched:** 12
2',3'-cyclic nucleotide 3' phosphodiesterase [synthetic construct]
gi|180687 **Mass:** 45469 **Score:** 56 **Expect:** 14 **Queries matched:** 11
2',3'-cyclic-nucleotide 3'-phosphodiesterase (EC 3.1.4.37)
gi|94721261 **Mass:** 47948 **Score:** 52 **Expect:** 38 **Queries matched:** 11
2',3'-cyclic nucleotide 3' phosphodiesterase [Homo sapiens]
gi|114667114 **Mass:** 59510 **Score:** 47 **Expect:** 1.3e+02 **Queries matched:** 11
PREDICTED: 2',3'-cyclic nucleotide 3' phosphodiesterase [Pan troglodytes]

---

gi|85014175 **Mass:** 96075 **Score:** 61 **Expect:** 4.6 **Queries matched:** 16
telomerase reverse transcriptase [Encephalitozoon cuniculi GB-M1]

---

gi|164658011 **Mass:** 10056 **Score:** 60 **Expect:** 6.4 **Queries matched:** 7
hypothetical protein MGL_2513 [Malassezia globosa CBS 7966]

---

gi|399268 **Mass:** 45360 **Score:** 58 **Expect:** 9.3 **Queries matched:** 11
2',3'-cyclic-nucleotide 3'-phosphodiesterase (CNP) (CNPase)
gi|30794282 **Mass:** 45332 **Score:** 58 **Expect:** 9.3 **Queries matched:** 11
2',3'-cyclic nucleotide 3' phosphodiesterase [Bos taurus]

---

gi|75042630 **Mass:** 47949 **Score:** 53 **Expect:** 32 **Queries matched:** 11
2',3'-cyclic-nucleotide 3'-phosphodiesterase (CNP) (CNPase)

---

gi|18026841 **Mass:** 11961 **Score:** 52 **Expect:** 39 **Queries matched:** 6
P12 [Rice tungro bacilliform virus]

gi|84687463 **Mass:** 15348 **Score:** 51 **Expect:** 48 **Queries matched:** 6
hypothetical protein RB2654_17936 [Rhodobacterales bacterium HTCC2654]

gi|38085189 **Mass:** 103631 **Score:** 50 **Expect:** 54 **Queries matched:** 17
PREDICTED: hypothetical protein [Mus musculus]
gi|148710101 **Mass:** 55561 **Score:** 47 **Expect:** 1.2e+02 **Queries matched:** 12
mCG148476 [Mus musculus]

Search Parameters

Type of search : **Peptide Mass Fingerprint**
Enzyme : **Trypsin**
Fixed modifications : **Carbamidomethyl (C)**
Variable modifications : **Oxidation (M)**
Mass values : **Monoisotopic**
Protein Mass : **Unrestricted**
Peptide Mass Tolerance : **± 50 ppm**
Peptide Charge State : **1+**
Max Missed Cleavages : **1**
Number of queries : **71**

Gamma actin proteomic analysis data

gi|151176139 **Mass:** 42053 **Score:** 100 **Expect:** 0.00063 **Queries matched:** 16
beta-actin [Anas platyrhynchos]
gi|15277503 **Mass:** 40536 **Score:** 92 **Expect:** 0.0036 **Queries matched:** 15
ACTB protein [Homo sapiens]
gi|1703127 **Mass:** 42163 **Score:** 92 **Expect:** 0.0038 **Queries matched:** 15
Actin, cytoplasmic type 8
gi|73964667 **Mass:** 42053 **Score:** 91 **Expect:** 0.0051 **Queries matched:** 15
PREDICTED: hypothetical protein XP_533132 [Canis familiaris]
gi|1703123 **Mass:** 42165 **Score:** 90 **Expect:** 0.0057 **Queries matched:** 15
Actin, cytoplasmic type 5
gi|56119084 **Mass:** 42151 **Score:** 90 **Expect:** 0.0057 **Queries matched:** 15
actin, gamma 1 propeptide [Gallus gallus]
gi|113271 **Mass:** 42163 **Score:** 90 **Expect:** 0.0057 **Queries matched:** 15
Actin, cytoplasmic 1 (Beta actin)
gi|148222128 **Mass:** 42119 **Score:** 90 **Expect:** 0.0057 **Queries matched:** 15
hypothetical protein LOC734918 [Xenopus laevis]
gi|126272476 **Mass:** 42169 **Score:** 90 **Expect:** 0.0057 **Queries matched:** 15
PREDICTED: hypothetical protein [Monodelphis domestica]
gi|126338084 **Mass:** 42311 **Score:** 90 **Expect:** 0.0057 **Queries matched:** 15
PREDICTED: similar to beta actin isoform 2 [Monodelphis domestica]
gi|118419977 **Mass:** 40894 **Score:** 90 **Expect:** 0.0066 **Queries matched:** 15
beta-actin [Eubalaena glacialis]
gi|809561 **Mass:** 41335 **Score:** 89 **Expect:** 0.0067 **Queries matched:** 15
gamma-actin [Mus musculus]
gi|157881403 **Mass:** 41921 **Score:** 89 **Expect:** 0.0069 **Queries matched:** 15

Chain A, The Structure Of Crystalline Profilin-Beta-Actin
gi|157878210 **Mass:** 41895 **Score: 89** **Expect:** 0.0069 **Queries matched:** 15
Chain A, Structure Of Bovine Beta-Actin-Profilin Complex With Actin Bound Atp Phosphates Solvent Accessible
gi|37698410 **Mass:** 41745 **Score: 89** **Expect:** 0.0074 **Queries matched:** 15
beta-actin [Passer domesticus]
gi|18034011 **Mass:** 42069 **Score: 89** **Expect:** 0.0074 **Queries matched:** 15
beta-actin [Morulius calbasu]
gi|16924319 **Mass:** 40819 **Score: 89** **Expect:** 0.0081 **Queries matched:** 15
Unknown (protein for IMAGE:3538275) [Homo sapiens]
gi|47550655 **Mass:** 41792 **Score: 88** **Expect:** 0.0083 **Queries matched:** 15
beta-actin [Seriola quinqueradiata]
gi|1703118 **Mass:** 42041 **Score: 88** **Expect:** 0.0093 **Queries matched:** 15
Actin, cytoplasmic 3 (Beta-actin C)
gi|148231177 **Mass:** 42082 **Score: 88** **Expect:** 0.0093 **Queries matched:** 15
hypothetical protein LOC398459 [Xenopus laevis]
gi|42560193 **Mass:** 42068 **Score: 88** **Expect:** 0.0093 **Queries matched:** 15
Actin, cytoplasmic 1 (Beta-actin)
gi|4501885 **Mass:** 42052 **Score: 88** **Expect:** 0.0093 **Queries matched:** 15
beta actin [Homo sapiens]
gi|1351867 **Mass:** 42053 **Score: 88** **Expect:** 0.0093 **Queries matched:** 15
Actin, cytoplasmic 1 (Beta-actin)
gi|82213656 **Mass:** 42066 **Score: 88** **Expect:** 0.0093 **Queries matched:** 15
Actin, cytoplasmic 2 (Gamma-actin)
gi|4501887 **Mass:** 42108 **Score: 88** **Expect:** 0.0093 **Queries matched:** 15
actin, gamma 1 propeptide [Homo sapiens]
gi|47498068 **Mass:** 42068 **Score: 88** **Expect:** 0.0093 **Queries matched:** 15
actin, beta [Xenopus tropicalis]

---

gi|3182899 **Mass:** 42098 **Score: 100** **Expect:** 0.00063 **Queries matched:** 16
Actin, cytoplasmic 1 (Beta-actin)
gi|67462093 **Mass:** 42082 **Score: 100** **Expect:** 0.00063 **Queries matched:** 16
Actin, cytoplasmic 1 (Beta-actin A)
gi|9049272 **Mass:** 42094 **Score: 100** **Expect:** 0.00063 **Queries matched:** 16
beta actin [Carassius auratus]
gi|62298523 **Mass:** 42082 **Score: 100** **Expect:** 0.00063 **Queries matched:** 16
Actin, cytoplasmic 1 (Beta-actin-1)
gi|45361511 **Mass:** 42080 **Score: 100** **Expect:** 0.00063 **Queries matched:** 16
actin, gamma 1 [Xenopus tropicalis]
gi|33415846 **Mass:** 42096 **Score: 100** **Expect:** 0.00063 **Queries matched:** 16
cytoplasmic actin type 4 [Rana lessonae]
gi|47218950 **Mass:** 42890 **Score: 94** **Expect:** 0.0024 **Queries matched:** 15
unnamed protein product [Tetraodon nigroviridis]
gi|27805142 **Mass:** 42050 **Score: 92** **Expect:** 0.0034 **Queries matched:** 15
beta actin [Dicentrarchus labrax]
gi|109716241 **Mass:** 42111 **Score: 91** **Expect:** 0.0047 **Queries matched:** 15
beta-actin [Spinibarbus denticulatus]
gi|28279111 **Mass:** 42068 **Score: 90** **Expect:** 0.0052 **Queries matched:** 15
Bactin1 protein [Danio rerio]
gi|33318285 **Mass:** 42098 **Score: 90** **Expect:** 0.0054 **Queries matched:** 15

beta-actin [Tigriopus japonicus]
gi|18858335 **Mass:** 42068 **Score:** 90 **Expect:** 0.0064 **Queries matched:** 15
bactin1 [Danio rerio]

---

gi|118419973 **Mass:** 40948 **Score:** 99 **Expect:** 0.00074 **Queries matched:** 16
beta-actin [Lagenorhynchus acutus]

---

gi|14250401 **Mass:** 41321 **Score:** 99 **Expect:** 0.00077 **Queries matched:** 16
actin, beta [Homo sapiens]
gi|66731680 **Mass:** 40495 **Score:** 91 **Expect:** 0.0045 **Queries matched:** 15
beta-actin [Pungitius pungitius]

---

gi|33318289 **Mass:** 42041 **Score:** 99 **Expect:** 0.00081 **Queries matched:** 16
beta-actin [Tigriopus japonicus]
gi|164472819 **Mass:** 42139 **Score:** 89 **Expect:** 0.0074 **Queries matched:** 15
actin [Ixodes persulcatus]

---

gi|49868 **Mass:** 39446 **Score:** 92 **Expect:** 0.004 **Queries matched:** 15
put. beta-actin (aa 27-375) [Mus musculus]

---

gi|74204169 **Mass:** 42039 **Score:** 91 **Expect:** 0.0044 **Queries matched:** 15
unnamed protein product [Mus musculus]

---

gi|156759 **Mass:** 42181 **Score:** 90 **Expect:** 0.0056 **Queries matched:** 15
actin

---

gi|47116231 **Mass:** 42034 **Score:** 90 **Expect:** 0.0066 **Queries matched:** 15
Actin, cytoplasmic 1 (Beta-actin)

---

gi|28336 **Mass:** 42128 **Score:** 89 **Expect:** 0.0077 **Queries matched:** 16
mutant beta-actin (beta'-actin) [Homo sapiens]

Search Parameters

Type of search : **Peptide Mass Fingerprint**
Enzyme : **Trypsin**
Fixed modifications : **Carbamidomethyl (C)**
Variable modifications : **Oxidation (M)**
Mass values : **Monoisotopic**
Protein Mass : **Unrestricted**
Peptide Mass Tolerance : **± 50 ppm**
Peptide Charge State : **1+**
Max Missed Cleavages : **1**
Number of queries : **118**

Purine rich element binding protein proteomic data

gi|6755252 **Mass:** 33995 **Score:** 151 **Expect:** 4.7e-09 **Queries matched:** 18

purine rich element binding protein B [Mus musculus]
gi|62945366 **Mass:** 33512 **Score: 124** **Expect:** 2.3e-06 **Queries matched:** 16
hypothetical protein LOC498407 [Rattus norvegicus]
gi|149047690 **Mass:** 33636 **Score: 124** **Expect:** 2.3e-06 **Queries matched:** 16
transcription factor Pur-beta [Rattus norvegicus]
gi|15147219 **Mass:** 33392 **Score: 105** **Expect:** 0.00019 **Queries matched:** 15
purine-rich element binding protein B [Homo sapiens]
gi|126302985 **Mass:** 34121 **Score: 103** **Expect:** 0.00029 **Queries matched:** 15
PREDICTED: hypothetical protein [Monodelphis domestica]
gi|74009720 **Mass:** 36909 **Score: 102** **Expect:** 0.00037 **Queries matched:** 15
PREDICTED: similar to purine rich element binding protein B [Canis familiaris]
gi|147899952 **Mass:** 35022 **Score:** 67 **Expect:** 1.1 **Queries matched:** 12
purine-rich element binding protein B [Xenopus laevis]
gi|82186781 **Mass:** 34702 **Score:** 58 **Expect:** 8.5 **Queries matched:** 11
Transcriptional activator protein Pur-beta-A (Purine-rich element-binding protein B-A)
gi|108744015 **Mass:** 32779 **Score:** 50 **Expect:** 57 **Queries matched:** 10
purine-rich element binding protein-beta [Astatotilapia burtoni]
gi|74228215 **Mass:** 11281 **Score:** 46 **Expect:** 1.4e+02 **Queries matched:** 6
unnamed protein product [Mus musculus]
gi|26340180 **Mass:** 11224 **Score:** 46 **Expect:** 1.4e+02 **Queries matched:** 6
unnamed protein product [Mus musculus]

---

gi|45768686 **Mass:** 32455 **Score:** 63 **Expect:** 3 **Queries matched:** 12
Purb protein [Danio rerio]
gi|41054521 **Mass:** 32586 **Score:** 62 **Expect:** 4 **Queries matched:** 12
purine-rich element binding protein B [Danio rerio]
gi|47221521 **Mass:** 31312 **Score:** 54 **Expect:** 23 **Queries matched:** 11
unnamed protein product [Tetraodon nigroviridis]

---

gi|108760572 **Mass:** 20846 **Score:** 61 **Expect:** 4.6 **Queries matched:** 9
hypothetical protein MXAN_3968 [Myxococcus xanthus DK 1622]

---

gi|148692166 **Mass:** 29682 **Score:** 61 **Expect:** 4.6 **Queries matched:** 9
sirtuin 2 (silent mating type information regulation 2, homolog) 2 (S. cerevisiae), isoform CRA_b [Mus musculus]

---

gi|68359605 **Mass:** 33852 **Score:** 59 **Expect:** 7.9 **Queries matched:** 12
PREDICTED: similar to Purine-rich element binding protein B isoform 1 [Danio rerio]

---

gi|47228540 **Mass:** 28639 **Score:** 56 **Expect:** 13 **Queries matched:** 10
unnamed protein product [Tetraodon nigroviridis]

---

gi|74138663 **Mass:** 40008 **Score:** 55 **Expect:** 19 **Queries matched:** 10
unnamed protein product [Mus musculus]
gi|12851673 **Mass:** 40155 **Score:** 55 **Expect:** 20 **Queries matched:** 10
unnamed protein product [Mus musculus]
gi|38258618 **Mass:** 43856 **Score:** 54 **Expect:** 23 **Queries matched:** 10
NAD-dependent deacetylase sirtuin-2 (SIR2-like protein 2) (mSIR2L2)
gi|31982681 **Mass:** 43866 **Score:** 54 **Expect:** 23 **Queries matched:** 10

sirtuin 2 (silent mating type information regulation 2, homolog) 2 [Mus musculus]
gi|11141704 **Mass:** 43872 **Score:** 53 **Expect:** 31 **Queries matched:** 10
SIR2L2 [Mus musculus]
gi|148692167 **Mass:** 46857 **Score:** 52 **Expect:** 34 **Queries matched:** 10
sirtuin 2 (silent mating type information regulation 2, homolog) 2 (S. cerevisiae), isoform CRA_c [Mus musculus]
gi|56605812 **Mass:** 39921 **Score:** 46 **Expect:** 1.6e+02 **Queries matched:** 9
sirtuin (silent mating type information regulation 2 homolog) 2 [Rattus norvegicus]
gi|149056443 **Mass:** 43763 **Score:** 45 **Expect:** 2e+02 **Queries matched:** 9
sirtuin (silent mating type information regulation 2 homolog) 2 (S. cerevisiae), isoform CRA_a [Rattus norvegicus]

---

gi|78045461 **Mass:** 80777 **Score:** 54 **Expect:** 25 **Queries matched:** 15
DNA topoisomerase TraE [Xanthomonas campestris pv. vesicatoria str. 85-10]

---

gi|90086129 **Mass:** 32300 **Score:** 53 **Expect:** 29 **Queries matched:** 10
unnamed protein product [Macaca fascicularis]

---

gi|76818822 **Mass:** 17404 **Score:** 53 **Expect:** 30 **Queries matched:** 7
hydrolase, NUDIX family [Burkholderia pseudomallei 1710b]

Search Parameters

Type of search : Peptide Mass Fingerprint
Enzyme : Trypsin
Fixed modifications : Carbamidomethyl (C)
Variable modifications : Oxidation (M)
Mass values : Monoisotopic
Protein Mass : Unrestricted
Peptide Mass Tolerance : ± 50 ppm
Peptide Charge State : 1+
Max Missed Cleavages : 1
Number of queries : 85

Myelin basic protein proteomic data

gi|69885056 **Mass:** 17272 **Score: 147** **Expect:** 1.2e-08 **Queries matched:** 15
myelin basic protein isoform 4 [Mus musculus]
gi|148677435 **Mass:** 31468 **Score: 113** **Expect:** 2.9e-05 **Queries matched:** 15
myelin basic protein, isoform CRA_a [Mus musculus]
gi|69885073 **Mass:** 14202 **Score: 139** **Expect:** 7.4e-08 **Queries matched:** 14
myelin basic protein isoform 6 [Mus musculus]
gi|4454313 **Mass:** 17254 **Score: 132** **Expect:** 3.7e-07 **Queries matched:** 13
myelin basic protein [Rattus norvegicus]

gi|114199083 **Mass:** 13863 **Score: 130** **Expect:** 5.9e-07 **Queries matched:** 13
myelin basic protein [Mus musculus]
gi|70166262 **Mass:** 17272 **Score: 130** **Expect:** 5.9e-07 **Queries matched:** 13
myelin basic protein isoform 3 [Rattus norvegicus]
gi|4454311 **Mass:** 14184 **Score: 124** **Expect:** 2.3e-06 **Queries matched:** 12
myelin basic protein [Rattus norvegicus]
gi|8393759 **Mass:** 14202 **Score: 121** **Expect:** 4.7e-06 **Queries matched:** 12
myelin basic protein isoform 5 [Rattus norvegicus]
gi|69885040 **Mass:** 20299 **Score: 113** **Expect:** 2.9e-05 **Queries matched:** 13
myelin basic protein isoform 2 [Mus musculus]
gi|69885032 **Mass:** 21546 **Score: 111** **Expect:** 4.7e-05 **Queries matched:** 13
myelin basic protein isoform 1 [Mus musculus]
gi|69885065 **Mass:** 17230 **Score: 108** **Expect:** 9.3e-05 **Queries matched:** 12
myelin basic protein isoform 5 [Mus musculus]
gi|69885049 **Mass:** 18476 **Score: 106** **Expect:** 0.00015 **Queries matched:** 12
myelin basic protein isoform 3 [Mus musculus]
gi|199051 **Mass:** 16216 **Score: 100** **Expect:** 0.00059 **Queries matched:** 11
myelin basic protein
gi|149015900 **Mass:** 31612 **Score: 98** **Expect:** 0.00095 **Queries matched:** 13
myelin basic protein, isoform CRA_b [Rattus norvegicus]
gi|4454317 **Mass:** 21528 **Score: 97** **Expect:** 0.0013 **Queries matched:** 11
myelin basic protein [Rattus norvegicus]
gi|70166245 **Mass:** 21546 **Score: 95** **Expect:** 0.0019 **Queries matched:** 11
myelin basic protein isoform 1 [Rattus norvegicus]
gi|6754658 **Mass:** 27151 **Score: 94** **Expect:** 0.0021 **Queries matched:** 12
Golli-mbp isoform 1 [Mus musculus]
gi|70166270 **Mass:** 17230 **Score: 92** **Expect:** 0.0039 **Queries matched:** 10
myelin basic protein isoform 4 [Rattus norvegicus]
gi|4454315 **Mass:** 18458 **Score: 91** **Expect:** 0.0043 **Queries matched:** 10
myelin basic protein [Rattus norvegicus]
gi|70166255 **Mass:** 18476 **Score: 90** **Expect:** 0.0066 **Queries matched:** 10
myelin basic protein isoform 2 [Rattus norvegicus]
gi|148677439 **Mass:** 34495 **Score: 88** **Expect:** 0.01 **Queries matched:** 13
myelin basic protein, isoform CRA_e [Mus musculus]
gi|158260809 **Mass:** 20320 **Score: 86** **Expect:** 0.014 **Queries matched:** 10
unnamed protein product [Homo sapiens]
gi|149015901 **Mass:** 27295 **Score:** 80 **Expect:** 0.063 **Queries matched:** 10
myelin basic protein, isoform CRA_c [Rattus norvegicus]
gi|149015899 **Mass:** 34639 **Score:** 74 **Expect:** 0.24 **Queries matched:** 11
myelin basic protein, isoform CRA_a [Rattus norvegicus]
gi|90075526 **Mass:** 15370 **Score:** 72 **Expect:** 0.39 **Queries matched:** 8
unnamed protein product [Macaca fascicularis]
gi|74268137 **Mass:** 19166 **Score:** 71 **Expect:** 0.45 **Queries matched:** 8
MBP protein [Bos taurus]
gi|69885018 **Mass:** 20991 **Score:** 69 **Expect:** 0.72 **Queries matched:** 9
Golli-mbp isoform 2 [Mus musculus]
gi|126796 **Mass:** 18312 **Score:** 69 **Expect:** 0.77 **Queries matched:** 8
Myelin basic protein (MBP) (Myelin A1 protein) (20 kDa
microtubule-stabilizing protein)
gi|126797 **Mass:** 18202 **Score:** 68 **Expect:** 1 **Queries matched:** 8

Myelin basic protein (MBP)
gi|12655896 **Mass:** 5865 **Score:** 64 **Expect:** 2.5 **Queries matched:** 6
myelin basic protein [Bos taurus]
gi|4505123 **Mass:** 20290 **Score:** 63 **Expect:** 3 **Queries matched:** 8
myelin basic protein isoform 2 [Homo sapiens]
gi|68509930 **Mass:** 21537 **Score:** 62 **Expect:** 4.2 **Queries matched:** 8
myelin basic protein isoform 1 [Homo sapiens]
gi|1162922 **Mass:** 22359 **Score:** 61 **Expect:** 5 **Queries matched:** 8
myelin basic protein
gi|3309629 **Mass:** 16334 **Score:** 59 **Expect:** 7.2 **Queries matched:** 7
myelin basic protein; MBP [Cavia porcellus]
gi|114673653 **Mass:** 28900 **Score:** 57 **Expect:** 11 **Queries matched:** 9
PREDICTED: similar to [Human Golli-mbp gene, complete cds.], gene product isoform 23 [Pan troglodytes]
gi|68509932 **Mass:** 17333 **Score:** 57 **Expect:** 12 **Queries matched:** 7
myelin basic protein isoform 4 [Homo sapiens]
gi|55731101 **Mass:** 17307 **Score:** 57 **Expect:** 12 **Queries matched:** 7
hypothetical protein [Pongo pygmaeus]
gi|90074964 **Mass:** 17335 **Score:** 57 **Expect:** 12 **Queries matched:** 7
unnamed protein product [Macaca fascicularis]
gi|60834666 **Mass:** 17448 **Score:** 57 **Expect:** 12 **Queries matched:** 7
myelin basic protein [synthetic construct]
gi|126802 **Mass:** 18548 **Score:** 57 **Expect:** 12 **Queries matched:** 7
Myelin basic protein (MBP)
gi|17378880 **Mass:** 18206 **Score:** 56 **Expect:** 13 **Queries matched:** 7
Myelin basic protein (MBP) (Myelin A1 protein) (Myelin P1 protein)
gi|55732188 **Mass:** 18553 **Score:** 56 **Expect:** 17 **Queries matched:** 7
hypothetical protein [Pongo pygmaeus]
gi|68509928 **Mass:** 18579 **Score:** 56 **Expect:** 17 **Queries matched:** 7
myelin basic protein isoform 3 [Homo sapiens]
gi|60652959 **Mass:** 18693 **Score:** 55 **Expect:** 17 **Queries matched:** 7
myelin basic protein [synthetic construct]
gi|70166179 **Mass:** 21303 **Score:** 55 **Expect:** 17 **Queries matched:** 7
Golli-mbp isoform 1 [Rattus norvegicus]

---

gi|49168552 **Mass:** 17337 **Score:** **81** **Expect:** 0.049 **Queries matched:** 10
MBP [Homo sapiens]

---

gi|223882 **Mass:** 21634 **Score:** 74 **Expect:** 0.22 **Queries matched:** 9
protein 21.5K,myelin basic

---

gi|116513410 **Mass:** 28552 **Score:** 52 **Expect:** 35 **Queries matched:** 7
hypothetical protein LBUL_0202 [Lactobacillus delbrueckii subsp. bulgaricus ATCC BAA-365]

---

gi|149185269 **Mass:** 66748 **Score:** 52 **Expect:** 38 **Queries matched:** 9
glucose-inhibited division protein A [Erythrobacter sp. SD-21]

---

gi|116749197 **Mass:** 36950 **Score:** 50 **Expect:** 55 **Queries matched:** 7
aldo/keto reductase [Syntrophobacter fumaroxidans MPOB]

Search Parameters

Type of search	:	Peptide Mass Fingerprint
Enzyme	:	Trypsin
Fixed modifications	:	Carbamidomethyl (C)
Variable modifications	:	Oxidation (M)
Mass values	:	Monoisotopic
Protein Mass	:	Unrestricted
Peptide Mass Tolerance	:	± 50 ppm
Peptide Charge State	:	1+
Max Missed Cleavages	:	1
Number of queries	:	48

Appendix C – Representative Graphs Showing TARP γ8/Actin for Mice with Altered $5HT_{2C}$ Receptor Expression.

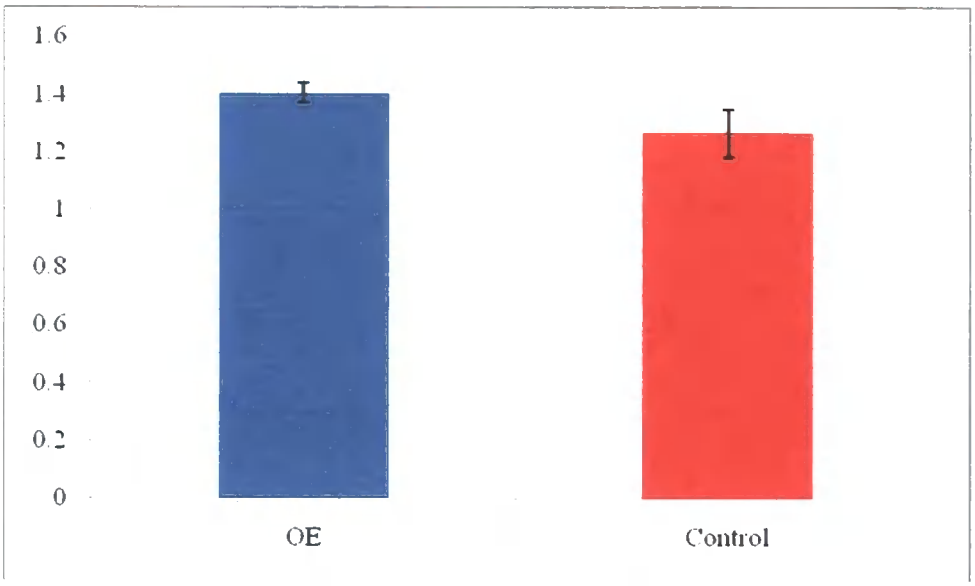

Figure C.1: TARP γ8/β-Actin Intensities for $5HT_{2C}$ Receptor Over-expressing Mice and their Respective Controls, *n = 3.*

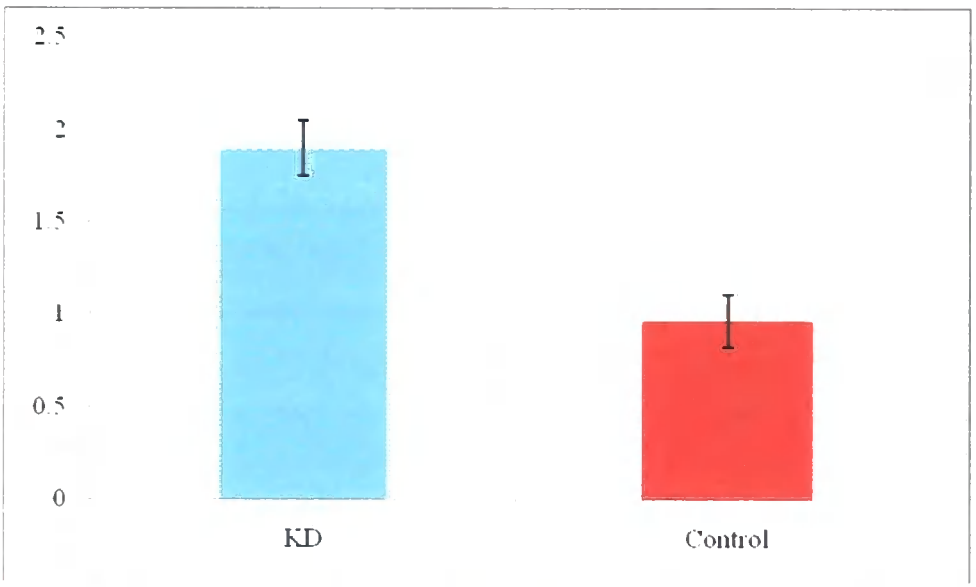

Figure C.2: TARP γ8/β-Actin Intensities for $5HT_{2C}$ Receptor Knockdown Mice and their Respective Controls, *n = 3.*

References

Abramowski D, Rigo M, Duc D, Hoyer D, Staufenbiel M (1995). "Localization of the 5-hydroxytryptamine2C receptor protein in human and rat brain using specific antisera." Neuropharmacology **34**(12): 1635-1645.

Abramowski D, Staufenbiel M (1995). "Identification of the 5-Hydroxytryptamine2C Receptor as a 60-kDa N-Glycosylated Protein in Choroid Plexus and Hippocampus." Journal of Neurochemistry **65**(2): 782-790.

Adesnik H, Nicoll RA, England PM (2005). "Photoinactivation of native AMPA receptors reveals their real-time trafficking." Neuron **38**(6): 977-985.

AM B, (2006). "Neurotransmitter-mediated calcium signalling in oligodendrocyte physiology and pathology." Glia **54**(7): 666-675.

Anantharam V, Panchal RG, Wilson A, Kolchine VV, Treistman SN, Bayley H (1992). "Combinatorial RNA splicing alters the surface charge on the NMDA receptor." Federation of European Biological Sciences Letters: 30527-30530.

Antri M, Auclair F, Albrecht J, Djeudjang N, Dubuc R. (2008). "Serotoninergic modulation of sensory transmission to brainstem reticulospinal cells." European Journal of Neuroscience **28**(4): 655-667.

Bachtell RK, Choi KH, Simmons DL, Falcon E, Monteggia LM, Neve RL, Self DW. (2008). "Role of GluR1 expression in nucleus accumbens neurons in cocaine

sensitization and cocaine-seeking behavior." European Journal of Neuroscience **27**(9): 2229-2240.

Bachtell RK, Self DW (2008). "Renewed cocaine exposure produces transient alterations in nucleus accumbens AMPA receptor-mediated behavior." Journal of Neuroscience **28**(48): 12808-12814.

Backstrom JR, Sanders-Bush E (1997). "Generation of anti-peptide antibodies against serotonin 5-HT2A and 5-HT2C receptors." Journal of Neuroscience Methods **77**(1): 109-117.

Backstrom JR, Westphal RS, Canton H, Sanders-Bush E (1999). "Identification of rat serotonin 5-HT2C receptors as glycoproteins containing N-linked oligosaccharides." Molecular Brain Research **33**(2): 311-318.

Bannerman P, Horiuchi M, Feldman D, Hahn A, Itoh A, See J, Jia ZP, Itoh T, Pleasure D. (2007). "GluR2-free alpha-amino-3-hydroxy-5-methyl-4-isoxazolepropionate receptors intensify demyelination in experimental autoimmune encephalomyelitis." Journal of Neurochemistry **102**(4): 1064-1070.

Bats C, Groc L, Choquet D (2007). "The interaction between stargazin and PSD-95 regulates AMPAR surface trafficking." Neuron **53**: 719-734.

Beattie EC, Carroll RC, Yu X, Morishita W, Yasuda H, von Zastrow M, Malenka RC (2000). "Regulation of AMPA receptor endocytosis by a signaling mechanism shared with LTD." Nature Neuroscience **3**(12): 1291-1300.

Beneyto, M. Meador-Woodruff JH (2006). "Lamina-Specific Abnormalities of AMPA Receptor Trafficking and Signalling Molecule Transcripts in the Prefrontal Cortex in Schizophrenia." Synapse **60**: 585-598.

Berg KA, Cropper JD, Niswender CM, Sanders-Bush E, Emeson RB, Clarke WP (2001). "RNA-editing of the 5-HT(2C) receptor alters agonist-receptor-effector coupling specificity." British Journal of Pharmacology **134**(2): 386-392.

Bespalov AY, Harich S, Jongen-Rêlo AL, van Gaalen MM, Gross G. (2007). "AMPA receptor antagonists reverse effects of extended habit training on signaled food approach responding in rats." Psychopharmacology **195**(1): 11-18.

Bettler B, Mulle C (1995). "Neurotransmitter Receptors II AMPA and Kainate Receptors." Neuropharmacology **34**(2): 123-139.

Black JL (2003). "The Voltage-gated calcium channel γ subunits: a review of the literature." JL Journal of Bioenergetics and Biomembranes **35**(6): 649-660.

Bocchiaro CM, Feldman JL (2004). "Synaptic activity-independent persistent plasticity in endogenously active mammalian motoneurons." Proceedings of the National Academy of Science USA **101**: 4292-4295.

Bockaert J, Pin J, Fagni L (1993). "Metabotropic glutamate receptors: an original family of G protein-coupled receptors." Fundamental Clinical Pharmacology 7(9): 473-485.

Boeckers TM (2006). "The postsynaptic density." Cell and Tissue Research **326**(2): 409-422.

Boggs JM (2006). "Myelin basic protein: a multifunctional protein." Cellular and Molecular Life Sciences **63**: 1945-1961.

Boothman L, Raley J, Denk F, Hirani E, Sharp T (2006). "In vivo evidence that 5-HT(2C) receptors inhibit 5-HT neuronal activity via a GABAergic mechanism." British Journal of Pharmacology **149**(7): 861-869.

Bouryi VA, Lewis DI (2003). "The modulation by 5-HT of glutamatergic inputs from the raphe pallidus to rat hypoglossal motoneurones, in vitro." Journal of Physiology **553**(3): 1019-1031.

Boylan CB, Blue ME, Hohmann CF. (2007). "Modeling early cortical serotonergic deficits in autism." Behavioural Brain Research **176**(1): 94-108.

Brunner C, Lassmann H, Waenheldt TV, Matthieu JM, Linington C (1989). "Differential Ultrastructural Localization of Myelin Basic Protein, Myelin/Oligodendroglial Glycoprotein, and 2',3'-Cyclic Nucleotide 3'-Phosphodiesterase in the CNS of Adult Rats." Journal of Neurochemistry **52**(1).

Buckland PR, Hoogendoorn B, Guy CA, Smith SK, Coleman SL, O'Donovan MC (2005). "Low gene expression conferred by association of an allele of the 5-HT2C receptor gene with antipsychotic-induced weight gain." American Journal of Psychiatry **162**(3): 613-615.

Buller AL, Larson HC, Schneider BE, Beaton JA, Morrisett RA, Monaghan DT (1994). "The molecular basis of NMDA receptor subtypes: native receptor diversity is predicted by subunit composition." Journal of Neuroscience **14**(9): 5471-5484.

Burns CM, Chu H, Rueter SM, Hutchinson LK, Canton H, Sanders-Bush E, Emeson RB (1997). "Regulation of serotonin-2C receptor G-protein coupling by RNA editing." Nature **387**: 303-308.

Chatterton JE, Awobuluyi M, Premkumar LS, Takahashi H, Talantova M, Shin Y, Cui J, Tu S, Sevarino KA, Nakanishi N, Tong G, Lipton SA, Zhang D (2002). "Excitatory glycine receptors containing the NR3 family of NMDA receptor subunits." Nature **415**: 793–798.

Chen H, Kintner DB, Jones M, Matsuda T, Baba A, Kiedrowski L, Sun D. (2007). "AMPA-mediated excitotoxicity in oligodendrocytes: role for Na(+)-K(+)-Cl(-) co-transport and reversal of Na(+)/Ca(2+) exchanger." Journal of Neurochemistry **102**(6): 1783-1795.

Chen L, Chetkovich DM, Petralia RS, Sweeney NT, Kawasaki Y, Wenthold RJ, Bredt DS, Nicoll RA (2000). "Stargazin regulates synaptic targeting of AMPARs by two distinct mechanisms." Nature **408**: 936-943.

Chen Q, Veenman L, Knopp K, Yan Z, Medina L, Song WJ, Surmeier DJ, Reiner A (1998). "Evidence for the preferential localization of glutamate receptor-1 subunits of AMPA receptors to the dendritic spines of medium spiny neurons in rat striatum." Neuroscience **83**(3): 749-761.

Chew LJ, Fleck MW, Wright P, Scherer SE, Mayer ML, Gallo V (1997). "Growth factor-induced transcription of GluR1 increases functional AMPA receptor density in glial progenitor cells." Journal of Neuroscience **17**(1): 227-240.

Chourbaji S, Vogt MA, Fumagalli F, Sohr R, Frasca A, Brandwein C, Hörtnagl H, Riva MA, Sprengel R, Gass P. (2008). "AMPA receptor subunit 1 (GluR-A) knockout mice model the glutamate hypothesis of depression." The FASEB Journal **22**: 3129-3134.

Chu P, Robertson HM, Best PM (2001). "Calcium channel γ subunits provide insights into the evolution of this gene family." Gene **280**: 37-48.

Chung HJ, Xia J, Scannevin RH, Zhang X, Huganir RL (2000). "Phosphorylation of the AMPA receptor subunit GluR2 differentially regulates its interaction with PDZ domain-containing proteins." Journal of Neuroscience **20**(19): 7258-7267.

Clenet F, De Vos A, Bourin M (2001). "Involvement of 5-HT(2C) receptors in the anti-immobility effects of antidepressants in the forced swimming test in mice." Neuropsychopharmacology **11**(2): 145-152.

Coleman SK, Möykkynen T., Cai C, von Ossowski L, Kuismanen E, Korpi ER, Keinänen K (2006). "Isoform-specific early trafficking of AMPA receptor flip and flop variants." Journal of Neuroscience **26**(43): 11220-11229.

Colledge M, Snyder EM, Crozier RA, Soderling JA, Jin Y, Langeberg LK, Lu H, Bear MF, Scott JD (2003). "Ubiquitination regulates PSD-95 degradation and AMPA receptor surface expression." Neuron **40**(3): 595-607.

Coppell AL, Pei Q, Zetterström TS (2003). "Bi-phasic change in BDNF gene expression following antidepressant drug treatment." Neuropharmacology **44**(7): 903-910.

Crozatier C, Farley S, Mansuy IM, Dumas S, Giros B, Tzavara ET. (2007). "Calcineurin (protein phosphatase 2B) is involved in the mechanisms of action of antidepressants." Neuroscience **144**(4): 1470-1476.

Cuadra AE, Kuo SH, Kawasaki Y, Bredt DS, Chetkovich DM (2004). "AMPA receptor synaptic targeting regulated by stargazin interactions with the Golgi-resident PDZ protein nPIST." Journal of Neuroscience **24**(34): 7491-7502.

Dakoji S, Tomita S, Karimzadegan S, Nicoll RA, Bredt DS (2003). "Interaction of Transmembrane AMPA receptor regulatory proteins with multiple membrane associated guanylate kinases." Neuropharmacology **45**: 849-856.

Davies J, Evans RH, Francis AA, Watkins, JC (1979). "Excitatory amino acid receptors and synaptic excitation in the mammalian central nervous system." Journal of Physiology **75**: 641-654.

Daw MI, Chittajallu R, Bortolotto ZA, Dev KK, Duprat F, Henley JM, Collingridge GL, Isaac JT (2000). "PDZ proteins interacting with C-terminal GluR2/3 are involved in a PKC-dependent regulation of AMPA receptors at hippocampal synapses." Neuron **27**(3): 873-876.

De Luca V, Müller DG, Hwang R, Lieberman JA, Volavka J, Meltzer HY, Kennedy JL (2007). "HTR2C haplotypes and antipsychotics-induced weight gain: X-linked multimarker analysis." Human Psychopharmacology **22**(7): 463-467.

Deng F, Price MG, Davis CF, Mori M, Burgess DL (2006). "Stargazin and other transmembrane AMPA receptor regulating proteins interact with synaptic scaffolding protein MAGI-2 in brain." Journal of Neuroscience **26**(30): 7884-7875.

Deng W, Neve RL, Rosenberg PA, Volpe JJ, Jensen FE. (2006). "Alpha-amino-3-hydroxy-5-methyl-4-isoxazole propionate receptor subunit composition and cAMP-response element-binding protein regulate oligodendrocyte excitotoxicity." Journal of Biological Chemistry **281**(47): 36004-36011.

Derkach VA, Oh MC, Guire ES, Soderling TR (2007). "Regulatory Mechanisms of AMPA Receptors in Synaptic Plasticity." Nature Reviews Neuroscience **8**: 101-114.

Dong H, O'Brian RJ, Fung ET, Lanahan AA, Worley PF, Huganir RL (1997). "GRIP: a synaptic PDZ domain-containing protein that interacts with AMPA receptors." Nature **386**(6622): 279-284.

Dracheva S, Davis KL, Chin B, Woo DA, Schmeidler J, Haroutunian V (2006). "Myelin-associated mRNA and protein expression deficits in the anterior cingulate cortex and hippocampus in elderly schizophrenia patients." Neurobiology of Disease **21**(3): 531-540.

Dremencova E, Newman ME, Kinora N, Blatman-Jana G, Schindlera CJ, Overstreetc DH, Yadid G (2005). "Hyperfunctionality of serotonin-2C receptor-mediated inhibition of accumbal dopamine release in an animal model of depression is reversed by antidepressant treatment." Neuropharmacology **48**: 34-42.

Duggan MJ, Pollard S, Stephenson FA (1991). "Immunoaffinity purification of GABAA receptor alpha-subunit iso-oligomers. Demonstration of receptor populations containing

alpha 1 alpha 2, alpha 1 alpha 3, and alpha 2 alpha 3 subunit pairs." Journal of Biological Chemistry **266**(36): 24778-24784.

Durand GM, Bennett MV, Zukin RS (1993). "Splice variants of the N-methyl-D-aspartate receptor NR 1 identify domains involved in regulation by polyamines and protein kinase C." Proceedings of the National Academy of Sciences USA **90**: 6731-6735.

Dusseldorp E, Spinhoven P, Bakker A, van Dyck R, van Balkom AJ (2007). "Which panic disorder patients benefit from which treatment: cognitive therapy or antidepressants?" Psychotherapy and Psychosomatics **76**(3): 154-161.

Earnshaw BA, Bressloff PC (2006). "Biophysical Model of AMPA Receptor Trafficking and Its Regulation during Long-Term Potentiation/Long-Term Depression." Journal of Neuroscience **26**(47): 12362-12373.

Ehlers MD (2000). "Reinsertion or degradation of AMPA receptors determined by activity-dependent endocytic sorting." Neuron **28**(2): 511-525.

Ehrlich I, Malinow R (2004). "Postsynaptic density 95 controls AMPA receptor incorporation during long-term potentiation and experience-driven synaptic plasticity." Journal of Neuroscience **24**(4): 916-927.

Engblom D, Bilbao A, Sanchis-Segura C, Dahan L, Perreau-Lenz S, Balland B, Parkitna JR, Luján R, Halbout B, Mameli M, Parlato R, Sprengel R, Lüscher C, Schütz G, Spanagel R. (2008). "Glutamate receptors on dopamine neurons control the persistence of cocaine seeking." Neuron **59**(3): 497-508.

Engels AS, Heller W, Mohanty A, Herrington JD, Banich MT, Webb AG, Miller GA (2007). "Specificity of regional brain activity in anxiety types during emotion processing." Psychophysiology **44**(3): 352-363.

Ennaceur A, Michalikova S, van Rensburg R, Chazot PL (2006). "Models of anxiety: responses of mice to novelty and open spaces in a 3D maze." Behavioural Brain Research **174**(1): 9-38.

Ferraguti F, Shigemoto R (2006). "Metabotropic Glutamate Receptors." Cell Tissue Research **326**: 483-504.

Flomen R, Knight J, Sham P, Kerwin R, Makoff A (2004). "Evidence that RNA editing modulates splice site selection in the 5-HT2C receptor gene." Nucleic Acids Research **32**(7): 2113-2122.

Follett PL, Rosenberg PA, Volpe JJ, Jensen FE. (2000). "NBQX attenuates excitotoxic injury in developing white matter." Journal of Neuroscience **20**(24): 9235-9241.

Francis PT (2008). "Glutamatergic approaches to the treatment of cognitive and behavioural symptoms of Alzheimer's disease." Neuro-degenerative Diseases **5**(3-4): 241-243.

Frank MG, Stryker MP, Tecott LH (2002). "Sleep and sleep homeostasis in mice lacking the 5-HT2c receptor." Neuropsychopharmacology **27**(5): 869-873.

Fukaya M, Hayashi Y, Watanabe M (2005). "NR2 to NR3B subunit switchover of NMDA receptors in early postnatal motoneurons." European Journal of Neuroscience **21**(5): 1432-1436.

Gajendiran M (2008). "In vivo evidence for serotonin 5-HT2C receptor-mediated long-lasting excitability of lumbar spinal reflex and its functional interaction with 5-HT1A receptor in the mammalian spinal cord." Brain Research Bulletin **75**(5): 674-681.

Gallo V, Ghiani CA (2000). "Glutamate receptors in glia: new cells, new inputs and new functions." Trends in Pharmacological Sciences **21**(7): 252-258.

Gallo V, Zhou JM, McBain CJ, Wright P, Knutson PL, Armstrong RC. (1996). "Oligodendrocyte progenitor cell proliferation and lineage progression are regulated by glutamate receptor-mediated K+ channel block." Journal of Neuroscience **16**: 2659-2670.

Gao C, Wolf ME (2007). "Dopamine alters AMPA receptor synaptic expression and subunit composition in dopamine neurons of the ventral tegmental area cultured with prefrontal cortex neurons." Journal of Neuroscience **27**(52): 14275-14285.

Gao XM, Sakai K, Roberts RC, Conley RR, Dean B, Tamminga CA (2000). "Ionotropic glutamate receptors and expression of N-methyl-D-aspartate receptor subunits in subregions of human hippocampus: effects of schizophrenia." American Journal of Psychiatry **157**(7): 1141-1149.

Gartside SE, Cole AJ, Williams AP, McQuade R, Judge SJ. (2007). "AMPA and NMDA receptor regulation of firing activity in 5-HT neurons of the dorsal and median raphe nuclei." European Journal of Neuroscience **25**(10): 3001-3008.

Gavarini S, Bécamel C, Chanrion B, Bockaert J, Marin P (2004). "Molecular and functional characterization of proteins interacting with the C-terminal domains of 5-HT2 receptors: emergence of 5-HT2 "receptosomes"." Biology of the Cell **96**(5): 373-381.

Gerges NZ, Tran IC, Backos DS, Harrell JM, Chinkers M, Pratt WB, Esteban JA (2004). "Independent functions of hsp90 in neurotransmitter release and in the continuous synaptic cycling of AMPA receptors." Journal of Neuroscience **24**(20): 4758-4766.

Giorgetti M, Tecott LH (2004). "Contributions of 5-HT2C receptors to multiple actions of central serotonin systems." European Journal of Pharmacology **488**: 1-9.

Guiard BP, Guilloux JP, Reperant C, Hunt SP, Toth M, Gardier AM. (2007). "Substance P neurokinin 1 receptor activation within the dorsal raphe nucleus controls serotonin release in the mouse frontal cortex." Molecular Pharmacology **72**(6): 1411-1418.

Hannon J, Hoyer D (2008). "Molecular biology of 5-HT receptors." Behavioural Brain Research **195**(1): 198-213.

Hayashi T, Rumbaugh G, Huganir RL (2005). "Differential regulation of AMPA receptor subunit trafficking by palmitoylation of two distinct sites." **47**(5): 709-723.

Herrick-Davis K, Grinde E, Mazurkiewicz JE (2008). "Ligand sensitivity in dimeric associations of the serotonin 5HT2c receptor." European Molecular Biology Organisation Reports **9**(4): 363-369.

Herrick-Davis K, Grinde E, Niswender CM (1999). "Serotonin 5-HT2C receptor RNA editing alters receptor basal activity: implications for serotonergic signal transduction." Journal of Neurochemistry **73**: 1711-1717.

Hertzmann M, Reba RC, Kotlyarov EV (1990). "Single photon emission computed tomography in phencyclidine and related drug abuse." American Journal of Psychiatry **147**: 255-256.

Hollmann M, Boulter J, Maron C, Beasley L, Sullivan J, Pecht G, Heinemann S (1993). "Zinc potentiates agonist-induced currents at certain splice variants of the NMDA receptor." Neuron **10**: 943-954.

Hollmann M, Heineman S (1994). "Cloned Glutamate Receptors." Annual Review Neuroscience **17**: 31-108.

Holmes MC, French KL, Seckl JR (1997). "Dysregulation of diurnal rhythms of serotonin 5-HT2C and corticosteroid receptor gene expression in the hippocampus with food restriction and glucocorticoids." Journal of Neuroscience **17** (11): 4056-4065

Hoyer D, Clarke DE, Fozard JR, Hartig PR, Martin GR, Mylecharane EJ, Saxena PR, Humphrey PP (1994). " International Union of Pharmacology classification of receptors for 5-hydroxytryptamine (Serotonin)." Pharmacological Review **46**(2): 157-203.

Hoyer D, Hannon J, Martin GR (2002). "Molecular, pharmacological and functional diversity of 5-HT receptors." Pharmocology, Biochemistry and Behaviour **71**(4): 533-554.

Hsu PC, Yang UC, Shih KH, Liu CM, Liu YL, Hwu HG (2008). "A protein interaction based model for schizophrenia study." BMC Bioinformatics **9**(Suppl. 12): S23.

Huang Y, Man HY, Sekine-Aizawa Y, Han Y, Juluri K, Luo H, Cheah J, Lowenstein C, Huganir RL, Snyder SH (2005). "S-nitrosylation of N-ethylmaleimide sensitive factor mediates surface expression of AMPA receptors." Neuron **46**(4): 533-540.

Huettner JE (2003). "Kainate Receptors and Synaptic Transmission." Progress in Neurobiology **70**: 387-407.

Ishii T, Moriyoshi K, Sugihara H, Sakurada K, Kadotani H, Yokoi M, Akazawa C, Shigemoto R, Mizuno N, Masu M, Nakanishi S (1993). "Molecular characterization of the family of the N-methyl-D-aspartate receptor subunits." Journal of Biological Chemistry **268**: 2836-2843.

Ives JH, Drewery DL, Thompson CL(2002). "Differential cell surface expression of GABAA receptor alpha1, alpha6, beta2 and beta3 subunits in cultured mouse cerebellar granule cells influence of cAMP-activated signalling. Journal of Neurochemistry **80**(2): 317-327.

Ives JH, Fung S, Tiwari P, Payne HL, Thompson CL (2004). "Microtubule-associated protein light chain 2 is a stargazin-AMPA receptor complex-interacting protein in vivo." Journal of Biochemistry **279**(30): 31002-31009.

Iwakura Y, Nagano T, Kawamura M, Horikawa H, Ibaraki K, Takei N, Nawa H (2005). "N-methyl-D-aspartate-induced alpha-amino-3-hydroxy-5-methyl-4-isoxazoleproprionic acid (AMPA) receptor down-regulation involves interaction of the carboxyl terminus of

GluR2/3 with Pick1. Ligand-binding studies using Sindbis vectors carrying AMPA receptor decoys." Journal of Biological Chemistry **276**(43): 40025-40042.

Jenck F, Moreau JL, Berendsen HH, Boes M, Broekkamp CL, Martin JR, Wichmann J, Van Delft AM (1998). "Antiaversive effects of 5HT2C receptor agonists and fluoxetine in a model of panic-like anxiety in rats." European Neuropsychopharmacology **8**(3): 161-168.

Jin R, Clark S, Weeks AM, Dudman JT, Gouaux E, Partin KM. (2005). "Mechanism of Positive Allosteric Modulators Acting on AMPA Receptors." Journal of Neuroscience **25**(39): 9027-9036.

Kannenberg K, Baur R, Sigel E (1997) "Proteins associated with alpha 1-subunit-containing GABAA receptors from bovine brain." Journal of Neurochemistry **68**(4): 1352-1360.

Káradóttir R, Cavalier P, Bergersen LH, Attwell D (2005). "NMDA receptors are expressed in oligodendrocytes and activated in ischaemia." Nature **438**(7071): 1162-1166.

Kato AS, Zhou W, Milstein AD, Knierman MD, Siuda ER, Dotzlaf JE, Yu H, Hale JE, Nisenbaum ES, Nicoll RA, Bredt DS (2007). "New transmembrane AMPA receptor regulatory protein isoform γ7 differentially regulates AMPA receptors." Journal of Neuroscience **27**(18): 4969-4977.

Kauer JA, Malenka RC (2006). "LTP: AMPA receptors trading places." Nature Neuroscience **9**(5): 593-594.

Kia HK, Brisorquiel MJ, Hamon M, Calas A & Verge D (1996). "Ultrastructural localization of 5-hydroxytryptamine1A receptors in the rat brain." Journal of Neuroscience Research **46**: 697-708.

Kim CH, Chung HJ, Lee HK, Huganir RL (2001). "Interaction of the AMPA receptor subunit GluR2/3 with PDZ domains regulates hippocampal long-term depression." Proceedings of the National Academy of Science USA **98**(20): 11725-11730.

Kim M, Au E, Neve R, Yoon BJ. (2008). "AMPA receptor trafficking in the dorsal striatum is critical for behavioral sensitization to cocaine in juvenile mice." Biochemical Biophysical Research Communications **379**(1): 65-69.

Köpke AK, Bonk I, Sydow S, Menke H, Spiess J (1993). "Characterization of the NR1, NR2A, and NR2C receptor proteins." Protein Science **2**(12): 2066-2076.

Kornguth SE, Anderson JW (1965). "Localization of a basic protein in the myelin of various species with the aid of fluorescence and electron microscopy." Journal of Cell Biology **26**(1): 157-166.

Kott S, Werner M, Korber C, Hollmann M (2007). "Electrophysiological properties of AMPA receptors are differentially modulated depending on the associated member of the TARP family." Journal of Neuroscience **27**(14): 3780-3789.

Kusiak JW, Norton DD (1993). "A splice variant of the N-methyl-Daspartate (NMDAR1) receptor." Molecular Brain Research **20**: 64-70.

Kwon OB, Parades D, Gonzalez CM, Neddens J, Hernandez L, Vullhorst D, Buonanno A (2008). "Neuregulin-1 regulates LTP at CA1 hippocampal synapses through activation of dopamine D4 receptors." Proceedings of the National Academy of Science USA **105**(40): 15587-15592.

LaLumiere RT, Kalivas PW (2008). "Glutamate release in the nucleus accumbens core is necessary for heroin seeking." Journal of Neuroscience **28**(12): 3170-3177.

Lane DA, Lessard AA, Chan J, Colago EE, Zhou Y, Schlussman SD, Kreek MJ, Pickel VM. (2008). "Region-specific changes in the subcellular distribution of AMPA receptor GluR1 subunit in the rat ventral tegmental area after acute or chronic morphine administration." Journal of Neuroscience **28**(39): 9670-9681.

Lee J, Gravel M, Zhang R, Thibault P, Braun PE. (2005). "Process outgrowth in oligodendrocytes is mediated by CNP, a novel microtubule assembly myelin protein." Journal of Cell Biology **170**(4): 661-673.

Lee SH, Liu L, Wang YT, Sheng M (2002). "Clathrin Adaptor AP2 and NSF Interact with Overlapping Sites of GluR2 and Play distinct Roles in AMPA Receptor Trafficking and Hippocampal LTD." Neuron **36**: 661-674.

Lerer B, Macciardi F, Segman RH, Adolfsson R, Blackwood D, Blairy S, Del Favero J, Dikeos DG, Kaneva R, Lilli R,vMassat I, Milanova V, Muir W, Noethen M, Oruc L, and P. G. Petrova T, Rietschel M, Serretti A, Souery D, Van Gestel S, Van Broeckhoven C, Mendlewicz J. (2001). "Variability of 5-HT2C receptor cys23ser polymorphism among European populations and vulnerability to affective disorder." Molecular Psychiatry **6**(579-585).

Li R, Huang FS, Abbas AK, Wigström H (2007). "Role of NMDA receptor subtypes in different forms of NMDA-dependent synaptic plasticity." Biomed Central Neuroscience **8**(55).

Li S, Stys PK (2000). "Mechanisms of Ionotropic Glutamate Receptor-Mediated Excitotoxicity in Isolated Spinal Cord White Matter." Journal of Neuroscience **20**(3): 1190-1198.

Lia X, Witkin JM, Need AB, Skolnick P (2002) Enhancement of antidepressant potency by a potentiator of AMPA receptors." Cellular and Molecular Neurobiology **23**(3): 419-439

Liang F, Huganir RL (2001). "Coupling of agonist-induced AMPA receptor internalization with receptor recycling." Journal of Neurochemistry **77**(6): 1626-1631.

Lin JW, Ju W, Foster K, Lee SH, Ahmadian G, Wyszynski M, Wang YT, Sheng M (2000). "Distinct molecular mechanisms and divergent endocytotic pathways of AMPA receptor internalization." Nature Neuroscience **3**(12): 1282-1290.

Liu S, Bubar MJ, Lanfranco MF, Hillman GR, Cunningham KA (2007). "Serotonin2C receptor localization in GABA neurons of the rat medial prefrontal cortex: implications for understanding the neurobiology of addiction." Neuroscience Research **146**(4): 1677-1688.

Lowry OH, Rosebrough NJ, Farr AL, Randall RJ (1951). "Protein measurement with the Folin phenol reagent." Journal of Biological Chemistry **193**: 265-275.

Lucaites VL, Nelson DL, Wainscott DB, Baez M (1996). "Receptor subtype and density determine the coupling repertoire of the 5-HT2 receptor subfamily." Life Sciences **59**(13): 1081-1095.

Lüscher C, Xia H, Beattie EC, Carroll RC, von Zastrow M, Malenka RC, Nicoll RA (1999). "Role of AMPA receptor cycling in synaptic transmission and plasticity." Neuron **24**(3): 649-658.

Man HY, Ju WH, Ahmadian G, Liu L, Becker LE, Sheng M, Wang YT (2000). "Regulation of AMPA receptor-mediated synaptic transmission by clathrin-dependent receptor internalization." Neuron **25**(3): 649-662.

Marek GJ (2008). "Cortical 5-hydroxytryptamine2A-receptor mediated excitatory synaptic currents in the rat following repeated daily fluoxetine administration." Neuroscience Letters **438**(3): 312-316.

Marsden CA, Fone KC, Jonson JV, Crespi F, Martin KF, Garrett JC, Bennett GW (1989). "Functional identification of 5HT receptor subtypes." Comparative Biochemical and Physiological Anatomy **93**(1): 107-114.

Martínez-Turrillas R, Del Río J, Frechilla D (2005). "Sequential changes in BDNF mRNA expression and synaptic levels of AMPA receptor subunits in rat hippocampus after chronic antidepressant treatment." Neuropharmacology **49**(8): 1178-1188.

Martinez-Turrillas R, Frechilla D, Del Río J (2002). "Chronic antidepressant treatment increases the membrane expression of AMPA receptors in rat hippocampus." Neuropharmacology **43**(8): 1230-1237.

Martins-de-Souza D, Gattaz WF, Schmitt A, Maccarrone G, Hunyadi-Gulyás E, Eberlin MN, Souza GH, Marangoni S, Novello JC, Turck CW, Dias-Neto E. (2008). "Proteomic analysis of dorsolateral prefrontal cortex indicates the involvement of cytoskeleton, oligodendrocyte, energy metabolism and new potential markers in schizophrenia." Journal of Psychiatric Research **E pub**.

Mathew SJ, Keegan K, Smith L (2005). "Glutamate modulators as novel interventions for mood disorders." Revista brasileira de psiquiatria **27**(3): 243-248.

Matsuda S, Mikawa S, Hirai H (1999). "Phosphorylation of serine-880 in GluR2 by protein kinase C prevents its C terminus from binding with glutamate receptor-interacting protein." Journal of Neurochemistry **73**(3): 1765-1768.

Matute C (2007). "Interaction between glutamate signalling and immune attack in damaging oligodendrocytes." Neuron Glia Biology **3**(4): 281-285.

McCarran WJ, Goldberg MP (2007). "White matter axon vulnerability to AMPA/kainate receptor-mediated ischemic injury is developmentally regulated." Journal of Neuroscience **27**(15): 4220-4229.

McCormack SG, Stornetta RL, Zhu JJ (2006). "Synaptic AMPA receptor exchange maintains bidirectional plasticity." Neuron **50**(1): 75-88.

McCullumsmith RE, Gupta D, Beneyto M, Kreger E, Haroutunian V, Davis KL, Meador-Woodruff JH (2007). "Expression of transcripts for myelination-related genes in the anterior cingulate cortex in schizophrenia." Schizophrenia Research **90**(1-3): 15-27.

Meador-Woodruff JH, Hogg AJ, Smith RE (2001). "Striatal ionotropic glutamate receptor expression in schizophrenia, bipolar disorder, and major depressive disorder." Brain Research Bulletin **55**(5): 631-640.

Michael-Titus AT, Albert M, Michael GJ, Michaelis T, Watanabe T, Frahm J, Pudovkina O, van der Hart MG, Hesselink MB, Fuchs E, Czéh B. (2008). "SONU20176289, a compound combining partial dopamine D(2) receptor agonism with specific serotonin reuptake inhibitor activity, affects neuroplasticity in an animal model for depression." European Journal of Pharmacology **598**(1-3): 43-50.

Micu I, Jiang Q, Coderre E, Ridsdale A, Zhang L, Woulfe J, Yin X, and M. J. Trapp BD, Rehak R (2006). "NMDA receptors mediate calcium accumulation in myelin during chemical ischaemia." Nature **439**: 988-992.

Monyer H, Sprengel R, Schoepfer R, Herb A, Higuchi M, Lomeli H, Bumashev N, Sakmann B, Seeburg PH (1992). "Heteromeric NMDA receptors: molecular and functional distinction of subtypes." Science **256**: 1217-1221.

Moreau JL, Bös M, Jenck F, Martin JR, Mortas P, Wichmann J (1996). "5HT2c receptor agonists exhibit antidepressant-like properties in the anhedonia model of depression in rats." European Neuropsychopharmacology **6**: 169-175.

Musse AA, Harauz G (2007). "Molecular "negativity" may underlie multiple sclerosis: role of the myelin basic protein family in the pathogenesis of MS." International Review of Neurobiology **79**: 149-172.

Nakae A, Nakai K, Tanaka T, Takashina M, Hagihira S, Shibata M, Ueda K, Mashimo T (2008). "Serotonin2C receptor mRNA editing in neuropathic pain model." Neuroscience Research **60**(2): 228-231.

Nakanishi N, Axel R, Shneider NA (1992). "Alternative splicing generates functionally distinct N-methyl-D-aspartate receptors." Proceedings of the National Academy of Sciences USA **89**: 8552-8556.

Nakanishi S (1992). "Molecular diversity of glutamate receptors and implications for brain function." Science **258**: 597-603.

Nakanishi S, Nakajima Y, Masu M, Ueda Y, Nakahara K, Watanabe D, Yamaguchi S, Kawabata S, Okada M (1998). "Glutamate receptors: brain function and signal transduction." Brain Research: Brain Research Reviews **26**(2-3): 230-235.

Neverova NV, Saywell SA, Nashold LJ, Mitchell GS, Feldman JL. (2007). "Episodic stimulation of alpha1-adrenoreceptors induces protein kinase C-dependent persistent changes in motoneuronal excitability." Journal of Neuroscience **27**(16): 4435-4442.

Nishi M, Hinds H, Lu HP, Kawata M, Hayashi Y (2001). "Motorneuron-specific expression of NR3B, a novel NMDA-type glutamate receptor subunit that works in a dominant-negative manner." Journal of Neuroscience **21**(23): RC185.

Nishimune A, Isaac JT, Molnar E, Noel J, Nash SR, Tagaya M, Collingridge GL, Nakanishi S, Henley JM (1998). "NSF binding to GluR2 regulates synaptic transmission." Neuron **21**(1): 87-97.

Nishizawa Y, Kurihara T, Takahashi Y (1981). "Immunohistochemical localization of 2',3'-cyclic nucleotide 3'-phosphodiesterase in the central nervous system." Brain Research **212**: 219-222.

Niswender CM, Copeland SC, Herrick-Davis K, Emeson RB, Sanders-Bush E (1999). "RNA editing of the human serotonin 5-hydroxytryptamine 2C receptor silences constitutive activity." Journal of Biological Chemistry **274**(14): 9472-9478.

Niswender CM, Herrick Davis K, Dilley GE, Meltzer HY, Overholser JC, Stockmeier CA, Emeson RB, Sanders-Bush E (2001). "RNA editing of the human serotonin 5-HT2C receptor: Alterations in suicide and implications for serotonergic pharmacotherapy." Neuropsychopharmacology **24**(5): 478-491.

Nunes-de-Souza V, Nunes-de-Souza RL, Rodgers RJ, Canto-de-Souza A (2008). "5-HT2 receptor activation in the midbrain periaqueductal grey (PAG) reduces anxiety-like behaviour in mice." Behavioural Brain Research **187**(1): 72-79.

Oh MC, Derkach VA, Guire ES, Soderling TR (2005). "Extrasynaptic membrane trafficking regulated by GluR1 serine 845 phosphorylation primes AMPA receptors for long-term potentiation." Journal of Biological Chemistry **281**(2): 752-758.

Ohashi S, Matsumoto M, Otani H, Mori K, Togashi H, Ueno K, Kaku A & Yoshioka M (2002). "Changes in synaptic plasticity in the rat hippocampo-medial prefrontal cortex pathway induced by repeated treatments with fluvoxamine." Brain Research **949**: 131-138.

Osten P, Khatri L, Perez JL, Köhr G, Giese G, Daly C, Schulz TW, Wensky A, Lee LM, Ziff EB (2000). "Mutagenesis reveals a role for ABP/GRIP binding to GluR2 in synaptic surface accumulation of the AMPA receptor." Neuron **27**(2): 313-325.

Osten P, Stern-Bach Y (2006). "Learning from stargazin: the mouse, the phenotype and the unexpected." Current Opinion in Neurobiology **16**: 1-6.

Pan JT, Gala RR (1988). "The serotonin 5-HT2 receptor system, but not the alpha 1-adrenergic receptor system, is involved in the estrogen-induced afternoon prolactin surge in the rat." Life Sciences **42**(19): 1869-1874.

Pandey SC, Davis JM, Pandey GN (1995). "Phosphoinositide system-linked serotonin receptor subtypes and their pharmacological properties and clinical correlates." Journal of Psychiatry and Neuroscience **20**(3): 215-225.

Paoletti P, Neyton J (2007). "NMDA receptor subunits: function and pharmacology." Current Opinion in Pharmacology **7**: 39-47.

Park E, Liu Y, Fehlings MG (2003). "Changes in glial cell white matter AMPA receptor expression after spinal cord injury and relationship to apoptotic cell death." Experimental Neurology **182**: 35-48.

Parker LL, Backstrom JR, Sanders-Bush E, Shieh BH (2003). "Agonist-induced Phosphorylation of the Serotonin 5-HT2C Receptor Regulates Its Interaction with Multiple PDZ Protein 1." Journal of Biological Chemistry **278**(24): 21576-21583.

Patneau DK, Wright PW, Winters C, Mayer ML, Gallo V (1994). "Glial cells of the oligodendrocyte lineage express both kainate- and AMPA-preferring subtypes of glutamate receptor." Neuron **12**(2): 357-371.

Payne HL, Donoghue PS, Connelly WM, Hinterreiter S, Tiwari P, Ives JH, Hann V, Sieghart W, Lees G, Thompson CL (2006). "Aberrant GABA(A) receptor expression in the dentate gyrus of the epileptic mutant mouse stargazer." Journal of Neuroscience **26**(33): 8600-8608.

Peddie CJ, Davies HA, Colyer FM, Stewart MG, Rodríguez JJ. (2008). "Colocalisation of serotonin2A receptors with the glutamate receptor subunits NR1 and GluR2 in the dentate gyrus: an ultrastructural study of a modulatory role." Experimental Neurology **211**(2): 561-573.

Pende M, Holtzclaw LA, Curtis JL, Russell JT, Gallo V (1994). "Glutamate regulates intracellular calcium and gene expression in oligodendrocyte progenitors through the activation of DL-a-amino-3-hydroxy-5-methyl-4-isoxazolepropionic acid receptors." Proceedings of the National Academy of Sciences USA **91**: 3215-3219.

Perez JL, Khatri L, Chang C, Srivastava S, Osten P, Ziff EB (2001). "PICK1 targets activated protein kinase Calpha to AMPA receptor clusters in spines of hippocampal neurons and reduces surface levels of the AMPA-type glutamate receptor subunit 2." Journal of Neuroscience **21**(15): 5417-5428.

Petralia RS, Wang YX, Wenthold RJ (1994). "The NMDA receptor subunits NR2A and NR2B show histological and ultrastructural localization patterns similar to those of NR1." Journal of Neuroscience **14**(10): 6102-6120.

Pinilla L, Gonzalez LC, Tena-Sempere M, Aguilar E. (2001). "5-HT1 and 5-HT2 receptor agonists blunt +/- -alpha-amino-3-hydroxy-5-methylisoxazole-4-propionic acid (AMPA)-stimulated GH secretion in prepubertal male rats." European Journal of Endocrinology **144**(5): 535-541.

Pittaluga A, Raiteri L, Longordo F, Luccini E, Barbiero VS, Racagni G, Popoli M, Raiteri M. (2007). "Antidepressant treatments and function of glutamate ionotropic receptors mediating amine release in hippocampus." Neuropharmacology **53**(1): 27-36.

Pittaluga A, Segantini D, Feligioni M, Raiteri M (2005). "Extracellular protons differentially potentiate the responses of native AMPA receptor subtypes regulating neurotransmitter release." British Journal of Pharmacology **144**(2): 293-299.

Pizzi M, Boroni F, Bianchetti KM, Memo M, Spano P (1999). "Reversal of glutamate excitotoxicity by activation of PKC-associated metabotropic glutamate receptors in cerebellar granule cells relies on NR2C subunit expression." European Journal of Neuroscience **11**(7): 2489-2496.

Priel A, Kolleker A, Ayalon G, Gillor M, Osten P, Stern-Bach Y (2005). "Stargazin reduces desensitization and slows deactivation of the AMPA-type glutamate receptors." Journal of Neuroscience **25**(10): 2682-2686.

Roth BL, Willins DL, Kristiansen K, Kroeze WK (1998). "5-Hydroxytryptamine2-family receptors (5-hydroxytryptamine2A, 5-hydroxytryptamine2B, 5-hydroxytryptamine2C): where structure meets function." Pharmacology and Therapeutics **79**(3): 231-257.

Rouach N, Byrd K, Petralia RS, Elias GM, Adesnik H, Tomita S, Karimzadegan S, Kealey C, Bredt DS, Nicoll RA (2005). "TARP gamma-8 controls hippocampal AMPA

receptor number, distribution and synaptic plasticity." Nature Neuroscience **8**(11): 1525-1533.

Saint-Cyr JA, Taylor AE, Nicholson K (1995). "Behavior and the basal ganglia." Advances in Neurology **65**: 1-28.

Salter MG, Fern R (2005). "NMDA receptors are expressed in developing oligodendrocyte processes and mediate injury." Nature **438**: 1167-1171.

Sánchez-Gómez MV, Matute C (1999). "AMPA and Kainate Receptors Each Mediate Excitotoxicity in Oligodendroglial Cultures." Neurobiology of Disease **6**: 475-485.

Sans N, Racca C, Petralia RS, Wang YX, McCallum J, Wenthold RJ (2001). "Synapse-associated protein 97 selectively associates with a subset of AMPA receptors early in their biosynthetic pathway." Journal of Neuroscience **21**(19): 7506-7516.

Sarchielli P, Di Filippo M, Candeliere A, Chiasserini D, Mattioni A, Tenaglia S, Bonucci M, Calabresi P (2007). "Expression of ionotropic glutamate receptor GLUR3 and effects of glutamate on MBP- and MOG-specific lymphocyte activation and chemotactic migration in multiple sclerosis patients." Journal of Neuroimmunology **188**(1-2): 146-158.

Schoepp DD (1994). "Novel functions for subtypes of metabotropic glutamate receptors." Neurochemistry International **24**(5): 439-449.

Seog DH (2004). "Glutamate receptor-interacting protein 1 protein binds to the microtubule-associated protein." Bioscience, Biotechnology and Biochemistry **68**(8): 1808-1810.

Sergeeva OA, Amberger BT, Haas HL. (2007). "Editing of AMPA and serotonin 2C receptors in individual central neurons, controlling wakefulness." Cellular and Molecular Neurobiology **27**(5): 669-680.

Shakesby AC, Anwyl R, Rowan MJ (2002). "Overcoming the effects of stress on synaptic plasticity in the intact hippocampus: rapid actions of serotonergic and antidepressant agents." Journal of Neuroscience **22**(9): 3638-3644.

Sheng M, Lee SH (2001). "AMPA receptor trafficking and the control of synaptic transmission." Cell **105**(7): 825-828.

Shi S, Hayashi Y, Esteban J. A. and Malinow R. (2001). "Subunit specific rules governing AMPA receptor trafficking to synapses in hippocampal pyramidal neurons." Cell **105**: 331-334.

Sommer B, Keinänen K, Verdoorn TA, Wisden W, Burnashev N, Herb A, Köhler M, Takagi T, Sakmann B, Seeburg PH (1990). "Flip and flop: a cell-specific functional switch in glutamate-operated channels of the CNS." Science **246**(2976): 1580-1585.

Song I, Kamboj S, Xia J, Dong H, Liao D, Huganir RL (1998). "Interaction of the N-ethylmaleimide-sensitive factor with AMPA receptors." Neuron **21**(2): 393-400.

Sossa KG, Beattie JB, Carroll RC (2007). "AMPAR exocytosis through NO modulation of PICK1." Neuropharmacology **53**: 92-100.

Sossa KG, Court BL, Carroll RC (2006). "NMDA receptors mediate calcium-dependent, bidirectional changes in dendritic PICK1 clustering." Molecular Cellular Neuroscience **31**(3): 574-585.

Standaert DG, Testa CM, Penney JB Jr, Young AB (1993). "Alternatively spliced isoforms of the NMDAR1 glutamate receptor subunit: differential expression in the basal ganglia of the rat." Neuroscience Letters **152**: 161-164.

Steinberg JP, Huganir RL, Linden DJ (2004). "N-ethylmaleimide-sensitive factor is required for the synaptic incorporation and removal of AMPA receptors during cerebellar long-term depression." Proceedings of the National Academy of Sciences **101**(52): 18212-18216.

Steiner P, Sarria JC, Glauser L, Magnin S, Catsicas S, Hirling H (2002). "Modulation of receptor cycling by neuron-enriched endosomal protein of 21 kD." Journal of Cell Biology **157**(7): 1197-209.

Stern JN, Keskin DB (2008). "Strategies for the identification of loci responsible for the pathogenesis of multiple sclerosis." Cellular and Molecular Biology Letters **13**(4): 656-666.

Stoll L, Sequin S, Gentile L (2007). "Tricyclic antidepressants, but not the selective serotonin reuptake inhibitor fluoxetine, bind to the S1S2 domain of AMPA receptors." **458**(2): 213-219.

Sugihara H, Moriyoshi K, Ishii T, Masu M, Nakanishi S (1992). "Structures and properties of seven isoforms of the NMDA receptor generated by alternative splicing." Biochemical Biophysical Research Communications **185**: 826-832.

Summers DF, Maizel JV Jr, Darnell JE Jr (1965). "Evidence for virus-specific noncapsid proteins in poliovirus-infected HeLa cells." Proceedings of the National Academy of Sciences USA **54**(2): 505-513.

Sun Y, Olsen R, Horning M, Armstrong N, Mayer M, Gouaux E (2002). "Mechanism of glutamate receptor desensitization." Nature **417**(6886): 245-253.

Thompson CL, Drewery DL, Atkins HD, Stephenson FA, Chazot PL (2002). "Immunohistochemical localization of N-methyl-D-aspartate receptor subunits in the adult murine hippocampal formation: evidence for a unique role of the NR2D subunit." Molecular Brain Research **102**(55-61).

Thompson CL, Tehrani M, Barnes EM Jr, Stephenson FA (1998). "Decreased expression of GABAA receptor alpha6 and beta3 subunits in stargazer mutant mice: a possible role for brain-derived neurotrophic factor in the regulation of cerebellar GABAA receptor expression?" Brain Research Molecular Brain Research **60**(2): 282-290.

Tomita S, Adesnik H, Sekiguchi M, Zhang W, Wada K, Howe JR, Nicoll RA, Bredt DS (2005). "Stargazin modulates AMPA receptor gating and trafficking by distinct domains." Nature **435**(7045): 1052-1058.

Tomita S, Chen L, Kawasaki Y, Petralia RS, Wenthold RJ, Nicoll RA, Bredt DS (2003). "Functional studies and distribution define a family of transmembrane AMPAR regulatory proteins." Journal of Cell Biology **161**: 805-816.

Tomita S, Fukata M, Nicoll RA, Bredt DS (2004). "Dynamic interaction of stargazin-like TARPs with cycling AMPA receptors at Synapses." Science **303**: 1508-1511.

Tomita S, Shenoy A, Fukata Y, Nicoll RA, Bredt DS (2007). "Stargazin interacts functionally with the AMPAR glutamate binding module." Neuropharmacology **52**(1): 87-91.

Tomita S, Sekiguchi M, Wada K, Nicoll RA, Bredt DS (2006). "Stargazin controls the pharmacology of AMPA receptor potentiators." Proceedings of the National Academy of Sciences of the USA **103**(26): 10064-10067.

Tomita S, Stein V, Stocker TJ, Nicoll RA, Bredt DS (2005). "Bidirectional synaptic plasticity regulated by phosphorylation of stargazin-like TARPs." Neuron **45**: 269-277.

Turetsky D, Garringer E, Patneau DK (2005). "Stargazin modulates native AMPA receptor functional properties by two distinct mechanisms." Journal of Neuroscience **25**(32): 7438-7448.

Vallano ML, Lambolez B, Audinat E, Rossier J (1995). "Neuronal activity differentially regulates NMDA receptor subunit expression in cerebellar granule cells." Journal of Neuroscience **16**(2): 631-639.

Van Oekelen D, Luyten WH, Leysen JE (2003). "5-HT2A and 5-HT2C receptors and their atypical regulation properties." Life Sciences **72**: 2429-2449.

Vandenberghe W, Nicoll RA, Bredt DS (2005). "Interaction with the unfolded protein response reveals a role for stargazin in biosynthetic AMPA receptor transport." Journal of Neuroscience **25**(5): 1095-1102.

Vandenberghe W, Nicoll RA, Bredt DS (2005). "Stargazin is an AMPA receptor auxillary subunit." Proceedings of the National Academy of Sciences of the USA **102**(2): 485-490.

Wang B, Chehab FF (2006). "Deletion of the serotonin 2c receptor from transgenic mice overexpressing leptin does not affect their lipodystrophy but exacerbates their diet-induced obesity." Biochemical Biophysical Research Communications **351**(2): 418-423.

Wang Q, O'Brian PJ, Chen CX, Cho DS, Murray JM, Nishikura K (2000). "Altered G protein-coupling functions of RNA editing isoform and splicing variant serotonin2C receptors." Journal of Neurochemistry **74**(3): 1290-1300.

Watanabe Y, Gould E, McEwen BS (1992). "Stress induces atrophy of apical dendrites of hippocampal CA3 pyramidal neurons". Brain Research **588**(2).

Weiner N, Clement HW, Gemsa D, Wesemann W (1992). "Circadian and seasonal rhythms of 5-HT receptor subtypes, membrane anisotropy and 5-HT release in hippocampus and cortex of the rat." Neurochemistry International **21**(1): 7-14.

Wenzel A, Scheurer L, Künzi R, Fritschy JM, Mohler H, Benke D (1995). "Distribution of NMDA receptor subunit proteins NR2A, 2B, 2C and 2D in rat brain." Neuroreport **7**(1): 45-48.

Wessel D, Flügge UI (1984). "A method for the quantitative recovery of protein in dilute solution in the presence of detergents and lipids." Analytical Biochemistry **138**(1): 141-143.

Wiedholz LM, Owens WA, Horton RE, Feyder M, Karlsson RM, Hefner K, Sprengel R, Celikel T, Daws LC, Holmes A (2008). "Mice lacking the AMPA GluR1 receptor exhibit striatal hyperdopaminergia and 'schizophrenia-related' behaviors." Molecular Psychiatry **13**(6): 631-640.

Wyszynski M, Valtschanoff JG, Naisbitt S, Dunah AW, Kim E, Standaert DG, Weinberg R, Sheng M (1999). "Association of AMPA receptors with a subset of glutamate receptor-interacting protein in vivo." Journal of Neuroscience **19**(15): 6528-6537.

Yin X, Baek RC, Kirschner DA, Peterson A, Fujii Y, Nave KA, Macklin WB, Trapp BD (2006). "Evolution of a neuroprotective function of central nervous system myelin." Journal of Cell Biology **172**(3): 469-478.

Yuen EY, Yan Z (2009). "Dopamine D4 receptors regulate AMPA receptor trafficking and glutamatergic transmission in GABAergic interneurons of prefrontal cortex." Journal of Neuroscience **29**(2): 550-562.

Zhang C, Marek GJ (2008). "AMPA receptor involvement in 5-hydroxytryptamine2A receptor-mediated pre-frontal cortical excitatory synaptic currents and DOI-induced head shakes." Progress in Neuro-Psychopharmacology & Biological Psychiatry **32**: 62-71.

Zhong P, Liu W, Gu Z, Yan Z. (2008). "Serotonin facilitates long-term depression induction in prefrontal cortex via p38 MAPK/Rab5-mediated enhancement of AMPA receptor internalization." Journal of Physiology **586**(18): 4465-4479.

Zhu Y, Pak D, Qin Y, McCormack SG, Kim MJ, Baumgart JP, Velamoor V, Auberson YP, Osten P, van Aelst L, Sheng M, Zhu JJ (2005). "Rap2-JNK removes synaptic AMPA receptors during depotentiation." Neuron **46**(6): 905-916.

Ziff EB (2007). "TARPs and the AMPA receptor trafficking paradox." Neuron **53**: 627-633.

Manuscripts and Communications Published or in Preparation as a Consequence of this Thesis and the Journals they will be Directed Towards:

Aberrant GABA(A) receptor expression in the dentate gyrus of the epileptic mutant mouse stargazer. **Payne HL, Donoghue PS, Connelly WM, Hinterreiter S, Tiwari P, Ives JH, Hann V, Sieghart W, Lees G and Thompson CL** J Neurosci **26** (33) (2006) 8600-8

AMPA receptor activation downregulates TARP γ 2 expression in mouse cerebellar granule neurones. **Payne HL, PS Donoghue, V Hann, CL Thompson** J Neurochem

Proteomic approaches to identify native TARP γ8 interacting proteins. **V Hann, H Payne, PS Donoghue, Robson, JL, Chazot PL, Slabas, A and Thompson CL** J Neurochem

Direct evidence for robust heterologomeric TARP gamma 2 and gamma 8 complexes in the mouse cortex and cerebellum **Hann, V, Payne, H, Donoghue, PS, Chazot, PL and Thompson, CL.** Neuroscience Letts

Biochemical evidence for AMPA-5HT2C interactions via TARP γ8 in the mammalian cortex **PS Donoghue, PL Chazot, M Holmes, CL Thompson and M Spedding.** Biochem J

Detailed anatomical topology of the major *TARP γ2, TARP γ4 and TARP γ8 proteins in the murine CNS.* **PS Donoghue, PL Chazot, M Holmes, CL Thompson and M Spedding.** Neuroscience

Relevance of AMPA receptor trafficking to new therapeutic strategies for neurological and psychological disorders. **PS Donoghue and PL Chazot.** Curr Annaesthesia and Critical Care (Review)